Scalable separation methods for the isolation of monosaccharides in a biorefinery context

David Ward

A thesis submitted to University College London for the degree of

Doctor of Philosophy

2017

The Advanced Centre for Biochemical Engineering
Department of Biochemical Engineering
University College London

Declaration of authorship

I, David Ward confirm that the work presented in this thesis is my own. Where information has been derived from other sources, I confirm that this has been indicated in the thesis.

Abstract

Biorefineries allow for the sustainable production of higher value products from biomass. In addition to bioethanol, they can produce added value chemicals and pharmaceutical intermediates from isolated component compounds such as sugars. Sugar beet pulp (SBP) is a high volume, low value by-product from sugar beet processing with a low lignin and a high carbohydrate content, making it an attractive biomass feedstock for biorefinery processing. The pectin fraction of SBP can be isolated via steam explosion, which, after complete acid hydrolysis, gives a hydrolysate rich in monosaccharides: primarily L-arabinose (Ara) and D-galacturonic acid (GA), with some D-galactose (Gal) and L-rhamnose (Rha). Isolation of these sugars is therefore a critical step in realising an integrated, whole crop biorefinery. Currently, little work has been reported on the separation and utilisation of SBP hydrolysates.

The aim of this thesis is to establish novel, scalable separation processes for the isolation of the component monosaccharides from crude hydrolysed sugar beet pulp pectin.

Centrifugal partition chromatography (CPC) is a liquid-liquid separation technique with no solid stationary phase and offers an alternative to traditional resin-based chromatographic techniques. As such it can more easily cope with crude feedstreams such as hydrolysates. Hydrophilic ethanol : ammonium sulphate two-phase systems were examined based on monosaccharide partition coefficients and phase settling times. An ethanol : aqueous ammonium sulphate (300 g L^{-1}) (0.8:1.8 v:v) system was chosen for CPC separations of the crude SBP hydrolysate and was shown to be capable of removing the coloured contaminants and isolating three sugar fractions in a single step: Rha, Ara and Gal, and GA. The separation was optimised and the throughput was increased by maximising the sample loading. Operation in an elution-extrusion mode allowed for reproducible separations in 100 min without additional column regeneration. The process was scaled up from a 250 to a 950 mL column providing a final throughput of 1.9 $g_{monosaccharides}$ L^{-1}_{column} h^{-1} using the crude SBP. The following purities and recoveries of the three main fractions were achieved: Rha at 92% purity

and 93% recovery; Ara at 84% purity and 97% recovery; and GA at 96% purity and 95% recovery.

Simulated moving bed (SMB) allows for continuous chromatographic separations using multiple columns, improving separation performance and throughputs. Isolation of Ara from the neutral sugars Gal and Rha was performed with resins and conditions screened on single columns leading to the selection of a Dowex 50W X8 resin in the Ca^{2+} form. SMB separation using 8 columns was performed in the 4-zone and 3-zone setups and achieved 94% purity with 99% recovery at a throughput of 4.6 $g_{monosaccharides}$ L^{-1}_{column} h^{-1} with a synthetic mixture of the neutral sugars (Ara, Gal and Rha). However, equivalent separations could not be achieved using the crude SBP hydrolysate which needed pretreatment before SMB.

Decolourisation with activated carbon was able to remove 97% of the coloured contaminants with sugar losses of 15% (w/w) in a batch process demonstrated to 50 mL scale. Anion exchange chromatography using a Dowex 1x8 resin was then found to be capable of isolating GA from a synthetic crude mixture of GA and neutral sugars with a dynamic binding capacity of 1.31 mmol mL^{-1}_{resin}. However, further work is needed to enable this anion exchange step to achieve satisfactory separations with the decolourised crude hydrolysate. The isolated neutral sugars, after GA removal, can be processed on the SMB with comparable separation performance and throughput to a mixture of neutral sugars prepared without GA.

In summary, this thesis presents two possible process paths each with their own benefits and drawbacks. CPC is capable of processing the crude SBP hydrolysate directly, isolating the sugars and removing the coloured contaminants in a single step. However, Ara co-elutes with Gal providing a stream that is only 84% pure. In SMB, the potential throughputs and separation performance are higher, however, this could only be experimentally demonstrated with synthetic crude mixtures of sugars and not with the crude SBP hydrolysate. Further pretreatment or SMB method development would be required in order to process the crude hydrolysate, and the resulting multistep processes may reduce the overall viability. Overall this thesis demonstrates two feasible approaches to the preparative scale separation of SBP pectin hydrolysates and supports development of an integrated SBP biorefinery.

Impact Statement

Biorefineries convert biomass into a range of added-value chemicals and products such as bioethanol. However, there often remains a portion of the crop which is underexploited with high potential for upgrading. A major hurdle in the further development of these processes is the isolation of the main components from these by-products. The work presented in this thesis provides two scalable separation methods for the isolation of monosaccharides, a key building block in many biorefinery feedstreams. While hydrolysates from sugar beet pulp are examined, the impact is applicable to a wide range of biomass sources and hydrolysates.

Traditionally, monosaccharide separations have been performed on cleaner feedstreams such as sugar juices. Hydrolysates tend to contain more contaminants and the presence of D-galacturonic acid as a major target compound further complicates pretreatment. The process options presented explore different methods of dealing with these contaminants as well as two different separation methods. This thesis thus provides additional options for the processing of biomass by-products and hydrolysates.

Overall, the work in this thesis will help towards the development of whole crop biorefineries by providing additional applications for biomass by-products and hydrolysates.

Acknowledgements

Firstly, I must thank my supervisor, Professor Gary Lye, for giving me the opportunity to undertake this PhD and for his continuous support and encouragement throughout. I gratefully acknowledge the financial support from the EPSRC.

I would like to thank Max Cárdenas-Fernández for his considerable assistance, particularly in my first year, in the progression of my laboratory skills and personal development as a researcher.

A special thanks must be given both to AB Sugar, for providing the sugar beet group with the sugar beet pulp for this and related projects, and to Charlotte Hamley-Bennett from the University of Bath for the steady supply of the steam exploded hydrolysed sugar beet pulp pectin used in this thesis.

My thanks also go to Svetlana Ignatova and Peter Hewitson from Brunel University for their invaluable expertise in countercurrent separations and for allowing me the use of the Advanced Bioprocessing Centre.

At GSK, I must firstly thank Nathalie Douillet and Joe Adams for letting me use your labs and equipment at Stevenage, but also Alba Díaz-Rodríguez and Bruce Stevenson for all their help and support day to day.

Additionally, I thank Laszlo Nemeth and Laszlo Lorantfy and the team at RotaChrom for their hospitality in Hungary and giving me the time and opportunity to use your industrial scale CPC machine.

I thank my parents for their endless support and everyone I've met along the way for the good times.

My final thanks go to my fiancée Courtney for her unwavering support, encouragement and love throughout. Thank you, I couldn't have got this far without you.

Table of contents

List of Figures

List of Tables

Nomenclature and abbreviations

Nomenclature

$BV_{0\%}$	Breakthrough volume (initial breakthrough)	mL
$BV_{10\%}$	Breakthrough volume (10% breakthrough)	mL
$BV_{100\%}$	Breakthrough volume (complete breakthrough)	mL
C_{ads}	Concentration adsorbed to resin	mg mL^{-1}
C_D	Column diameter	cm
C_F	Concentration in the feed	mg mL^{-1}
C_L	Column length	cm
C_{liq}	Concentration in liquid phase	mg mL^{-1}
C_{LP}	Concentration in the lower phase	mg mL^{-1}
C_M	Concentration in the mobile phase	mg mL^{-1}
C_S	Concentration in the stationary phase	mg mL^{-1}
C_{UP}	Concentration in the upper phase	mg mL^{-1}
$DBC_{0\%}$	Dynamic binding capacity at initial breakthrough	mmol g^{-1}
$DBC_{10\%}$	Dynamic binding capacity at 10% breakthrough	mmol g^{-1}
H_i	Henry constant of component i	-
$k^R{}_i$	Retention factor of component i	-
$k^{R'}{}_i$	Adjusted retention factor of component i	-
K_i	Partition coefficient of component i	-
$K_{LP/UP}$	Partition coefficient (lower phase over upper phase)	-
$\dot{m}_i$	Mass flow rate of component i	mg min^{-1}
m_n	Flow rate ratio in zone n	-
m_{resin}	Mass of resin	g
P_q	Backpressure on pump q	psi
Q	Flow rate	mL min^{-1}
Q_D	Desorbent flow rate	mL min^{-1}
Q_E	Extract flow rate	mL min^{-1}
Q_F	Feed flow rate	mL min^{-1}
Q_n	Flow rate in zone n	mL min^{-1}
Q_{Raf}	Raffinate flow rate	mL min^{-1}
Q_{Rec}	Recycle flow rate	mL min^{-1}
RSD	Relative standard deviation	-
S_F	Stationary phase retention	%

t_0	Void retention time	min
t'_0	Adjusted void retention time	min
t_i	Retention time of component i	min
t'_i	Adjusted retention time of component i	min
T_S	Valve switch time	min
V_C	Column volume	mL
V_D	Dead volume	mL
V_E	Elution volume	mL
V_I	Injection volume	mL
V_S	Volume of stationary phase	mL
$V_{S\text{-eluted}}$	Volume of stationary phase eluted from the column	mL
α^R	Selectivity	-
$\alpha^{R'}$	Adjusted selectivity	-
α_i	Separation factor of component i	-
ε	Void fraction	-
σ	Population standard deviation	-
μ	Mean	-

Abbreviations

ACN	Acetonitrile
AFEX	Ammonia fibre explosion
Ara	L-arabinose
AS	Ammonium sulphate
ATPS	Aqueous two-phase systems
BD	Blue dextran
BuOH	n-butanol
CCC	Countercurrent chromatography
CCS	Countercurrent separations
ChMWat	Chloroform : methanol : water
CPC	Centrifugal partition chromatography
DBC	Dynamic binding capacity
DMSO	Dimethyl sulfoxide
EBuWat	Ethyl acetate : butanol : water
EtOH	Ethanol
G.U.E.S.S	Generally useful estimation of solvent systems
GA	D-galacturonic acid
Gal	D-galactose
Glu	D-glucose
HEMWat	Hexane : ethyl acetate : methanol : water
HMF	Hydroxymethyl furfural
HPAEC	High performance anion exchange chromatography
HPLC	High performance liquid chromatography
HPLC-RI	High performance liquid chromatography with refractive index detection
HSCCC	Highspeed countercurrent chromatography
ICS	Ion chromatography system
LP	Lower phase
LP-Disp	Lower phase with displacer
MeOH	Methanol
MW	Molecular weight
NaOAc	Sodium acetate
N.D.	Not determined
PEG	Polyethylene glycol
PrOH	Propanol

RCF	Relative centrifugal force
Rha	L-rhamnose
RI	Refractive index
RT	Room temperature
SBP	Sugar beet pulp
SMB	Simulated moving bed
SMCC	Sequential multicolumn chromatography
TFA	Trifluoroacetic acid
THF	Tetrahydrofuran
TMB	True moving bed
UP	Upper phase
UP-Exch	Upper phase with exchanger
v/v	Volume per volume
v:v	Volume ratio
w/v	Weight per volume
w/w	Weight per weight
Xyl	D-xylose

Chapter 1 Introduction

1.1 Sugar beet pulp as a renewable feedstock for biorefinery applications

1.1.1 Sustainable chemical feedstocks

Biomass is increasingly being used for the production of biofuels and chemicals as a result of volatility in oil price and availability, a desire for energy independence, and a need to reduce greenhouse gas emissions from fossil fuels [1]. Utilising biomass for the sustainable production of added value chemical and pharmaceutical intermediates could provide economic advantages to biorefineries, while working towards the concept of a whole crop biorefinery, as well improving the sustainability of industries currently reliant on petrochemical derived feedstocks.

Lignocellulosic biomass is available cheaply and abundantly from a number of sources from both agricultural residues and waste by-products such as wheat straw, corn stover, sugarcane bagasse and sugar beet pulp (SBP) [2]. These biomass feedstocks comprise a number of biological polymers in varying proportions: cellulose, made up of polymeric D-glucose; hemicellulose, a polymer made up of other sugars such as D-xylose and D-mannose; pectin, a polymeric D-galacturonic acid (GA) backbone with neutral sugar side chains containing sugars such as L-arabinose (Ara), D-galactose (Gal) and L-rhamnose (Rha); and lignin, a polymer of phenolic and other aromatic compounds [2]. The isolation of the sugars or aromatics from these polymers allows for conversion into a number of products [3] as discussed in Section 1.1.6.

Considerable progress has been made towards the production of bioethanol from biomass by-products such as wheat straw and commercial biorefineries are currently producing bioethanol on an industrial scale [4]. However, there remains a large amount of other lignocellulosic material that may be unsuitable for bioethanol production still being used for animal feed, such as SBP, that has potential for the production of value-added chemicals within the context of a whole crop biorefinery [5].

1.1.2 Sugar beet pulp as a renewable feedstock

Over 8 million tonnes of sugar beet are grown annually in the UK and SBP is a significant by-product product from beet processing. The Wissington Factory, operated by AB Sugar, processes sugar beet in an already highly integrated process as shown in Figure 1-1. It produces sugar products, primarily sucrose; bioethanol, betaine and vinasse from sugar side streams; topsoil and stones, cleaned from the sugar beet; and even tomatoes, utilising the low-grade heat from the onsite combined heat and power plant.

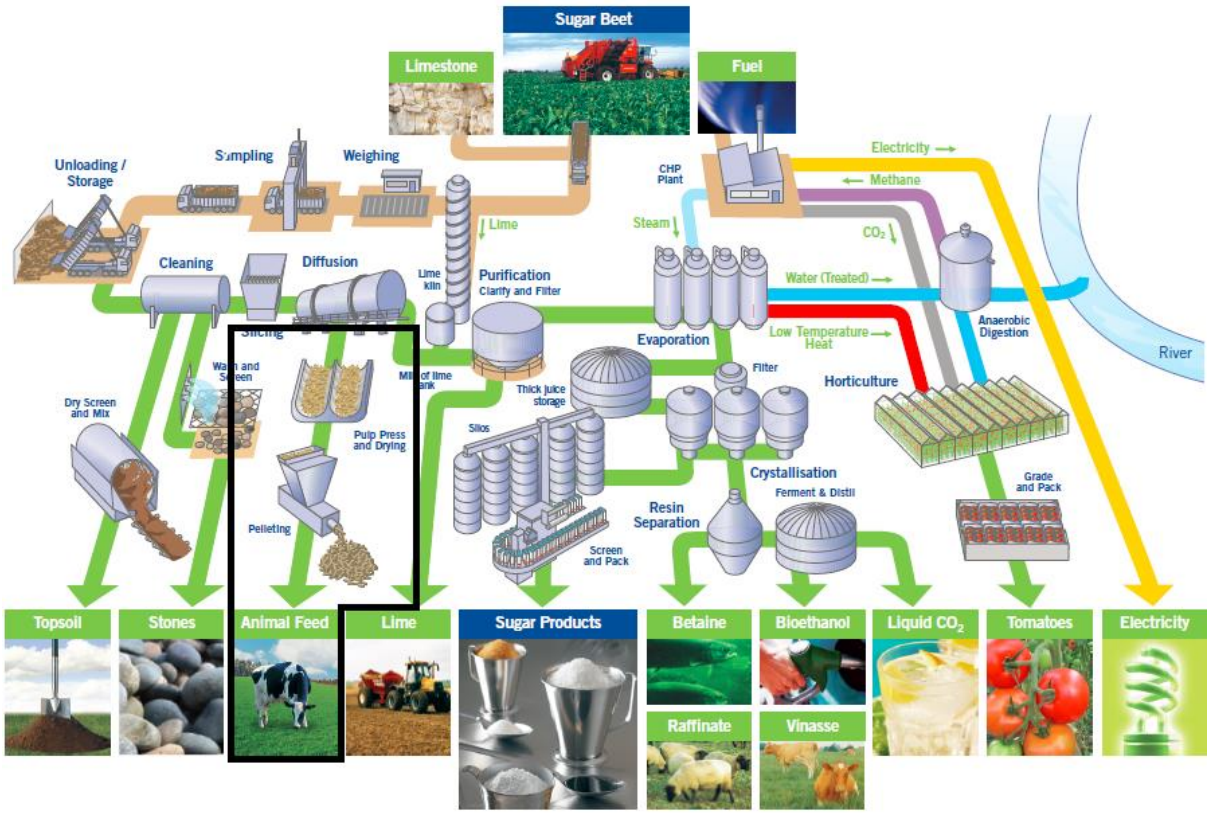

Figure 1-1: Sugar beet processing at AB Sugar's Wissington Factory – modified from graphic provided by AB Sugar. The highlighted black box represents the current processing method for the conversion of sugar beet pulp to animal feed.

Sucrose is isolated from sugar beet in a hot water extraction step known as diffusion. After pressing to remove more of the sucrose, the remaining solids, the sugar beet pulp, is dried and pelleted before being sold as animal feed [6]. This process is highlighted in Figure 1-1. The SBP is still a rich source of carbohydrates, consisting primarily of cellulose, polymeric Glu; and sugar beet pectin, a polymeric GA backbone with side chains of Ara and Gal [7]. It has a reported total carbohydrate content of up to 85%

(w/w, dry basis) and a very low lignin content of 1-2% (w/w, dry basis) [6]. Figure 1-2 shows the overall composition of sugar beet pulp as calculated by Micard et al. [7], showing a total carbohydrate content of ~72%. It shows almost equal amounts of Ara, GA and Glu with lesser amounts of Gal, Rha and Xyl. The Glu was found to be entirely present in the cellulose [7] and so could potentially be isolated during initial hydrolysis of the SBP. The "other" portion in Figure 1-1 contains a number of components, including methanol, acetic acid, ash and lignin.

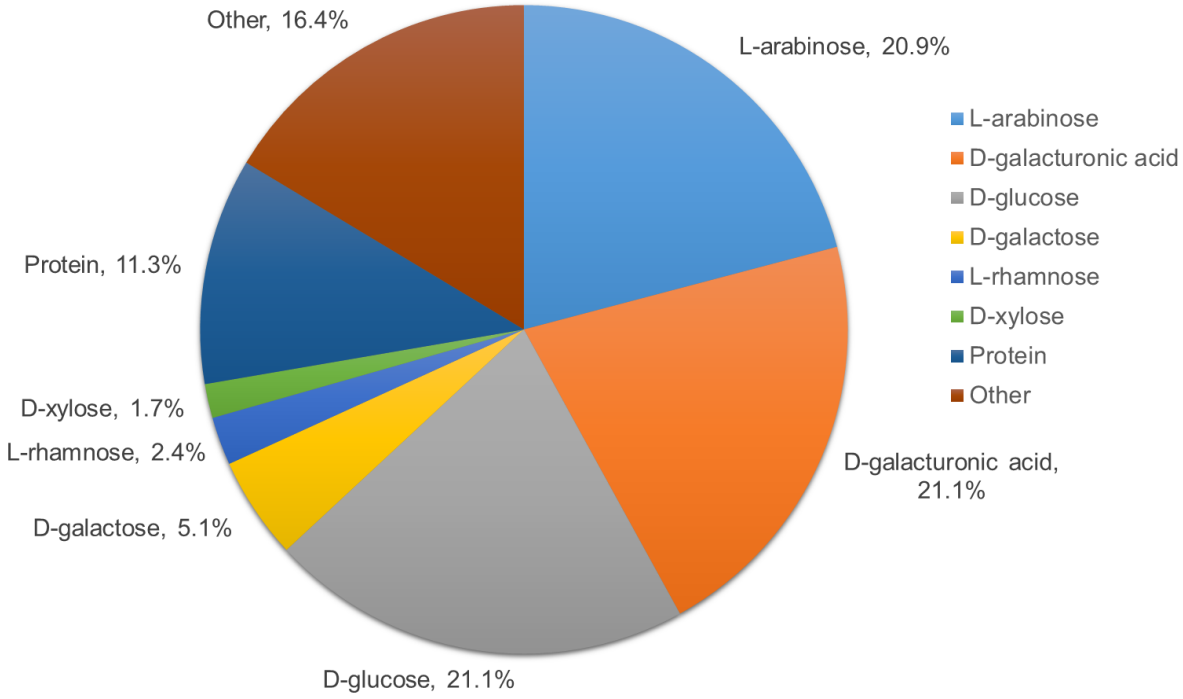

Figure 1-2: Total composition of sugar beet pulp. Data taken from Micard et al. [7].

Adding value to this SBP process stream to produce sustainable chemical feedstocks can be realised through a chemical processing route outlined in Figure 1-3. Hydrolysis involves methods of breaking down the SBP into the constituent sugars and is discussed in Section 1.1.4. The separation stage will be the emphasis of this thesis, focussing on the isolation of the component monosaccharides and removing any crude contaminants remaining after the hydrolysis steps. Synthetic applications of the isolated sugars are discussed in Section 1.1.6. The overall aim and objectives are detailed in Section 1.7.

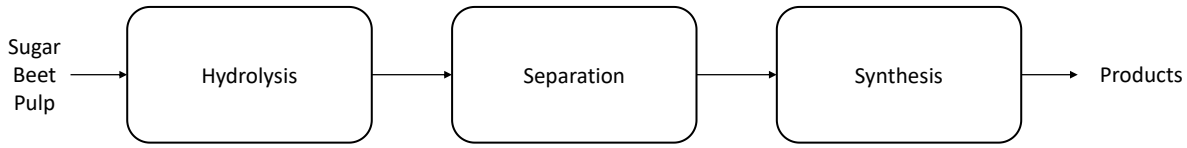

Figure 1-3: Schematic process overview for producing sustainable chemical feedstocks from sugar beet pulp.

1.1.3 Biomass hydrolysis methods

Hydrolysis of biomass has a critically important role in the production of bioethanol and other products from lignocellulosic feedstocks. The primary goal is to hydrolyse the biomass into the component monosaccharides, usually for fermentation into products such as ethanol or butanol, without producing too many toxic degradation products [8]. Methods of hydrolysing the biomass fall into three categories: physical, chemical or biological hydrolysis [9].

Physical hydrolysis breaks down the biomass without further addition of chemicals, such as steam explosion and liquid hot water treatment. Steam explosion uses high pressure steam followed by explosive decompression to hydrolyse the polymers [10]. Liquid hot water treatment is similar to steam explosion but uses pressurised water in the liquid phase at a lower temperature to reduce the amount of degradation products formed [10]. Steam explosion and liquid hot water treatment act primarily on hemicellulose, pectin and lignin, solubilising them and leaving the cellulose as a solid phase for easier isolation and further processing [8]. The hydrolysis releases acidic groups, such as GA, which leads to further catalysis of the hydrolysis and the formation of degradation products [9] although they tend to be lower than for chemical methods.

Chemical methods include dilute acid hydrolysis, acid catalysed steam explosion, ammonia fibre explosion, and alkaline hydrolysis. Dilute acid hydrolysis uses a strong acid such as sulphuric acid at concentrations of <4% (w/w) to hydrolyse the polysaccharides. Its use for hydrolysing biomass is well researched. It is effective at hydrolysing both hemicellulose and cellulose at different severity levels, however, it is more likely to produce degradation products and fermentation inhibitors [10] and can cost more than physical methods due to the reagents needed and the additional treatment required to remove the neutralised salts [9]. Catalysed steam explosion employs steam explosion with the addition of an acid to catalyse the hydrolysis. This

results in the increased hydrolysis of hemicellulose but also an increase in the amount of degradation products formed [9]. Ammonia fibre explosion (AFEX) is very similar but uses added liquid ammonia instead of acid. It is less effective for lignin removal but provides a nitrogen source for subsequent fermentation [8]. Alkaline hydrolysis is effective at removing lignin and solubilising hemicellulose. Furthermore it can operate at much milder conditions, or even ambient, however, the hydrolysis time is considerably longer than other methods, often lasting hours or days [9].

Biological hydrolysis utilises enzymes or microorganisms such as fungi or bacteria, to degrade the biomass. Enzymes allow for the breakage of specific polymer bonds, however, accessibility of enzymes to the polysaccharides can dramatically effect hydrolysis rates and so enzyme treatments are sometimes performed after a physical or chemical hydrolysis [2]. It is also possible to use microorganisms such as white rot fungi to selectively degrade lignin however, these methods can be limited by extended operating times [2].

1.1.4 Hydrolysis of sugar beet pulp

A number of different hydrolysis methods have been applied to sugar beet pulp to isolate the component sugars. In general, milder methods than for other biomass sources are required due to the lower lignin content and easier accessibility of the polysaccharides. It is possible to directly use enzyme preparations in order to selectively hydrolyse the sugars using pectinase [7][11] or arabinase [12]. Zheng et al. used cellulases and pectinases to fully hydrolyse all of the polysaccharides in a simultaneous enzyme saccharification and fermentation into ethanol [6]. Dilute acid hydrolysis has also been used, either as a sole hydrolysis method [13] or prior to complete enzyme hydrolysis [14][15], for ethanol fermentation. A modified AFEX process has been used for SBP hydrolysis, followed by complete hydrolysis using cellulases and pectinases, however, it only benefitted enzymatic hydrolysis of cellulose and not pectin [16].

Finally, steam explosion has been used effectively by Hamley-Bennett et al. to solubilise the pectin without the addition of enzymes, acids or ammonia, while leaving the cellulose intact [17]. This allowed for a simple solid-liquid separation to obtain

cellulose for ethanol fermentation and pectin for further processing. While it may be possible to selectively, enzymatically hydrolyse the solubilised pectin and separate the monosaccharides from the remaining polymer, it will still require some form of ultrafiltration. It is noted by Kuhnel et al. that enzymatic methods may provide efficient hydrolysis of the sugars but current methods are not feasible due to the costs and amounts of the enzymes required [14]. Dilute sulphuric acid hydrolysis can fully hydrolyse the pectin into monomeric sugars and so the method proposed by Hamley-Bennett et al. can provide a selective removal of cellulose as well as full hydrolysis of the pectin into monomeric sugars. However, there will be more degradation products produced than in an enzymatic hydrolysis step and these could cause further downstream processing difficulties. These degradation products are discussed in Section 1.1.5 and often require further treatment such as decolourisation (discussed in Section 1.3) before the hydrolysate can be used for synthetic applications.

The work in this thesis will focus on the separation of the monosaccharides present in this crude SBP pectin fraction after steam explosion and full acid hydrolysis, provided by Bath University (for a photograph of the material see Figure 2-1). This will be referred to throughout this work as “crude hydrolysate”. It contains a number of monosaccharides, primarily Ara and GA; lesser amounts of Gal, Rha and Glu; and a number of degradation products, discussed in Section 1.1.5. The pyranose ring structures of the four main monosaccharides present in the crude (Ara, Rha, Gal and GA) are shown in Figure 1-4.

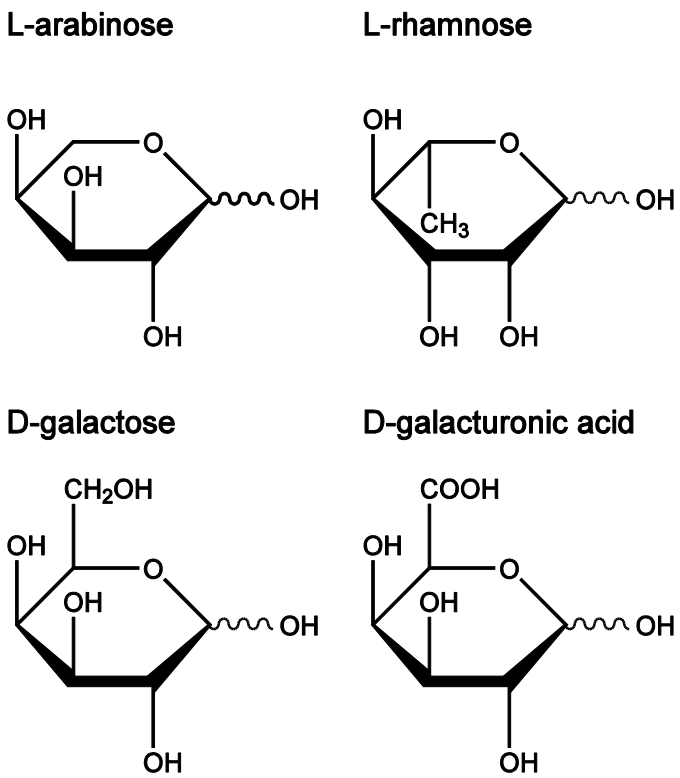

Figure 1-4: Pyranose ring structures of the main monosaccharides present in the SBP pectin crude hydrolysate.

1.1.5 Degradation products

While a hot acidic environment is effective at hydrolysing polymeric sugars, it can also degrade those sugars into other products. For example, a number of products can be produced from the acid-catalysed degradation of a single sugar, fructose, including furans, such as furfural, as well as formic acid and acetic acid [18]. Ara and GA are the primary sugars in SBP and both are known to form browning products under heated acidic conditions [19], however, the reactions involved are complex and produce a wide variety of compounds and, so, characterisation is difficult [20]. GA is known to undergo decarboxylation to Ara and thus produce similar degradation products, however, most of the GA does not follow this pathway and produces other colour precursors and different predicted coloured compounds [21]. Furthermore the presence of amino acids leads to additional browning products such as pyrroles [20][22]. Amino acids could be present in crude hydrolysed SBP due to the hydrolysis of any protein present.

Both Zheng et al. [15] and Kuhnel et al. [14] found the presence of furfural and hydroxymethylfurfural (HMF) in dilute acid treated SBP hydrolysate, however, Zheng

et al. noted that furfural and HMF yields were significantly reduced under milder conditions. Hamley-Bennett et al. could not detect furfural or HMF in the acid hydrolysed SBP pectin (crude hydrolysate), as will be used here, after steam explosion [17].

The hydrolysis step can also release non-sugar products into the liquid phase. In SBP, acetic acid, methanol and ferulic acid can be formed during hydrolysis from the de-esterification of the pectin due to the presence of acetyl, methyl and feruloyl esters [14].

Phenolic compounds can also be released due to the degradation of lignin during the hydrolysis step [23]. However, this may be limited relative to other lignocellulosic feedstocks due to the low lignin content in SBP, as discussed in Section 1.1.2.

The crude used in this thesis, described in Section 1.1.4, is dark in colour, indicating that, although there is no detectable furfural, HMF or acetic acid, there are browning products from the sugars present in the pectin. It is also possible it contains some methanol and ferulic acid, from deesterification during the hydrolysis process; and sulphates, from the sulphuric acid used for hydrolysis and the subsequent neutralisation. Full characterisation of the browning and degradation products formed is beyond the scope of this thesis. Methods of decolourisation and removal of degradation products is discussed in Section 1.3.

1.1.6 Separation targets and applications

The crude hydrolysate used in this thesis, contains a number of monosaccharides: Rha, Glu, Gal, Ara and GA, as described in Section 1.1.4, as well as a number of unknown contaminants, discussed in Section 1.1.5. The overarching separation targets are the isolation of GA and Ara, as the two primary monosaccharides in SBP pectin, from the remaining sugars and from any other contaminants. The potential applications of Ara and GA are discussed below.

Bioethanol is an established, high volume, product that can be produced from almost all biomass hydrolysates [3], however the fermentation of ethanol from Ara remains difficult [24] and, although it is improving with engineered strains [25], the metabolic

pathway involved is more complex than for using D-xylose or D-glucose [26] limiting its potential. GA cannot be fermented into ethanol by yeasts [14] although it is possible using engineered bacterial strains [27].

The possibility to produce higher value products from both Ara and GA, avoiding the associated limitations of bioethanol production, represents an important factor in developing SBP as a renewable feedstock for biorefinery applications. Oxidised sugars, such as GA, have been highlighted as important building blocks from biomass for the production of hyperbranched polyesters and plasticisers [28]. It has also been used to produce adipic acid, a precursor to nylon-6,6 [29]. Ara can be used to produce biopolymers [30] or reduced to arabinitol, listed as an important value added chemical from biomass, for the production of unsaturated polyester resins [28]. Recent work has examined biocatalytic approaches to producing products from sugars from biomass. For example, Ara can be upgraded using transketolase to produce L-gluco-heptulose, which has potential therapeutic applications [31].

1.2 Countercurrent separations

1.2.1 Countercurrent separations

Countercurrent separations (CCS) are a range of liquid-liquid separation techniques which utilise the partitioning of dissolved solutes between two immiscible liquids in order to separate them. The process holds one of the phases stationary with the aid of a centrifugal field and flows the other (mobile) phase past it. The phases repeatedly mix and settle allowing the solutes to partition between the phases; the more the solute partitions into the stationary phase the slower it elutes through the column. CCS is similar to partition chromatography, except the stationary liquid phase is retained through centrifugal force rather than on a solid support. CCS can also be thought of as a method of sequential liquid-liquid extraction.

CCS overcome many of the disadvantages associated with solid-liquid chromatography systems. The most important difference is the use of a liquid stationary phase and the lack of a solid support. Some advantages of the liquid stationary phase are outlined below:

- The system is much more robust than systems such as resin-based chromatography: contaminants, unreacted compounds and ions are generally tolerable, passing through, dissolved or in suspension, without damaging or clogging the column [32].
- Recovery of the product can reach as high as 100%. Solutes strongly retained in the stationary phase can be recovered simply by extruding, or pumping out, that phase from the column [33].
- Sample loading can be up to 10-30% of the column volume, much higher than for preparative, resin-based chromatography, as a result of the high fraction of the column that is stationary phase rather than solid support [34].
- Elution profiles are both predictable and reproducible as no irreversible binding or denaturation occurs in the column [34] and separation occurs through partitioning alone [35]. This also means that there is no permanent damage to the stationary phase and fresh stationary phase can be used every time. Furthermore, column packing is not a concern, the column is filled by simply pumping the stationary phase.

1.2.2 Types of CCS

There are two major categories of CCS machines, differing in the way that they retain the stationary phase. Countercurrent chromatography (CCC) utilises a continuous tube coiled around a rotating bobbin on a coil planet centrifuge. This is an example of a hydrodynamic CCS device, where, if the flow stops, the upper phase will "rise" to one end of the column while the lower phase will "fall" to the other end.

The coil planet centrifuge has a multitude of configurations, the most popular of which is the type-J coil planet centrifuge (referred to as HSCCC). This involves a column wound around a bobbin and rotating around its own axis on a “planet” gear which is, in turn, revolving around a stationary “sun” gear to provide two rotational fields. As the bobbin rotates and revolves with the same angular velocity, such that one “day” (bobbin rotation) is equal to one “year” (bobbin revolution), the motion is described as synchronous [36]. Figure 1-5 shows the two gears and axes of rotation and revolution.

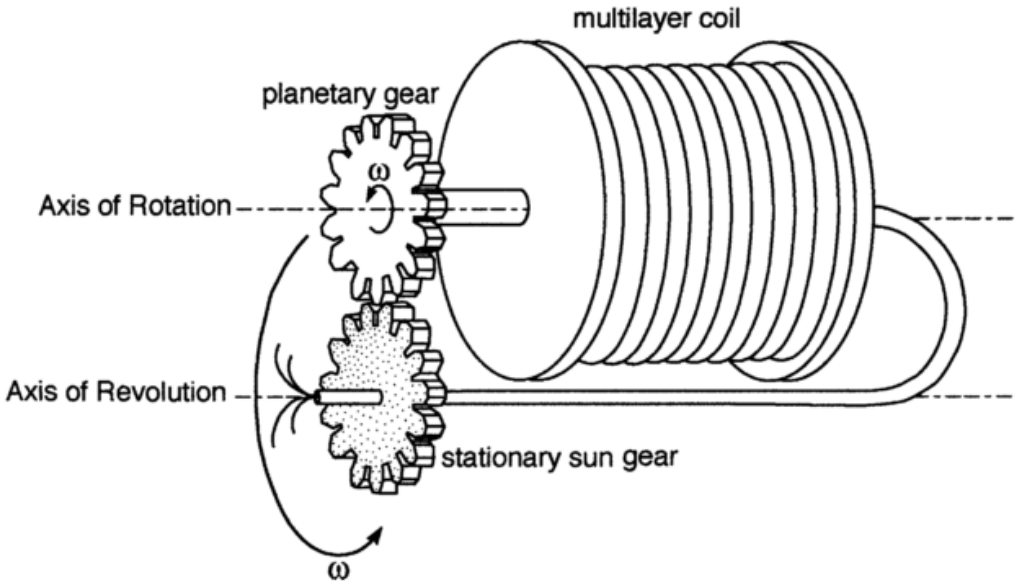

Figure 1-5: Type-J planetary motion with a multilayer coil. The angular velocities (ω) of the stationary sun gear and the planetary gear are the same, giving synchronous motion. From [37].

Synchronous planetary motion allows for continuous rotation, and therefore continuous elution through the column without the use of rotary seals, preventing leakage, corrosion and contamination [38]. CCC is operationally robust and scalable [39] and able to generate stationary phase retentions of greater than 95% in some instances [40]. The stationary phase retention is a key characteristic of CCS performance and represents the percentage of the column which is stationary phase. Stationary phase retention is discussed in detail in Section 1.2.3.3.

While older HSCCC machines needed a counterweight, newer ones simply operate with two bobbins opposite each other connected in series, eliminating the need to balance the system. Column geometry is also important to the performance, each with different mixing and retention patterns. The multilayer coil is the most common geometry but toroidal and spiral columns are sometimes used, offering improved mixing and retention of more difficult, polar phase systems [41].

The alternative to CCC is a hydrostatic device, termed centrifugal partition chromatography (CPC). In this instance, a single rotational axis is used with the flow path made up of twin cells to retain the stationary phase with interconnecting channels on a disk (Figure 1-6). The twin cell geometry has been shown to improve the

stationary phase retention [42]. Multiple disks are stacked on top of each other to form the column, with gaskets in between. The flow path is such that stopping the flow does not affect the distribution of stationary phase throughout the column. Mass transfer is a result of cascade mixing as the mobile phase cascades through the stationary phase in each cell [43]. The number of partition steps is equal to the number of cells and a single axis of rotation provides a constant centrifugal field [44].

There are two possible operating directions, or modes: ascending and descending (Figure 1-7). In the ‘ascending’ mode, the heavier phase acts as the stationary phase and the mobile phase is fed from the bottom where it ascends to the top of the column. In this mode the mobile phase flows against the direction of the centrifugal force within each cell. In the ‘descending’ mode, the lighter phase acts as the stationary phase and the mobile phase is fed from the top where it descends to the bottom of the column. In this mode the mobile phase flows in the direction of the centrifugal force within each cell.

Figure 1-6: Individual disk (~6.7 cm radius) from an Armen CPC machine (Vannes, France) featuring a twin cell design.

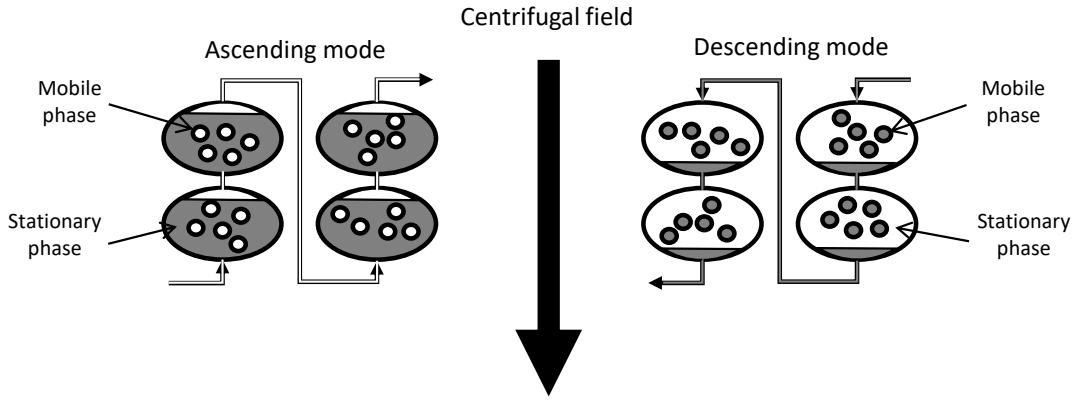

Figure 1-7: Schematic showing the ascending and descending CPC modes with the mobile flow direction relative to the centrifugal field.

The hydrostatic nature of CPC can assist in the retention of the stationary phase, particularly for systems which are difficult to retain such as highly polar two-phase systems [35]. CPC also suffers less when the hydrodynamic equilibrium is briefly disrupted, e.g. by changes in rotational speed, however, rotary seals are required, which can be prone to leaking and require frequent replacement. Furthermore, the narrow interconnecting channels make it more sensitive to disruption or blocking from solids or precipitate [35]. As a hydrostatic device, the CPC builds hydrostatic pressure

throughout the column, and the use of rotary seals limits the maximum pressure drop to around 80 bar [45] which can lead to practical limitations of flow rate and rotational speed. CPC performance is also more dependent on the hydrodynamics of mixing in the cells [46]; although, its ability to retain the stationary phase, particularly for highly polar phase systems, makes it a promising candidate for the separation of hydrophilic compounds such as sugars. The rest of this section will therefore focus on CPC, although, the majority of the concepts discussed are applicable to CCS in general, including hydrodynamic CCC.

1.2.3 CPC operational considerations

1.2.3.1 Phase system

As CCS is a liquid-liquid separation technique, it utilises two immiscible phases (the phase system) and the difference in partitioning of solutes between them to perform separation. The phase system consists of a stationary phase and a mobile phase, which can be alternated by switching the flow direction. The mobile phase, like in other chromatography techniques, carries the injected sample through the column. The stationary phase, retained by centrifugal forces, slows down the solutes at different rates dependent on the ratio at which the components partition between the stationary and mobile phases (the partition coefficient – see Section 1.2.3.2). The phase systems that can be used for CCS have essentially no limitations beyond the requirement that they form two phases. The phase systems need not be limited to two components but frequently utilises three, four or even five solvents [47]. Furthermore, phase systems are not restricted to pure solvents and can incorporate salts and other additives in order to enhance or fine-tune the properties of the phase systems e.g. solute partition coefficient [46].

This is one of the most powerful advantages of CCS: an unlimited number of potential phase systems and a wide scope to fine tune the composition to optimise performance. In solid-liquid chromatography the solid phase is generally not easily modified meaning that optimisation is restricted to the mobile phase [48]; this further illustrates the advantage of CCS where both phases can be fine-tuned. Selecting an appropriate phase system in CCS is thus analogous to selecting both the column and the mobile

phase simultaneously in solid-liquid chromatography [48], and can be the most time consuming part of developing a CCS separation method [37].

Ito outlined four main requirements for any phase system [37]:

1. Solutes must be stable and soluble in both phases;
2. A two-phase system should form with similar volume ratios to avoid wastage;
3. Suitable partition coefficients should be achieved for the solutes;
4. Satisfactory stationary phase retention should be attainable.

Point 1 is a standard requirement for any phase system. Degradation of compounds or poor solubility in the phase system will hinder the performance of any separation process. Point 2 requires the ratio of volumes in the upper and lower phases to be similar. While not a strict requirement, this can assist in the amount of solvent wasted by not producing too much of one phase in order to form enough of the other. This requirement can be neglected if the phases can be made up independently. Points 3 and 4 are more subjective in what defines a suitable partition coefficient and a satisfactory stationary phase retention and will be discussed in Section 1.2.3.2 and 1.2.3.3 respectively.

1.2.3.2 Partition Coefficients and Separation Factors

The partition coefficient (K) is probably the most important parameter for any CPC separation. It is defined as the concentration ratio of a solute between the two phases at equilibrium. Convention in CPC literature is to use the ratio of concentration in the stationary phase (C_S) to the concentration in the mobile phase (C_M) (Equation 1-1). Importantly, it also gives an indication of when a solute will elute from the column.

$$K = \frac{C_S}{C_M} \qquad \textbf{Equation 1-1}$$

A partition coefficient of K = 1 indicates an even concentration distribution between the two phases and is considered to be the best partition coefficient for separating a target compound with an optimal resolution [49]. Solutes with higher partition coefficients are retained more by the stationary phase, taking longer to elute and giving broader peaks, while those with lower partition coefficients are less retained in the

stationary phase, eluting quickly through the column with peaks getting closer together [50].

Partition coefficients are entirely independent of the CPC device, dependent only on the phase system and the solute. They can easily be determined in a simple shake flask method by adding a solute to a two-phase system, vigorously mixing the two phases two ensure equilibrium and allowing to settle [51]. The concentration of solute in each phase can then be analytically measured by any means (TLC, spectroscopy, HPLC etc.).

Generally, it is preferable to operate such that $K<1$ so that the solute partitions more into the mobile phase, thus eluting more quickly, resulting in shorter elution times, higher product concentrations and reduced solvent usage. The partition coefficients are thus generally used to determine the operating mode (ascending or descending), i.e. which phase operates as the stationary phase and which as the mobile phase (see Figure 1-7). Switching the operating mode will entirely reverse the elution order about the point $K=1$, with each compounds partition coefficient becoming the reciprocal of its original value.

Although aiming for a partition coefficient of close to 1 is generally accepted as good practice, there is little consensus on any upper or lower limit on this value to achieve a suitable separation and recommendations generally stem from personal experience. Friesen and Pauli recommended a “sweet spot” range of between $0.4 < K < 2.5$ [50] in 2005 while Ito recommended a partition coefficient of between $0.5 < K < 1$ [37] in the same year, with the stationary and mobile phases reversed if necessary to ensure partition coefficients below 1. In a 2008 review of CCS, it was found that over half of separations took place within the range $0.5 < K < 2$ while over 85% were in the range $0.25 < K < 4$ [35].

It is not enough to make sure that all the relevant solutes have partition coefficients in the "sweet spot"; if two solutes have very similar partition coefficients, they will co-elute and not be separated. The separation factor (α) demonstrates this chromatographic selectivity. Defined as the ratio of the partition coefficients of the two solutes (Equation 1-2), the separation factor is recommended to be greater than

1.5 in order to provide good resolution between solutes [37]. Although, resolution is ultimately dependent on the stationary phase retention achievable (Section 1.2.3.3), and so is phase system and device dependent.

$$\alpha = \frac{K_1}{K_2} \qquad \textbf{Equation 1-2}$$

1.2.3.3 Stationary phase retention

In CPC, the stationary phase is a liquid and not retained by a solid support but by the centrifugal force and the cell geometry [52]. The amount of stationary phase that can be retained in the column is vital to separation performance. Broadly speaking, the greater the stationary phase retention, the greater the contact with the mobile phase, and thus improvements in partitioning and separation are achieved (as shown in Figure 1-8); although, hydrodynamics and mixing within the cells is also important [53]. While Figure 1-8 uses data from a CCC separation, the same principle holds in CPC. Additionally, Figure 1-8 demonstrates how the column volume marks a centre point for the separation (compounds with K>1 will elute after this point, and compounds with K<1 will elute before this point), and how peak width increases retention volume.

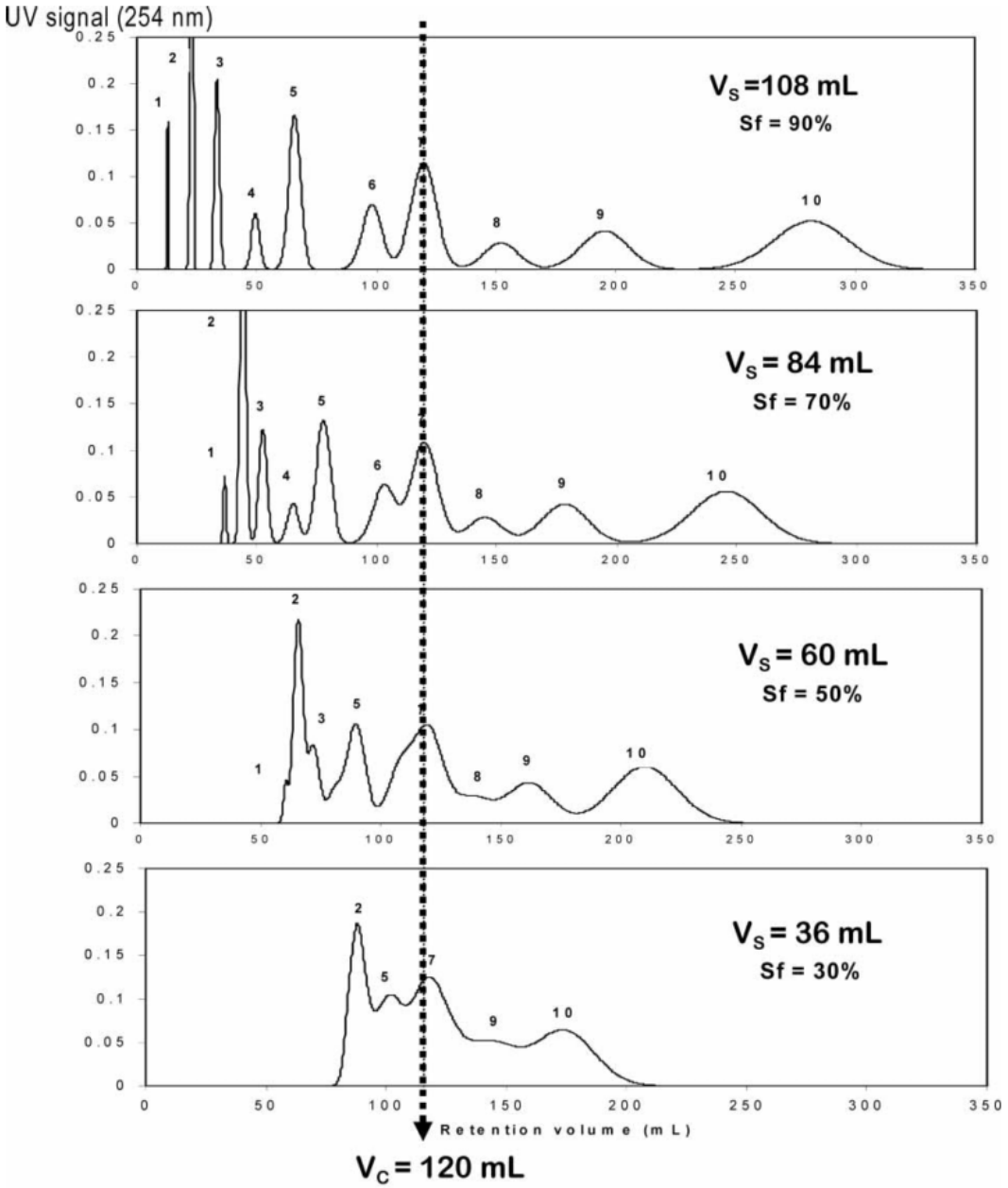

Figure 1-8: Effect of stationary phase retention (S_F) on a CCC chromatogram showing that increased S_F values give higher resolutions. The column volume (V_C = 120 mL) is represented by the vertical line in retention volume. From [54].

The stationary phase retention (S_F) is expressed (Equation 1-3) as the fraction or percentage of the total column volume (V_C) that is filled with stationary phase (V_S). It is calculated from the volume of stationary phase eluted ($V_{S\text{-eluted}}$) from the column when mobile phase is first introduced until a hydrodynamic equilibrium is reached (Equation 1-4). As a dimensionless parameter, the stationary phase retention is also useful for comparing different CCS equipment [44].

$$S_F = \frac{V_S}{V_C} \qquad \textbf{Equation 1-3}$$

$$V_S = V_C - V_{S-eluted} \qquad \textbf{Equation 1-4}$$

Through a combination of the volume of stationary phase in the column, the partition coefficient, and the volume of mobile phase (V_M, simply calculated from V_C) it is possible to predict the elution volume for each solute using Equation 1-5.

$$V_R = V_M + K \cdot V_S \qquad \textbf{Equation 1-5}$$

The stationary phase retention is heavily affected by the phase system used. Retention has been shown to be dependent on the interfacial tension, density difference and, more recently, the viscosity ratio of the two phases [52]. As a general rule a phase system should have a short settling time for good retention [37]. Advances in both CPC and CCC have sought to improve the stationary phase retention in difficult to retain systems such as aqueous two-phase systems (ATPS).

Adelmann et al. discovered that stationary phase retention behaviour can be markedly different between the ascending and descending modes of operation [53], and so a phase system should ideally be tested in both modes if retention is low.

In CCC, the stationary phase retention drops linearly to the square root of the flow rate [55], however, the relationship between retention and flow rate is more complicated in CPC. Retention is found to decrease linearly with increasing flow rate, however, this appears to hold true only up to a certain linear velocity, at which point, increasing the flow rate further reduces the retention without improving the linear velocity [56]. The

rotational speed was found to have little impact on retention at lower flow rates [53], but it has been shown to increase the maximum linear velocity achievable [56].

Settling time has frequently been used as a guide to the level of stationary phase retention that can be achieved. The settling time is essentially a manifestation of the interfacial tension between the two phases. The higher the interfacial tension, the shorter the settling time, and the higher the stationary phase retention [39]. Multiple settling times have been recommended as a maximum value: Ito recommends a settling time of less than 20 seconds (based on 2 mL of each phase in a test tube or graduated cylinder) [37] while Oka et al. recommend less than 30 seconds. While these guidelines have found their way into most solvent selection criteria [36][57][58] they should not be used as hard and fast rules. Improvements in modern CPC equipment and cell design allows for the retention of phase systems with long settling times such as ATPS [42]. ATPS are further described in Section 1.2.4.4.

1.2.4 Phase system selection

As discussed in Section 1.2.3.1, there are an unlimited number of potential phase systems that can be prepared with mixtures of any number of different solvents or additives. Thus, it becomes necessary to have clear guidelines and systematic ways of developing a method for any potential solute. Without such a method, selection is limited to existing literature and trial and error based development. The lack of guidelines was reported as a major stumbling block towards the general acceptance and application of CCS [50] in 2005 and since then, a number of phase system selection strategies have been introduced [59][60][61][62][63].

For the purposes of processing a low value feedstock such as SBP, CPC process development must be considered from a preparative perspective and, as such, the cost of solvents, safety and disposal concerns must be addressed and play a role in selection from the earliest stages [35].

1.2.4.1 Best solvent method

One of the earliest methods of developing a phase system relied on the "best solvent". This involves finding an intermediate solvent that the compound of interest is most soluble in and then adding two other solvents to create a two-phase system in which

the intermediate solvent is soluble in. The partitioning of the "best solvent" brings about the partitioning of the solute [48]. While this method can be a useful way of selecting a family of phase systems it gives no indication of the proportions that may give an effective separation, or even if effective separation is possible, while still requiring a fair amount of experimental work in finding the "best solvent". For highly hydrophilic compounds, this method is not particularly helpful as the "best solvent" is frequently water with no suitable intermediate solvents.

1.2.4.2 Screening tables

An alternative is to use solvent screening tables to rapidly narrow down semi-optimised conditions based on phase system families (a selection of solvents that can give a wide range in polarity depending on their relative proportions). The predominant family, HEMWat (hexane - ethyl acetate - methanol - water) has been described as the "workhorse" of CCS and is usually the first port of call when developing a method [35]. Hexane and water are the primary two-phase forming solvents while ethyl acetate and methanol act as modifiers to adjust the partition coefficients. Partitioning into the organic phase is enhanced by increasing the ethyl acetate proportion while partitioning into the aqueous phase is enhanced by increasing the proportion of methanol [33]. Hexane is often replaced by heptane to prevent the toxicity problems of using hexane for industrial applications [47]. Furthermore, limonene has been proposed as a “green” and renewable replacement for heptane [45]. While the HEMWat system is suitable for covering a wide range of solutes, it has poor performance for more polar solutes [50].

If a compound’s polarity falls outside of the range of HEMWat then other phase systems must be used. The HEMWat system can be further added to with extra modifiers such as TFA or NaCl for more polar compounds [37] but it is often necessary to use an entirely different phase system family and thus a different screening table. The addition of acids assists in the separation of negatively charged solutes by protonating them. The result is that the peak slims as only 1 form is present and the partition coefficient moves slightly towards the non-polar phase [37].

The EBuWat (ethyl acetate – n-butanol - water) system acts as an extension of the HEMWat table and allows for the screening of phase systems for more polar

compounds [59]. Table 1-1 shows a combined EBuWat (1-6) HEMWat (6-28) screening table [47] with highlighted starting points with simple volume ratios to simplify phase system selection. The EBuWat system only provides a small extension of the polarity range; at its most polar (butanol – water) it is still essentially an organic/aqueous phase system and, as such, it is unlikely to be suitable for extremely hydrophilic compounds such as monosaccharides.

Table 1-1: Combined EBuWat (1-6), HEMWat (6-28) phase system screening table showing volume proportions of each solvent for each phase system. Highlighted rows show simple solvent proportions for rapid screening of partition coefficients. From [47].

No.	Heptane	EtOAc	MeOH	Butanol	Water
1	0	0	0	2	2
2	0	0.4	0	1.6	2
3	0	0.8	0	1.2	2
4	0	1.2	0	0.8	2
5	0	1.6	0	0.4	2
6	0	2	0	0	2
7	0.1	1.9	0.1	0	1.9
8	0.2	1.8	0.2	0	1.8
9	0.29	1.71	0.29	0	1.71
10	0.33	1.67	0.33	0	1.67
11	0.4	1.6	0.4	0	1.6
12	0.5	1.5	0.5	0	1.5
13	0.57	1.43	0.57	0	1.43
14	0.67	1.33	0.67	0	1.33
15	0.8	1.2	0.8	0	1.2
16	0.91	1.09	0.91	0	1.09
17	1	1	1	0	1
18	1.09	0.91	1.09	0	0.91
19	1.2	0.8	1.2	0	0.8
20	1.33	0.67	1.33	0	0.67
21	1.43	0.57	1.43	0	0.57
22	1.5	0.5	1.5	0	0.5
23	1.6	0.4	1.6	0	0.4
24	1.67	0.33	1.67	0	0.33
25	1.71	0.29	1.71	0	0.29
26	1.8	0.2	1.8	0	0.2
27	1.9	0.1	1.9	0	0.1
28	2	0	2	0	0

These phase system screening tables all represent established phase system families. The fact that so many separations and so much guidance focuses on just a few families and a relatively small range of solvents shows that a major advantage of CCS, the flexibility and limitless range of phase systems, is not being fully exploited [61]. The HEMWat family, by far the most popular, does work well for an intermediate polarity range, however, it is possible that this has led to little development of other phase system families which may provide improved performance [35].

1.2.4.3 Generally useful estimation of solvent systems

The "generally useful estimation of solvent systems" (G.U.E.S.S.) is a method for phase system selection based on the performance of 22 commercially available natural products in a range of HEMWat or ChMWat (chloroform, methanol, water) phase systems [50]. By comparing the performance of a new solute to those in the 'G.U.E.S.S. Mix' based on TLC experiments, the performance in CCS can be predicted. The 'G.U.E.S.S. Mix' has also been applied to other phase system families including EBuWat [59], however, this may not be a suitably polar phase system for the partitioning of extremely hydrophilic solutes such as sugars.

1.2.4.4 Aqueous two-phase systems

ATPS are two-phase systems with water as the main component in both phases. They have applications for liquid-liquid extraction and CCS of very polar compounds, due to the high polarity of both phases; and biomolecules, due to the gentler conditions of ATPS over organic solvents for maintaining biological activities [64]. ATPS are generally categorised as either polymer-salt systems or polymer-polymer systems [65], however, there are also ionic-liquid based ATPS, and alcohol-salt ATPS [64]. There are also micelle-based and reverse-micelle-based ATPS for the separation of proteins but as these are based on the electrostatic interaction between the protein and the surfactant, they will not be discussed further in this thesis [66].

Polymer-salt ATPS are two-phase systems produced between a polymer, usually polyethylene glycol (PEG), and a salt, usually a phosphate or a sulphate [65]. They are useful for separating a range of biomolecules, such as proteins, while retaining their structures and biological activity [67]. The partitioning of proteins in a stable polymer-salt phase system can be modified by changing the molecular weight or concentration

of the polymer, concentration of the salt [64], or by adjusting the pH of the system [68].

Polymer-salt ATPS do, however, suffer from high viscosities, low interfacial tensions and similar densities when compared with organic-aqueous phase systems. This can lead to poor stationary phase retention in CCS [69], and while modern CPC equipment is much more capable of retaining these systems, it can still be difficult [68]. Polymer-salt ATPS are also associated with stationary phase bleed, continuous loss of the stationary phase throughout a separation [68][70].

Polymer-polymer ATPS are two-phase systems produced by two water-soluble polymers, usually PEG and dextran. Polymer-polymer ATPS, however, are generally less suitable than polymer-salt ATPS due to their increased cost, higher viscosity, reduced density difference, and lower selectivity [65] which limit their potential applications in CPC.

The sheer number of possible combinations of polymer-salt and polymer-polymer ATPS, including different salts and different molecular weight PEG compounds, complicates the development of a screening table for extremely hydrophilic compounds. Extensive use of statistical "Design of Experiment" software is often required to develop ATPS extraction methods [65].

Ionic liquids cannot generally be used directly in CCS due to their high viscosity, however, by adding them to an organic solvent or an aqueous salt, a two-phase system can be formed with acceptable physical characteristics and have been used for the separation of a range of products [71]. Research into their use in CCS appears to be focussed on their applications as modifiers rather than phase-forming components [46].

Alcohol-salt phase systems are generally not useful for the separation or extraction of biomolecules due to denaturation and the loss of biological activity, however they can be useful for the separation of hydrophilic compounds such as dyes [72], butanediol [73] and sugars [74]. These phase systems form such that the upper phase has a high alcohol concentration and the lower phase has a high salt concentration. Furthermore,

they are cheaper and have lower viscosities and shorter settling times [64], assisting stationary phase retention in CCS.

While methanol, ethanol and propanol are fully miscible in water, they are still organic compounds. Furthermore, the primary application of ATPS in CPC is for biomolecule separations, and the use of alcohols in the phase system can lead to denaturation or loss of bioactivity. Throughout this thesis, alcohol-salt phase systems will be referred to simply as "alcohol-salt phase systems", rather than as a type of ATPS.

Polymer-salt and polymer-polymer phase systems may be useful for the separation of hydrophilic separations but the problems mentioned above, including their cost, viscosity, difficulty of retention and stationary phase bleed are causes for concern. In addition, their primary advantage, maintaining biological activity, is not of importance to the separation of sugars. As such, phase system selection in this thesis will focus on alcohol-salt phase systems.

1.2.5 Separation of sugars in CCS

The application of CCS to the separation of sugars is limited in comparison to the separation of natural products [48][50][60][75][76][77][78][79] (which has sparked a number of reviews [35][46][80]) and even protein separations [67][68][81][82][83][84], with only a handful of articles published on the separation of sugars.

While some research has been performed on natural products containing sugars (for example glycosides [79][85][86] and glucosinolates [75][87][88]), they often contain large non-polar or ionic regions which allows for the use of organic-aqueous phase systems or ion exchange CCS (described in Section 1.2.7). Looking specifically at the separation of carbohydrates, there are only a few literature examples:

- Lau et al. were able to separate a number of xylose oligomers using a DMSO : THF : water (1:6:3 v:v:v) phase system [89], and improved the separation further using a butanol : methanol : water (5:1:4 v:v:v) phase system [90]. The separation of xylose oligomers has also been applied to dried crude feedstocks [91][92], although separation times are between 300-350 min. Zhang et al.

even managed to apply a non-aqueous phase system to the separation of xylose oligomers based on a heptane : butanol : acetonitrile (9:4:5 v:v:v) phase system [93], however, the requirement to fully dry crude aqueous samples prior to separation and the limited solubility in organic solvents dramatically hinders the practical application of this method.

- Chevolot was able to separate sulphated oligofucans using an ion-exchange method with a methyl *tert.*-butyl ether : water phase system [94]. Amberlite LA2 was used as an ion exchanger in the organic phase and NaOH as displacer. However, these oligofucans are charged and the separation method takes advantage of this, so this cannot be used for the separation of monosaccharides from crude hydrolysed sugar beet pulp except, perhaps, for the isolation of GA.

The above CCS separations have examined oligosaccharides but have not attempted the separation of monosaccharides as will be attempted in this work. Monosaccharides have very similar structures and sizes to each other (Figure 1-4) and so their separation is extremely challenging. The few CCS studies to address monosaccharide separations are described below:

- Early work was carried out by Murayama on the separation of sugars using CCC with a butanol : ethanol : water (10:2.5:10 v:v:v) phase system. The monosaccharides used had very low partition coefficients, with the sugars partitioning very strongly into the aqueous phase, leading to very long retention times and poor separation [95].

- Shinomiya improved on this work slightly using a butanol : acetic acid : water (4:1:5 v:v:v) phase system, however, the partition coefficients were still poor. Partition coefficients for GA, Ara, Gal and Rha were 0.14, 0.27, 0.29 and 0.31 respectively. The phase system was heavily flow rate limited (0.1 mL min^{-1} on a 26.5 mL column) with separation times of 400 min for the separation of sucrose and fucose [96].

- Shinomiya and Ito were able to further improve their earlier separation of sugars in CCC using an ethanol : aqueous 2 M ammonium sulphate (3:5 v:v) phase system [74] to give improved partition coefficients. They achieved partition coefficients for GA, Ara, Gal and Rha of 0.18, 0.64, 0.39 and 0.97

respectively. However, retention of the stationary phase was limited even at flow rates of 0.2 mL min^{-1} on a 26.5 mL column, leading to excessive separation times.

The literature on monosaccharide separations using CCS is thus extremely limited and has primarily focussed on CCC, using the non-conventional cross-axis coil planet centrifuge to increase the stationary phase retention. The studies in the literature have also focused on model mixtures of pure monosaccharides rather than the crude hydrolysates that are more relevant in biorefinery applications (Section 1.1). With advances in CPC technology, allowing for much greater retention of the stationary phase, it may be possible to overcome the flow-limitations experienced in the literature and dramatically reduce separation times and increase throughput. Alcohol-salt phase systems could be a useful place to start for the separation of sugars in CCS.

1.2.6 Preparative CPC and scale-up

The problems associated with solid supports in resin-based chromatography are still present at large scale for these systems, notably limited lifetime through irreversible effects (permanent adsorption, denaturation etc.) on the solid support, contamination and blockages. Some analytical resins can even be far too costly to run at preparative scale and so alternative columns and resins must be sought. This can add further development steps to find suitable packing materials and can limit the application of preparative scale resin-based chromatography or lead to decreased performance [97]. Also, non-specific adsorption in resin-based chromatography can lead to regulatory issues [34].

CPC overcomes many of these problems and retains all of the features that make it useful at an analytical scale, most notably: flexibility, the whole column contents can be pumped out and new stationary and mobile phases pumped in with no resultant cross contamination; and 100% sample recovery, any highly retained solute can be recovered by extruding the stationary phase [98]. Furthermore, any problems with column packing and flow-distribution for resin-based chromatography are inherently removed due to the lack of solid-phase, and CPC is more tolerant than resin-based chromatography to the presence of particulate matter, improving process robustness

[99]. Reduced solvent consumption can also be achieved relative to preparative resin-based chromatography [76].

Scale-up in resin-based chromatography features the equivalence of residence times over the column between scales. As the column length is generally kept constant (resulting in short, wide columns), chromatographs can be almost identical to their analytical counterparts. In CPC scale-up, larger machines requires larger volume equipment with possible variations in cell number or cell design, which can alter the performance and lead to variations between scales [79]. However, fundamentally, the partition coefficients and stationary phase retention determine the solute elution volume. Therefore, the elution volume (i.e. the x-axis on a chromatogram) can be normalised to partition coefficients by taking into account the amount of stationary phase lost throughout the separation [100].

Scale-up can be performed linearly, generally with improvements in process performance as scale increases [70]. However, improvements in performance effectively underestimates the potential of the larger scale, and so recent efforts have been made to optimise large scale performance directly from smaller-scale experiments (free space between peaks method) [101], and to determine scale-up invariants in order to understand the non-linear phenomena during scale-up [99][102].

Linear scale-up has been performed in CPC by scaling up the flow rate and sample volume using the ratio of the two column volumes as a linear scale-up factor [70][103][104]. Sutherland et al. used this method to scale-up a protein separation using an ATPS (12.5% (w/w) PEG-1000 : 12.5% (w/w) K_2HPO_4) from a 500 mL CPC to a 6.25 L CPC [70]. A scale-up factor of 12.5 was therefore applied to the flow rate, increasing it from 10 mL min^{-1} to 125 mL min^{-1}, and sample volume, increasing from 40 mL to 500 mL. Improved separation performance was achieved at the larger scale, with the resolution increasing from 1.28 to 1.88. The rotational speed was adjusted in order to maintain the centrifugal force between scales due to different rotor diameters [70].

The linear scale-up method underestimates the performance of larger scale CPC equipment. The improved separation performance on the larger scale could have

allowed for a larger sample injection to be performed, further increasing the throughput at the larger scale. It is even possible for linear scale-up to be restricted based on pressure limitations on the column, forcing reduced rotational speeds and resulting in reduced separation performance [105]. Bouju et al. developed a novel scale-up methodology, allowing for the prediction of maximum loading on a large-scale column based on an optimised smaller scale CPC separation and a single analytical injection on a large scale column [101]. The "free-space between peaks" method determines the free space volume between two peaks at both the small (ΔV_1) and large scales (ΔV_2). The ratio of the free-spaces between the peaks ($\Delta V_2 / \Delta V_1$) is used as a scale-up factor for the sample volume of the maximal loading on the small scale equipment.

An alternative approach to scale-up was made by attempting to determine more useful scale-up invariants associated with scale-up, rather than simply tying mobile phase flow rate to the total volume ratio. Kotland et al. utilised a "global mass transfer coefficient", linked to the efficiency of the column design; and the stationary phase retention, a measure of the capacity of the column as scale-up invariants [102]. Keeping stationary phase constant between scales is relatively simple, whereas the global mass transfer coefficient is column dependent and involves more detailed calculations on both columns. The results, however, allow for more predictive scale-up between column types of different designs.

1.2.7 Alternative operating methods

Due to the liquid nature of the stationary phase in CCS (Section 1.2), it can be manipulated much more easily than in resin-based chromatography. In resin-based chromatography, gradients are often required in order to more rapidly elute strongly retained components [106]. With a liquid stationary phase, these compounds can simply be pumped out by switching from the mobile phase to the stationary phase (elution-extrusion). Strongly retained compounds which may take significant volumes of mobile phase to eventually elute in broad bands can be rapidly eluted with much reduced solvent usage in narrower peaks [106]. Furthermore, it is possible to use elution-extrusion to reduce band broadening for all peaks by extruding as soon as bands are separated within the column rather than waiting for them to elute and

broaden further [107]. Another benefit is that after extrusion, the column is regenerated with stationary phase and so can be immediately used for further separations [108]. This could be an important factor in increasing process throughput.

Dual-mode CPC involves switching from ascending to descending mode within a run. This involves switching both the phase being pumped and the direction of flow [109]. The method is similar to elution-extrusion but the change in flow direction reverses the elution order after the switch [35]. This allows for rapid elution of very strongly retained compounds that may still be towards the start of the column [110]. Multiple switches can be made (multiple dual-mode), allowing for an artificially longer column while maintaining a higher resolution than a classical elution mode [111]. It is thus useful for difficult to separate compounds where longer column volumes would otherwise be required. However, while the elution-extrusion mode can be performed by programming the run method into the pump software, the dual-mode and multiple dual-mode require manual switching of the flow direction valve.

Chiral separations, ion exchange, and pH zone refining in CCS involve the addition of selectivity modifiers to the phase system. Chiral separations utilise chiral selectors in the stationary phase, allowing for the selective modification of one of the enantiomer's partition coefficients [112]. Ion exchange CPC takes advantage of a retainer, often an ionic liquid, in the stationary phase; and a displacer, a salt, in the mobile phase. Operation without displacer in the mobile phase allows for partitioning into the stationary phase and then addition of the displacer shifts these compounds back into the mobile phase, eluting in reverse order of their affinity for the retainer [113][114]. This displacement mode allows for highly selective separations. Another displacement technique for ionisable analytes is pH zone refining. Acids and bases are used as retainers or displacers and manipulate the pH through the column. Compounds are confined into pH zones based on their dissociation constants due to differences in partition coefficients between their neutral and ionised forms [115][102]. This leads to sharp peak boundaries with much increased capacities and solute concentration [116]. In principle it is similar to ion exchange CPC but using pH rather than ionic strength [46]. These techniques demonstrate that it is possible for phase system additives to have an important impact on separation selectivity and performance.

1.3 Pretreatment options for crude SBP hydrolysate

The crude hydrolysate used in this thesis (steam exploded, fully hydrolysed SBP pectin, as described in Section 1.1.4) is a black solution, containing sugars, salts, and a number of unknown coloured contaminants. Unlike CPC, resin-based chromatography for the separation of sugars requires a much cleaner feed stream due to the solid nature of the stationary phase as it is susceptible to variation and irreversible binding by certain compounds and contaminants. Furthermore, as explained in Section 1.5.1, the resins often used for the separation of sugars tend to be cation exchange resins and so the presence of certain cations could prove problematic to separation performance and reproducibility. Pretreatment and decolourisation is likely required before the crude hydrolyse SBP can be used for separations of the sugars using resin chromatography and simulated moving bed technologies. The two primary methods of decolourisation are the use of resins or activated carbon [117] and are discussed in Sections 1.3.1 and 1.3.2 respectively.

1.3.1 Resins for decolourisation

While activated carbon has historically been used for decolourisation of sugar juices, the use of resins for pretreatment and decolourisation has been used since 1970 [118]. However, it has primarily been applied to sugarcane decolourisation and not for sugar beet decolourisation. This is due to the level of coloured compounds present in the sugar beet juices being an order of magnitude higher than in sugar cane juices [119]. Resin based treatments allow for robust and reproducible decolourisation and regeneration, reducing the extra costs associated with replacing the resins. Decolourising resins are routinely used in the manufacture of sucrose, from sugar cane or sugar beet [120]; and fructose syrups [117].

1.3.1.1 Ion exchange resins

Ion exchange resins are the most common type of resin used for decolourisation of sugar juices and hydrolysates [121]. They contain functional groups associated with either an anion or cation that can exchange for ions of the same charge. Equation 1-6 shows the reversible process of sorption and desorption of an anionic contaminant onto an anion exchange resin in the Cl^- form. In contaminant sorption (left to right), the

contaminant exchanges with the Cl^- ion, releasing Cl^- ions in the effluent. In contaminant desorption/regeneration (right to left), NaCl is passed through the column and exchanges with the contaminant, releasing the contaminant and regenerating the column back into its original Cl^- form.

$$Resin^+Cl^- + contaminant^- \rightleftarrows Resin^+contaminant^- + Cl^- \qquad \textbf{Equation 1-6}$$

As coloured contaminants from sugar hydrolysates and liquors are generally anionic, anion exchange resins in the Cl^- form are predominantly used for decolourisation, with further anion and cation exchange resins used for softening and demineralisation [118]. Decolourisation of sugar liquors using resins was initially prevalent primarily for sugarcane juices [120][122]. Sugar beet juices have proved more difficult to decolourise due to much increased colouration relative to sugarcane juice [119][120]. A large amount of related research, however, has been focussed on the decolourisation of agricultural waste hydrolysates [123][124][125][126].

There are two main types of resins based on the material used for the matrix: polystyrene resins and acrylic resins [118]. The different materials allow for different interactions with the coloured contaminants. Polystyrene resins have higher decolourisation efficiencies [118], however they are more easily fouled and have more difficult to regenerate due to hydrophobic interactions in addition to ion exchange interactions [122]. Acrylic resins tend to only exhibit ion exchange interactions and so, while the decolourising potential may be lower, they are less easily fouled and much easier to regenerate using only NaCl [118].

Coca et al. [120] decolourised sugar beet juice using Lewatit 6368 anion exchange resin in the Cl^- form and succeeded in removing 75-80% of the colour. The authors note that a demineralisation step would be required before further processing due to the high Cl^- concentration present in the decolourised product stream, a result of the Cl^- ions released after organic coloured compounds and other inorganic anions exchanged with the Cl^- on the anion exchange resin (Equation 1-6).

De Mancilha and Karim examined the use of ion exchange resins in the detoxification of corn stover hydrolysates, focussing on the recovery of D-xylose [123]. From a range

of ion exchange resins, including both anion and cation exchange resins. All of the resins were able to remove a considerable amount of the colour (41-95%), recover almost all of the D-xylose (94-100%) while only one of the resins was able to remove any acetic acid. This resin (Purolite A 103 S in the NH_3 form) performed the best out of all of the resins for colour and contaminant removal. The removal of acetic acid could be problematic as it indicates that GA could also be removed if present, however the other anion exchangers in the Cl^- form did not remove any acetic acid indicating that this could be a preferred ionic form for decolourisation, even if the colour removal is not as great.

Gong et al. [125] examined the pretreatment of sugar cane bagasse hemicellulose after acid hydrolysis using a cation exchange resin (Dowex 50W-X4) for the production of ethanol and demonstrated an improvement on the ethanol production by the removal of inhibitory compounds.

Chandel et al. used an anion exchange resin to remove furans and phenolics from a sugarcane bagasse hydrolysate to produce ethanol [126]. They also found that the anion exchange resin performed better than activated carbon treatment for removal of contaminants and yield of ethanol.

For the work to be conducted in this thesis, it is important to consider the effects of any pretreatment method on the removal of GA from the crude sample (Section 1.1.4). While sucrose and high-fructose corn syrup productions can use a wide range of resins capable of removing effectively all contaminants other than neutral sugars, the ionic nature of GA makes things more difficult in the case of the crude hydrolysate examined in this thesis. It would not be possible to simply run a complete demineralisation using a combination of anion and cation exchangers in the OH^- and H^+ forms respectively, as the GA would also be lost.

1.3.1.2 Adsorption resins

In addition to ion-exchange resins, adsorption resins have also been examined for decolourisation. These operate in a similar method to activated carbon, utilising hydrophilic or hydrophobic adsorption of compounds to the resin, and while they have a reduced effective surface area, they are more durable and chemically stable while

maintaining high capacities [124]. Furthermore the regeneration is simple with the use of alcohols, allowing for solvent recycling to reduce the amount of liquid waste [127].

These resins have predominantly been used for the adsorption of phenolic compounds [128][129][130], which could arise from the degradation of any lignin present. Okuno and Tamaki used an octadecylsilyl-silica gel to adsorb polyphenols from sugarcane juice [127]. A colour reduction of 90% was achieved and the resin used can be regenerated with ethanol and water rather than salts. Optipore SD-2 was used by Van Duc Long et al. [131] as part of a de-ashing step for decolourisation, followed by a cation and anion exchange column in order to completely demineralise a sugar mixture for simulated moving bed separation of psicose and fructose. The resin was also used for the decolourisation of apple juice by adsorption of phenolic compounds without affecting the levels of sugars or organic acids [132]. This is important for the proposed SBP decolourisation as it would not be desirable to remove any of the neutral sugars or the GA from the feedstream during a decolourisation step.

1.3.2 Activated carbon for decolourisation

Activated carbon is an extremely versatile adsorbent that can be used for the bulk adsorption of a wide variety of compounds in both gaseous and liquid phases [133]. It has a polymodal porous structure and variable surface composition, which, combined with its large surface area and adsorption capacity makes it an effective adsorbent [134]. The adsorption capacity is dependent on both the internal surface area and the pore size and differences in chemical structure affect specificity of adsorption of different compounds [135], thus, activated carbons produced from different sources and with different activation methods can result in different capacities and adsorption specificity. This allows a broad range of compounds to be adsorbed, useful for decolourisation in the sugar industry where there are many contaminants. The relatively non-polar nature of activated carbon also provides a specificity for less polar compounds, meaning that polar sugars are less likely to be adsorbed.

The use of carbon-based adsorbents has long been used for water purification, both for industrial wastewaters [134][136][137][138] and drinking water [139][140]. They have also been used for centuries in sugar decolourisation with the use of wood

charcoals [141] before being replaced with bone char [127] and activated carbon with much higher capacities [141].

Activated carbons are commonly used for decolourisation of sugar liquors [142][143][144][145][146] after the diffusion step (Figure 1-1) and prior to softening and demineralisation steps. They are also used for the decolourisation of lignocellulosic hydrolysates, and this is where most research on activated carbon decolourisation of liquids containing sugars has developed. Research in this area is primarily focussed on the decolourisation and detoxification of these hydrolysates [8] to increase the productivity of fermentation of the sugars into xylitol [147][148][149][150][151][152] and ethanol [126].

The hydrolysates examined are from a range of different biomass sources including corn fibre [151], corn stover [153] eucalyptus [150] and other hardwoods [148][152][154], and sugarcane bagasse [126][149]. However, only one previous article has described the decolourisation or detoxification of a sugar beet pulp hydrolysate using activated carbon [13]. This examined the use of SBP hydrolysate for fermentation into ethanol, and uses activated carbon to primarily remove furans and phenolic compounds as well as acetic acid. It was found that 98% of furans and 71% of phenolic compounds could be removed, however, no mention is made of the colour of the hydrolysate either before or after detoxification.

Activated carbon can be produced from any lignocellulosic material [144] and is commonly produced from coal or agricultural residues [133][145][146][155]. It can be produced through physical activation: pyrolyzing the material at high temperature (<800°C) in the absence of oxygen and then adding a non-oxidising gas such as steam, air or CO_2; or chemical activation, by adding chemicals such as $ZnCl_2$, KOH or H_3PO_4 and heating to ~800°C [133].

A lot of research has focussed on producing activated carbon from a range of different agricultural residues [133] including sugarcane bagasse [136][144], sugar beet pulp [143], rice hulls [155] and a wide variety of nut shells [133] to produce activated carbons for decolourising sugar juices and cleaning up wastewaters.

Regeneration of the activated carbon adsorbent is a key consideration for the economic feasibility of an adsorption process [124]. It can be performed in a similar way to activated carbon production, primarily pyrolysis and high temperature addition of steam or CO_2 [156]. However, regeneration changes the internal structure of the adsorbent, affecting pore size and total surface area and so tends to decrease the total capacity of the activated carbon [157].

1.3.3 Other adsorbents

Other novel methods of decolourisation of sugar juices include the use of pulp materials as an adsorbent after modification, such as unmodified sugarcane bagasse (59% decolourisation) [158] and sugar beet pulp (44% decolourisation) [159], although it is noted that decolourisation was not complete using these adsorbents and further decolourisation would be required, likely using either ion exchange resins or activated carbon. Ultrafiltration has also been used for the decolourisation of cane sugar juice [160], although the use of ion exchange resins afterwards was still required.

1.4 Isolation of GA from neutral sugars

Similar to the decolourisation step (Section 1.3), it is perhaps easiest to isolate GA from the other neutral sugars in the crude hydrolysate (Section 1.1.4) using an anion exchange resin, with the galacturonate ions binding and the neutral sugars not binding. The galacturonate ions could then be eluted using a regenerating salt.

Anion exchange resins have been utilised for the separation of uronic acids and the isolation of uronic acids from neutral sugars. Suzuki et al. [161] separated a mixture of oligogalacturonic acids on a DEAE Sephadex A-25 resin using NH_4HCO_3 as the eluent. The reported advantage of this eluent is that it can be completely removed by lyophilisation, allowing for simplified further purification of the fractions. However, this would not be feasible at the scale and throughputs required. Khym and Doherty were able to separate GA and glucuronic acid using a Dowex 1 anion exchanger in the acetate form with acetic acid as an eluent [162]. The isocratic method they used also fractionated the uronic acids from the neutral sugars Gal and Ara which were also present in the mixture. This method could easily be used as a starting point for the development of a step elution method to maximise the capacity of the anion exchange

resin as no glucuronic acid is likely to be present in the crude sample. This anion exchange method, using acetate as an eluent, is also employed for analytical separations of neutral sugars and uronic acids [163] using high performance anion exchange chromatography (HPAEC).

Selectivity of the anions to the exchanger is also important. Too strong an anionic form and the galacturonate will not bind. Too weak and desorption will take a much higher volume of desorbent (diluting the GA); or require a stronger desorbent, adding an additional regeneration step to convert the resin back to its original form. The Dow Chemical Company (Midland, Michigan, United States) provide selectivity coefficients indicating the relative strength of common anions for type 1 and type 2 anion exchangers [164]. For type 1 anion exchangers, acetate is 3.2 times as strong as OH^-, while Cl^- is 22 times as strong as OH^-. In HPAEC, NaOH cannot be used to elute galacturonate from the column, indicating that it is stronger than OH^-, while it readily elutes using NaOAc. This indicates that its strength is around that of acetate and thus likely lower than Cl^-. This is particularly useful due to the general preference for Cl^- anion exchange resins used for decolourisation, discussed in Section 1.3.1, indicating that GA may not readily bind to these columns.

1.5 Neutral sugar separations

1.5.1 Cation exchange chromatography

Cation exchange resins have long been used for the separation of neutral sugars for preparative separations. Kumanotani et al. worked on preparative separations of acidic and neutral monosaccharides using a cation exchange resin in the H^+ form in 1979 [165]. Hicks et al. [166] were able to use preparative HPLC in 1987 to separate a range of sugars, sugar acids, lactones and other sugar derivatives on silica columns, and cation exchange columns in the H^+ and Ca^{2+} forms. They found that silica gel gave better resolution for monosaccharides but cation exchange columns had better capacity, durability and economics. Further advantages for the use of cation exchange columns over silica gel columns was the recovery of 100% of the injected sugars and a more robust separation media, with much reduced need for regeneration or repacking and reusability over several years [166].

These works are based on scaling up the processes used for analytical separations of sugars and generating purified samples from a single column. While this may be useful to develop a generic method for routine preparative separations of unknown mixtures of sugars, industrial scale separations of sugars generally work with known separation criteria. As a result, they are able to work with lower resolution, higher capacity systems and take advantage of multiple columns, or recycling of partially separated compounds in order to achieve the desired separation most effectively. Simulated moving bed (SMB) systems are generally used to fill this role, allowing for continuous binary separations based on strict input criteria but allowing for much increased resin utilisation, capacity and throughput. SMB is discussed further in Section 1.6.1.

Cation exchange resins are often used for the separation of sugars both analytically [167], at preparative scale [131] and industrially [168], however, the method of separation is not obvious due to the non-ionic nature of these sugars. Water is often used as an eluent with little need for regeneration unless any other ions are present in the stream [169], although at preparative and industrial scales ions can be removed with the use of de-ashing and demineralisation prior to loading onto the columns [131]. Importantly, the cation form of the resin (the cation that is normally exchanged in cation exchange chromatography) dictates the retention times of different carbohydrates [169]. This indicates that while there is no direct exchange, there is some interaction between the immobilised cation on the ligand and the carbohydrates in the sample. The use of water as an eluent and the lack of a regeneration step is a key factor in the use of cation exchange resins for the separation of sugars.

The actual separation is based on complex formation between the sugars and the metal ions and the mechanism can be described as a combination of ligand exchange, steric exclusion, partitioning, hydrophobic adsorption, and electrostatic attraction and repulsion [170]. It is generally referred to as ligand exchange chromatography. The metal cation is associated with a number of water molecules which are displaced by the carbohydrates as they pass the ligand, forming a donor-acceptor complex [170]. The stability of the complex varies between sugars, with more stable complexes retaining the sugar for longer on the column, resulting in longer elution times [169]. The result is a separation mechanism that is capable of separating sugars yet does not require the addition of any modifiers or regular regeneration of the stationary phase.

This puts cation exchange resins as prime contenders for use in preparative and industrial scale separations where the operating costs of modifiers and regeneration must be considered.

1.5.2 Other resin based chromatography methods

Reverse phase liquid chromatography of sugars is difficult, even at an analytical scale, due to the high polarity of the sugars. As a result, sugars tend to elute very early off the column unresolved and this method is rarely used without some form of derivatisation [171], which limits the applications to purely analytical.

Hydrophilic interaction liquid chromatography (HILIC) has been used to analytically separate a number of carbohydrates [172][173], however, high percentages of acetonitrile are used in the mobile phase and so this method was deemed unsuitable for further exploration.

Anion exchange resins can also be used to separate monosaccharides with high pH causing ionisation of the sugars [174]. While these resins may be useful for analytical systems, such as HPAEC, the use of high pH in order to ionise the sugars could cause issues at an industrial scale. Ideally it would be possible to operate using a water mobile phase, as with cation exchange resins.

1.6 Simulated moving bed chromatography

1.6.1 Simulated moving bed concept

The concept of simulated moving bed chromatography (SMB) stems out of a practical approach to the true moving bed (TMB) concept where the solid adsorbent and fluid move in countercurrent directions, with the feed injected into the centre of the moving bed. The countercurrent motion of the solid and liquid phases can be adjusted such that the faster eluting (least adsorbing) compound travels in the direction of the fluid, while the slower eluting (more adsorbing) compound travels in the direction of the solid. This is shown in the TMB schematic in Figure 1-9. This method allows for a much higher proportion of the resin to be active in achieving the separation at any one time, as opposed to batch chromatography, where the active portion of the resin is much

smaller and moves down the column. The result is high purity, high throughput, continuous processing, with reduced solvent/desorbent usage and reduced dilution of target compounds.

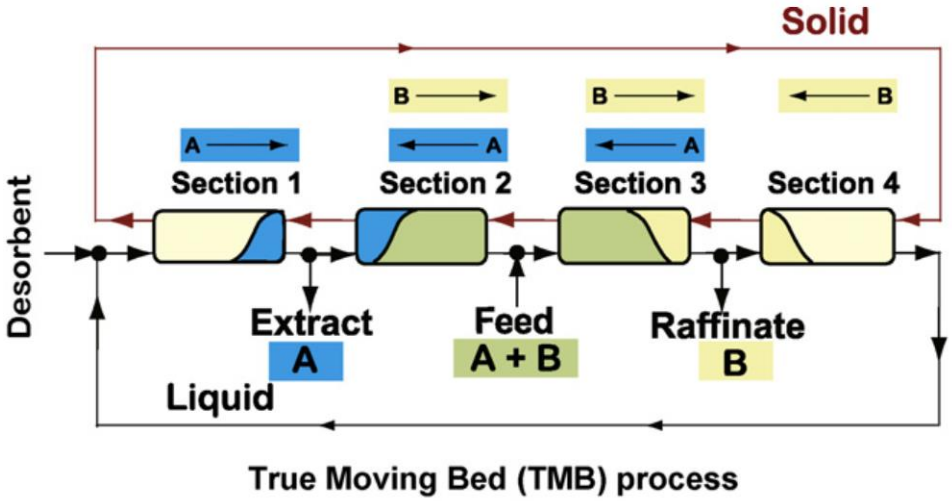

Figure 1-9: Schematic diagram showing the principle of a true moving bed (TMB) process with four sections separating a mixture of A and B. The flow directions of the solid and liquid, and the relative movement of components A and B are shown. From [175].

The movement of the solid phase provides a severe practical difficulty to the application of TMB systems. To fix this problem, the solid phase is split up into multiple smaller columns with adjustable inlet/outlet ports between each. The port position moves at intervals in the direction of fluid flow, thus simulating the countercurrent movement of the solid phase. This “Simulated Moving Bed”, shown in Figure 1-10, allows for the countercurrent nature of TMB to be achieved using ordinary solid-phase chromatography columns.

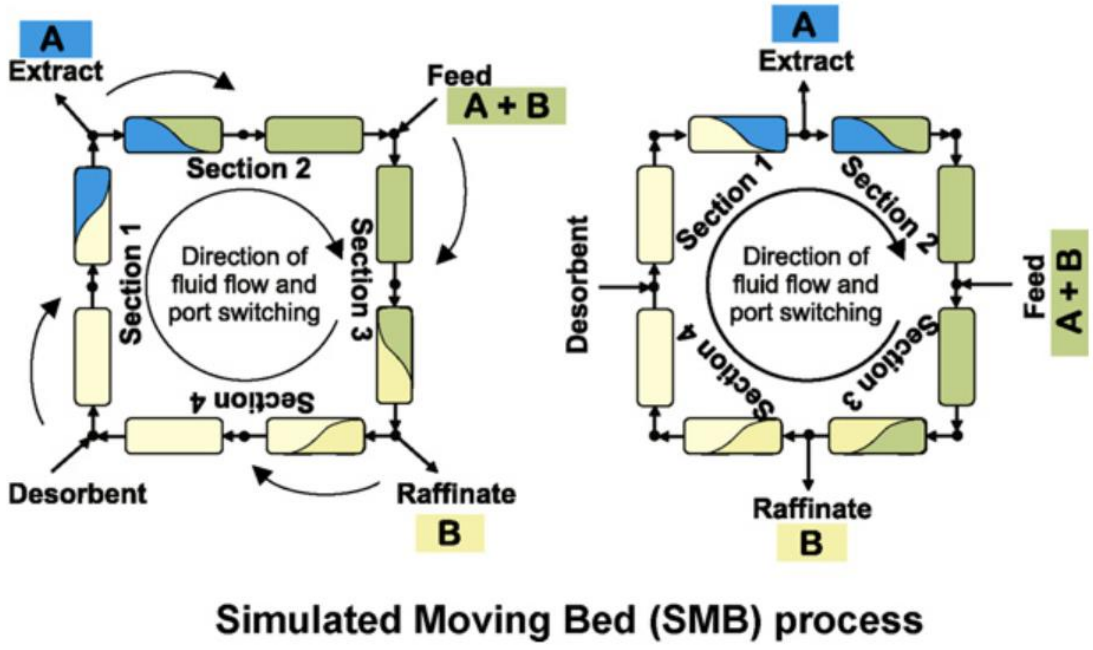

Figure 1-10: Schematic diagram showing the operation of a four-zone simulated moving bed (SMB) process separating a mixture of A and B. The clockwise direction of liquid flow and port switching is shown. From [175].

There are a number of advantages to using SMB processes over batch chromatography. First is the issue of resolution and purity: batch chromatography generally requires high resolutions in order to achieve high purity products; in SMB, the extract and raffinate are effectively only collecting the peak tails and so high purity is achievable even with lower resolutions [176]. Second is the improvement in throughput: as a much higher proportion of the resin is active in separating the compounds of interest, throughputs per volume of resin can be significantly higher than batch separations [177]. Furthermore, the improvements in active resin usage leads to shorter solute migration distances resulting in reduced solvent consumptions and reduced product dilution [178].

The most common SMB setup uses four sections, or "zones", as shown in Figure 1-10, and each is responsible for a specific role. In zone 1, the resin is regenerated and the adsorbed components are desorbed and eluted in the extract [179]. Separation occurs in zones 2 and 3 with the weaker adsorbing compounds moving "forwards" relative to port switching, ending up in zone 4; and the stronger adsorbing compounds moving "backwards" relative to port switching, ending up in zone 1 [180]. The weaker adsorbing compound is moved "forwards" into zone 4 by the mobile phase where it is

retained. This allows the mobile phase, free of any solutes, to be recycled back into zone 1 and mixed with fresh desorbent. The weaker adsorbing compound retained in zone 4 is shifted back into zone 3 where it is then eluted as the raffinate.

It is important during SMB method development to ensure that the port shifting timing is not so slow that it allows for the extract component to continue moving "backwards" from zone 1 into zone 4; similarly, that it is not so fast that it allows for the raffinate component to continue moving "forwards" through the recycle from zone 4 into zone 1.

1.6.2 SMB theory and method development

A typical, four-zone SMB process has four key operating constraints [177]:

- In zone 1, the strongly retained compound must be completely desorbed.
- In zone 2, the weakly retained compound must be completely desorbed.
- In zone 3, the strongly retained compound must be completely adsorbed.
- In zone 4, the weakly retained compound must be completely adsorbed.

A trial and error approach to the main operating flow rates and interval switch time would be extremely unlikely to find an optimal operating condition that meets these constraints. As a result, models have been developed in order to predict acceptable operating conditions. The equilibrium theory (or triangle theory) can be used to model SMB processes for separating components with linear isotherms [175].

The equilibrium theory assumes there is no axial dispersion and no mass transfer resistance, and, thus, linear isotherms can be expressed in terms of the Henry adsorption constant (H_i) for each component (i) according to Equation 1-7, where $C_{ads,i}$ is the concentration of the component adsorbed to the adsorbent and C_i is the concentration of the component in the liquid phase [175]. Higher Henry constants result in stronger adsorption to the adsorbent and, consequently, longer elution times on a single column batch separation. For linear isotherms, these Henry constants can be calculated from the retention times of batch column experiments [181].

$$C_{ads,i} = H_i \cdot C_i \qquad \textit{Equation 1-7}$$

The dimensionless flow rate ratios (m_n) in each zone (n) (Equation 1-8) are then used for the SMB triangle theory model, calculated from the flow rate in each zone (Q_n), the switch time (T_S), the column volume (C_V), the void fraction (ε), and the dead volume (V_D). These flow rate ratios show the relative flow rates of the liquid and solid phases [175].

$$m_n = \frac{Q_n T_S - C_V \epsilon - V_D}{C_V(1-\epsilon)} \qquad \textbf{Equation 1-8}$$

Applying the flow rate ratios and the Henry constants to the operating constraints described previously in this section yields four key inequalities to successful SMB separation [182] (Equation 1-9 to Equation 1-12).

$$H_A < m_1 \qquad \textbf{Equation 1-9}$$

$$H_B < m_2 < H_A \qquad \textbf{Equation 1-10}$$

$$H_B < m_3 < H_A \qquad \textbf{Equation 1-11}$$

$$m_4 < H_B \qquad \textbf{Equation 1-12}$$

As the separation is dependent only on zones 2 and 3, the values of m_1 and m_4 are of less importance so long as the inequalities Equation 1-9 and Equation 1-12 are satisfied. The m_2-m_3 plane (Figure 1-11) is a useful tool to predict separation performance and shows the expected separation performance in different regions based on the Henry constants of the two components and the m_2 and m_3 values. The region where both the extract and raffinate are expected to be pure forms a triangle in the centre of the plane, giving the name to the triangle theory. The size of this region is therefore dependent on the selectivity between the two components (the ratio of the two Henry constants). Alternative methods have been studied which take into account the axial dispersion and mass transfer resistance [131], however, they increase the complexity of the models.

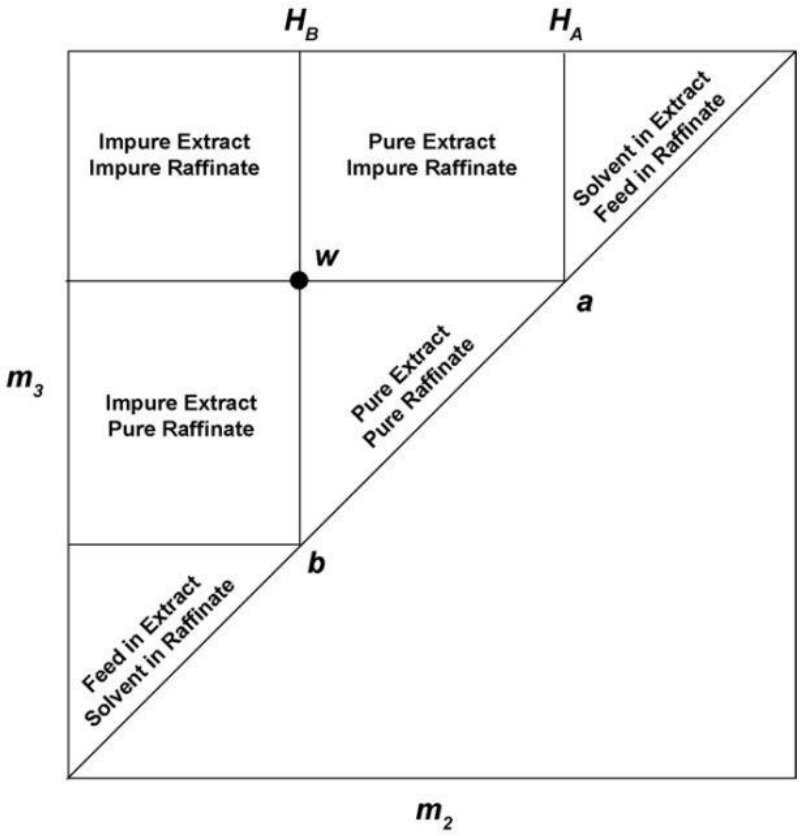

Figure 1-11: SMB separation regions on the m_2-m_3 plane for the separation of a mixture of A and B, based on linear adsorption isotherms. From [175].

Separations with non-linear isotherms, where species propagate at rates that are dependent on the composition, pose an extra difficulty for SMB method development. Modified versions of the triangle theory for non-linear isotherms have been developed which can be used for Langmuir, Anti-Langmuir, and mixed isotherms [175]. These effectively result in models that deviate slightly from the m_2-m_3 triangular operating window. However, due to the strong linearity of isotherms for sugars on cation exchange columns [183][184] this will not be examined in further detail.

1.6.3 Alternative SMB setups

While SMB traditionally operates using a four-zone, closed loop setup, it is possible to remove zone 4 and operate without an internal recycle in a three-zone, open loop setup. In this setup, zone three feeds directly into the raffinate [181] and, as there is no risk of raffinate products being recycled back into zone 1, the triangle theory model can still be used, although without the zone 4 constraint (Equation 1-12). This can lead

to simpler setups but higher desorbent usage due to the lack of an internal desorbent recycle.

SMB systems are generally restricted to the isolation of two fractions from a separation, the extract (more retained solutes) and the raffinate (the less retained solutes). Thus, if it is required to isolate multiple compounds or fractions from a sample, multiple SMB steps may be required. Tandem SMB has been developed to facilitate the isolation of multiple fractions using SMB. For example: Xie et al. developed a tandem SMB process to remove high molecular weight proteins from insulin in the first SMB and remove $ZnCl_2$ from insulin in the second SMB [185]. Mun used tandem SMB for the removal of acetic acid and sulphuric acid from glucose and xylose for fermentation, demonstrated in Figure 1-12 [186].

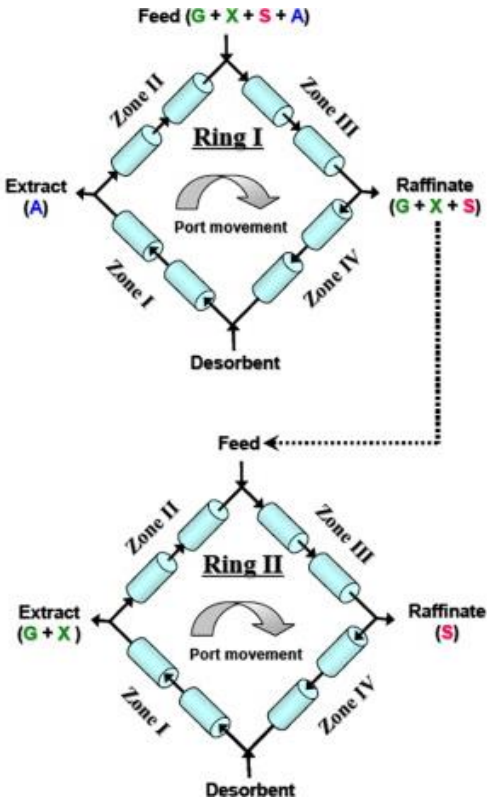

Figure 1-12: Schematic diagram of a ternary separation using a tandem SMB to separate a four component mixture. The raffinate from the first SMB is used as the feed for the second SMB. G, X, S and A represent example components to demonstrate the separation. Adapted from Mun [186]**.**

Other modified methods also exist, such as the five-zone setup as an alternative to tandem SMB, incorporating 4 inlets (wash, regeneration, desorbent, and feed) and 4 outlets (three waste and one product) [187]. Wooley [188] has even developed a nine-

zone SMB system in place of a tandem SMB setup, however, this rapidly adds complexity to method development and optimisation.

SMB processes are generally restricted to isocratic elution methods [177], whereas, in the vast majority of bioseparations, gradient elution methods are applied in discontinuous single column operations. As a way around this restriction, a number of alternative systems have been developed to allow for gradient elution.

The main method of performing a gradient elution is the step gradient SMB, essentially adding a modifier to the desorbent or reducing the amount of modifier in the feed [189]. This allows for more selective adsorption and desorption of compounds in each zone rather than relying on a single isotherm for the whole separation [189], effectively splitting the SMB into two isocratic halves: before the feed (Zones I and II), with a higher desorbing potential; and after the feed (Zones III and IV), with a lower desorbing potential. However, this step gradient SMB requires a more complicated model due to the coupling of the two isotherm equations under different modifier concentrations [190].

Linear gradients can be performed with an alternative method termed multicolumn countercurrent solvent gradient purification [191]. This method "short-circuits" some of the columns, allowing for batch gradient elution combined with SMB as well as ternary separations in a single unit operation [192]. It is worth noting that these gradient systems require additional hardware as they need a more complicated valve system allowing for independent port switching [193] relative to isocratic methods which are traditionally operated using a simpler rotary valve system [194].

The Varicol operating mode is similar to isocratic SMB but instead of a synchronous switching of all ports, the switching is non-synchronous with 4 subintervals, where some ports switch while others don't, until all ports are switched as in a normal SMB interval [195]. This method adds flexibility to the SMB system and the additional optimisation can provide productivity increases of up to 30% [179].

"Intermittent SMB" (ISMB), sometimes referred to as "Improved SMB", is another SMB operating mode used in the sugar industry [179]. Each interval is split up into

two steps: firstly, with no recycle flow in Zone IV; and secondly, with all system inlets and outlets closed, and the recycle between Zones IV and I activated. After the recycle the ports are switched one position and the process is repeated [196]. The ISMB method allows for a reduced number of columns, typically four, and a simpler setup, further reducing capital costs [175].

Other operating methods also exist such as PowerFeed, where the flow rate of the feed is modified [197]; ModiCon, where the concentration of the feed is modified [198]; and Fractionation and Feed-back SMB (FF-SMB), where the raffinate stream is fractionated within an interval and partially fed back into the feed [199].

Sequential multicolumn chromatography (SMCC) is another method that can be used for applications with high selectivities such as Protein A affinity chromatography for monoclonal antibody purification. The method features the feed passing through multiple columns until the first is fully loaded, as shown in Figure 1-13. This column is then take out of the sequence for washing, elution and regeneration while the feed is loaded directly onto the partially loaded second column [200]. The result is a much higher utilisation of the resin than in traditional batch chromatography [201].

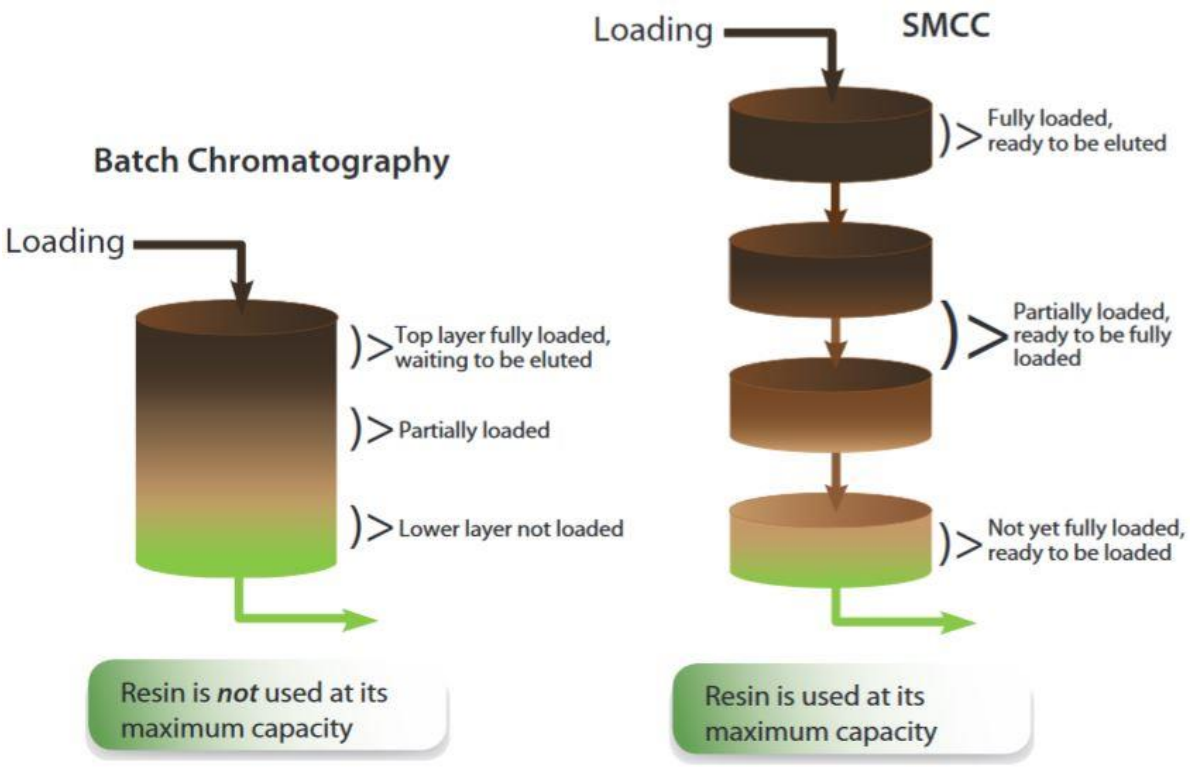

Figure 1-13: Comparison of the loading step on a batch chromatography separation and a sequential multicolumn chromatography separation (SMCC) to demonstrate the increased resin loading achievable in SMCC. From [200]**.**

These operating modes show that SMB forms the basis of a number of flexible continuous chromatographic separations. They tend to increase the degrees of freedom, possibly complicating method development, but have the potential to provide considerable improvements to the traditional isocratic SMB method.

1.6.4 Applications of SMB

SMB was originally used for the separation of petrochemicals by Universal Oil Products titled the Sorbex Process, first patented in 1961 [202]. Since then, SMB has been transferred into a much wider range of chromatographic separations, from sugars [203] (most notably for fructose-glucose separations for the production of high fructose corn syrup [168][204][205]) to xylenes [206]

While SMB has major applications in the sugar industry (where single column separations are difficult, the scales are large and the products are generally low value), it is also applied in the area of chiral separations for pharmaceuticals [175]; proteins,

for example insulin [185] and monoclonal antibodies [177]; as well as gas phase separations [207].

Isolation of other sugars and products from biomass is also a large research area such as sucrose and betaine from molasses [208][209]; dextran from fructose [210]; psicose from fructose [131]; xylose from glucose [188]; sucrose from salts [208]; fructose from cashew juice [211]; and rhamnose from xylose [212]. These SMB sugar separations primarily use cation exchange resins as adsorbents. SMB has also been used for the separation of fermentation products such as lactic acid [213] and other carboxylic acids [214]. Furthermore, research into isolating compounds from biomass hydrolysates such as ionic liquids from sugars [215][216] and other hydrolysate by-products (sulphates, acetates, furfural and HMF) from sugars [187] has been reported using SMB.

1.6.5 Simulated moving bed reactors

In addition to chromatographic separations, simulated moving bed technology has been used for reactions, termed simulated moving bed reactors (SMBR). SMBR is often applied to isomerisation or other enzyme reactions where conversions are inhibited by the presence of the product. SMBR allows for combined enzyme reaction and separation, allowing for much increased conversions in a continuous process. It has been applied to the production of *p*-xylene, combining isomerisation of xylenes into *p*-xylene and isolation of the *p*-xylene product [217]; lactosucrose, preventing the back reaction of lactosucrose and glucose into lactose and sucrose formation by separating the two products [218]; and high-fructose corn syrup production, combining inversion of sucrose and separation of fructose and glucose [219][220].

An alternative method of high-fructose corn syrup production was sought by Zhang et al. who coupled the isomerisation of glucose to fructose with the glucose-fructose separation traditionally used for high-fructose corn syrup production [221]. This allows for the direct production of 55% fructose HFCS directly from an inverted sucrose mixture of glucose and fructose. Furthermore, the overall desorbent usage is much reduced across the isomerisation and separation steps than the standard method

of producing 90% fructose via SMB and blending with 42% fructose from isomerisation.

1.7 Aim and objectives

As described in Section 1.1.2, SBP is currently a by-product from existing sugar beet biorefineries. It represents an interesting renewable feedstock due to its abundance, low cost, high in carbohydrate content and low lignin content. Current processing of SBP involves energy intensive drying and pelleting processes prior to sale as low value animal feed. Based on an integrated biorefinery approach SBP could become a significant sustainable feedstock for the production of chemical and pharmaceutical intermediates, producing a number of higher value products.

It has already been shown that steam explosion can effectively isolate the cellulose from the SBP, leaving a solubilised pectin fraction (Section 1.1.4). The cellulose can be readily broken down using commercial cellulases and fermented by yeast to produce ethanol. Meanwhile, the pectin can be broken down into its component monosaccharides by dilute acid hydrolysis; it is this hydrolysed pectin fraction that will be used as an example crude feedstock throughout this thesis. This crude hydrolysate primarily contains Ara and GA with lesser amounts of Gal and Rha as well as a number of unknown impurities (Section 1.1.4).

Current research has largely focussed on the breakdown of lignocellulosic biomass, including SBP, for the production of bioethanol (Section 1.1.1). Specifically, for SBP, the pectin is often fully hydrolysed with the cellulose for bioethanol fermentation [15]. There remains considerable potential for the pectin fraction to be separated further into its component sugars, primarily Ara and GA. These have further applications in the production of higher value products such as biopolymers [28] or therapeutic intermediates [31] (Section 1.1.6).

As described in Section 1.1, pretreatment and separation steps are key operations in overall biorefinery process design. The separation of carbohydrate components from renewable feedstocks is particularly challenging (Sections 1.3, 1.4 and 1.5). As described previously, there are a number of interesting novel separation methods for

sugar separations including centrifugal partition chromatography (CPC, Section 1.2) and simulated moving bed chromatography (SMB, Section 1.6).

CPC is a liquid-liquid chromatography technique (Section 1.2) for which there has been little previous work on the separation of highly hydrophilic compounds such as carbohydrates (Section 1.2.5). However, its ability to process contaminated crude feed streams without prior clean-up [32] could be a major benefit to the processing of SBP hydrolysates within the context of an integrated biorefinery. In contrast, SMB technology (Section 1.6) uses traditional resin-based chromatography columns in a multicolumn, continuous setup to maximise productivity and product purity [179]. It is already well established within the sugar industry, however, its application tends to focus on separating sugars from sugar juices, such as glucose-fructose separations [211], which tend to be 'cleaner' process streams than waste stream hydrolysates. The application of SMB to separating sugars from hydrolysates is much less explored because of the pretreatment necessary to remove the contaminating compounds (Section 1.3). Both CPC and SMB will be examined in this thesis as potential separation technologies to facilitate the utilisation of SBP pectin components.

The aim of this thesis is to establish novel, scalable separation pathways for the isolation of the component monosaccharides from crude hydrolysed sugar beet pulp pectin. The specific objectives are outlined below. Figure 1-14 provides a diagrammatic overview of the two process options, CPC and SMB, and highlights their relation to each chapter.

- To develop a method for separating a model synthetic mixture of the monosaccharides in hydrolysed SBP pectin using CPC. This will involve the development of a two-phase system capable of partitioning the monosaccharides and demonstration separations of a synthetic monosaccharide mixture. This work is described in Chapter 3.
- To demonstrate the potential of the CPC method developed in Chapter 3 to the processing of crude SBP hydrolysates. This will involve modification of the sample preparation methods to accommodate differences between the synthetic and crude hydrolysate mixtures as well as studies on optimisation and scale-up

of operating conditions to increase experimental throughput and yield. This work is described in Chapter 4.

- To develop a method for isolating L-arabinose from a synthetic neutral mixture of the neutral sugars in hydrolysed SBP pectin using SMB. This will involve resin and condition screening in single column runs before an 8 column SMB separation. An SMB model will be used to predict SMB operating conditions in both a 4-zone and 3-zone setup. These conditions will be tested and optimised based on experimental results. This work is described in Chapter 5.
- To develop a method of isolating D-galacturonic acid from a synthetic crude mixture and develop pretreatment methods to move towards complete processing of the crude hydrolysate. This will involve examining suitable anion exchange resins for D-galacturonic acid isolation and activated carbon and various resins for decolourisation of contaminants from the crude hydrolysate. It will also look at incorporating the decolourisation and D-galacturonic acid isolation from this chapter with the SMB separation of L-arabinose developed in Chapter 5. This work is described in Chapter 6.

In addition, Chapter 2 describes all the equipment, methods and analytical techniques used in this thesis. Finally, Chapter 7 provides an overall summary and comparison of the two separation approaches and suggestions for further work.

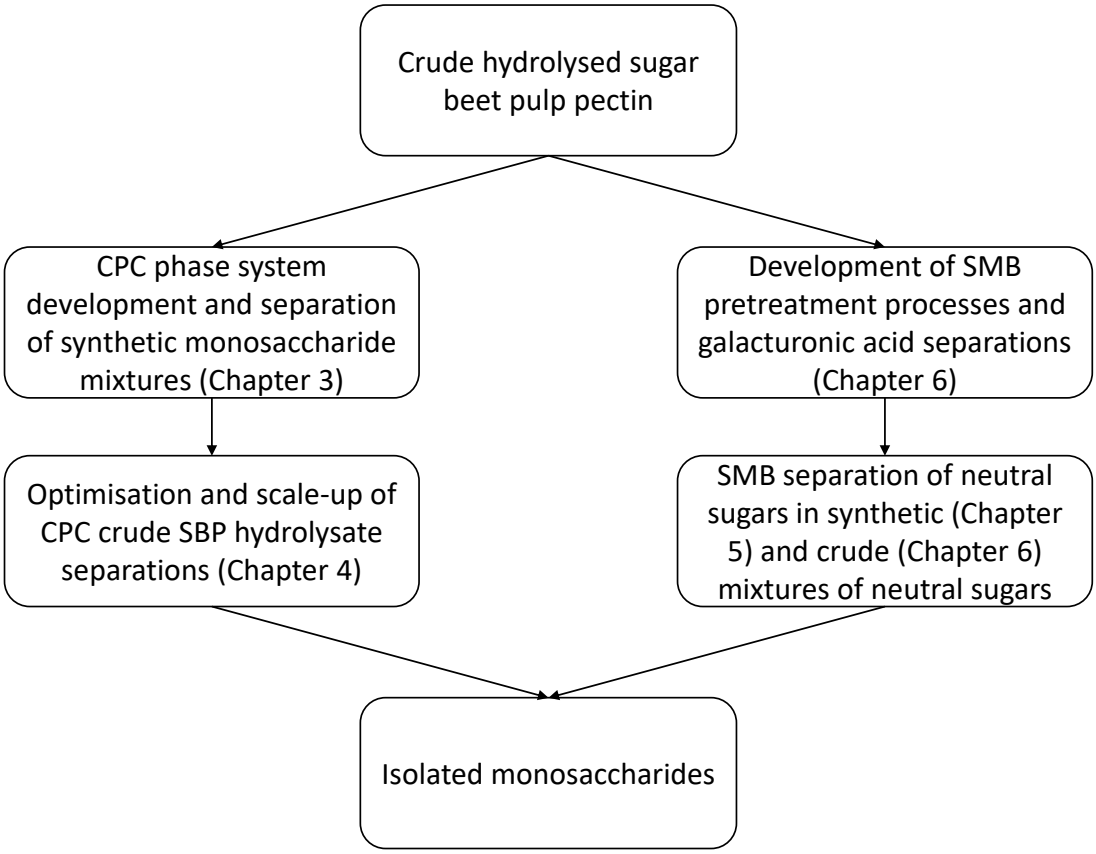

Figure 1-14: Overview of the two process options and experimental strategies pursued in this thesis.

Chapter 2 Materials and Methods

2.1 Reagents

The sugars L-arabinose (99% w/w), L-rhamnose (99% w/w), D-galacturonic acid sodium salt (98% w/w) and D-galactose (99% w/w) were purchased from Sigma-Aldrich (Gillingham, UK). The solvents acetonitrile, methanol, n-propanol, n-butanol, ethyl acetate and hexane were also purchased from Sigma-Aldrich. Dimethyl sulfoxide (DMSO) (99%) and sodium acetate trihydrate (HPLC grade) were purchased from Fisher (Loughborough, UK). Aliquat 336, sodium iodide and trifluoroacetic acid (TFA) were purchased from Sigma-Aldrich. Absolute ethanol was purchased either from Fisher or Sigma-Aldrich. Water was purified to 18.2 MΩ by either a Millipore Synergy UV Water Purification System (Watford, UK) or a Purite Select Fusion purification system (Thame, UK).

The resins Dowex 50W X2 (200-400), Dowex 50W X4 (200-400) and Dowex 50W X8 (200-400) were purchased from VWR (Lutterworth, UK). Dowex Monosphere 99 320/Ca was provided courtesy of the DOW Chemical Company (Chauny, France). Calcium chloride dihydrate was purchased from VWR (Lutterworth, UK). Glacial acetic acid was purchased from Sigma-Aldrich (Gillingham, UK).

The resins Marathon A, Marathon A2, Marathon C and Marathon MSA were purchased from Sigma-Aldrich. The resins Amberlite IRA-400 and Dowex 1x8 (200-400 mesh) were purchased from VWR. Activated carbon (Darco 100 mesh) was purchased from Sigma-Aldrich. NaOAc was purchased from Fisher Scientific. NaCl and NaOH were purchased from VWR.

2.2 CPC phase system development and solute partition coefficients

Two-phase systems were prepared by combining all components in the specified volume ratios, mixing to allow dissolution of any precipitated salts, and were then left to settle for 2 hours in a separation funnel prior to separation of the two phases. In each case the volumes of the upper phase (UP) and lower phase (LP) were recorded and the

interface was discarded. The fraction of LP to the total volume is referred to as the LP volume fraction and expressed as a decimal fraction between 0 and 1.

Settling times were measured by adding 2 mL of each separated phase into a test tube, vortexing for 15 seconds, and measuring the time taken to settle completely; defined as the appearance of a distinct, flat interface. Three repeats were performed for each phase system.

Solute equilibrium partition coefficients (K) were individually determined for the sugars (Rha, Ara, Gal and GA) by adding 10 mg of the sugar to 2 mL of the LP and leaving to dissolve completely. 1 mL of this solution was added to 1 mL of the UP, and thoroughly mixed for 45 min to reach equilibrium. The partition coefficients were calculated using Equation 2-1, where C_{LP} and C_{UP} are the concentrations in the lower and upper phases respectively. C_{LP} and C_{UP} were determined by HPLC-RI, as described in Section 2.8.1.

$$K = \frac{C_{LP}}{C_{UP}} \qquad \textbf{Equation 2-1}$$

Separation factors (α) between two solutes were calculated using the partition coefficients of each solute (K_1 and K_2) using Equation 2-2. The solutes are categorised such that $K_1 > K_2$ and thus $\alpha > 1$. Unless otherwise stated, separation factors are given relative to Ara, meaning that Ara is one of the two solutes.

$$\alpha_{1/2} = \frac{K_1}{K_2} \qquad \textbf{Equation 2-2}$$

A number of phase systems were considered in this study. Initially, solvent-based phase systems were explored comprising either a traditional HEMWat system (hexane : ethyl acetate : methanol : water 1:5:1:5 v:v:v:v) or a polar EBuWat (ethyl acetate : butanol : water 0:1:1 v:v:v) system. HEMWat 1:5:1:5 is near the polar end of the HEMWat phase system family and EBuWat is the most polar of the EBuWat phase system family (see Section 1.2.4) [37]. Following this, a number of ammonium-

sulphate based phase systems were used in order to increase the partition coefficients of the sugars. The phase systems investigated are detailed in Table 2-1.

Table 2-1: Summary of the highly polar phase systems investigated for fractionation of crude hydrolysed SBP pectin. Values represent volumetric ratios of solvents used in phase system preparation. Phase systems were formed as described in Section 2.2.

Phase system	Hex	EtOAc	MeOH	EtOH	PrOH	BuOH	DMSO	ACN	Sat. AS	2 M AS	Water	2 M AS +1% TFA
HEMWat 1:5:1:5	1	5	1	-	-	-	-	-	-	-	5	-
EBuWat 0:1:1	-	-	-	-	-	1	-	-	-	-	1	-
I	-	-	-	3	-	-	-	-	-	4	-	-
I + TFA	-	-	-	3	-	-	-	-	-	-	-	4
II	-	-	-	3	-	-	-	-	-	5	-	-
II + TFA	-	-	-	3	-	-	-	-	-	-	-	5
III	-	-	-	3	-	-	-	-	-	6	-	-
IV	-	-	-	-	1	-	-	0.5	1.2	-	1	-
V	-	-	-	0.5	0.5	-	-	0.5	1.2	-	1	-
VI	-	-	-	0.5	-	0.5	-	0.5	1.2	-	1	-
VII	-	-	-	1	-	-	-	-	1	-	0.8	-
VIII	-	-	-	0.8	-	-	-	-	1	-	0.8	-
IX	-	-	0.1	0.8	-	-	-	-	1	-	0.8	-
X	-	-	-	0.5	-	-	-	0.5	1	-	0.8	-
XI	-	-	0.2	0.5	-	-	-	0.5	1	-	0.8	-
XII	-	-	0.4	-	-	-	-	0.5	1	-	0.8	-
XIII	-	-	-	-	-	-	0.3	0.5	1	-	0.8	-
XIV	-	-	-	0.6	-	-	0.1	-	1	-	0.8	-
XV	-	-	-	0.8	-	-	0.1	-	1	-	0.8	-

Hex, hexane; ETOAc, ethyl acetate; MeOH, methanol; EtOH, ethanol; PrOH, n-propanol; BuOH, n-butanol; DMSO, dimethyl sulfoxide; ACN, acetonitrile; Sat. AS, saturated amomnium sulphate; 2 M AS, 2 molar ammonium sulphate; TFA, trifluoroacetic acid.

Saturated ammonium sulphate was prepared by adding 550 g of ammonium sulphate to warm deionised water until it completely dissolved. This solution was then made up to 1 L before cooling to room temperature overnight and the supernatant decanted. A 2 M ammonium sulphate solution was prepared by fully dissolving the required amount of ammonium sulphate in water and making up to the desired total volume. For phase systems containing TFA, 1% (v/v) TFA was added to the 2 M AS prior to formation of the phase system.

A solution of saturated ammonium sulphate and water (1.0:0.8 v:v) was gravimetrically determined (see Section 2.8.2) to have a concentration of approximately 300 g L^{-1}. This concentration was used with a relative volume of 1.8 when preparing phase systems for CPC separations using phase systems VIII and XV in order to reduce phase system preparation time and improve batch to batch consistency. Phase system XV can thus be expressed as ethanol : 300 g L^{-1} aqueous ammonium sulphate (0.8:1.8 v:v).

Additionally, an ion-exchange based phase system was examined, based on a butanol : water (1:1 v:v) phase system with the use of Aliquat 336 as an ion exchanger in the UP (UP-Exch) and NaI as a displacer in the LP (LP-disp). A phase system containing no ion exchanger or displacer was first prepared and the two phases separated. Ara and GA (2.5 mM of each) were added to the LP. The UP-Exch was prepared by adding 25 mM of Aliquat 336 (10 times the concentration of GA) to a portion of the separated UP. The LP-Disp was prepared by adding 50 mM NaI (twice the concentration of ion exchanger in the UP-Exch) to a portion of the LP containing Ara and GA. There were therefore four phases: UP; LP; UP-Exch; and LP-Disp. Partition coefficients for this system were determined in three separate mixtures simulating the conditions in ion exchange CPC: UP – LP (normal partitioning when not in ion exchange mode); UP-Exch – LP (exchange of the GA into the UP); and UP-Exch – LP-Disp (displacement of the exchanged GA back into the LP). In each case, the sample was introduced in the LP and partition coefficients determined as described in Equation 2-1. Settling times were also determined as stated previously.

2.3 Ethanol : ammonium sulphate : water ternary phase diagram

A ternary phase diagram was established for ethanol : ammonium sulphate : water phase systems by adding ethanol, saturated ammonium sulphate and water in various volumetric ratios and observing the phase behaviour and settling times at room temperature. The mass ratios of each component were then calculated, taking into account the fact that the saturated ammonium sulphate contained both water and ammonium sulphate. Phase systems were categorised as ‘single-phase’, ‘two-phase’ or ‘precipitate’. ‘Precipitate’ describes any phase system where salt precipitation was observed, even if two immiscible liquid phases were still present, as these systems are not suitable for CPC operation due to the likelihood of precipitate formation within the column.

2.4 Centrifugal partition chromatography equipment

Centrifugal partition chromatography (CPC) was performed on an FCPC-A machine (fast centrifugal partition chromatography – Roussalet Robatel Kromaton, Annonay, France).

The CPC was connected to one of two pumping and fraction collection setups. Firstly, in Chapter 3, it was connected to an Agilent G1361A preparative pump and an Agilent G1364B fraction collector (Agilent Technologies UK, Cheadle, UK). Secondly, in Chapter 4, it was connected to a puriFlash 450 system (Interchim, Montluçon, France), which provided a pump, injection valve and fraction collector.

Two columns were used; a semi-preparative and a preparative one, detailed in Table 2-2. Both columns feature a twin-cell design (Figure 1-6 in Section 1.2.2). Total volumes were experimentally determined for each column by filling the column with the LP of phase system VIII (prepared as described in Section 2.2) and eluting with the UP in the descending mode at a rotational speed of 1000 rpm. The total LP collected gives the total volume of the column. The reverse process was performed as a control, by filling the column with the UP and eluting with the LP in the ascending mode at 1000 rpm. These experiments were performed with the minimal possible extra tubing volume either side of the column.

Table 2-2: Volumes of the two CPC columns based on manufacturer provided data and experimentally determined data (determined as described in Section 2.4).

Column	Manufacturer stated volume (mL)	Manufacturer cell volume (mL)	Manufacturer total volume (mL)	Number of cells	Experimental total volume (mL)
Semi-prep.	200	268	205	840	250
Preparative	1000	1049	863	800	950

For experiments performed using the Agilent pump system in Chapter 3, a sample loop of 10.8 mL was used for sample injection. Fractions were collected every 0.6 min into 5 mL test tubes from 15 min after the sample injection.

For experiments performed using the puriFlash Interchim pump system in Chapter 4, various sample loop volumes were tested. On the semi-preparative column, sample loops of 10, 20 30 or 40 mL were used with fractions collected every 2 min in the ascending mode and every 1 min in the descending mode. The ascending and descending mode are discussed in Section 1.2.3.2. Operating conditions and fraction collection for the preparative column are described in Section 2.6. All fractions were immediately sealed and kept at 4°C for subsequent analysis.

For separations performed on the semi-preparative column, a mobile phase flow rate of 8 mL min^{-1} and a rotational speed of 1000 rpm were used unless otherwise stated. Operating conditions for the preparative column are discussed in Section 2.6.

2.5 CPC operating conditions

2.5.1 Stationary phase retention

Stationary phase retention studies were performed in the ascending mode on the semi-preparative column at various flow rates (2, 4, 8, 12 and 16 mL min^{-1}) at 1000 rpm and various rotational speeds (600, 800, 1000, 1500 and 2000 rpm) at 8 mL min^{-1} and observing the total elution volume of stationary phase (V_E) at initial mobile phase breakthrough. The stationary phase retention (S_F) was then calculated using the total column volume (V_C), given in Table 2-2, and the total dead volume (V_D) either side of the column, according to Equation 2-3.

$$S_F = \frac{V_C - V_E + V_D}{V_C}$$ **Equation 2-3**

For CPC separations with the sample prepared in the mobile phase, Equation 2-3, was used to calculate the stationary phase retention, whereas, for CPC separations with the sample prepared in the mobile phase, Equation 2-4, was used to calculate the stationary phase retention, taking into account the injection volume (V_I).

$$S_F = \frac{V_C - V_E + V_I + V_D}{V_C}$$ **Equation 2-4**

The stationary phase retention values are calculated at the initial mobile phase breakthrough except where stated. The stationary phase retention throughout a CPC separation can be estimated by summing the volume of stationary phase in collected fractions to give a value for V_E. The equilibration S_F values are defined as the S_F when no further stationary phase is observed in the collected fractions.

2.5.2 Operating methods

All CPC separations were performed in the ascending mode unless explicitly described as being performed in the descending mode. Ascending and descending modes are described in Section 1.2.3.2. Ascending mode separations used the LP as the stationary phase and the UP as the mobile phase; descending mode separations used the UP as the stationary phase and the LP as the mobile phase. All separations were performed without establishing hydrodynamic equilibrium prior to separation. Samples were thus injected with the first introduction of mobile phase to the column. Sample preparation methods are discussed in 2.7.

Both the semi-preparative and preparative columns were filled by pumping the appropriate stationary phase for the operating mode used for the separation (LP in the ascending mode for ascending mode separations, or UP in the descending mode for descending mode separations). The stationary phase was pumped at a flow rate of 20 mL min^{-1} at a rotational speed of 600 rpm.

The elution-extrusion mode, described in Section 1.2.7, was performed by switching from pumping the mobile phase (UP) to the stationary phase (LP) after 72 min on both the semi-preparative and preparative columns. With the change in phase, the flow rate is kept constant (8 mL min^{-1} on the semi-preparative column, as described in Section 2.4, and 30.4 mL min^{-1} on the preparative column, as described in Section 2.6).

Sequential injections (sequential elution-extrusion) were performed on the semi-preparative column using 30 mL of crude sample prepared in the UP as described in Section 2.7.3. Sequential injections were performed using the elution-extrusion mode. Extrusion was performed after 72 min, as described above, and stopped after a further 28 min when the flow was switched back to the mobile phase. The next sample was immediately injected and the elution-extrusion process was repeated. This gave a total run time of 100 min per sample. A total of 3 sequential injections were performed.

2.6 CPC scale-up

Scale-up between the semi-preparative and preparative columns (detailed in Table 2-2) was performed linearly using the experimentally determined total column volumes based on work by Sutherland et al. [70]. Scale-up methods in CPC are discussed further in Section 1.2.6. The ratio of total volumes gives a scale-up factor of 3.8 which was used to linearly scale-up the mobile phase flow rate (from 8 to 30.4 mL min^{-1}) and sample volume (from 40 to 152 mL). Both columns have the same diameter and so rotational speed was kept constant in order to maintain the same g-force between scales. Fractions were collected every 1.5 min from the start of separation giving a volume of 45.6 mL per fraction. During the elution-extrusion mode, the extrusion step was performed after 72 min, as on the semi-preparative column, and the flow rate was kept constant at 30.4 mL min^{-1} with the change in phase.

2.7 Sample preparation

2.7.1 Crude hydrolysate

Fully hydrolysed, crude SBP pectin (“crude hydrolysate”) was prepared and donated by the Department of Biology and Biochemistry at the University of Bath, UK. The cellulose was fractionated from the SBP by steam explosion, described by Hamley-

Bennett et al. [17], which solubilised the pectin fraction. This pectin fraction was then fully hydrolysed by adding H_2SO_4 up to 2.5% (v/v) and heating to 121°C in an autoclave before adjusting to pH 6 with NaOH. The crude contained a total dissolved solids content of ~100 g L^{-1} with a total sugar concentration of ~20 g/L^{-1}. It is worth noting that there was some batch to batch variation in the total dissolved solids content, the total sugars concentration and the relative concentrations of the individual sugars in the crude.

Figure 2-1: Photograph of fully hydrolysed, crude SBP pectin (crude hydrolysate).

2.7.2 Synthetic CPC samples

Two types of synthetic samples were employed with different monosaccharide compositions: an 'illustrative mixture' of Rha, Ara and GA, and a 'model synthetic mixture' of Ara, GA, Gal and Rha. Both synthetic samples were prepared by dissolving the sugars directly in the UP, unless explicitly stated, before being made up to the desired final volume with additional phase. All synthetic samples were filtered through a 0.45 µm syringe filter (Millex hydrophilic polyvinylidene fluoride syringe filter, Millipore, Watford, UK) prior to injection.

The illustrative mixture was prepared with Rha, Ara and GA at 50 g L^{-1} of each, giving a total dissolved sugars concentration of 150 g L^{-1}. The model synthetic mixture was prepared with a monosaccharide composition of 43, 41, 11 and 5 g L^{-1} of Ara, GA, Gal and Rha respectively, giving a total concentration of 100 g L^{-1}. These values were chosen prior to receiving the crude hydrolysate and so were based on the relative values of the sugars found in SBP by Micard et al. [7], with the exclusion of glucose based on the assumption of complete cellulose removal in the steam explosion step.

2.7.3 Crude CPC samples

Crude samples were prepared for CPC separation in four different ways described below:

1. No additional preparation.
2. Preparation in the UP: 44% (v/v) ethanol and 54 g L^{-1} ammonium sulphate
3. Preparation in a lower salt modified UP: 44% (v/v) ethanol and 25 g L^{-1} ammonium sulphate
4. Preparation in the LP: 13% (v/v) ethanol and 332 g L^{-1} ammonium sulphate

To maximise the solute dissolved in the sample, the crude solution took the place of water during phase system preparation. Ammonium sulphate was first dissolved in a small amount of crude before the required amount of ethanol was added. More crude was then added slowly to dissolve any precipitated salts caused by the addition of ethanol, and then up to the desired final volume. All crude samples were filtered through a 0.45 µm filter prior to injection, as described in Section 2.7.2.

2.7.4 SMB samples

For single column screening and SMB separations, samples were prepared by dissolving the required monosaccharides in a minimal volume of water and topping up to the desired volume in a volumetric flask.

For single column screening experiments, individual samples were prepared for each sugar at a concentration of 10 g L^{-1}. Additionally, a mixed sample was prepared with

a concentration 10 g L^{-1} of each sugar (Rha, Ara and Gal). Blue dextran solution was prepared by first dissolving the blue dextran in a minimal volume of water; subsequently an appropriate volume of water was added to reach the desired concentration (1% w/v).

For SMB separations, a "synthetic neutral mixture" was prepared at a concentration of 13 g L^{-1} Ara, 3 g L^{-1} Gal, and 1 g L^{-1} Rha. These concentrations were selected as representative of the neutral sugars in the crude hydrolysate batch (determined as described in 2.8.3).

2.7.5 Samples for the isolation of D-galacturonic acid

Samples for the isolation of GA from the neutral sugars were prepared by dissolving the required monosaccharides in a minimal volume of water and topping up to the desired volume in a volumetric flash.

For resin ionic form screening, a "synthetic crude mixture" was prepared based on the sugars composition of the crude hydrolysate and consisted of 13 g L^{-1} Ara, 3 g L^{-1} Gal, 1 g L^{-1} Rha, and 5 g L^{-1} GA. This synthetic crude mixture is similar to the synthetic neutral mixture described in Section 2.7.4.

2.8 Analytical methods

2.8.1 HPLC-RI

For partition coefficient calculations, concentrations of sugars were determined by HPLC using a Dionex P680 HPLC pump, an ASI-100 autosampler injector (Dionex, Hemel Hempstead, UK) and an Aminex-87H column (Bio-Rad, Watford, UK) kept at 60°C. A mobile phase of 5 mM H_2SO_4 was used with an isocratic elution at 0.6 mL min^{-1} for 30 min. An injection volume of 10 µL was used and a refractive index (RI) detector (Shodex RI-101 (Shodex, Munich, Germany)) was used to monitor the separation. Quantitative analysis was performed by the integration of peak areas using the external standard method. Calibration was run daily due to small variations in the retention times. An example chromatogram and example calibration curves are shown in Figure A-1 Figure A-2 respectively in Appendix A.

This HPLC method was also used for the determination of ethanol and DMSO concentrations in each phase. An example chromatogram showing the retention of ethanol and DMSO is shown in Figure A-3 in Appendix A, with example calibration curves shown in Figure A-4.

2.8.2 Gravimetric analysis

Gravimetric analysis was of dissolved solids was performed by drying 0.5 mL of a solution in an oven overnight at 100°C and measuring the remaining mass.

2.8.3 Ion Chromatography (ICS)

Ion chromatography (ICS) was performed for the quantitative analysis of CPC fractions containing multiple sugar species. It was performed using a Reagent-Free Ion Chromatography System (ICS 5000+, Thermo Scientific, Hemel Hempstead, UK) fitted with either a CarboPac PA1 (4 x 250 mm) (Thermo Scientific) with corresponding guard column (4 x 50 mm) in Chapter 3 and an AminoPac PA10 (2 x 250 mm) (Thermo Scientific) with corresponding guard column (2 x 50 mm) in Chapter 4. For both columns, an injection volume of 10 µL and a column temperature of 30°C were used. An electrochemical detector system (gold detector) was used for detection. Quantitative analyses were performed measuring peak height or area using the external standard method. Calibration curves were performed daily due to variations in the retention times over many injections. Example chromatograms are shown in Figure A-5 to Figure A-10 in Appendix A with example calibration curves shown in Figure A-11 and Figure A-12.

For quantification of neutral sugars (Ara, Rha and Gal), 15 or 7.5 mM KOH was used, generated by a KOH 500 eluent generator cartridge. A flow rate of 1.5 mL min^{-1} was used with the CarboPac PA1 column. On the AminoPac PA10 column, a flow rate of 0.25 mL min^{-1} was used.

For quantification of GA on the CarboPac PA1, a mobile phase of 25% 0.5 M aqueous sodium acetate, 75% water at 1 mL min^{-1} was used, with a GA retention time of 3.0 min. On the AminoPac PA10, a mobile phase of 5% 1 M aqueous sodium acetate, 95% water was used.

All CPC fractions were diluted with Milli Q water to “break” any two-phase systems which formed as a result of stationary phase bleed from the column, ensuring that the analytical methods were not affected by solute partitioning.

Purity and recovery from CPC separations were calculated from ICS analysis. Recovery is defined as the mass of the target monosaccharide in a pooled fraction as a percentage of the mass of the same target monosaccharide in all fractions. Purity is defined as the mass of the target monosaccharide in a pooled fraction as a percentage of the mass of all the monosaccharides in that same pooled fraction. Both purity and recovery values are based on optimised pool fraction times to maximise their values and are given as percentages (w/w).

2.8.4 Conductivity

Conductivities of solutions were measured using a Mettler Toledo Seven2Go S3 conductivity probe.

2.8.5 UV scanning

UV scanning was performed on a Tecan Infinite M200 microplate reader, with a scan range of 230-400 nm, a step length of 2 nm, and 5 flashes per well.

2.9 SMB resins and column packing

2.9.1 Resin preparation

The resins examined for SMB separation in Chapter 5 are shown in Table 2-3. The number at the end of the three Dowex 50W X resins represents different crosslinking percentages. All resins used are made up of a polystyrene matrix with divinylbenzene crosslinking. Resin masses were measured directly from their container as shipped with no prior hydration or change in ionic form. Once weighed, the resins were hydrated in deionised water in a beaker for 2 hours.

Table 2-3: SMB resins examined in batch experiments for resin and condition screening in Section 5.2.

Resin	Particle size (μm)	Ionic form as shipped
Dowex 50W X2	37-74	H^+
Dowex 50W X4	37-74	H^+
Dowex 50W X8	37-74	H^+
Monosphere 99	320	Ca^{2+}

The hydrated resins were then poured directly into a column (GE XK16/20 with a packing reservoir funnel attached) half-filled with deionised water. This column has an internal diameter of 1.6 cm. The resin was left to settle for 30 min and the top adapter connected with the plunger adjusted to approximately 2 cm above the resin bed. The column was then attached to an Akta Purifier system (GE Healthcare, Little Chalfont, UK) with a conductivity detector. The ionic form was modified by pumping 0.2 M of the desired ion (acetic acid for conversion to H^+ form, $CaCl_2$ for conversion to Ca^{2+} form) at 5 mL min^{-1} and waiting for the eluate conductivity to become constant. Excess ions were removed by pumping deionised water through the column until the conductivity again became constant.

2.9.2 Column packing

A resin-containing column, prepared as described in Section 2.9.1, was packed by removing the top adapter, topping up the column with deionised water and reattaching the top adapter to attain the maximum total column volume with no air bubbles. The column was then vigorously shaken until the resin formed a homogenous slurry within the column and then left vertical for 1 hour to settle. The column was then attached to the Akta Purifier system and deionised water passed through the column at 10 mL min^{-1} for 20 min. The top adapter was then adjusted to the top of the packed bed of resin.

2.10 SMB resin and condition screening

For batch experiments, 20 g of each resin was prepared in the appropriate ionic form and packed into a column as described in Sections 2.9.1 and 2.9.2. For the three Dowex 50W resins, both the H^+ and Ca^{2+} ionic forms were examined. For the Monosphere 99 resin, only the Ca^{2+} form was examined. All resins and their various ionic forms were examined at both room temperature and 50°C. The column temperature was elevated to 50°C by heating water in a water bath to 55°C and using a peristaltic pump to feed

the heated water to the column temperature-control jacket, recycling the water from the jacket outlet. By using a water bath temperature of 55°C, the temperature of the water leaving the temperature reached a steady state value of 50°C.

The column was connected to a Semba Octave 100 pump with a manual injection valve (with 100 µL loop) prior to the column and a Shimadzu RID-20A RI detector (Shimadzu, Milton Keynes, UK) after the column. Water at a flow rate of 2 mL min^{-1} was used as the mobile phase. For experiments at 50°C the mobile phase bottle was placed in the water bath used for heating the column. 100 µL injections were performed and retention times measured on the RI detector. Solutions of individual sugars (Ara, Gal, Rha or Glu) and blue dextran were prepared as described in Section 2.7.4.

Retention times were taken from the peak maximum time from the RI detector. Retention factors (k_i^R) for each sugar were calculated using the blue dextran retention time (t_0) as a void volume marker according to Equation 2-5, with the retention time of compound "i" (t_i).

$$k_i^R = \frac{t_i - t_0}{t_0} \qquad \textbf{Equation 2-5}$$

The selectivity (α^R) of the separation between two sugars was calculated according to Equation 2-6. In Chapter 5, the selectivity values are always given relative to Ara with Ara being the numerator in Equation 2-6. The "selectivity of Gal" therefore refers to the selectivity between Gal and Ara, with k_1^R as the retention factor for Ara, and k_2^R as the retention factor of Gal.

$$\alpha^R = \frac{k_1^R}{k_2^R} \qquad \textbf{Equation 2-6}$$

2.11 SMB column packing comparison

Once a desired resin and operating condition was selected, 28 g of the selected resin (Dowex 50W X8 (200-400)), exchanged into the desired ionic form (Ca^{2+}), was packed

onto 8 columns as described in Section 2.9. Blue dextran, Ara, Rha and Gal samples, prepared as described in Section 2.7.4, were loaded onto each column at room temperature and the retention times, retention factors and selectivities of each sugar were calculated as described in Section 2.10.

To compare the 8 columns, the retention times, retention factors and selectivities of each sugar, and the retention times of blue dextran were examined. The mean values (μ) and population standard deviations (σ) were calculated and used to calculate the relative standard deviations (RSD) as a percentage. These relative standard deviation values were used to directly compare the columns.

$$RSD = \frac{\sigma}{\mu} \cdot 100\% \qquad \textbf{Equation 2-7}$$

2.12 SMB equilibrium theory model

2.12.1 SMB Model inputs

The SMB equilibrium theory model uses data from the resin and condition screening tests, described in Section 2.10, to predict the outcome of SMB separation on the longer columns, as described in Section 2.11. The following input data is required from the batch experiments: column diameter (C_D), column length (C_L), flow rate (Q), retention times of the sugars (t_i), retention time of blue dextran (t_0), and the extra dead volume around the column (V_D).

For all these experiments, a column with a diameter of 1.6 cm (GE XK16/20) was used and the column length was calculated to the top of the resin bed. A flow rate of 2 mL min^{-1} was used for all batch experiments as described in Section 2.10. The retention times were also calculated as described in Section 2.10. The extra dead volume was estimated using the height between the top of the packed bed and the top adapter, and the volume of extra column tubing.

Adjusted retention times (t_i') were calculated for the sugars, using Equation 2-8, and for blue dextran (t_0'), using Equation 2-9, to remove the time added by the dead volume. This is important to calculate the effect of just the column on the retention times through adjusted retention factors and Henry constants. These values are independent of both the column dimensions and the dead volume either side of the column.

$$t_i' = t_i - \frac{V_D}{Q} \qquad \textbf{Equation 2-8}$$

$$t_0' = t_0 - \frac{V_D}{Q} \qquad \textbf{Equation 2-9}$$

Adjusted retention factors ($k_i^{R\prime}$) were calculated using Equation 2-10. In order to calculate the Henry constants, the void fraction (ε) of the resin was required, calculated using Equation 2-11. The Henry constants were thus calculated using Equation 2-12 based on the assumption that the isotherms are linear [183][184].

$$k_i^{R\prime} = \frac{t_i' - t_0'}{t_0'} \qquad \textbf{Equation 2-10}$$

$$\epsilon = \frac{F \cdot t_0'}{V_C} \qquad \textbf{Equation 2-11}$$

$$\frac{\epsilon}{1-\epsilon} \cdot k_i^{R\prime} = H_i \qquad \textbf{Equation 2-12}$$

The adjusted selectivity ($\alpha^{R\prime}$) can then be calculated from either the adjusted retention factors or the Henry constants using Equation 2-13.

$$\alpha^{R\prime} = \frac{k_1^{R\prime}}{k_2^{R\prime}} = \frac{H_1}{H_2}$$ **Equation 2-13**

These Henry constant values form the basis of the SMB equilibrium theory model and are used for defining limits on operability (m_2 and m_3) which allow for theoretical separation of the compounds. The SMB model uses two Henry constants, one for the slower eluting compound and one for the faster eluting compound. As the target SMB separation is to isolate Ara from Rha and Gal, the Henry constants of Ara and the closest eluting other sugar were used, with the order of Henry constants in the adjusted selectivity calculation given such that the value is greater than 1.

2.12.2 SMB equilibrium theory model

2.12.2.1 General considerations

The SMB equilibrium theory model uses the Henry constants, calculated as described in Section 2.12.1, and relevant inputs (C_L, C_D and V_D) from the longer columns for SMB separation, packed as described in Section 2.11. The two SMB zone setups (4-zone closed loop and 3-zone open loop) use different experimental configurations and so, while each model is similar, there are some differences between them including the number of variables. The 4-zone model is described in Section 2.12.2.2 and the 3-zone model is described in Section 2.12.2.3. Both models are based on the equilibrium theory, first proposed by Storti et al. [222] and further adapted by a number of authors including Rajendran [182] for SMB separation with linear isotherms.

2.12.2.2 4-zone, closed loop SMB model

For the 4-zone, closed loop SMB setup, there are 4 main variables: switch time (T_S), feed flow rate (Q_F), desorbent flow rate (Q_D), extract flow rate (Q_E), and recycle flow rate (Q_{Rec}). The flow rate in the raffinate (Q_{Raf}) can thus be calculated from an input = output flow rate balance, as described in Equation 2-14.

$$Q_F + Q_D = Q_E + Q_{Raf}$$ **Equation 2-14**

The 4-zone setup operates in a closed loop with an internal recycle between zones 4 and 1, fed by a recycle pump before zone 1 (shown in Figure 2-2). The flow rates (Q_n) in each zone (n), shown in Equations 2-15 to 2-18, can be calculated by looking at the inputs of each zone.

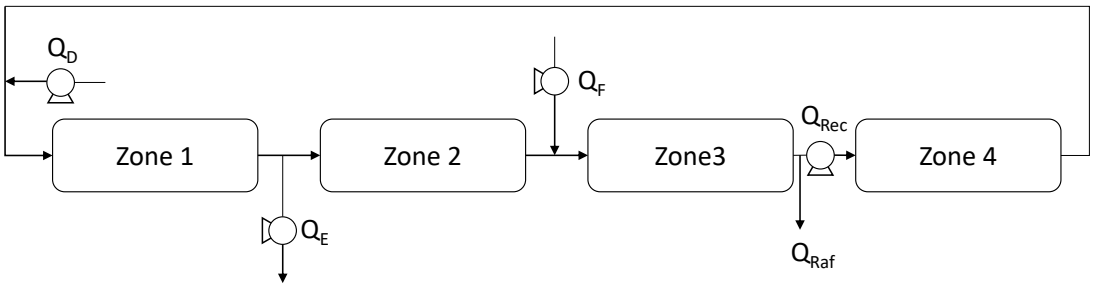

Figure 2-2: Overview diagram of pumps and zones within the 4-zone SMB setup.

$$Q_1 = Q_D + Q_{Rec}$$ **Equation 2-15**

$$Q_2 = Q_D + Q_{Rec} - Q_E = Q_1 - Q_E$$ **Equation 2-16**

$$Q_3 = Q_D + Q_{Rec} - Q_E + Q_F = Q_2 + Q_F$$ **Equation 2-17**

$$Q_4 = Q_{Rec}$$ **Equation 2-18**

Using the flow rate in each zone it is possible to calculate the flow rate ratios (m_n) in each zone (n) which can be compared with the Henry constants in order to predict SMB performance. Flow rate ratios (or m-values) are calculated using Equation 1-8, taking into account the void fraction (ε) and, additionally, the dead volume.

$$m_n = \frac{Q_n T_S - C_V \epsilon - V_D}{C_V(1-\epsilon)}$$ **Equation 2-19**

Successful SMB operation is modelled using these flow rate ratios and the Henry constants according to Equation 2-20 where H_1 is the lower value Henry constant (faster eluting) and H_2 is the higher value Henry constant (slower eluting). Plotting the m_2 and m_3 values on the m_2-m_3 plane with the Henry constant constraints gives an operating triangle where both the extract and raffinate should be pure. This is described in further detail in Section 1.6.2.

$$m_1 > H_2 > m_3 > m_2 > H_1 > m_4 \qquad \textbf{Equation 2-20}$$

2.12.2.3 3-zone, open loop SMB model

The 3-zone, open loop SMB model is very similar to the 4-zone SMB model with some modifications. The recycle loop is removed (and the recycle pump) and so the SMB operates in an open loop format. The overview schematic demonstrating the pumps, zones, inputs and outputs is shown in Figure 2-3 and the flow rates in each zone are redefined in Equations 2-21 to 2-23. The removal of the recycle pump means that the 3-zone SMB has one fewer variable than the 4-zone SMB.

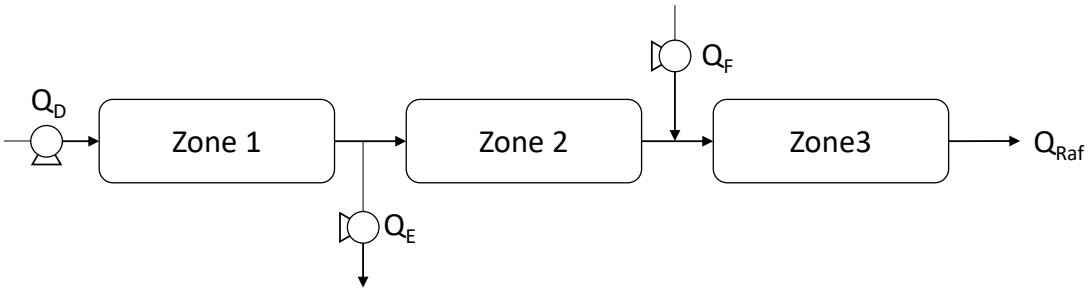

Figure 2-3: Overview diagram of pumps and zones within the 3-zone SMB setup.

$$Q_1 = Q_D \qquad \textbf{Equation 2-21}$$

$$Q_2 = Q_D - Q_E = Q_1 - Q_E \qquad \textbf{Equation 2-22}$$

$$Q_3 = Q_D - Q_E + Q_F = Q_2 + Q_F$$ **Equation 2-23**

Calculation of the flow rate ratios for each zone uses Equation 2-19, as for the 4-zone SMB setup, in Section 2.12.2.2. Equation 2-20, used to predict successful SMB separation, was also modified to remove m_4 and becomes Equation 2-24.

$$m_1 > H_2 > m_3 > m_2 > H_1$$ **Equation 2-24**

2.13 SMB separation

2.13.1 The SMB system

SMB was performed on a Semba Biosciences Octave 10 SMB (Semba Biosciences, Madison, WI, USA) consisting of an Octave 10 Chromatography Valve Block, Octave Control Module and 4 Octave 12 Pumps. Nitrogen was supplied to the valve block at 300 psi to enable valve switching. Each column was connected directly to the valve block. A Shodex RID-20 RI detector was attached to either the raffinate or the extract port. Back pressure regulators were attached to pump outlets to control the back pressure through each zone and maintain the correct flow direction. These were added such that the backpressure (P_q) on any pump (q) during SMB separation was below 270 psi and that the pressure on each pump met the requirements defined in Section 2.13.2 and 2.13.3 for 4-zone and 3-zone SMB setups respectively.

Port switching was automated using the Semba Pro software, with an 8-step repeating cycle. Switch time and pump flow rates were kept constant for all steps. Each step shifts the inputs to the next column and loops from column 8 back to column 1. Specific column configurations for the 4-zone and 3-zone SMB setups are shown in Sections 2.13.2 and 2.13.3 respectively. The extract and raffinate outlet ports were manually directed to waste for the first three full SMB cycles to allow for steady state operation to be achieved. The outlets were then manually directed into collection bottles for 1 or more whole cycles.

The feed was a 'synthetic neutral mixture' unless otherwise stated. This solution of Ara, Gal and Rha, was representative of the neutral sugars found in the crude hydrolysate and was prepared as described in Section 2.7.4. The desorbent was purified water, unless otherwise stated.

2.13.2 4-zone, closed loop SMB setup

For the 4-zone SMB setup, four pumps, as shown in Figure 2-4, were used: feed and desorbent pumps for the inputs, fed directly into the valve block; extract pump on one of the outputs to control the extract flow rate; and a recycle pump fed from one of the outputs and into one of the inputs. There is no pump attached to the raffinate outlet as its flow rate is defined by the flow rate balance (Equation 2-14).

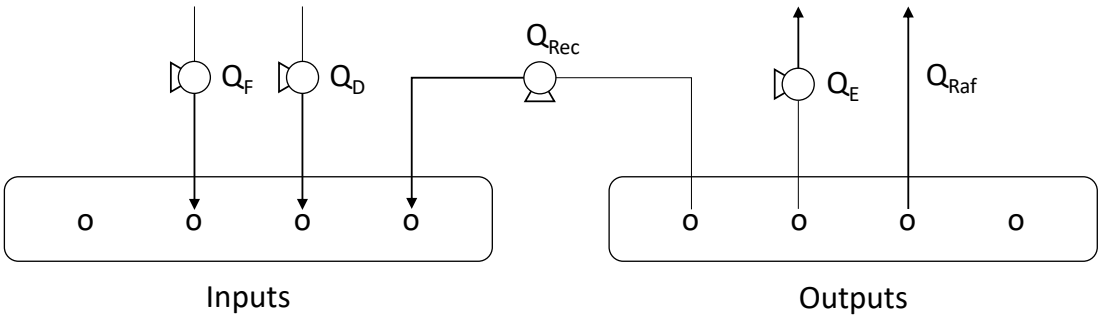

Figure 2-4: Inputs and outputs of the SMB valve block in the 4-zone SMB setup with recycle.

The backpressure regulators were set to meet the criteria (Equation 2-25 to Equation 2-27) recommended by Semba Biosciences for 4-zone SMB setup to ensure the correct flow direction through the valve block and flow rates through the recycle, extract and raffinate outlets.

$$P_E > P_{Rec} + 30$$ **Equation 2-25**

$$P_{Rec} > P_F + 30$$ **Equation 2-26**

$$P_{Rec} > P_D + 30$$ **Equation 2-27**

The columns were programmed in a 2-2-2-2 configuration (2 columns in each zone, as shown in Figure 2-5) in the Semba Pro software.

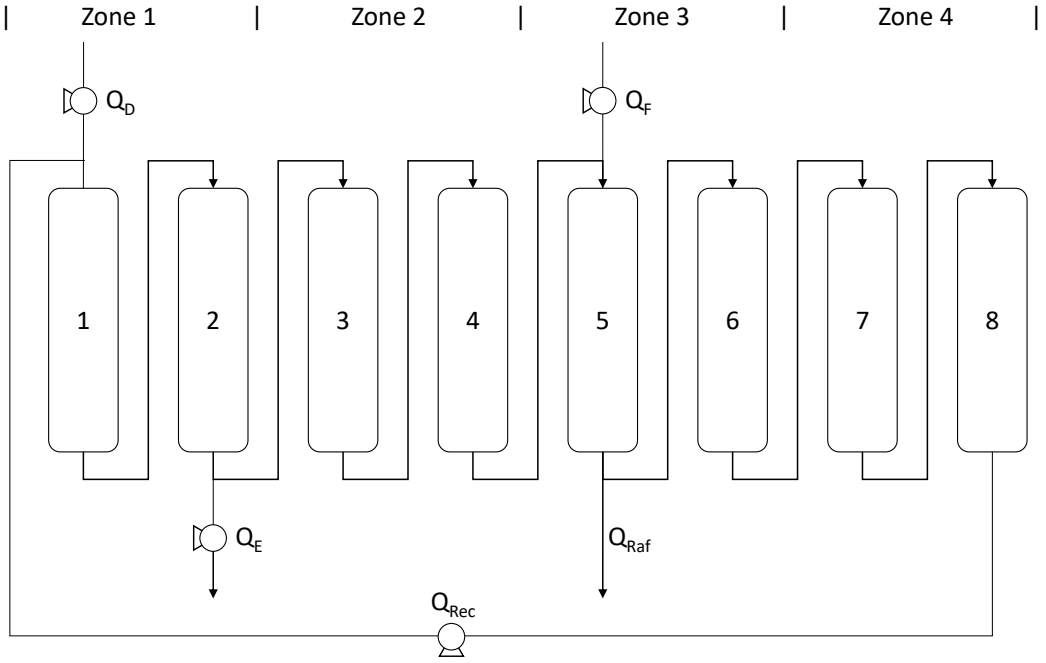

Figure 2-5: Illustration of 2-2-2-2 column configuration and zone locations for 4-zone SMB setup with recycle.

2.13.3 3-zone, open loop SMB setup

For the 3-zone SMB setup, three pumps, shown in Figure 2-6, were used: feed and desorbent pumps for the inputs, fed directly into the valve block; and an extract pump on the extract output to control its flow rate. As in the 4-zone setup, there is no pump attached to the raffinate outlet as its flow rate is defined by the flow rate balance (Equation 2-14).

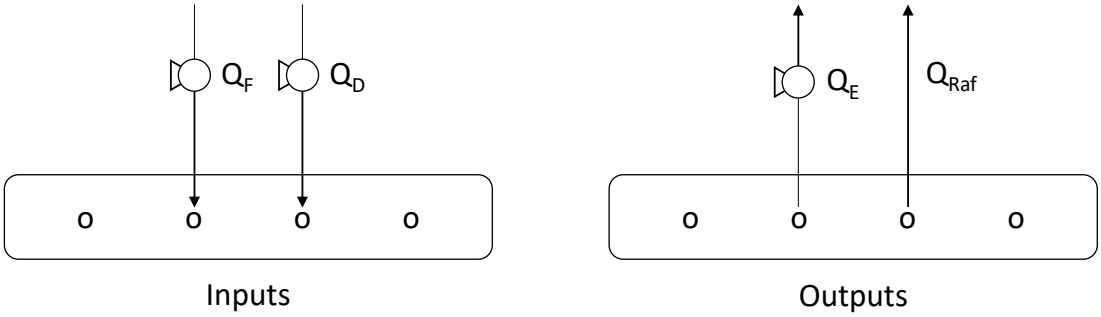

Figure 2-6: Inputs and outputs of the SMB valve block in the 3-zone SMB setup.

The backpressure regulators were set to meet the criteria (Equation 2-28) recommended by Semba Biosciences for the 3-zone SMB setup to ensure the correct flow-rates through the extract and raffinate outlets.

$$P_E > P_D + 30\ psi \qquad \textbf{Equation 2-28}$$

The columns were programmed in a 2-3-3 configuration (2 columns in zone 1, and 3 columns in zones 2 and 3, as shown in Figure 2-7) in the Semba Pro software.

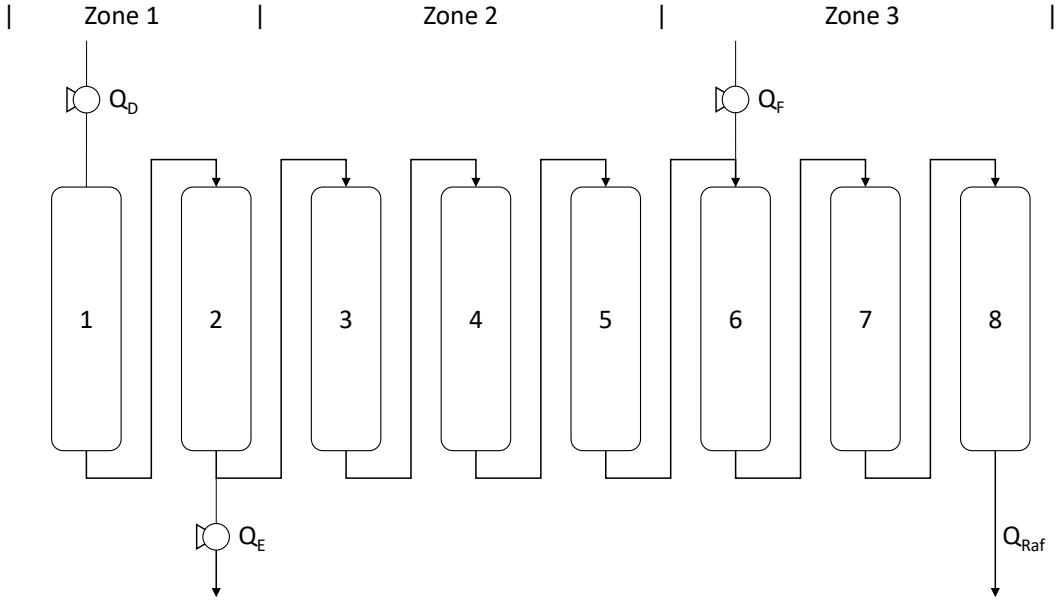

Figure 2-7: Illustration of 2-3-3 column configuration and zone locations for the 3-zone SMB setup.

2.13.4 Analysis of the extract and raffinate streams

The collected extract and raffinate were analysed using ICS on the AminoPac PA10 column as described in Section 2.8.3. Purity and recovery from SMB separations were calculated from ICS analysis of the extract and raffinate outlet streams. Purity is defined as the mass of the target monosaccharide in the extract or raffinate streams as a percentage of the mass of all the monosaccharides in that stream. Calculation of the recovery of each sugar in each outlet stream requires calculation of the mass flow rates. Mass flow rates ($\dot{m}$) of each sugar in each stream are calculated from the concentration, from ICS analysis, multiplied by the outlet flow rates of the extract (Q_E) and raffinate (Q_{Raf}) (Equation 2-29). The extract flow rate is set by the extract pump and the raffinate flow rate is calculated according to the flow rate balance (Equation 2-14) described in Section 2.12.2. The recovery of each sugar in each stream is then calculated from the mass flow rate of the sugar in the stream divided by the sum of the mass flow rates in both the extract and raffinate streams. The recovery of each sugar in the extract and raffinate streams thus add up to a total of 100%.

$$\dot{m} = C_i \cdot Q \qquad \textbf{Equation 2-29}$$

2.14 D-galacturonic acid isolation from neutral sugars

2.14.1 Resin hydration and column packing

Resins for GA isolation were prepared and packed according to the protocol described in Section 2.9. The column was connected to an Akta Purifier system and the top adapter was adjusted to 2 cm above the resin bed to allow for any bed volume expansion due to changes in the ionic form. The ionic form was altered into either Cl^-, OH^- or $C2H3O2^-$ (acetate) by pumping 200 mM NaCl, NaOH or NaOAc respectively at 2 mL min^{-1} until the conductivity value became constant. Deionised water was then flushed through the column at 2 mL min^{-1} until the conductivity value became constant. The top adapter was then readjusted to 1 cm above the resin bed to allow for any bed volume expansion due to changes in the ionic form during experiments.

2.14.2 Resin ionic form screening

Dowex 1x8 (200-400 mesh) resin was examined for use in different ionic forms. 3 g of the resin was packed as described in Section 2.14.1 without changing the ionic form. The column was connected to an Akta Purifier system. Three different ionic forms were tested: hydroxide, acetate and chloride.

Resin ionic form screens were performed by injection of 10 mL of the "synthetic crude mixture", prepared as described in Section 2.7.5.

A flow rate of 5 mL min^{-1} was used with the following protocol:

1. Load: 10 mL injection of 10 g L^{-1} GA
2. Wash: 15 mL deionised water
3. Elute: 50 mL 200 mM of NaCl, NaOH or $C_2H_3NaO_2$
4. Wash: 15 mL deionised water

Each step was collected as a whole fraction and analysed by ICS for the presence of neutral sugars and GA as described in Section 2.8.3.

2.14.3 Resin screening

Four different resins, detailed in Table 2-4, were examined, with 3 g of the resin prepared and packed in the acetate form as described in Section 2.14.1. The columns were then connected between a Semba Biosciences Octave 12 Pump and a Shimadzu RID-20A refractive index detector. A solution of GA (10 g L^{-1}), prepared as described in Section 2.7.5, was pumped directly onto the column at 5 mL min^{-1} for 40 min to allow for complete exchange of the anionic form from acetate to galacturonate.

Table 2-4: Resins examined for D-galacturonic acid isolation from neutral sugars. Particle size values are given in units provided by the manufacturers in the form shipped (Cl^-) and converted to µm if necessary. For Marathon A and A2 resins, crosslinking values are not available.

Resin	Anion exchanger type	Particle size range	Exchange capacity (mEq mL^{-1})	Crosslinking
Marathon A	1	500-600 µm	1.3	n.a.
Marathon A2	2	525-625 µm	1.2	n.a.
Amberlite IRA-400	1	20-25 mesh (0.707-0.841 µm)	1.4	8%
Dowex 1x8	1	200-400 mesh (37-74 µm)	1.2	8%

Refractive index detection was used to allow for the detection of both the galacturonate and acetate eluting from the column. Comparisons were made based on the time and slope of the breakthrough curves observed.

2.14.4 Dynamic binding capacities

Columns containing 3 g and 14 g of Dowex 1x8 resin in the acetate form were prepared as described in Section 2.14.1. The columns were connected to an Akta Purifier system with a conductivity detector and fraction collector. The synthetic crude mixture, detailed in Section 2.7.5, was used for dynamic binding capacity studies. Prior to loading, the column was flushed with 200 mM NaOAc and then with deionised water until the conductivity became constant. Each binding capacity experiment was split into 4 steps, with each step performed for the length of time detailed in Table 2-5, dependent on the resin mass. A flow rate of 5 mL min^{-1} was used for all steps.

1. Load - Synthetic crude mixture
2. Wash – Deionised water
3. Elute – 200 mM NaOAc
4. Wash – Deionised water

Table 2-5: Step times at different column masses for dynamic binding capacity experiments.

Step	3 g column	14 g column
Load time (min)	80	325
Wash time (min)	10	20
Elute time (min)	20	50
Wash time (min)	10	20

On the 3 g column, fractions were collected every 2 min and analysed for GA concentration using the ICS analysis method as described in Section 2.8.3. The neutral sugars concentrations were not calculated individually with additional ICS runs but the area of the combined neutral sugars peak in the GA analysis was used to demonstrate the elution of neutral sugars. On the 14 g column, the load and elution steps were collected as single fractions.

Dynamic binding capacity (DBC) was calculated at the volume of initial breakthrough ($BV_{0\%}$) using Equation 2-30, and at 10% breakthrough ($BV_{10\%}$) using Equation 2-31. Both equations have the units (mmol g^{-1}_{resin}) and use the concentration of GA in the feed (C_F = 5 g L^{-1}), the molecular weight of D-galacturonic acid monohydrate (MW = 212.15 mg $mmol^{-1}$), and the mass of resin (m_{resin} = 3 g or 14 g).

$$DBC_{0\%} = \frac{BV_{0\%} \cdot C_F}{MW \cdot m_{resin}} \qquad \textbf{Equation 2-30}$$

$$DBC_{10\%} = \frac{BV_{10\%} \cdot C_F}{MW \cdot m_{resin}} \qquad \textbf{Equation 2-31}$$

On the 3 g column the breakthrough volumes $BV_{0\%}$ and $BV_{10\%}$ were calculated from either the GA analysis or based on the conductivity values. On the 14 g column, the breakthrough volumes were determined solely from the conductivity values. For the DBC from GA, the initial breakthrough $BV_{0\%}$ represents the first fraction where GA was detected, and $BV_{10\%}$ represents the first fraction where the GA concentration rises above 0.5 g L^{-1} (10% of the feed concentration).

Using the conductivity, the initial breakthrough volume ($BV_{0\%}$) was calculated from the volume at which the conductivity rises after the initial increase at the beginning of

the load step. The 10% breakthrough volume ($BV_{10\%}$) was calculated from the volume at which the change in conductivity before and after breakthrough reaches 10% of the total change. The breakthrough curve length was calculated from the difference in volume between initial breakthrough ($BV_{0\%}$) and complete breakthrough ($BV_{100\%}$) (when the conductivity becomes constant). The breakthrough volume per mass of resin was determined from the initial breakthrough volume ($BV_{0\%}$) divided by the resin mass.

Noise reduction of the conductivity trace for the 14 g column was performed by applying a 21-point symmetric moving average, by taking the average value of the original volume and the 10 volume points before and after.

2.14.5 Crude hydrolysate separations

Crude hydrolysate separations for the isolation of GA were performed on a 14 g Dowex 1x8 column prepared in the acetate form as described in Section 2.14.1. Crude hydrolysate was loaded directly onto the column with no prior treatment. The method described in Section 2.14.4 was employed with varying load times. Column cleaning was performed after each run with 20 column volumes of 2 M NaCl and 1 M NaOH in succession at 0.5 mL min^{-1}.

2.15 Decolourisation of crude hydrolysate

2.15.1 Batch decolourisation screening

All resins for decolourisation were used in the ionic form as shipped (Cl^- for anion exchange resins and Na^+ for cation exchange resin) with no prior hydration or form change. Activated carbon was also used as shipped with no hydration or pretreatment. The mass of resin/carbon (200 mg unless otherwise stated) was contacted with 1 mL of the crude hydrolysate in a microcentrifuge tube and shaken horizontally on a thermomixer at room temperature for the desired contact time before centrifugation (Hettich Mikro 120) at 14,000 rpm (~18,000 RCF) for 4 minutes. Loadings are given as the mass of resin/carbon per mL of crude (mg mL^{-1}). Experiments were run overnight (16 hours) unless otherwise stated. The supernatant was then taken for sugar and UV analysis.

Table 2-6: Properties of the resins examined for decolourisation of the crude hydrolysate.

Resin	Exchanger	Type	Form
Marathon A	Anion	1	Cl^-
Marathon A2	Anion	2	Cl^-
Amberlite IRA-400	Anion	1	Cl^-
Marathon MSA	Anion	1	Cl^-
Dowex 1x8 (200-400 mesh)	Anion	1	Cl^-
Marathon C	Cation	-	Na^+
Activated carbon	-	-	-

Analysis of GA and neutral sugars was performed as described in Section 2.8.3. Analysis of the UV profile was performed as described in Section (2.8.5). Samples were diluted to ensure the whole spectrum (230-400 nm) fell within detectable limits. The 'level of decolourisation' is given as the percentage change of the decolourised sample to the crude and is based on the average value between 230-400 nm unless otherwise stated.

2.15.2 Larger scale batch decolourisation

Larger scale decolourisation experiments were performed by maintaining both the loading and the contact time. An activated carbon loading of 100 mg mL^{-1} with a contact time of 10 min was scaled up to 5 g of activated carbon to decolourise 50 mL of crude hydrolysate. Decolourisation was performed by adding the activated carbon to a 50 mL centrifuge tube and adding the crude hydrolysate. The tube was then mixed horizontally on a shaker platform (Heidolph UNIMAX 2010) at 400 rpm for 10 min before being centrifuged (Eppendorf 5810 R) for 15 min at 4000 rpm (~3200 RCF). The supernatant was filtered through a 0.22 µm filter to remove any residual activated carbon before analysis of the GA and neutral sugars, as described in Section 2.8.3, and the UV profile, as described in Section 2.15.1. The material produced using this method is referred to as the 'decolourised crude hydrolysate'.

2.15.3 D-galacturonic acid isolation from decolourised crude hydrolysate

The decolourised crude hydrolysate, prepared as described in Section 2.15.2, was loaded onto a 14 g Dowex 1x8 column in the acetate form, prepared as described in Section 2.14.1. Each injection followed the method described in Section 2.14.4 for a 14 g column with the decolourised crude hydrolysate in place of the synthetic crude mixture and varying the load times (injection volumes).

Chapter 3 Phase system development and separation of synthetic monosaccharide mixtures using centrifugal partition chromatography[†]

3.1 Introduction, aim and objectives

It was described in Section 1.2.5 that CPC has considerable potential for biorefinery applications, although presently this has been relatively unexplored. CPC is able to process crude samples with little to no pretreatment and at high sample loadings (Section 1.2.1). Furthermore, the lack of any solid phase removes any risk irreversible adsorption and concerns over resin costs and lifetime. CPC could thus be an important addition to methods for the processing of crude hydrolysates of renewable feedstocks (Section 1.2.1).

The aim of this first results chapter is to develop a method for separating a model synthetic mixture of the monosaccharides present in hydrolysed SBP pectin (Section 1.1.4) using CPC. The specific objectives of this chapter are to:

- Screen for a suitable family of phase systems based on the partition coefficients of the individual monosaccharides.
- Develop ternary phase diagrams for further understanding the operating limits of the selected phase system family.
- Optimise the phase system based on monosaccharide partition coefficients and settling times, and explore the effects of different additives on the phase system behaviour.
- Examine the retention characteristics of the phase system in CPC and select preliminary operating conditions.

[†] The results presented in this chapter have been published as: Ward, David P., et al. "Centrifugal partition chromatography in a biorefinery context: separation of monosaccharides from hydrolysed sugar beet pulp." *Journal of Chromatography A* 1411 (2015): 84-91.

- Perform example CPC separations based on model synthetic mixtures of monosaccharides.

3.2 Phase system development

3.2.1 Phase system requirements

The first step in CPC method development is to identify suitable phase systems for separation. As discussed in Section 1.2.3, phase systems are selected based on solute partition coefficients and phase system settling times. Partition coefficients are indicators of retention factors and a value of K=1 is considered the target value to provide optimal resolution [49] while a "sweet spot" of $0.4<K<2.5$ should provide sufficient performance for CPC separations [50]. The settling time of a two-phase system is an important metric for understanding stationary phase retention in CPC, with shorter settling times generally giving higher retention [37]. High stationary phase retentions, in turn, allow for higher mobile phase flow rates, increasing solute throughput.

3.2.2 Organic : aqueous phase systems

This section examines organic : aqueous two-phase systems as a first step in phase system development. Partition coefficients were determined for Ara, Gal, Rha, Xyl and GA, as described in Section 2.2, in HEMWat 1:5:1:5, one of the most polar HEMWat phase systems, and EBuWat 0:1:1, the most polar of the EBuWat phase systems. The HEMWat family of phase systems is a usual starting point for separating natural products and EBuWat 0:1:1 is one of the most polar organic : aqueous two-phase systems. The partition coefficients of the sugars in these phase systems should give a gauge as to how polar the monosaccharides are and how feasible an organic : aqueous phase system would be for separating them. The partition coefficient results are shown in Table 3-1.

Table 3-1: Partition coefficients ($K_{LP/UP}$) of L-arabinose, D-galactose, L-rhamnose and D-galacturonic acid and separation factors (α) relative to L-arabinose for two organic : aqueous phase systems. Phase systems were prepared as described in Section 2.2. Partition coefficient and separation factor values were determined as described in Section 2.2 and represent one standard deviation about the mean (n=2 for these initial studies).

Phase system	K_{Ara} ($\alpha_{Ara/Ara}$)	K_{Gal} ($\alpha_{Gal/Ara}$)	K_{Rha} ($\alpha_{Ara/Rha}$)	K_{GA} ($\alpha_{Ara/GA}$)
HEMWat 1:5:1:5	200 (1.0)	120 (1.7)	460 (2.3)	N.D.
EBuWat 0:1:1	19 (1.0)	N.D.	N.D.	170 (8.9)

The results of both phase systems are poor, with the sugars almost exclusively partitioning into the aqueous lower phase (LP), and very little into the organic upper phase (UP). The Ara partition coefficient in EBuWat 0:1:1 (19) is an order of magnitude lower than for HEMWat 1:5:1:5 (200), but it is still far outside the "sweet spot" range of $0.4 < K < 2.5$ given by Friesen and Pauli [50]. This shows that even with the most polar of the organic : aqueous phase systems, the partition coefficients do not support separation by CPC. While the separation factors appear acceptable ($\alpha>1.5$) for all of the sugars relative to Ara, the poor partition coefficients would require excessive separation times and lead to band broadening, resulting in peak overlap and loss of resolution [56].

3.2.3 Ion exchange phase systems

In an attempt to improve the partition coefficient of GA, an ion exchange phase system was examined. The process is detailed in Section 1.2.7 and briefly described in Figure 3-1. In brief, it uses a soluble ion exchanger in the UP (UP-Exch) to adjust the partition coefficient of ionic compounds so that they partition more into the UP, and a modified LP containing a displacer (LP-Disp) to partition the ionic compounds back into the LP. This method could allow for the separation of GA from the neutral sugars directly from a crude sample, which may be difficult using ion exchange resins without some form of pretreatment. Ion exchange resins for the extraction of GA are discussed in Section 1.4 and examined in 6.2.

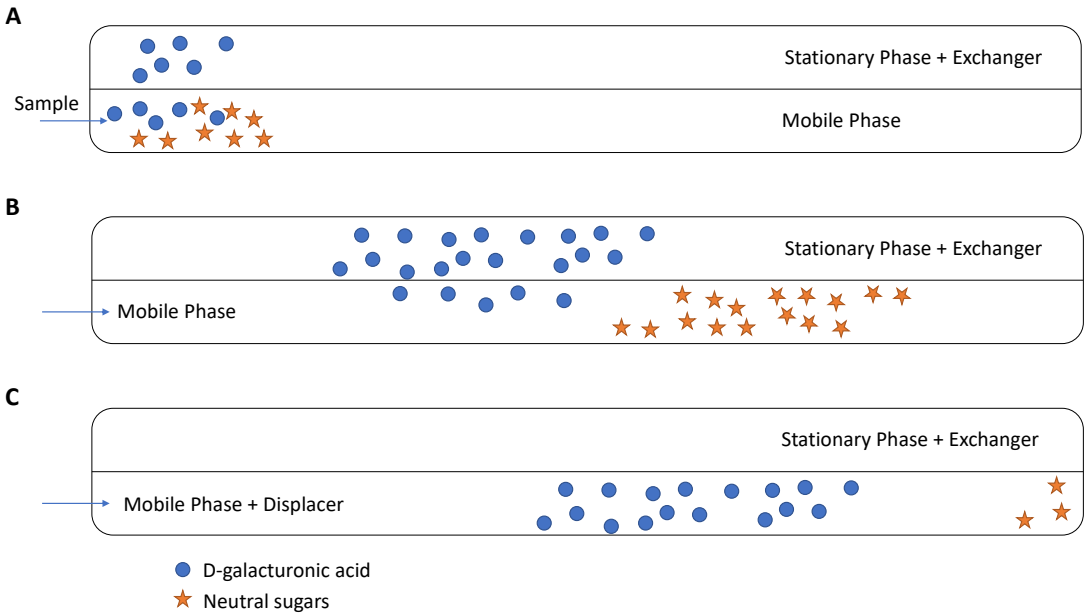

Figure 3-1: Schematic representation of how ion-exchange CPC could work for the isolation of D-galacturonic acid (GA) from neutral sugars. A: GA partitions more strongly into the UP-Exch stationary phase and the neutral sugars remain in the LP mobile phase. B: GA is thus retained in the UP-Exch while the neutral sugars elute from the column. C: Introduction of LP-Disp displaces the GA back into the mobile phase where it elutes from the column.

A method was sought which gave a higher GA partition in a UP-Exch – LP mixture and a lower GA partition coefficient in a UP-Exch – LP-Disp mixture. An EBuWat 0:1:1 phase system was used with 25 mM Aliquat 336 as the ion exchanger in the UP-Exch and 50 mM NaI as the displacer in the LP-Disp. 2.5 mM of both Ara and GA were used in the LP and LP-Disp. Table 3-2 shows the partition coefficients of Ara and GA in the different phase systems.

Table 3-2: Partition coefficients ($K_{LP/UP}$) of L-arabinose and D-galacturonic acid in different combinations of UP, UP-Exch, LP and LP-Disp to mimic the conditions of ion exchange CPC. Phase systems were prepared as described in Section 2.2. Partition coefficient values were determined as described in Section 2.2 and represent one standard deviation about the mean (n=2 for these initial studies).

	$\frac{\text{UP}}{\text{LP}}$	$\frac{\text{UP-Exch}}{\text{LP}}$	$\frac{\text{UP-Exch}}{\text{LP-Disp}}$	$\frac{\text{UP}}{\text{LP-Disp}}$
K_{Ara}	19.5±1.8	19.8±0.1	24.7±1.8	20.0±2.3
K_{GA}	164±15	1.5±0.1	∞	∞

The addition of the ion exchanger to the UP results in a greater than 100-fold reduction in the partition coefficient of GA, from 164 to 1.5, while it does not appear to affect the partition coefficient of Ara. This promotes the possibility of using this to remove GA in the Descending mode, slowing down only the GA and allowing the neutral

sugars to flow directly through the column. Addition of the displacer to the LP entirely displaces the GA from the UP or UP-Exch into the LP-Disp, with no GA detectable in the UP-Exch.

In the UP – LP mixture and the UP-Exch – LP-Disp mixture the settling time is approximately 20 sec; however, the UP-Exch – LP mixture causes settling times in excess of 2 min, even in the absence of GA. This could cause difficulties in retaining the stationary phase in CPC, even at higher rotational speeds. Furthermore, as the GA still partitions primarily into the LP ($K > 1$) in the UP-Exch – LP, the application of this method to a liquid-liquid extraction step may also be limited.

It is clear that there is potential for an ion-exchange step to isolate the GA from the neutral sugars, however, the current proposed system is limited by the settling time in the presence of the ion exchanger. It is possible that modifications to the phase system, ion exchanger, ion exchanger concentration or product:ion exchanger ratio could allow for an improved settling time and thus feasibility in a CPC separation. However, it remains unclear how the partition coefficients of GA would be affected in the crude hydrolysate, or if the anion exchanger would preferentially exchange other ionic contaminants in the crude hydrolysate with increased partitioning into the UP. As a result, ion exchange CPC methods were not explored further, and attention was directed towards more polar alcohol-salt phase systems.

3.2.4 Alcohol : salt phase systems

To improve the partition coefficients from the EBuWat 0:1:1 phase system in Section 3.2.2, alcohol : salt phase systems were examined, primarily based on the ethanol-ammonium sulphate phase system, discussed in Section 1.2.5).

A ternary phase diagram for ethanol : saturated ammonium sulphate solution : water was developed based on the volumes of each (Figure 3-2). This data was then developed into a ternary phase diagram for ethanol : ammonium sulphate : water on a mass basis (Figure 3-3) to avoid the necessity of preparing saturated ammonium sulphate. The ternary phase diagrams demonstrate a relatively small range of compositions under which two-phase systems form which are suitable for CPC.

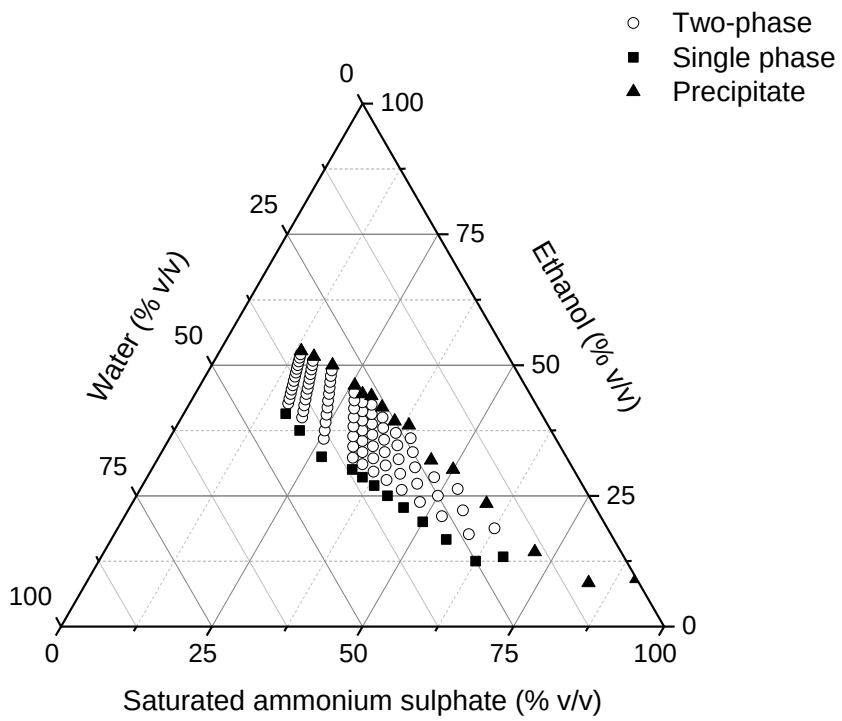

Figure 3-2: Ternary phase diagram (% v/v) showing the two-phase region of ethanol : ammonium sulphate : water phase systems. Experiments were performed as described in Section 2.3.

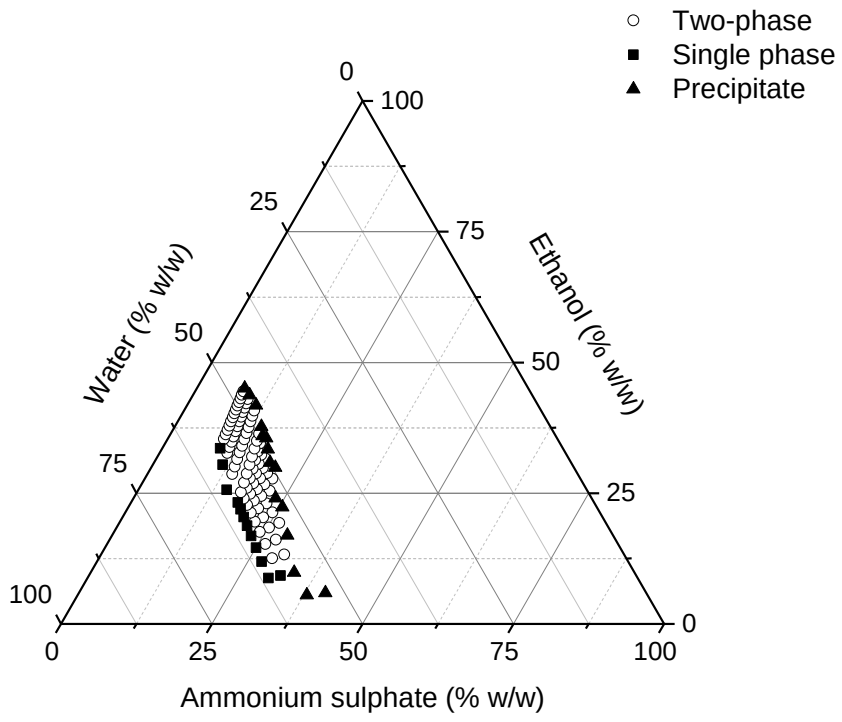

Figure 3-3: Ternary phase diagram (% w/w) showing the two-phase region of ethanol : ammonium sulphate : water phase systems. Experiments were performed as described in Section 2.3.

While binodal curve data for ethanol : ammonium sulphate : water phase systems has been published previously [223], it does not demonstrate the effective two-phase region for CPC operation, nor the region in which precipitation occurs with further addition of ammonium sulphate or ethanol. Figure 3-4 represents the same data as in Figure 3-3 in the form of such a binodal curve showing both the single-phase boundary and the precipitation boundary.

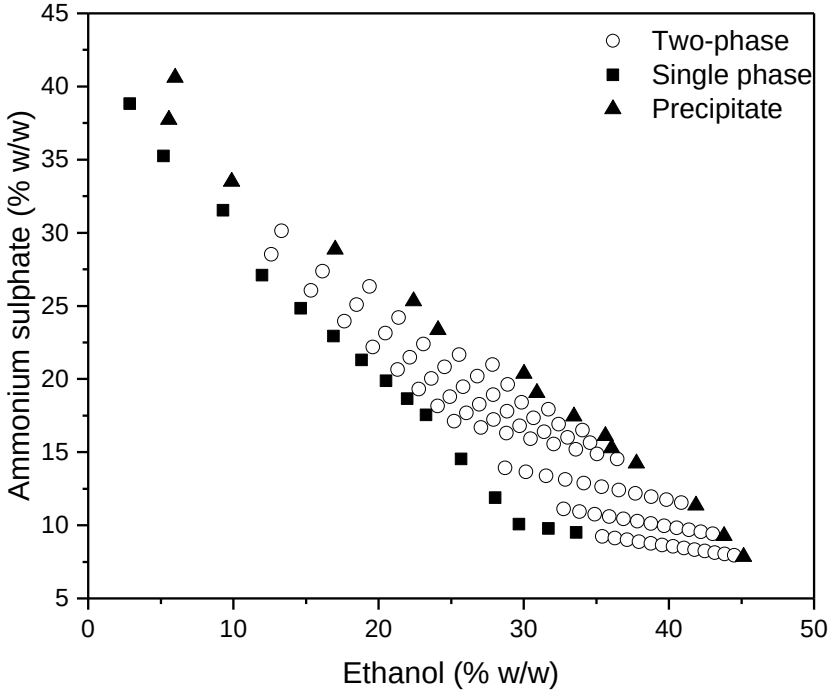

Figure 3-4: Binodal curve phase diagram (% w/w) showing the two-phase region of ethanol : ammonium sulphate : water phase systems. Experiments were performed as described in Section 2.3.

The settling times of the phase systems should also be considered due to its relationship with the stationary phase retention in CPC. It was observed that systems containing more ammonium sulphate and ethanol (i.e. closer to the precipitate phase boundary) exhibit shorter settling times (<30 s) indicating a likely improvement in retention. Systems with a higher percentage of water (closer to the single-phase boundary) exhibit longer settling times (>60 s), indicating that the retention could be lower.

Phase systems I-III (Table 2-1), from Shinomiya and Ito [74], use a constant salt concentration (2 M ammonium sulphate) in varying volumetric ratios with ethanol to demonstrate how the location of the phase system in the two-phase region affects settling time and partition coefficient. With a lower ethanol proportion (phase system

III – closer to the single phase boundary in Figure 3-3) the partition coefficients (K_{Ara} = 2.2) (Table 3-3) are closer to the target of 1 (Section 3.2.1) but the settling time is increased (31 s) (Table 3-4). A higher ethanol proportion (phase system I – closer to the precipitate boundary) results in a shorter settling time (21 s) but also partition coefficients further from 1 (K_{Ara} = 4.3). There is therefore a trade-off required between the separation achievable (K values) and the throughput (settling times). Using an even lower ethanol proportion (3:7) results in excessive settling times that would result in poor retention while a higher ethanol proportion (3:3) resulted in some salt precipitation. The requirement for short settling times (<30 s) effectively shrinks the practicable two-phase region in Figure 3-3, where phase systems with suitable characteristics can be formed.

Table 3-3: Partition coefficients ($K_{LP/UP}$) of the monosaccharides present in hydrolysed SBP pectin. Phase systems were prepared as described in Section 2.2. Partition coefficient values were determined as described in Section 2.2 and represent one standard deviation about the mean (n=2 for these initial experiments).

Phase system	Partition coefficient ($K_{LP/UP}$)			
	Ara	Gal	Rha	GA
I	4.3 ± 0.2	5.2 ± 0.1	1.3 ± 0.1	13.0 ± 1.9
I + TFA	3.8±0.1	N.D.	N.D.	7.1±0.1
II	3.0 ± 0.2	3.5 ± N.D.	1.2 ± 0.0	8.7 ± 0.9
II + TFA	3.0 ± 0.1	N.D.	N.D.	5.0±0.5
III	2.2 ± N.D.	2.5 ± 0.1	1.2 ± 0.1	4.2 ± N.D.
IV	16 ± 2	24 ± 0	3.9 ± 0.0	33 ± 3
V	7.7 ± 0.0	12 ± 0	2.1 ± 0.1	33 ± 8
VI	10.0 ± 0.5	15 ± 0	2.4 ± N.D.	33 ± 2
VII	4.0 ± 0.2	N.D.	N.D.	N.D.
VIII	2.8 ± 0.0	N.D.	N.D.	7.2 ± 0.0
IX	2.8 ± 0.0	N.D.	N.D.	7.3 ± 0.1
X	5.3 ± 0.1	N.D.	N.D.	N.D.
XI	4.0 ± 0.7	N.D.	N.D.	N.D.
XII	3.7 ± 0.1	N.D.	N.D.	N.D.
XIII	2.9 ± 0.1	N.D.	N.D.	N.D.
XIV	1.8 ± 0.0	2.1 ± 0.1	1.0 ± 0.0	3.6 ± 0.1
XV	2.6 ± 0.0	3.5 ± 0.0	1.2 ± 0.1	7.2 ± 0.2

Ara, L-arabinose; Gal, D-galactose; Rha, L-rhamnose; GA, D-galacturonic acid; N.D., not determined.

Table 3-4: Lower phase (LP) volume fractions and settling times of the highly polar phase systems described in Table 2-1. Experiments were performed as described in Section 2.2. Values represent one standard deviation about the mean (n=3).

Phase system	LP volume fraction	Settling time (s)
I	0.32	19.4 ± 0.3
II	0.38	25.3 ± 0.1
III	0.44	37 ± 1
IV	0.47	16.0 ± 0.3
V	0.44	14.6 ± 0.4
VI	0.51	18.3 ± 0.4
VII	0.44	20.3 ± 0.5
VIII	0.53	29.5 ± 0.4
IX	0.46	29.8 ± 0.5
X	0.76	19.9 ± 0.4
XI	0.43	20.6 ± 0.5
XII	0.58	28.3 ± 0.5
XIII	0.52	41.4 ± 0.8
XIV	0.57	89.8 ± 0.4
XV	0.42	31.4 ± 0.7

Adding an acid to the phase system has the potential to modify solute partition coefficients, particularly for GA, by manipulating which ionic form it is present in. Phase systems I and II were modified by adding 1% (v/v) TFA to the 2 M ammonium sulphate solution used, as described in Section 2.2. This reduced the pH of both phases from ~5 to below 3 (see Table 3-5) which is below the pKa for GA of 3.5 [224]. This adjustment in the pH should force GA into the non-ionic form when dissolved in these phase systems.

Table 3-5: pH of the upper (UP) and lower (LP) phases of phase systems I and II with and without TFA (Table 2-1). Phase systems were prepared as described in Section 2.2.

Phase system	LP	UP
I	4.9	5.4
I + TFA	2.4	2.8
II	4.9	5.4
II + TFA	2.5	2.7

Calculated partition coefficients of Ara and GA are shown in Table 3-3. The TFA appears to have little to no effect on the partition coefficients of Ara (no change in

phase system II and only a small change in phase system I). For GA, the changes are more pronounced, with the partition coefficient dropping from 13.0 to 7.1 in phase system I and 8.7 to 5.0 in phase system II. This represents a higher proportion of GA in the upper phase when in the non-ionic form, however, these changes bring the GA partition coefficient closer to that of the other sugars, reducing the separation factors. As a result, TFA was not added to future phase systems.

In an attempt to improve both stationary phase retention and settling times, various other modifiers were tested in the ethanol : ammonium sulphate systems. Phase systems IV-VI use a combination of acetonitrile, propanol or butanol as phase system modifiers and have previously been used for the separation of glucosinolates [78][225]. For these phase systems, the settling times were shorter than 20 s (Table 3-4), however, the partition coefficients were much higher than for phase systems I, II and III (Table 3-3) suggest long and poor CPC separations. It is evident that these systems, while useful for glucosinolate isolation, are not suitable for the separation of sugars, which partition too strongly into the lower aqueous phase.

All of the phase systems I-VI followed the same order of partition coefficients ($K_{LP/UP}$) for the SBP solutes i.e. Rha < Ara ≤ Gal < GA. It was therefore decided to look primarily at improving the Ara partition coefficient (bringing it closer to 1) by addition of further phase modifiers.

Phase systems VII-XIII examine the effect of methanol and acetonitrile as alternatives to ethanol in forming two-phase systems with ammonium sulphate as well as modifying the partition coefficient in ethanol systems. From these systems, the lower phase volume fractions (defined in Section 2.2) were generally around 0.5 and settling times between 20 and 30 s (Table 3-4). Phase system VIII (ethanol : saturated ammonium sulphate : water (0.8:1.0:0.8 v:v:v)) shows a relatively high Ara partition coefficient (K_{Ara} = 2.8) but maintains a large separation factor (2.6) between the two main targets (Ara and GA) with a reasonable settling time (30 s). This phase system was used as the basis of further modifications and as a standard for comparison.

Methanol, as a more polar alcohol than ethanol, could provide a way of improving the solute partition coefficients by reducing the polarity difference between the two

phases. Phase system IX introduces a small proportion of methanol (Table 2-1), which has no effect on the partition coefficients (Table 3-3) or the settling time (Table 3-4). The use of methanol as a modifier is limited as it readily precipitates the ammonium sulphate and so can only be used in low proportions, requiring another compound to stabilise the phase system.

Replacing the ethanol in phase system VIII for propanol led to the formation of a two-phase system with a much increased settling time of longer than 1 min. Furthermore, as it was seen in phase systems IV and V, increasing the proportion of propanol had a negative effect on the partition coefficients; hence, this solvent was not examined further as a phase system modifier.

Phase system X examines the addition of acetonitrile to the phase system. While the settling time is reduced to 20 s from phase system VIII (30 s), the Ara partition coefficient almost doubles (K_{Ara} = 5.3) as shown in Table 3-3. To improve the partition coefficient, ethanol and methanol were examined as phase system modifiers (systems XI and XII). Settling times for these systems were 21 and 28 s respectively, however, the partition coefficients were much higher than phase system VIII containing only ethanol as organic solvent.

DMSO was also investigated as a potential phase system modifier to improve partition coefficients of the monosaccharides. It is a polar aprotic solvent which is capable of dissolving a wide range of organic compounds with high loadings [226] and is effective at solubilising even long chain carbohydrates [227]. Adding DMSO to an acetonitrile-ammonium sulphate phase system reduced the partition coefficient of Ara from 5.3 (phase system X) to 2.9 (phase system XIII) but increases the settling time from 30 s to 41 s.

DMSO was then tested in an ethanol-salt phase system, however, the addition of DMSO readily precipitated the salt and a low concentration was required in order for a two-phase system to form. Phase system XIV uses a lower ethanol proportion and provides the lowest achieved monosaccharide partition coefficients of all the phase systems tested (K_{Ara} = 1.8). The settling time, however, is 90 s, which is excessive and could lead to significant problems with stationary phase retention in the CPC column.

As SBP is a high volume feedstock (Section 1.1.2), increasing CPC throughput is considered to be an overriding consideration and so improvements in the settling time were sought to allow for higher mobile phase flow rates. An increase in the ethanol proportion to 0.8 (system XV) shortened the settling time to 31 s and increased the partition coefficient (K_{Ara} = 2.6). Importantly, the separation factor for GA and Ara in system XV (2.8) is higher than both phase system XIV (2.0) and VIII (2.6). Based on these results, phase system XV was selected for subsequent CPC separations in Section 3.3.

Analysis of the composition of the two phases formed showed that the ammonium sulphate concentration was 376 g L^{-1} in the LP and 63 g L^{-1} in the UP (determined gravimetrically, as described in Section 2.8.2). The ethanol concentration in the LP and UP was 97 g L^{-1} and 333 g L^{-1} respectively, while the DMSO concentration was 23 g L^{-1} and 56 g L^{-1}, respectively. Ethanol and DMSO concentrations were determined using HPLC-RI, as described in Section 2.8.1.

3.3 CPC separations

3.3.1 Stationary phase retention studies

Initial CPC experiments with phase system XV were used to determine the retention of stationary phase at a rotational speed of 1000 rpm and flow rates (Q) between 2 and 16 mL min^{-1}. These experiments were performed as described in Section 2.5.1. A linear relationship was found for the stationary phase retention (S_F) with varying flow rate as shown in Figure 3-5 ($S_F = -3.7Q + 86.6$ with r^2=0.996). Further experiments at 8 mL min^{-1} with various rotational speeds between 600 and 2000 rpm yielded no significant variation in the stationary phase retention (Figure 3-6). At higher rotational speeds, the column pressure increased, and at 2000 rpm, was close to the maximum operating pressure of 80 bar. This rotational speed would leave little allowance for any pressure increase caused by sample injection. A rotational speed of 1000 rpm was selected which gave a maximum pressure of 22 bar at 8 mL min^{-1}. These conditions were selected for CPC separations, giving a stationary phase retention of 57%.

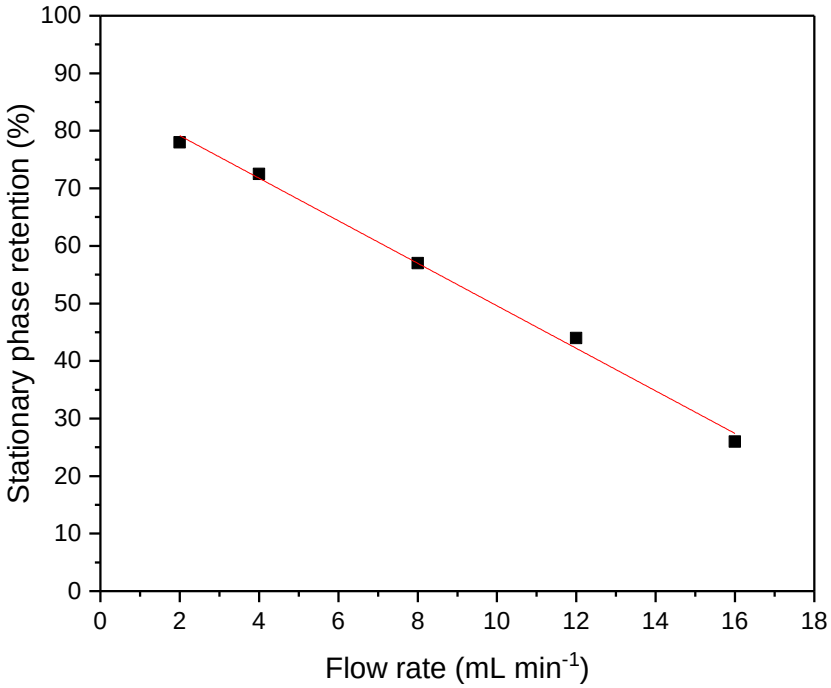

Figure 3-5: Effect of flow rate on stationary phase retention in the ascending mode on the semi-preparative CPC column at 1000 rpm using phase system XV (Table 2-1). Experiments were performed as described in Section 2.5.1. Stationary phase retention was calculated as described in Section 2.5.1.

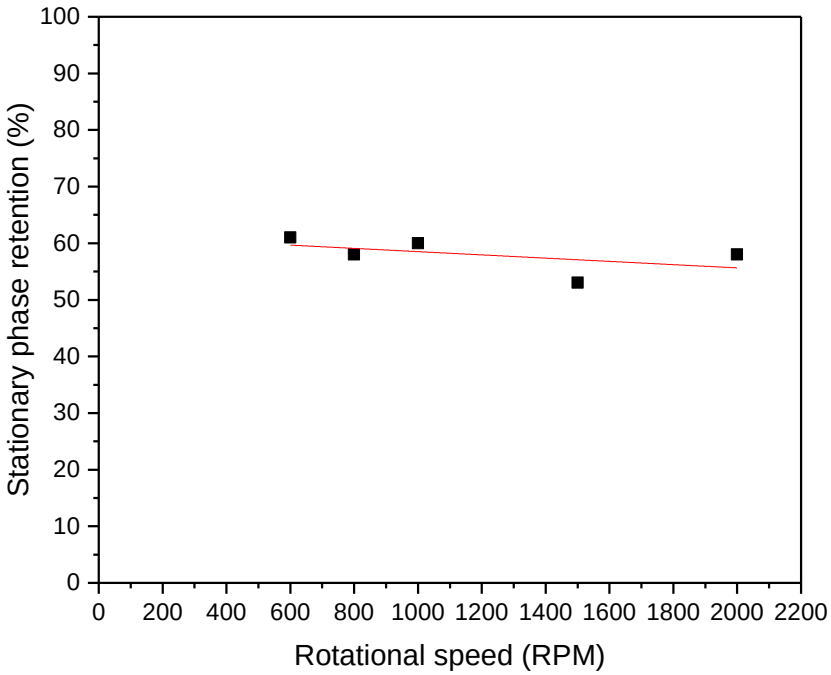

Figure 3-6: Effect of rotational speed on stationary phase retention in the ascending mode on the semi-preparative CPC column at 8 mL min^{-1} using phase system XV (Table 2-1). Experiments were performed as described in Section 2.5.1. Stationary phase retention was calculated as described in Section 2.5.1.

3.3.2 CPC separations

As the primary constituents of hydrolysed SBP pectin, Ara and GA were studied in initial separation experiments. Rha was also included as its partition coefficient is lower than both Ara and GA while providing a reasonable separation factor with Ara (2.2, based on partition coefficients values). The expected elution order from the partition coefficient data (Table 3-3) would thus be Rha – Ara – GA for CPC operated in the ascending mode, with the upper phase mobile and the lower phase stationary.

In order to clearly demonstrate this predicted elution profile, equal concentrations of the monosaccharides were used at concentrations of 50 g L^{-1} each, prepared as described in Section 2.7.2. CPC separation was performed as described in Section 2.4 and Figure 3-7 shows the CPC elution profile achieved with this 'illustrative' mixture based on ICS analysis of the monosaccharide composition in collected fractions. This matches the expected elution order from partition coefficient data and shows that there is good separation achieved between Rha and Ara, and baseline resolution achieved between Ara and GA.

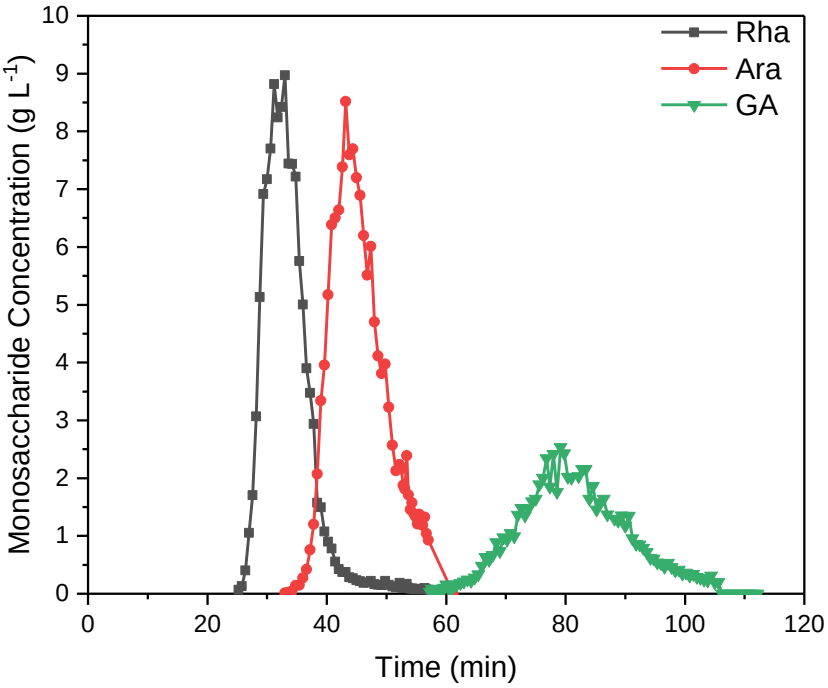

Figure 3-7: CPC separation of an illustrative mixture of L-rhamnose, L-arabinose and D-galacturonic acid using phase system XV (Table 2-1). Separation was performed in the ascending mode with a flow rate of 8 mL min^{-1}, a rotational speed of 1000 rpm, at room temperature and with an injection volume of 10.81 mL. The illustrative mixture was prepared in the upper phase, as described in Section 2.7.2. Experiments were performed as described in Section 2.4. Concentrations were determined by ICS as described in Section 2.8.3.

Subsequently, a CPC separation was performed using all of the four main sugars present in SBP pectin. This 'model synthetic mixture' contained the monosaccharides at a concentration ratio expected in hydrolysed SBP pectin after cellulose removal, i.e. 43% Ara, 41% GA, 11% Gal and 5% Rha [7], and was prepared as described in Section 2.7.2. A total solute concentration of 100 g L^{-1} was used. As shown in Figure 3-8, elution of Rha started after 22 min and the whole separation process was completed within 2 h. The 'model synthetic mixture' was separated into three main fractions; a highly pure Rha fraction (>90% w/w) eluted between 27 - 37 min, a mixed Ara-Gal fraction eluted between 38 – 63 min (comprising 76% Ara and 22% Gal) and a highly pure GA fraction (>90%) eluted between 67 - 111 min.

Figure 3-9 shows example analytical chromatograms for specific points in the CPC elution profile demonstrating the sugars present in each fraction: Figure 3-9A, Rha fraction at 33 min; Figure 3-9B Ara and Gal fraction at 45 min; and Figure 3-9C, GA fraction at 79.8 min. Two analytical methods are required to fully analyse each

fraction: one for neutral sugars and one for GA (as described in Section 2.8). Fractions A and B showed no presence of GA and so only the neutral sugar analyses are shown. Similarly, fraction C showed no presence of neutral sugars and only the GA analysis is shown. It is important to note that, for biorefinery applications, complete fractionation of all four sugars into separate fractions is not necessarily required. For example, selective enzymatic modification of Ara in the presence of Gal could be performed.

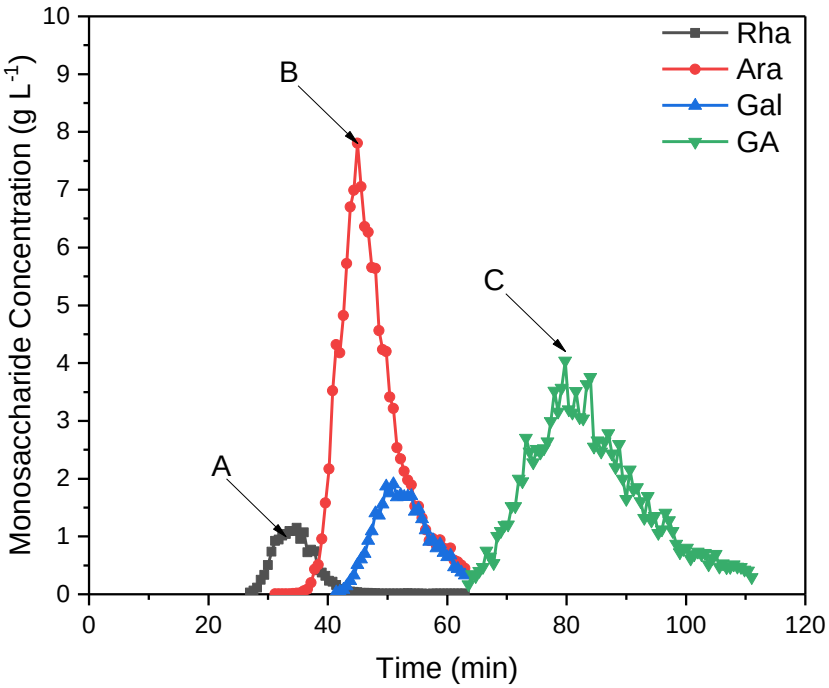

Figure 3-8: CPC separation of a model synthetic mixture of L-rhamnose, L-arabinose, D-galactose and D-galacturonic acid using phase system XV (Table 2-1). Separation was performed on the semi-preparative column in the ascending mode with a flow rate of 8 mL min^{-1}, a rotational speed of 1000 rpm, at room temperature and with an injection volume of 10.81 mL. The model synthetic mixture was prepared in in the upper phase, as described in Section 2.7.2. Experiments were performed as described in Section 2.4. Analytical chromatograms at the marked points A, B and C are shown in Figure 3-9.

A comparison of Figure 3-7 and Figure 3-8 showed that the monosaccharide elution profiles and retention times did not change between the 'illustrative' and 'model synthetic mixture' separations. This indicates that the selected phase system (XV, Table 2-1) is stable to fluctuations in solute concentrations and the introduction of Gal into the feed stream. While the peaks appear in their expected order, the compounds eluted earlier than expected based on their partition coefficient values (Table 3-3). This is probably a result of the stationary phase stripping that occurs shortly after injection, resulting in a smaller stationary phase retention and compounds with K values higher

than 1 eluting faster [228]. The CPC separations were found to be reproducible after repeats with freshly prepared phase systems and samples.

In terms of CPC operation, these results show that Rha could be collected as a first fraction with high purity prior to the elution of Ara. While Ara has good separation from Rha and baseline separation from GA, it co-elutes with Gal in the second fraction. GA can be taken as a third and final fraction with high purity. However, it elutes as a broad peak, taking approximately 60 min (480 mL) for full recovery. In order to decrease the time of this separation process, and therefore increase the throughput, extrusion of the column contents after the Ara and Gal fraction could be considered. This would have the benefit of increasing the concentration of GA in the fraction, ensuring complete recovery and preparing the column for further injections. In the case of this elution-extrusion mode [106], the estimated throughput based on the current operating conditions at this semi-preparative scale would be 0.9 g $hour^{-1}$ with 0.62 L of solvent per gram of total sugars. This is based on an extrusion flow rate of 16 mL min^{-1} for 12 minutes after 1 hour of elution at 8 mL min^{-1}.

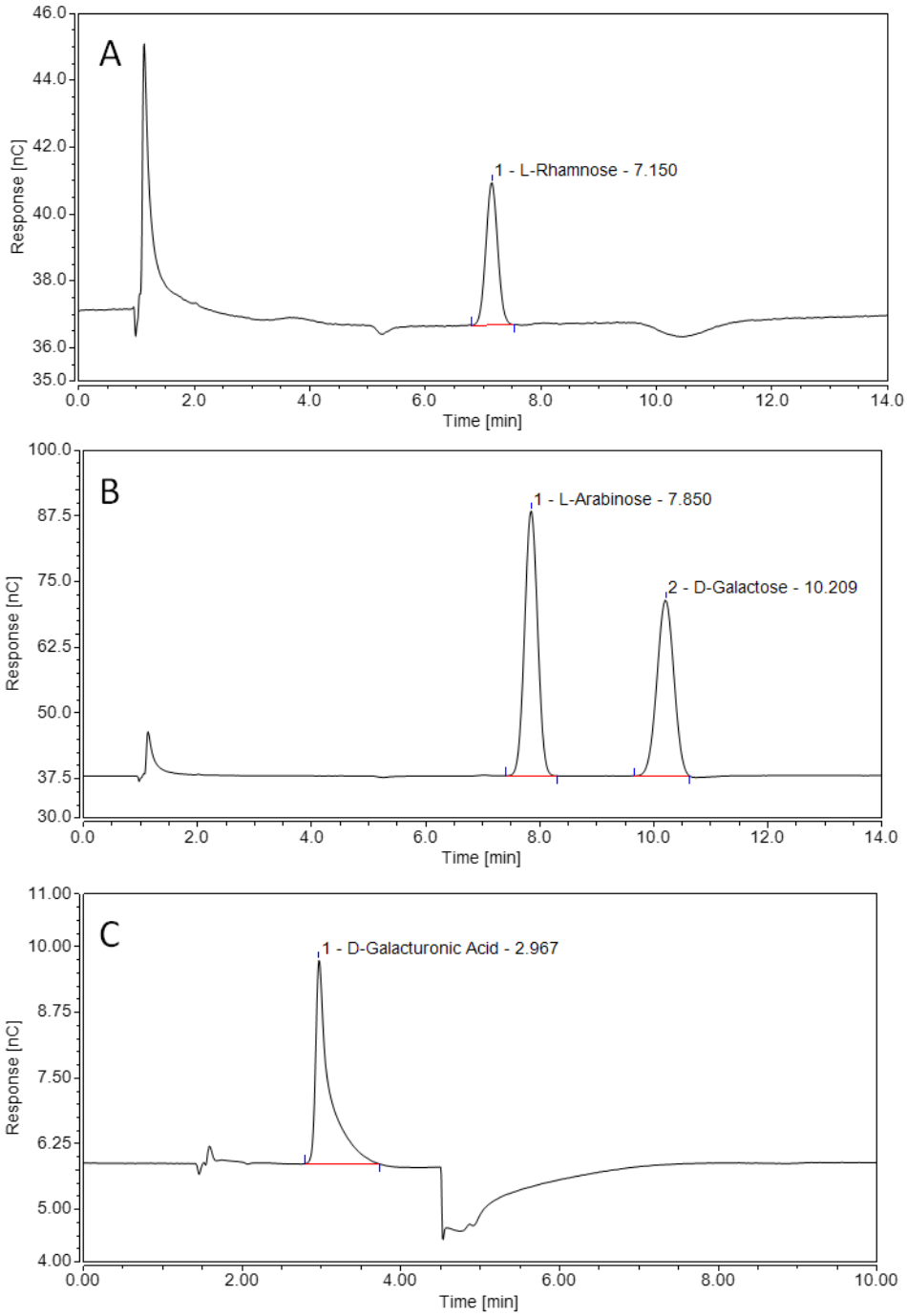

Figure 3-9: Analytical chromatograms of CPC fractions from the model synthetic mixture separation at A, 33 min; B, 45 min; and C, 79.8 min; (as shown in Figure 3-8). Figure 3-9A and Figure 3-9B show the analysis of neutral sugars. Figure 3-9C shows the analysis of GA. The two analytical methods used are described in Section 2.8.

3.4 Chapter Summary

This work represents an important first step in demonstrating the capability of CPC as a separation technology suitable for use within a whole-crop biorefinery context (Section 1.1.2). It demonstrates the ability to separate compounds in a low value feedstock like SBP, after hydrolysis, into various fractions for subsequent conversion into higher value products.

The aim of this chapter was to develop a method for separating a model synthetic mixture of the monosaccharides in hydrolysed SBP pectin using CPC and this was achieved as shown in Figure 3-8. The main conclusions of this chapter are:

- Organic – aqueous solvent-based phase systems are not capable of partitioning monosaccharides to a level suitable for CPC. The best partition coefficient achieved was 19 for L-arabinose in an EBuWat 0:1:1 phase system (Table 2-1). This is far from a desirable partition coefficient of $K<2.5$.
- An ion-exchange phase system has some potential to isolate GA from the neutral sugars and it was possible to improve the partition coefficient more than 100-fold from 164 to 1.5 without modifying the partition coefficient of Ara (Table 2-2 in Section 3.2.3). However, the ion-exchanger dramatically increased the settling time of the EBuWat 0:1:1 phase system, making it impractical for CPC separation.
- An ethanol : aqueous ammonium sulphate phase system was studied in detail (Section 3.2.4) with the development of a ternary phase diagram (Figure 3-3). The impact of different ethanol and ammonium sulphate ratios, and solvent modifiers on the solute partition coefficients (Table 3-3) and settling times (Table 3-4) was examined. A highly polar ethanol : DMSO : aqueous ammonium sulphate (300 g L^{-1}) (0.8:0.1:1.8 v:v:v) phase system was selected for CPC separations with the DMSO improving the partition coefficient of the Ara.
- CPC stationary phase retention studies were performed varying the rotational speed and flow rate (Section 3.3.1). It was found that a rotational speed of 1000

rpm and a mobile phase flow rate of 8 mL min^{-1} in the ascending mode gave a suitable stationary phase retention of 57% (Figure 3-5).

- CPC separation was performed on an illustrative mixture and a model synthetic mixture of SBP pectin monosaccharides (Section 3.3.2) using the DMSO modified phase system. It was found that the CPC method was able to isolate three relatively pure fractions from the four target sugars: Rha (>90%), Ara (76%) and Gal, and GA (>90%) as shown in Figure 3-8.

In the next chapter, the focus will shift to the separation of crude SBP hydrolysate, examining crude sample preparation, throughput maximisation, and scale-up.

Chapter 4 Optimisation and scale-up of centrifugal partition chromatography crude hydrolysate separations[‡]

4.1 Introduction, aim and objectives

In Chapter 3 a range of phase systems (listed in Table 2-1) were examined based on phase system settling times (Table 3-4) and partition coefficients for the target sugars (Table 3-3). Phase system XV, comprised of ethanol : DMSO : 300 g L^{-1} aqueous ammonium sulphate (0.8:0.1:1.8 v:v:v) was selected for CPC separations and was tested in a semi-preparative CPC column for stationary phase behaviour and determination of suitable operating conditions. It was shown that CPC separation of a model synthetic mixture of monosaccharides at 100 g L^{-1} total sugars concentration was possible (Figure 3-8), separating the target sugars into three fractions: Rha; Ara and Gal; and GA.

This chapter will focus on transitioning the CPC method to the processing of crude SBP pectin hydrolysates as would be found in a sugar beet biorefinery (Section 1.1.4). As explained in Section 2.7.1, this crude hydrolysate was provided by the Department of Biology and Biochemistry at the University of Bath and is the soluble pectin fraction following steam explosion (Hamley-Bennett et al. [17]) and complete acid hydrolysis with H_2SO_4 to fully monomerise all of the remaining oligosaccharides.

The aim of this chapter is to demonstrate the potential of the CPC method developed in Chapter 3 to the processing of crude SBP hydrolysates. Given the integrated biorefinery context of the work (Section 1.1.2) it will be important to consider maximisation of material throughput and scale-up of the separation onto a larger CPC column. The specific objectives of this chapter are to:

[‡] The results presented in this chapter have been published as: Ward, David P., et al. "Centrifugal partition chromatography in a biorefinery context: Optimisation and scale-up of monosaccharide fractionation from hydrolysed sugar beet pulp." *Journal of Chromatography A* 1497 (2017): 56-63.

- Evaluate the benefits of DMSO on phase system development and CPC separation performance.
- Establish a simple sample preparation method for dealing with crude pectin hydrolysates that will enable sample injection onto the CPC without a loss in separation performance.
- Examine methods to improve the throughput of the CPC methods by either increasing the sample injection volume or implementing the elution-extrusion operation mode.
- Scale up the CPC separation method from a semi-preparative (250 mL) to a preparative (950 mL) scale column.

4.2 Impact of DMSO on CPC separation

In Section 3.2.4, DMSO was added to the phase system in order to improve the partition coefficient of Ara (Table 3-3). DMSO, however, poses potential difficulties to any additional purification step or solvent recycling technique used due to its high boiling point of 189°C [229]. The impact of DMSO on the actual separation achieved by CPC was examined based on the chromatograms shown in Figure 4-1, with DMSO (phase system XV), and Figure 4-2, without DMSO (phase system VIII). The operating conditions used, and the operating conditions of all of the CPC separations in this chapter are detailed in Table 4-1. Fraction purities and recoveries are shown in Table 4-2.

Table 4-1: Summary of CPC phase systems and operating strategies used in Chapter 4. Phase systems as described in Table 2-1. Preparation of model synthetic mixtures and crude samples are detailed in 2.7.2 and 2.7.3 respectively. Details of the two columns given in Section 2.4 with additional operating requirements for the preparative column given in Section 2.6. The ascending and descending mode are discussed in Section 1.2.3.2. The elution-extrusion operating modes is detailed in Section 2.5.2.

Experiment	Phase system	Sample type	Column	Sample preparation	Injection volume (mL)	Flow rate (mL min^{-1})	Rotational speed (rpm)	Mode	Operating Method	Resulting Chromatogram
1	XV	Synthetic	Semi-prep.	UP	10	8	1000	Ascending	Elution	Figure 4-1
2	VIII	Synthetic	Semi-prep.	UP	10	8	1000	Ascending	Elution	Figure 4-2
3	VIII	Synthetic	Semi-prep.	LP	10	8	1000	Ascending	Elution	Figure 4-3
4	VIII	Crude	Semi-prep.	LP	10	8	1000	Ascending	Elution	Figure 4-5 & 4-10A
5	VIII	Crude	Semi-prep.	LP	10	8	1600	Ascending	Elution	Figure 4-6
6	VIII	Crude	Semi-prep.	LP	10	8	1000	Descending	Elution	Figure 4-7
7	VIII	Crude	Semi-prep.	LP	10	8	1600	Descending	Elution	Figure 4-8
8	VIII	Crude	Semi-prep.	LP	10	6	1000	Descending	Elution	Figure 4-9
9	VIII	Crude	Semi-prep.	LP	20	8	1000	Ascending	Elution	Figure 4-10B
10	VIII	Crude	Semi-prep.	LP	30	8	1000	Ascending	Elution	Figure 4-10C
11	VIII	Crude	Semi-prep.	LP	40	8	1000	Ascending	Elution	Figure 4-10D
12	VIII	Crude	Semi-prep.	LP	30	8	1000	Ascending	Elution-Extrusion	Figure 4-11 & 4-12
13	VIII	Crude	Preparative	LP	152	30.4	1000	Ascending	Elution	Figure 4-13
14	VIII	Crude	Preparative	LP	152	30.4	1000	Ascending	Elution-Extrusion	Figure 4-14
15	VIII	Crude	Preparative	LP	152	30.4	1000	Ascending	Elution-Extrusion	Figure 4-15

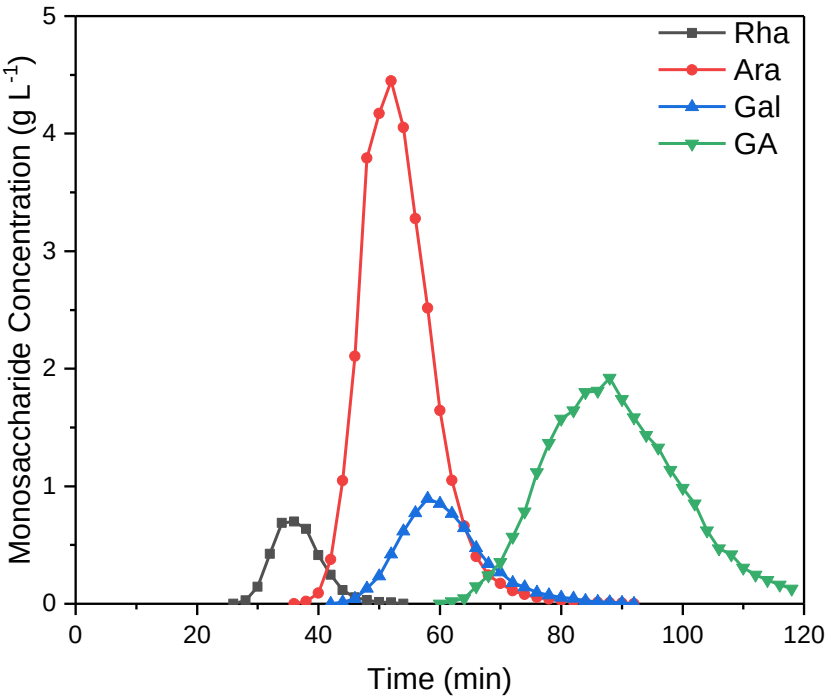

Figure 4-1: CPC separation of a model synthetic mixture of L-rhamnose, L-arabinose, D-galactose and D-galacturonic acid in the UP using phase system XV (Table 2-1). The sample was prepared as described in Section 2.7.2. Separation was performed on the semi-preparative column in the ascending mode with a flow rate of 8 mL min^{-1}, a rotational speed of 1000 rpm, at room temperature and with an injection volume of 10 mL, as described in Section 2.4. Full experimental details are given under Experiment 1 in Table 4-1.

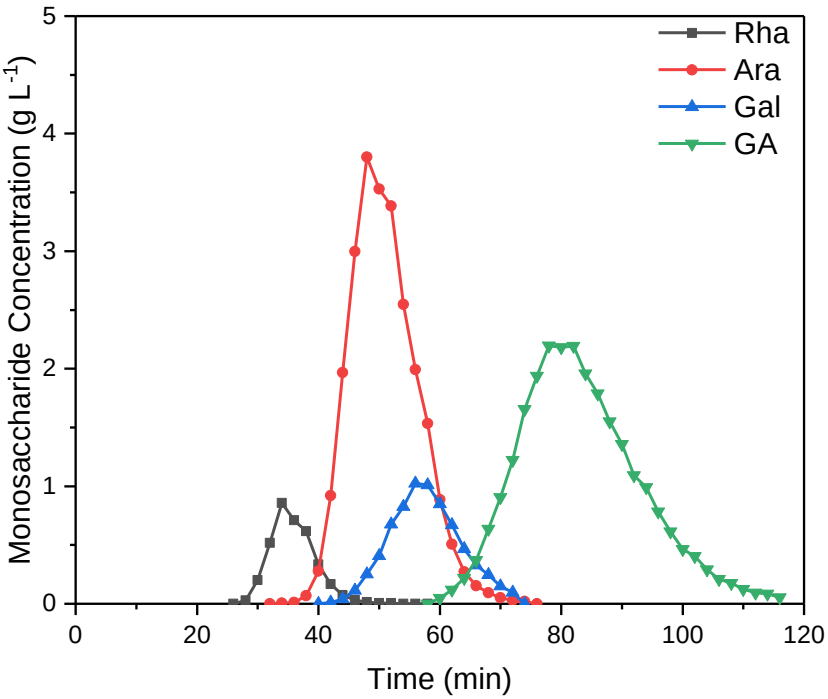

Figure 4-2: CPC separation of a model synthetic mixture of L-rhamnose, L-arabinose, D-galactose and D-galacturonic acid in the UP using phase system VIII (Table 2-1). The sample was prepared as described in Section 2.7.2. Separation was performed on the semi-preparative column in the ascending mode with a flow rate of 8 mL min^{-1}, a rotational speed of 1000 rpm, at room temperature and with an injection volume of 10 mL, as described in Section 2.4. Full experimental details are given under Experiment 2 in Table 4-1.

Table 4-2: Optimised purities and recoveries of target monosaccharides from CPC separation using phase systems XV and VIII (Table 2-1). Samples were 100 g L^{-1} model synthetic mixture samples prepared in the UP and prepared as described in Section 2.7.2. CPC separation was performed on a semi-preparative, 250 mL Kromaton CPC (full details of Experiment 1 and 2 given in Table 4-1). Purities and recoveries are given as % (w/w) as defined in Section 2.8.

Experiment	Phase System	S_F (%)	Rha			Ara			GA		
			Purity (%)	Recovery (%)	Time (min)	Purity (%)	Recovery (%)	Time (min)	Purity (%)	Recovery (%)	Time (min)
1	XV	55	96	87	28-40	81	98	42-68	94	98	70-118
2	VIII	58	90	91	28-42	81	94	44-62	97	97	70-118

It is clear from comparing Figure 4-1 and Figure 4-2 that the presence of DMSO does not have a strong impact on the retention times of the neutral sugars and only a small change in the GA retention time, where DMSO increases the peak maximum from 82 to 88 min. Furthermore, DMSO does not appear to affect the initial stationary phase retention value, and the fraction purities and recoveries are broadly the same (Table 4-2). As any improvement in CPC performance with DMSO is minor, it was subsequently removed from the phase system for future CPC experiments in favour of a simpler solvent recycling process and solute recovery. Phase system VIII was thus used in all subsequent work.

It is also worth noting that stationary phase retention values (Section 2.5.1) are calculated based on initial breakthrough and do not consider any stationary phase bleed caused by instability of the phase system or sample injection. Phase system XV, in the presence of DMSO, equilibrates at an S_F value of 34% during separation, while phase system VIII, without DMSO, S_F continues to drop during separation to approximately 24%. This suggests that the presence of DMSO helps to stabilise phase system hydrodynamics within the CPC machine and could provide improved separation for other applications. The equilibration stationary phase retention values were calculated as described in Section 2.5.1.

4.3 Crude sample preparation and impact on CPC separation

The most straightforward option to access all the monosaccharides present in a complex feedstock like sugar beet pectin is to carry out acid hydrolysis (Section 1.1.4). This was performed on the aqueous pectin fraction following steam explosion of the sugar beet pulp by the Department of Biology and Biochemistry at Bath University as described in Section 2.7.1. After full acid hydrolysis in an autoclave and adjustment to pH 6, a dark brown solution is formed with a mass of dried solids of approximately 100 g L^{-1} (determined gravimetrically, as described in Section 2.8.2) and a total monosaccharide concentration of approximately 20 g L^{-1} (Ara, 12 g L^{-1}; GA, 4 g L^{-1}; Gal, 3 g L^{-1}; Rha, 1 g L^{-1}, Glu 1 g L^{-1} as determined by ICS (Section 2.8.3)). The colouration could be the result of degradation of the GA [21,22] and neutral monosaccharides, such as fructose [18], during the hydrolysis step leading to the formation of browning products. These browning products are discussed further in

Section 1.1.5. Furthermore, some of the dissolved solids will be sodium sulphate salts due to the acid hydrolysis with H_2SO_4 and pH adjustment with NaOH.

Being a liquid-liquid separation technique with a high proportion of stationary phase in the column, CPC can cope with a large volume of sample [34], however, it is important to find a balance between high throughput, purity and yield without disturbing the hydrodynamic equilibrium within the column. It has also been shown that column hydrodynamics and thermodynamic equilibrium between the two phases can be greatly affected by sample preparation [230]. For model synthetic mixtures, the monosaccharides could be prepared in either of the two phases (UP or LP), however, for the crude hydrolysate, it proved impossible to prepare in the mobile phase (UP 44% v/v ethanol, 54 g L^{-1} ammonium sulphate) without precipitation of ammonium sulphate. There was no such precipitation or solubility difficulties when preparing crude hydrolysate in the stationary phase (LP, 13% v/v ethanol, 332 g L^{-1} ammonium sulphate). Full details of the sample preparation methodology are described in Section 2.7. Ethanol proportions for each were determined using HPLC-RI as described in Section 2.8.1. Ammonium sulphate concentrations were determined gravimetrically for each phase as described in Section 2.8.2.

It was clear from these initial investigations that sample preparation would be an important consideration for separation of the crude hydrolysate. Therefore, a CPC separation was run in the ascending mode using a model synthetic mixture of sugars dissolved in the LP. The same model synthetic mixture sugar concentrations were used as in Chapter 3 (100 g L^{-1} total sugars, as described in Section 2.7.2) in order to replicate the total dissolved solids content in the crude of 100 g L^{-1}. The resulting chromatogram is shown in Figure 4-3 which indicates a slight shortening of the retention times but similar separation performance when compared with sample preparation in the UP (Figure 4-2). Table 4-3 shows the maximum values of purity and recovery for the target monosaccharides in the pooled fractions from the CPC separation of the model synthetic mixture sample prepared in both the UP and LP. The purities and recoveries of Ara and GA are approximately the same between the two runs with a slight drop in Rha recovery from 90 to 80% (w/w).

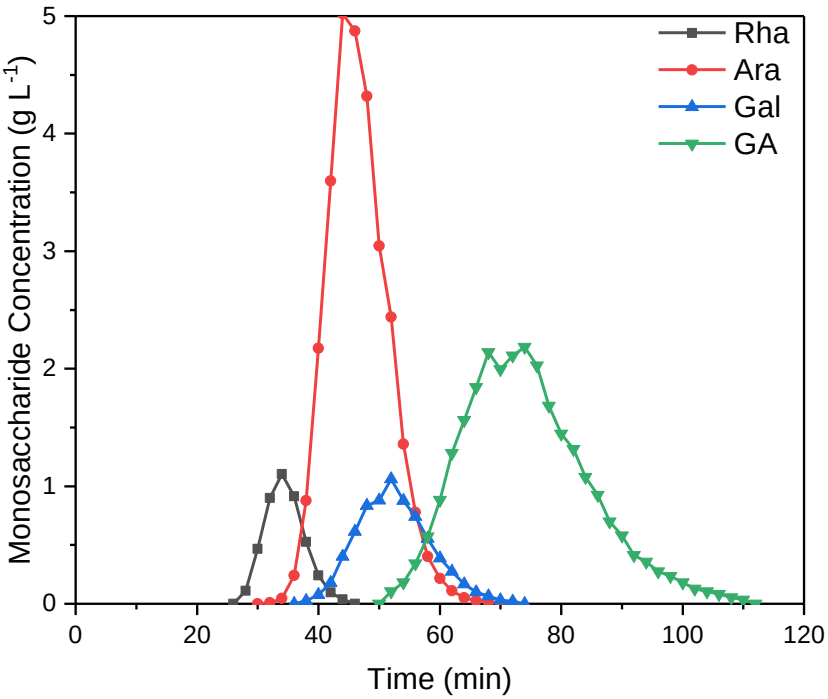

Figure 4-3: CPC separation of a model synthetic mixture of L-rhamnose, L-arabinose, D-galactose and D-galacturonic acid in the LP using phase system VIII (Table 2-1). The sample was prepared as described in Section 2.7.2. Separation was performed on the semi-preparative column in the ascending mode with a flow rate of 8 mL min^{-1}, a rotational speed of 1000 rpm, at room temperature and with an injection volume of 10 mL, as described in Section 2.4. Full experimental details are given under Experiment 3 in Table 4-1.

Table 4-3: Maximum purities and recoveries of target monosaccharides from CPC separation using different sample preparations. Model synthetic mixture samples (100 g L^{-1} of total sugars) were prepared in either the UP or LP as described in Section 2.7.2 and a crude sample (20 g L^{-1} total sugars and 100 g L^{-1} total solids) was prepared in the LP as described in Section 2.7.3. CPC separation was performed on a semi-preparative, 250 mL Kromaton CPC with full details given in Table 4-1 based on the Experiment number. Purities and recoveries are given as % (w/w) and calculated from ICS analysis as defined in Section 2.8.3.

	Experiment	Sample Phase	S_F (%)	Rha			Ara			GA		
				Purity (%)	Recovery (%)	Time* (min)	Purity (%)	Recovery (%)	Time* (min)	Purity (%)	Recovery (%)	Time* (min)
Model Synthetic mixture	2	UP	58	90	91	28-42	81	94	44-62	97	97	70-118
	3	LP	64	92	80	28-36	78	95	40-58	95	96	60-110
Crude	4	LP	51	94	96	28-44	88	97	46-66	99	99	78-110

It is worth noting that injection of a sample made in the stationary phase can overstate the loss of stationary phase, as sample injection will elute a volume of stationary phase equal to that of the sample injection volume (V_I). Stationary phase retention (S_F) for samples injected in the LP was therefore calculated using Equation 4-1, (where V_C is total column volume, V_E is total eluted volume until mobile phase breakthrough and V_D is total dead volume). This equation should be used to take into account V_I when running separations in this manner, particularly when varying the injection volume. Therefore, for the LP sample injection, the stationary phase retention becomes 64%; greater than that of the UP sample injection. Overall these results demonstrate that sample preparation in the stationary phase yields similar separation performance to that of the mobile phase and could be a useful option for crude samples that do not solubilise well in the mobile phase.

$$S_F = \frac{V_C - V_E + V_I + V_D}{V_C} \qquad \textbf{Equation 4-1}$$

With little difference in recovery and purity between model synthetic mixture sample preparation in the mobile (UP) or stationary (LP) phases, separations were attempted with the crude hydrolysate. As stated previously, sample preparation of the crude sugar beet pectin in the mobile phase (UP) led to precipitation of the ammonium sulphate. Dropping the concentration of ammonium sulphate to 25 g L^{-1} allowed the salts to fully dissolve but led to complete stripping of the stationary phase when injecting a 10 mL sample volume. In an attempt to fully utilise the liquid nature of the stationary phase, 10 mL of the neat crude sample (without mixing in either phase) was injected into the CPC column but this also resulted in complete stripping of the stationary phase.

Preparing the crude hydrolysate in the LP (stationary phase) (13% v/v ethanol and 332 g L^{-1} ammonium sulphate) led to its full solubilisation, however, a small volume (<10% v/v) of a new phase formed on top of the solution (Figure 4-4C). This new phase was black in colour, indicating a high concentration of impurities; conversely, the rest of the solution was a much lighter brown, indicating a reduction in the level of coloured impurities. It is likely that the impurities causing this colour were acting as phase forming compounds, interacting with the salt in a similar way to ethanol to partition into a new UP. By discarding the new upper phase, a proportion of the

impurities were removed with no effect on the concentration of monosaccharides in the sample (confirmed by ICS analysis), effectively utilising the sample preparation step as a form of purification.

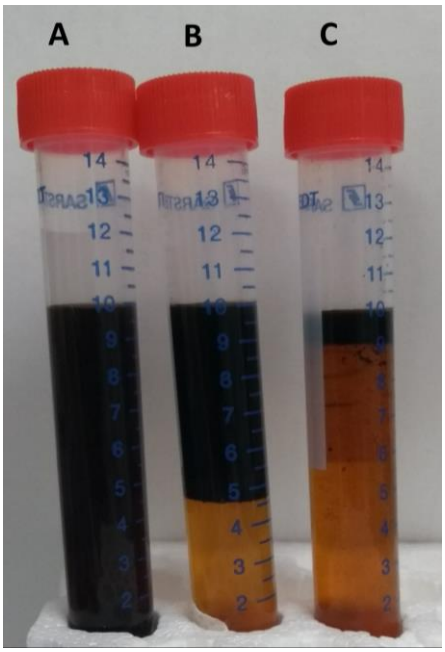

Figure 4-4: Crude CPC samples prepared A, in the UP; B, in a 50:50 mix of UP and LP; and C, in the LP. Samples were prepared as described in Section 2.7.3.

It is possible that using ammonia to adjust the pH of the acid hydrolysed SBP pectin instead of NaOH could be beneficial. This would form ammonium sulphate in the crude, reducing the amount of ammonium sulphate that would need to be added during sample preparation.

The purity and recovery values for injecting a crude sample prepared in the LP are also shown in Table 4-3 with the chromatogram shown in Figure 4-5. It is clear that the separation is improved relative to the LP model synthetic mixture separation despite a drop in stationary phase retention from 64% to 51%. This is likely a result of the lower monosaccharide concentration; the crude had a total dissolved solids loading of 100 g L^{-1}, similar to that of the model synthetic mixture, but total monosaccharides of only 20 g L^{-1}. This demonstrates that an optimised sample preparation methodology, which provides a partial or complete removal of these impurities prior to CPC separation, could allow similar total monosaccharide loadings. In addition to the sugars shown, a

very small amount of Glu (less than 1 g L^{-1} in the sample) from the crude was eluted, however, it co-elutes entirely with Ara peak and so is not shown.

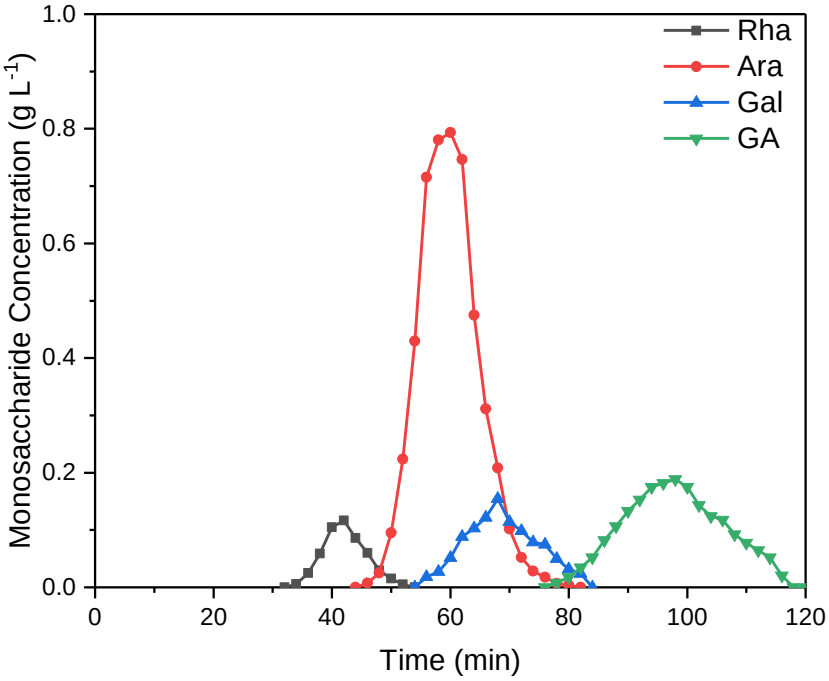

Figure 4-5: CPC separation of a crude sample prepared in the LP using phase system VIII (Table 2-1). The crude sample was prepared as described in Section 2.7.3. Separation was performed on the semi-preparative column in the ascending mode with a flow rate of 8 mL min^{-1}, a rotational speed of 1000 rpm, and with an injection volume of 10 mL, as described in Section 2.4. Full experimental details are given under Experiment 4 in Table 4-1.

4.4 Optimisation through variations in rotational speed, operating mode and flow rate

Further optimisation of CPC operating conditions can lead to improvements in separation performance as described in Section 1.2.3. An increase in the rotational speed was implemented to improve the stationary phase retention and interfacial area within the mixing chamber [52], and thus improve separation performance. Initially, the rotational speed was increased to the operating maximum of 2000 rpm, however, during a separation of 10 mL of crude, prepared in the LP, at 8 mL min^{-1} the pressure increased above 75 bar and so separation was halted. Repeating the experiment at a lower rotational speed of 1600 rpm allowed for a safe maximum working pressure of 48 bar during separation. For comparison, at 1000 rpm, the maximum pressure was 22 bar.

The resulting chromatogram at 1600 rpm is shown in Figure 4-6 and is very similar to the separation at 1000 rpm, as shown in Figure 4-5. The retention times of solutes in each separation and the purities and recoveries of each sugar are shown in Table 4-4. One main difference is that after 120 min at 1600 rpm, the GA peak is still eluting, whereas, at 1000 rpm, full elution of the GA peak had been achieved. This could be due to the small improvement in retention at 1600 rpm (55%, up from 51% at 1000 rpm). Furthermore, the separation performance appears to be slightly worse for each of the fractions at the higher rotational speed. As a result, a rotational speed of 1000 rpm continued to be used due to the slightly improved separation performance, reduced operating pressure and reduced run time.

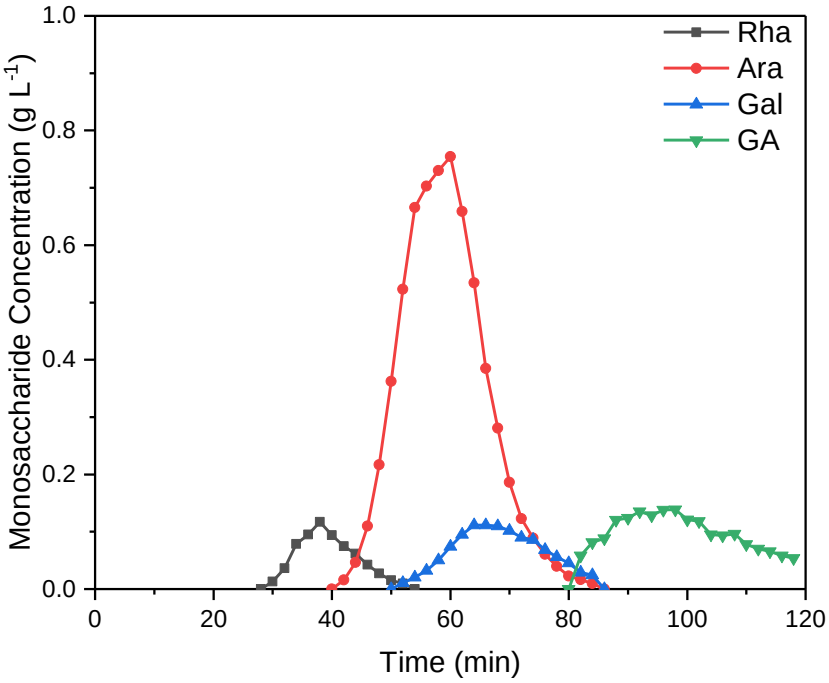

Figure 4-6: CPC separation of a crude sample at a rotational speed of 1600 rpm. The crude sample was prepared as described in Section 2.7.3. Separation was performed on the semi-preparative column using phase system VIII (Table 2-1) in the ascending mode with a flow rate of 8 mL min^{-1}, a rotational speed of 1600 rpm, and with an injection volume of 10 mL, as described in Section 2.4. Full experimental details are given under Experiment 5 in Table 4-1.

Table 4-4: Maximum purities and recoveries of target monosaccharides from crude CPC separations with varying rotational speed and flow mode and flow rate. CPC separation was performed on a semi-preparative, 250 mL Kromaton CPC with full details given in Table 4-1 based on the Experiment number. Purities and recoveries are given as % (w/w) and calculated from ICS analysis as defined in Section 2.8.3.

Exp.	Rotational Speed (rpm)	Mode	Flow rate (mL min^{-1})	S_F (%)	Rha			Ara			GA		
					Purity (%)	Recovery (%)	Time* (min)	Purity (%)	Recovery (%)	Time* (min)	Purity (%)	Recovery (%)	Time* (min)
4	1000	Asc	8	51	94	96	28-44	88	97	46-66	99	99	78-110
5	1600	Asc	8	55	97	76	30-42	84	95	44-80	96	100	82- >120
6	1000	Desc	8	54	82	86	26-33	83	98	20-25	89	90	16-19
7	1600	Desc	8	44	91	83	29-35	81	98	23-28	90	83	19-22
8	1000	Desc	6	60	-	-	-	83	99	27-43	82	89	21-26

Due to the requirement of preparing the crude sample in the LP (Section 4.3), a separation was performed in the descending mode to assess whether any improvement in the separation performance could be achieved. Operating in the descending mode allows the UP to act as the stationary phase while the LP acts as the mobile phase and flows from the centre to the outside of each chamber and from the top of the column to the bottom between plates (Section 1.2.3.2). The descending mode also means that the LP sample is prepared in what is now the mobile phase and can start to partition with the stationary phase immediately after sample injection. Furthermore, the elution order should be reversed, with GA eluting first and Rha last. All other operating conditions were kept constant, including the rotational speed (1000 rpm), crude sample preparation (in the LP) and flow rate (8 mL min^{-1}).

Figure 4-7 shows the chromatogram obtained in the descending mode. The most noticeable difference is the much reduced total run time, with full elution of all components in just 35 min (down from 110 min in the ascending mode). An elution volume of 1 column volume represents the central point of a CPC separation and the elution time of a solute with a partition coefficient of 1, as detailed in Section 1.2.3.3. Peaks eluting after this point in the ascending mode will elute prior to this point in the descending mode and vice versa. In this case, 1 column volume (250 mL) would be eluted after 31.25 min at 8 mL min^{-1} which appears to be around the point of inversion when comparing the ascending mode (Figure 4-5) with the descending mode (Figure 4-7). It is not possible to accurately plot the x-axis based on calculated partition coefficient values due to bleeding of the stationary phase during the separations and so a more theoretical comparison of the separations in the ascending and descending modes is not possible. The recoveries and purities, shown in Table 4-4, are lower than for operation in the ascending mode for all fractions, although the stationary phase retention is slightly increased from 51% to 54%.

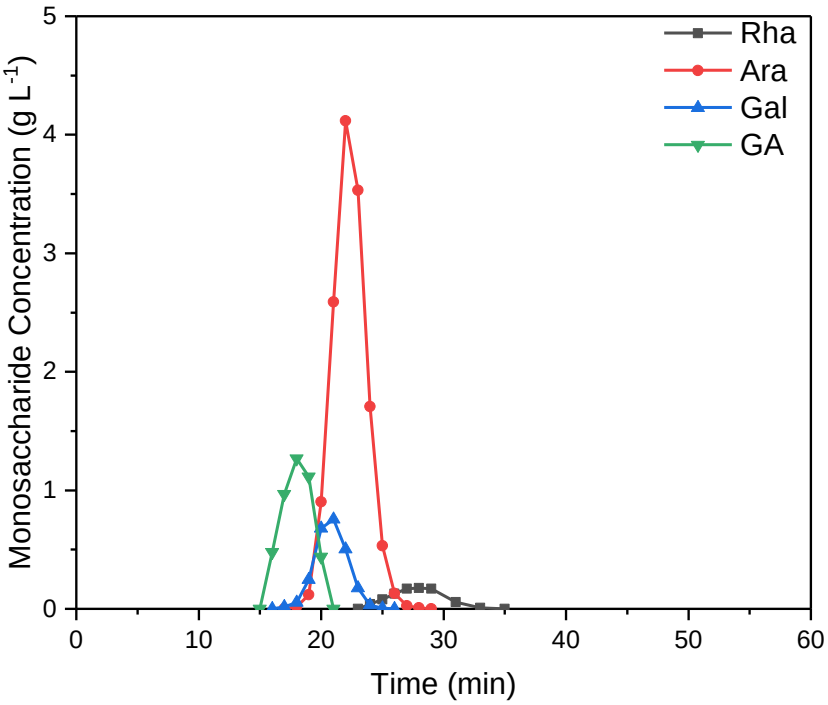

Figure 4-7: CPC separation of a crude sample in the descending mode at 1000 rpm. The crude sample was prepared as described in Section 2.7.3. Separation was performed on the semi-preparative column using phase system VIII (Table 2-1) with a flow rate of 8 mL min^{-1}, and with an injection volume of 10 mL, as described in Section 2.4. Full experimental details are given under Experiment 6 in Table 4-1.

Increasing the rotational speed to 1600 rpm also had little effect on the separation performance: the purity and recovery of Ara remain effectively constant, while for GA the recovery drops from 90% to 83%; although it did increase the retention times of all components. These results are also shown in Table 4-4 and the corresponding chromatogram in Figure 4-8. Furthermore, increasing the rotational speed led to an unexpected drop in stationary phase retention, from 54% to 44%.

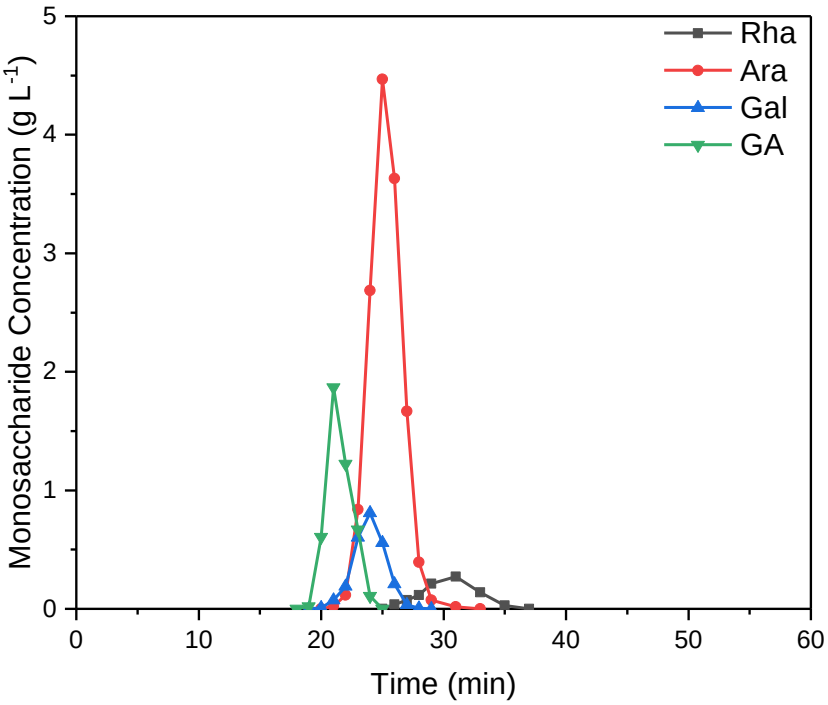

Figure 4-8: CPC separation of a crude sample in the descending mode at 1600 rpm. The crude sample was prepared as described in Section 2.7.3. Separation was performed on the semi-preparative column using phase system VIII (Table 2-1) with a flow rate of 8 mL min^{-1}, and with an injection volume of 10 mL, as described in Section 2.4. Full experimental details are given under Experiment 7 in Table 4-1.

Based on the above results it appears that the descending mode performs less well than the ascending mode for the same rotational speed at both 1000 and 1600 rpm, although separation times are dramatically reduced with full elution in descending mode before the elution of the first sugar in ascending mode. It is worth noting that the coloured impurities elute after the last sugars in the descending mode and they could take a long time to fully elute, making this a less attractive operating mode.

While the separation performance is lower, the much reduced separation time must be taken into consideration. In a further experiment at 1000 rpm, the flow rate was dropped from 8 to 6 mL min^{-1} in order to improve the stationary phase retention and thus separation performance. The results, shown in Figure 4-9 and Table 4-4, indicate an increase in Sf from 54 to 60% with the drop in flow rate, however, separation performance remains broadly the same for all fractions. Rha values were not calculated due to the programmed fraction collection ending before full elution of the peak.

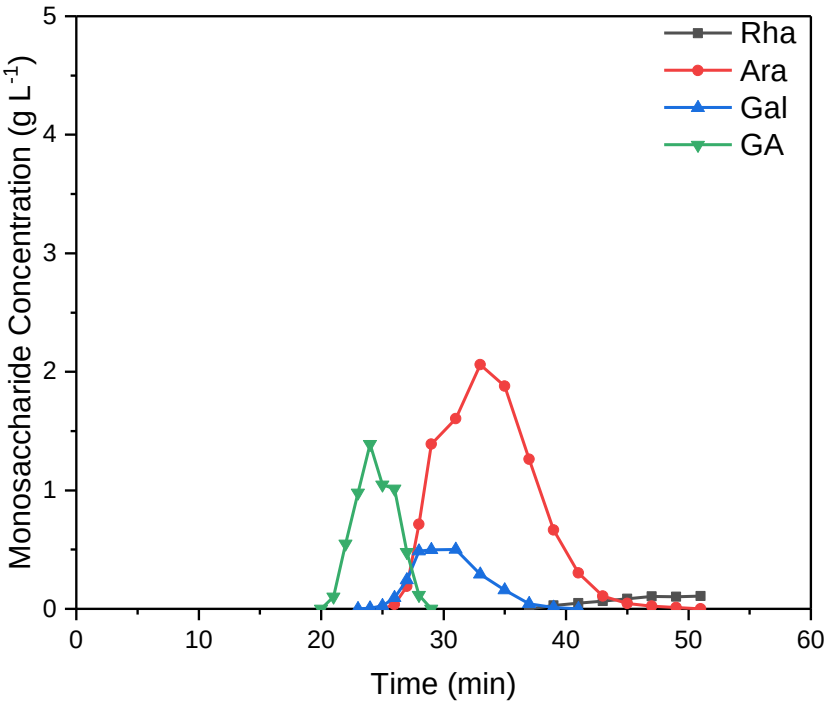

Figure 4-9: CPC separation of a crude sample in the descending mode at 1600 rpm and a flow rate of 6 mL min^{-1}. The crude sample was prepared as described in Section 2.7.3. Separation was performed on the semi-preparative column using phase system VIII (Table 2-1) with an injection volume of 10 mL, as described in Section 2.4. Full experimental details are given under Experiment 8 in Table 4-1.

Overall, the results in this section show that the descending mode did not provide improvements in the separation performance. Furthermore, while the descending mode could provide reduced run times and thus reduced solvent consumption, the fractions would be eluted in the LP and therefore contain a much higher concentration of ammonium sulphate which is likely to be more difficult and costly to remove than the lower salt, higher ethanol concentrations in the UP (Section 1.2.4.4). Taking these factors into consideration, it was decided to continue using the ascending mode, at 1000 rpm and 8 mL min^{-1}.

4.5 Increasing throughput by increasing injection volume

Throughput is a major consideration for any separation technique used in a biorefinery context where the quantities of feedstocks utilised can be large [3]. Separations using the crude hydrolysate were therefore performed with increasing injection volumes (from 10 - 40 mL, shown in Figure 4-10) to improve CPC throughput. In all cases, crude samples were prepared in the LP. As shown in Table 4-5, this quadrupling of the

sample volume resulted in relatively small reductions (within a 10% range) in purity and recovery of target monosaccharides in pooled fractions due to peak broadening. This broadening of the peaks extended the total elution time from 110 min to 140 min for 10 and 40 mL injections respectively.

Table 4-5: Maximum purities and recoveries of target monosaccharides from CPC separation of crude hydrolysate with varying sample volume. CPC separation was performed on a semi-preparative, 250 mL Kromaton CPC with full details given in Table 4-1 based on the Experiment number. Purities and recoveries are given as % (w/w) and calculated from ICS analysis as defined in Section 2.8.3.

Experiment	Sample Volume (mL)	S_F (%)	Rha			Ara			GA		
			Purity (%)	Recovery (%)	Time* (min)	Purity (%)	Recovery (%)	Time* (min)	Purity (%)	Recovery (%)	Time* (min)
4	10	51	94	96	28-44	88	97	46-66	99	99	78-110
9	20	50	98	93	28-42	85	96	44-66	97	98	78-122
10	30	56	90	88	28-42	79	96	44-66	94	92	76-124
11	40	57	86	88	28-44	79	96	46-70	92	93	78-140

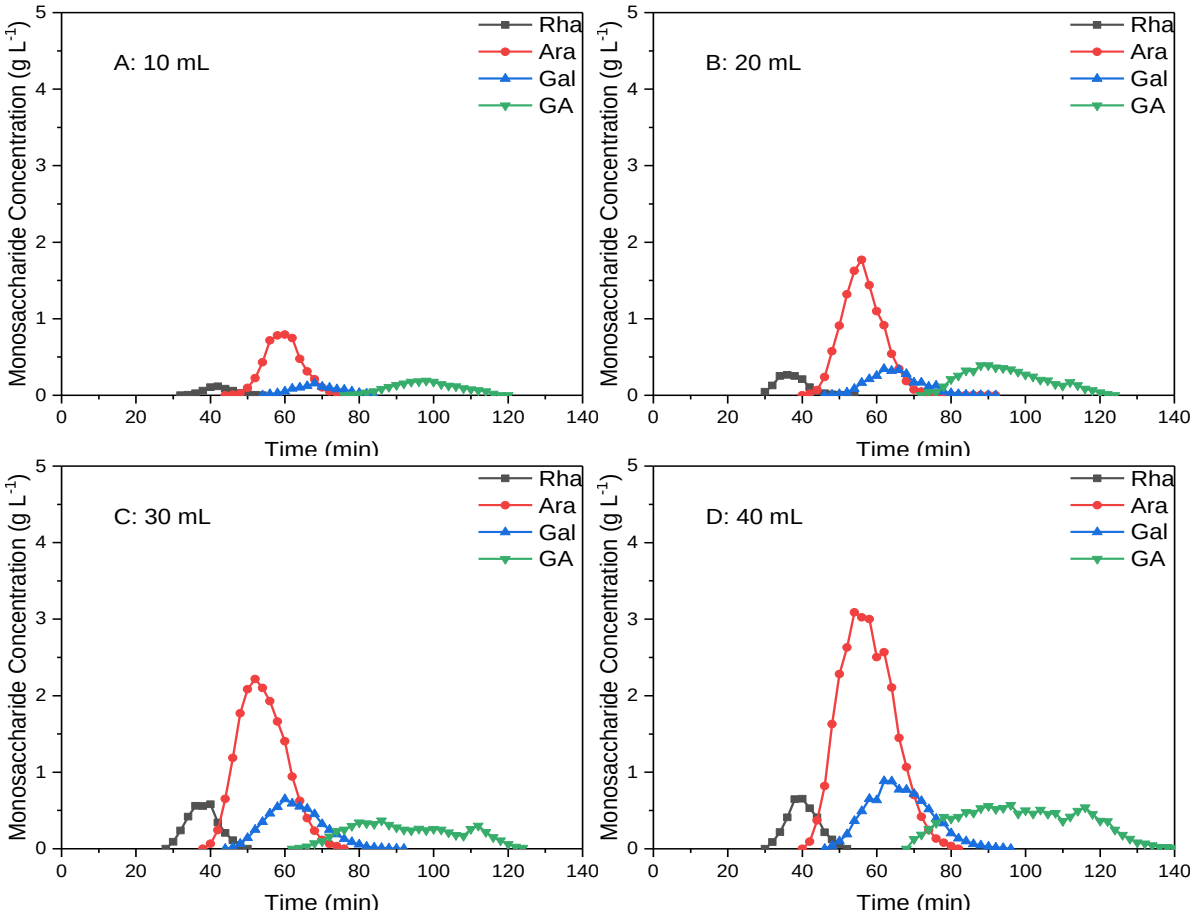

Figure 4-10: CPC separations of crude samples with varying sample injection volumes: A 10 mL; B 20 mL; C 30 mL; D 40 mL. The crude samples were prepared in the LP as described in Section 2.7.3. Separation was performed using phase system VIII (Table 2-1) on the semi-preparative column in the ascending mode at a flow rate of 8 mL min^{-1} and a rotational speed of 1000 rpm, as described in Section 2.4. Full experimental details are given under Experiment 4, 9, 10 and 11 for A, B, C and D respectively in Table 4-1.

Calculated throughputs for increasing injection sample volume are shown in Table 4-6. It is demonstrated that a four-fold increase in sample volume results in a three-fold increase in throughput, as peak widths increase with higher sample loads, increasing the total run time. Throughput values for operation in elution-extrusion mode and for CPC scale-up are also presented in Table 4-6 and will be discussed in detail in Sections 4.6 and 4.7 respectively.

Table 4-6: Monosaccharide and total solids throughputs for CPC separations with various operating strategies. Crude hydrolysate samples were prepared in the lower phase for injection, as described in Section 2.8. Throughputs are given in grams of monosaccharide processed, per litre of total column volume, per hour of run time. Run time is defined as the time taken for full elution of all solutes. CPC was performed on a Kromaton CPC with full details given in Table 4-1 based on the Experiment number. Elution-extrusion mode was performed, where stated, by switching to pump mobile phase 72 minutes after sample injection as described in Section 2.5.2.

Experiment	Column volume (mL)	Sample Volume (mL)	Mode	Run Time (min)	Total monosaccharide throughput ($g\ L^{-1}\ h^{-1}$)	Total solids throughput ($g\ L^{-1}\ h^{-1}$)
4	250	10	Elution	110	0.44	2.2
9	250	20	Elution	122	0.79	3.9
10	250	30	Elution	124	1.2	5.8
11	250	40	Elution	140	1.4	6.9
12	250	30	Elution-extrusion	100	1.4	7.2
13	950	152	Elution	117	1.6	8.2
14	950	152	Elution-extrusion	102	1.9	9.4

4.6 Operation in elution-extrusion mode and reproducibility

One of the advantages of CPC compared to conventional resin based chromatography is that it is possible to manipulate the column contents, particularly the stationary phase, within a run to improve separation performance or reduce separation times [106]. With increased injection volumes, as in Figure 4-10C and Figure 4-10D where 30 mL (12% of column volume) and 40 mL (16% of column volume) samples respectively were injected, the GA peak becomes excessively broad, taking upwards

of 1 h to fully elute (50% of total elution time). This band broadening primarily occurs as solutes leave the column as noted by Berthod et al. [107]. The use of elution-extrusion mode allows for shortening of the elution time of strongly retained compounds by rapidly extruding them from the column once the narrower, earlier fractions have eluted. Extrusion was performed by simply switching to pump stationary phase as described by Berthod et al. [106].

Extrusion also has the benefit of refreshing the stationary phase, an important aspect of improving throughput and reproducibility as separation will always occur on a regenerated column. Figure 4-11 demonstrates the performance of CPC separation using the elution-extrusion mode, with three sequential 30 mL injections of crude sample prepared in LP. The extrusion step was started 72 minutes after sample injection and lasted for 28 minutes, at which point the flow was switched back to the mobile phase (UP) and the next injection was started. This gave a total cycle time of 100 minutes per sample. Figure 4-12 shows an overlay of the total monosaccharide concentrations for each of the three injections based on ICS analysis. While there is an apparent shortening of the Rha and Ara retention times after the first injection, the subsequent retention times appear consistent and separation performance does not appear to be affected, demonstrating good reproducibility of the method.

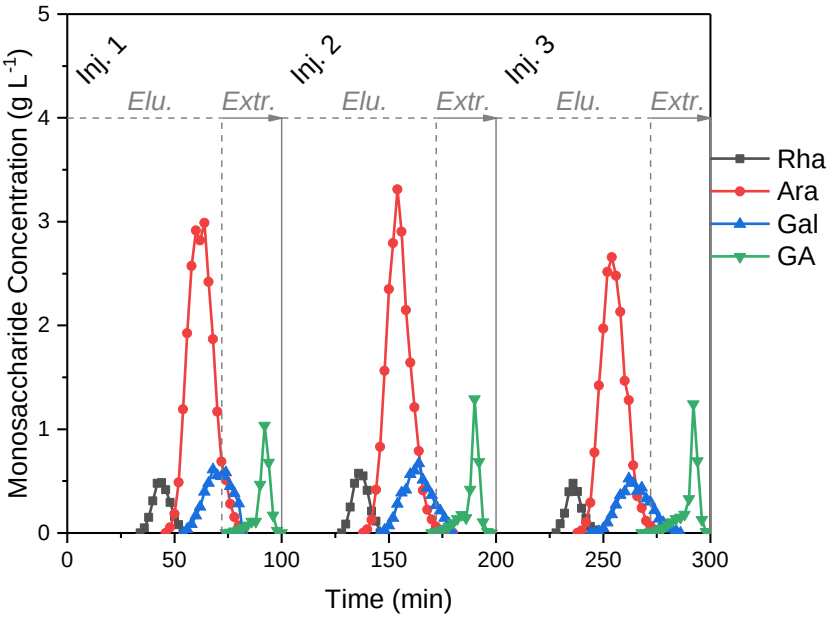

Figure 4-11: CPC separation of three sequential 30 mL crude hydrolysate samples performed in the elution-extrusion mode. The crude sample was prepared as described in Section 2.7.3. Separation was performed on the semi-preparative column, in the ascending mode, at a flow rate of 8 mL min^{-1} and a rotational speed of 1000 rpm, as described in Section 2.4. The chromatogram shows the concentrations of each individual sugar against the total elution time. Extrusion was performed 72 min after each injection. Injections 2 and 3 were performed 28 min after extrusion of the previous injection as described in Section 2.5.2. Full experimental details are given under Experiment 12 in Table 4-1.

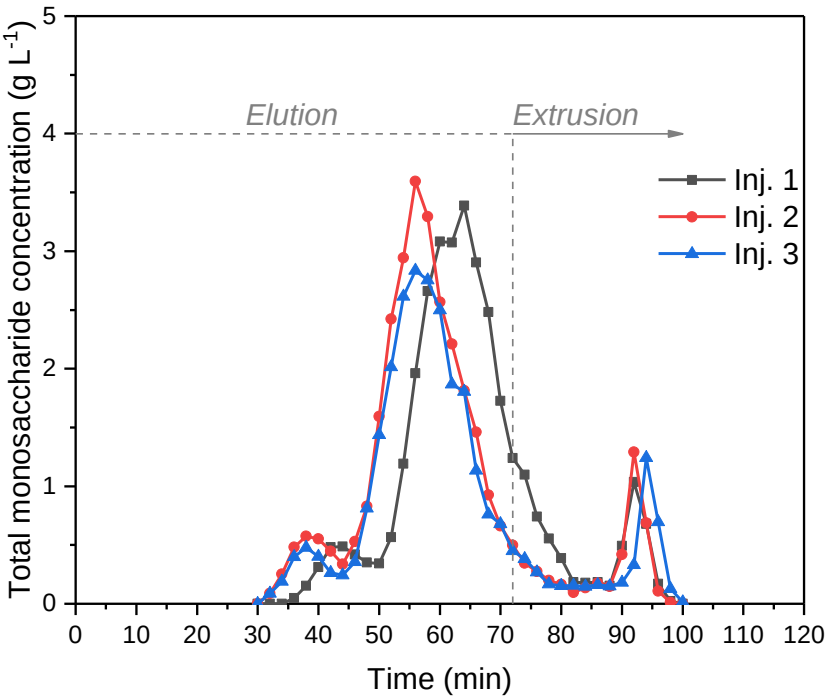

Figure 4-12: CPC separation of three sequential 30 mL crude samples performed in the elution-extrusion mode. The crude sample was prepared as described in Section 2.7.3. Separation was performed on the semi-preparative column, in the ascending mode, at a flow rate of 8 mL min^{-1} and a rotational speed of 1000 rpm, as described in Section 2.4. The chromatogram shows the total concentrations of sugars against the elution time for each individual injection. Extrusion was performed 72 min after each injection. Injections 2 and 3 were performed 28 min after extrusion of the previous injection as described in Section 2.5.2. Full experimental details are given under Experiment 12 in Table 4-1.

Throughput values are presented in Table 4-6 and show that throughput was increased from 1.2 g L^{-1} h^{-1} to 1.4 g L^{-1} h^{-1} using the elution-extrusion method, relative to full elution, based on total run time. As confirmed in Figure 4-11, this operating strategy had the added benefit of being able to perform consecutive injections immediately without the need for further column regeneration.

4.7 CPC process scale-up

Linear scale-up of the CPC column provides a further option for increasing throughput based on the volume ratio of the two columns. While this method can provide an effective method of scaling up, the separation behaviour is not expected to be strictly linear [105]. Improvements in separation performance can often be seen at the larger scale [70], and alternative scale-up methodologies have been developed to take advantage of this, including the free space between peaks method [101] and the use of

global mass transfer coefficients and the stationary phase retention as scale-up invariants [102].

The linear method is demonstrated here due to its simplicity and uses the working volumes of the columns, including extra volume before and after the column, to scale up from a semi-preparative to a preparative scale CPC machine. It is therefore important that this extra volume is minimised when calculating the working volumes of the columns. The working volumes of the columns were determined to be 250 mL and 950 mL, respectively, giving a scale-up factor of 3.8 using the method described in Section 2.6. This scale-up factor was used to linearly scale-up the mobile phase flow rate, injection volume and stationary phase flow rate in the extrusion step. The extrusion time was maintained at 72 minutes between scales and rotational speed was kept constant at 1000 rpm to maintain the same g-force as the columns had the same diameter (Section 2.6). A summary of the scale-up parameters is detailed in Table 4-7.

Table 4-7: Conditions used for linear scale-up of CPC separations from the semi-preparative column to the preparative column. CPC Columns and equipment are described in Section 2.4. The scale-up method used is described in Section 2.6.

Operating Conditions	Semi-preparative	Preparative
Working volume (mL)	250	950
Mobile phase flow rate (mL min^{-1})	8	30.4
Injection Volume (mL)	40	152

The scaled up separation process operated in full elution mode, shown in Figure 4-13, demonstrates good similarity in the elution profile compared with the semi-preparative scale, shown in Figure 4-10D. One difference is that the GA peak appears to be splitting into two separate peaks. On the semi-preparative scale the GA peak is very broad but it is not clear if the peak is splitting or it is just an effect of band broadening. At the preparative scale, the peak appears to be split in the middle which could be more noticeable due to improved separation performance at the larger scale [70]. However, it is unclear why the peak is splitting, and there is no apparent difference in the analytical chromatograms with either ICS analysis or HPLC-RI. The peak split could be due to the two ionic forms of GA (the ionised and non-ionised forms) which has a pKa of 3.5 [224]. However, the phase system has a pH 5.9 and 5.4 in the UP and LP respectively and the elution fractions containing GA also have a consistent pH of 5.8,

indicating that the GA may only be present in the acidic form. It is possible that adding an acid to the phase system would force the GA into the non-ionised form and elute as a single narrower peak. However, the solute partition coefficients in an acidified system were determined in Section 3.2.4 and, while the presence of TFA did shift the partition coefficient of GA, it shifted towards that of the other sugars, reducing the separation factor. This could shift the second peak earlier or into the first peak, and so may actually reduce separation performance. In the full elution mode, separation performance between the two scales, shown in Table 4-8, is comparable despite a drop in the stationary phase retention from 57 to 50%. This drop could be offset by improved mixing within the larger chambers of the preparative column.

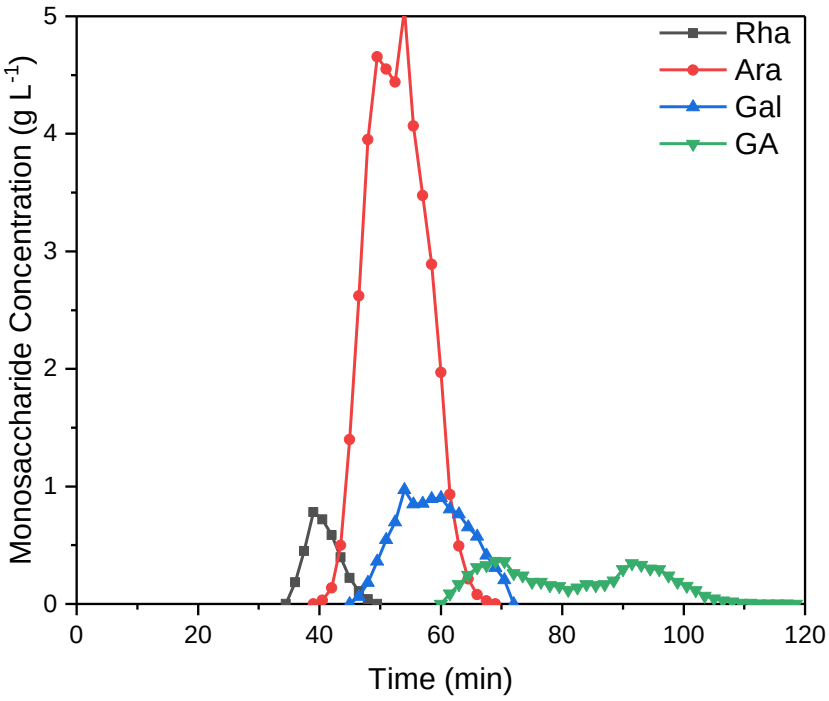

Figure 4-13: CPC separation of a crude sample performed on a preparative (950 mL) column. The crude sample was prepared as described in Section 2.7.3. Separation was performed using phase system VIII (Table 2-1) in the ascending mode and a rotational speed of 1000 rpm as described in Section 2.4. Mobile phase flow rate and injection volume were scaled up linearly based on column working volume from Experiment 9 (Table 4-1) from 8 to 30.4 mL min^{-1} and 40 to 152 mL respectively (Table 4-7) based on a scale-up factor of 3.8 as described in Section 2.6. Full experimental details are given under Experiment 13 in Table 4-1.

Table 4-8: Optimised purities and recoveries of target monosaccharides from CPC separation of a crude SBP hydrolysate at semi-preparative (250 mL) and preparative (950 mL) scales. Scale-up parameters are outlined in Table 4-7. Extrusion was performed after 72 min in the elution-extrusion mode at preparative scale as described in Section 2.5.2. Full experimental details are given in Table 4-1 based on the Experiment number. Purities and recoveries are given as % (w/w) as defined in Section 2.8.

Experiment	Scale	Mode	S_F (%)	Rha			Ara			GA		
				Purity (%)	Recovery (%	Time* (min)	Purity (%)	Recovery (%)	Time* (min)	Purity (%)	Recovery (%)	Time* (min)
4	Semi-prep.	Elution	57	86	88	28-44	79	96	46-70	92	93	78-100
13	Preparative	Elution	50	82	89	36-43.5	84	98	45-63	90	87	67.5-120
14	Preparative	Elution - Extrusion	50	92	93	33-45	84	97	46.5-66	96	95	78-100.5
15	Preparative	Elution - Extrusion	49	91	93	34.5-45	81	98	46.5-66	98	95	75-102

Operation of the preparative scale CPC machine in the elution-extrusion mode (Section 4.6) was also demonstrated to further enhance throughput at the larger scale. As shown in Figure 4-14, the performance is again similar, with a further improvement of the GA purity and recovery (Table 4-8). The stationary phase retention is constant at 50% between the full elution mode and the elution-extrusion mode. This is expected as the two methods only deviate after 72 min, well after the initial stationary phase breakthrough. As in the full elution mode, the GA peak appears split into two, with a small peak eluting after the start of extrusion but prior to the extrusion peak. Run time is comparable to the elution-extrusion mode on the semi-preparative column with full elution of all compounds with no GA detected after 102 min. It is possible that performing extrusion earlier could reduce the separation between the two GA peaks, increasing the concentration of the GA fraction and reducing the total run time.

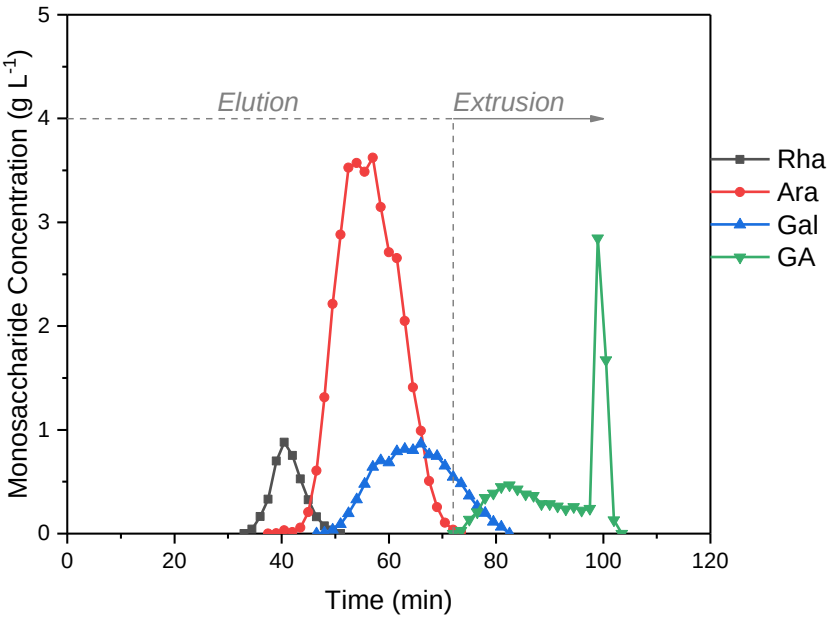

Figure 4-14: CPC separation of a crude sample performed on a preparative (950 mL) column in the elution-extrusion mode. The crude sample was prepared as described in Section 2.7.3. Separation was performed using phase system VIII (Table 2-1) in the ascending mode and a rotational speed of 1000 rpm as described in Section 2.4. Mobile phase flow rate and injection volume were scaled up linearly based on column working volume from Experiment 9 (Table 4-1) from 8 to 30.4 mL min^{-1} and 40 to 152 mL respectively (Table 4-7) based on a scale-up factor of 3.8 as described in Section 2.6. Extrusion was performed after 72 min as described in Section 2.5.2. Full experimental details are given under Experiment 13 in Table 4-1.

Overall, separation performance is similar at the two scales, demonstrating process stability and predictability with the elution-extrusion mode (Figure 4-14) again

outperforming the full elution method (Figure 4-13) in terms of product purity and recovery. Reproducibility has been confirmed at the preparative scale by repeating the elution-extrusion separation which generated a nearly identical chromatogram (Figure 4-15). The stationary phase retention (49%) is almost identical to the previous preparative scale separations (both 50%), and the purities and recoveries of each fraction in the two repeats demonstrates the reproducibility of the separation (Table 4-8).

Furthermore, throughput values, shown in Table 4-6, are improved beyond the linear scale-up factor of 3.8; when normalised per litre of column volume, the results give a throughput of monosaccharides of 1.4 g L^{-1} h^{-1} at the semi-preparative scale and 1.7 g L^{-1} h^{-1} at the preparative scale under full elution conditions. Under elution-extrusion conditions, this throughput is increased even further to 1.9 g L^{-1} h^{-1}.

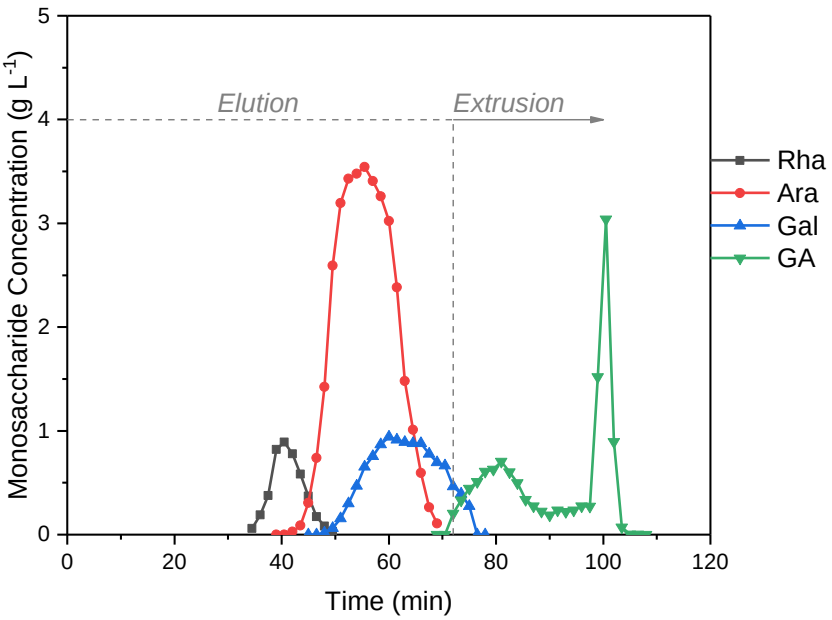

Figure 4-15: Repeat of CPC separation of a crude sample performed on a preparative (950 mL) column in the elution-extrusion mode (shown in Figure 4-14). The crude sample was prepared as described in Section 2.7.3. Separation was performed using phase system VIII (Table 2-1) in the ascending mode and a rotational speed of 1000 rpm as described in Section 2.4. Mobile phase flow rate and injection volume were scaled up linearly based on column working volume from Experiment 9 (Table 4-1) from 8 to 30.4 mL min^{-1} and 40 to 152 mL respectively (Table 4-7) based on a scale-up factor of 3.8 as described in Section 2.6. Extrusion was performed after 72 min as described in Section 2.5.2. Full experimental details are given under Experiment 13 in Table 4-1.

Preliminary work on scale-up to industrial scale CPC devices is shown in Appendix B.

4.8 Chapter summary

The aim of Chapter 4 was to demonstrate the potential of the CPC method developed in Chapter 3 to the processing of crude SBP hydrolysates. This represents a key step forward in showing that CPC is applicable to the separation of biorefinery feedstocks that can contain a large number of impurities and a high solids loading. As shown in Figure 4-5, the CPC separation method developed in Chapter 3 is applicable to the separation of the monosaccharides from crude hydrolysate simultaneously removing impurities and isolating the three target monosaccharides (Rha, Ara and GA) into separate fractions. The main conclusions of this chapter are:

- DMSO, used in the method described in Section 4.2, was shown not to have a major effect on the CPC separation of the target monosaccharides (Table 4-2) and so was removed from the phase system in order to assist in future downstream processing and solvent recycling.
- Crude sample preparation in the stationary phase (LP) allows for complete solubilisation of the sample without any precipitation of monosaccharides or salts. Furthermore, this approach enables removal of some coloured contaminants due to a small volume of a new phase forming on top of the prepared sample which can easily be discarded (Figure 4-4C).
- CPC separation using the crude SBP hydrolysate (Figure 4-5) is improved relative to the model synthetic mixture. It is able to separate the sample into the same three fractions (Rha, Ara and Gal, and GA) at higher purities and recoveries (Table 4-3) while simultaneously removing the coloured contaminants earlier in the elution profile.
- Increasing the sample volume from 4 to 16% v/v (Figure 4-10) allowed for a three-fold improvement in throughput with only minor losses in separation performance (Table 4-5).
- The elution-extrusion mode reduced the total run time by 24% by extruding the column contents during the elution of the final GA fraction. This allowed for sequential injections to be performed without a separate stationary phase regeneration step (Figure 4-11).

- Linear scale-up based on the total column volumes from the semi-preparative 250 mL column to the preparative 950 mL column showed comparable separation performance (Table 4-8) and an improvement in total sugars throughput. Final optimised throughput in the elution-extrusion (chromatogram shown in Figure 4-14) gave a total monosaccharide throughput of 1.9 g L^{-1} h^{-1} and a total solids throughput of 9.4 g L^{-1} h^{-1}.

The work presented in Chapter 3 and Chapter 4 has established a novel CPC methodology for the recovery and purification of hydrophilic solutes, such as carbohydrates, from crude biorefinery feedstocks. In the following chapters simulated moving bed chromatography (Section 1.6.1) is explored as an alternative to CPC separation for the isolation of monosaccharides from the crude hydrolysate. Chapter 5 examines SMB as a method of isolating Ara from a synthetic neutral mixture of the neutral sugars present in the crude hydrolysate.

Chapter 5 Design of a simulated moving bed chromatography method for the isolation of L-arabinose from synthetic neutral monosaccharide mixtures.

5.1 Introduction, aim and objectives

As an alternative to CPC, as described in Chapter 3 and Chapter 4, SMB provides a proven large scale technology for sugar separations (Section 1.6). However, its industrial applications have focussed on cleaner feedstreams such as glucose-fructose separations (Section 1.6.4) rather than hydrolysates. The SMB separation examined in this chapter will focus on the isolation of Ara from a synthetic mixture of the neutral sugars (a synthetic neutral mixture – Section 2.7.4) present in the crude hydrolysate (Ara, Rha and Gal). GA will likely have to be isolated prior to this SMB separation. This will be examined in Chapter 6 along with the removal of contaminants from the crude hydrolysate and crude processing considerations for SMB.

Design of an SMB system initially requires a detailed understanding of how the separation behaves on a conventional batch column. As such, a number of resin and condition screening experiments need to be run on a batch column in order to determine component retention times under different conditions (Section 1.6.2). These retention times can be used to calculate the selectivity of the resin under the operating conditions which can then be used to model SMB separations using the equilibrium theory. However, this SMB model does not consider peak shape or width, which must be used as qualitative metrics during resin and condition selection. The equilibrium theory model can be used to predict SMB operating conditions in the 4-zone, closed loop; and 3-zone, open loop setups, however, additional optimisation may be required based on experimental results.

The aim of this chapter is to develop a method for isolating L-arabinose from a synthetic neutral mixture of the neutral sugars in hydrolysed SBP pectin using SMB. The specific objectives of this chapter are to:

- Screen a number of different resins, their ionic forms and chromatography operating conditions to provide a suitable separation factor and peak shape for subsequent SMB separation.
- Pack 8 columns for SMB separation and compare their packing to ensure consistent column performance.
- Predict operating conditions using an SMB model for SMB separations in the 4-zone setup (Section 1.6.1), with an internal recycle; and the 3-zone setup (Section 1.6.3), without an internal recycle.
- Perform SMB experiments in both the 4-zone (Section 5.4.2) and 3-zone (Section 5.4.3) setups based on the conditions from the SMB model and optimise performance by adjusting operating conditions.

5.2 Resin and condition screening

5.2.1 Monosphere 99 resin in the Ca^{2+} form

Initially, a Monosphere 99 Ca/320 resin was examined and the retention factors of the different individual neutral sugars, and the selectivities relative to Ara, were determined. This resin is provided in the Ca^{2+} form and is primarily used for sugar separations (fructose from glucose) [231]. 20 g of dry resin was hydrated, packed and equilibrated according to the method described in Section 2.9. The resin's size and high particle uniformity (320µm) makes it a good option for large scale SMB separations by providing more consistent column packing and a lower pressure drop [231]. However, it is possible that the large particle size could cause issues on small columns, such as broad peaks, and so the benefit would be restricted to larger columns.

Blue dextran was used as an inert tracer to provide a zero-interaction front from which to calculate retention factors. Individual injections of Ara, Rha and Gal were used to examine the retention times, retention factors and selectivities (prepared as described in Section 2.7.4. Calculation of retention factors and selectivity were performed as described in Section 2.10. All injections were performed once and so error values are not available. However, Table 5-8 shows consistent retention times (within ~1%) for

all components performed on 8 individually packed columns, and so the lack of repeats was not thought to be a concern (Section 5.3).

Figure 5-1 and Figure 5-2 show the overlaid chromatograms of Ara, Rha and Gal, as well as blue dextran as a void volume marker, at room temperature and 50°C respectively. It is apparent that retention factors are low for both columns, eluting rapidly after the blue dextran, however, the peak shape varies significantly with increasing temperature. At room temperature, the sugar peaks have exaggerated peak tails. This is much reduced, although still present, at 50°C. Peak retention times also increase with increasing temperature, although this is likely due to improved peak shape shifting the peak maximum to the right. The blue dextran peak does not shift with increased temperature and thus the increased retention times of the sugars results in increased retention factors.

In terms of separation performance, Gal and Rha effectively co-elute, with only a very small difference in retention factors (shown in Table 5-1). Ara elutes slightly later, giving a higher retention factor. At 50°C a selectivity of 1.75 is produced, however, the resolution is poor due to the broad peaks.

Table 5-1: Retention times (t_i), retention factors (k_i^R) and selectivities (α^R) of individual sugars on a 20 g Monosphere 99 column in the Ca^{2+} form at room temperature (RT) and 50°C. The retention time of blue dextran is also given for reference. Experiments were performed as described in Section 2.10 with retention factors and selectivities also calculated as described in Section 2.10.

Sugar	t_i (RT)	k_i^R (RT)	α^R (RT)	t_i (50°C)	k_i^R (50°C)	α^R (50°C)
Rha	6.2	0.15	2.07	6.9	0.28	1.75
Ara	7.1	0.31	-	8.1	0.49	-
Gal	6.4	0.19	1.63	7.0	0.29	1.69
Blue Dextran	5.4	-	-	5.4	-	-

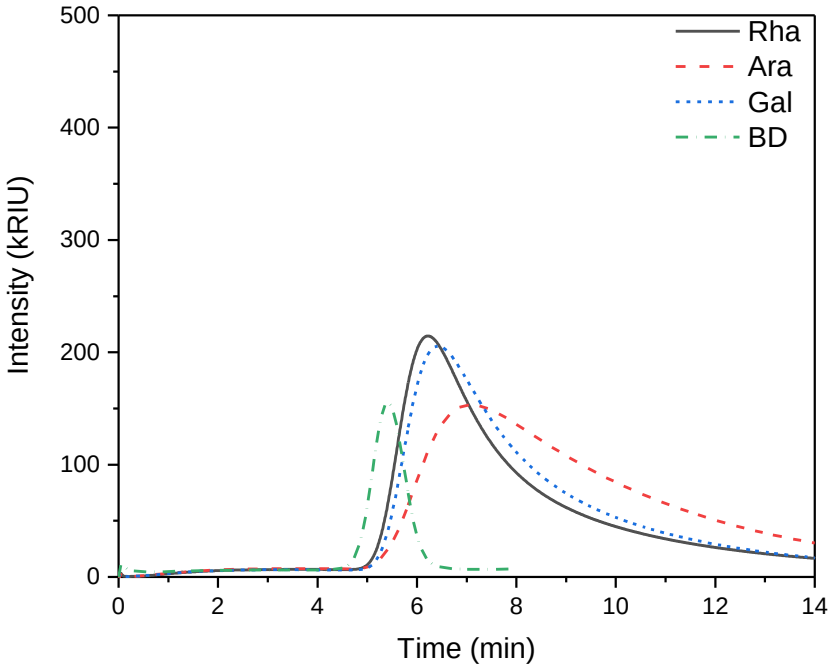

Figure 5-1: Batch separations of neutral monosaccharides a Monosphere 99 column in the Ca^{2+} form at room temperature. 100 µL injections of individual sugars (Ara, Rha and Gal (10 g L^{-1} each)) and blue dextran (1% w/v) were performed as described in Section 2.10 with the column prepared with 20 g of resin as described in Section 2.9. Rha, L-rhamnose; Ara, L-arabinose; Gal, D-galactose; BD, blue dextran.

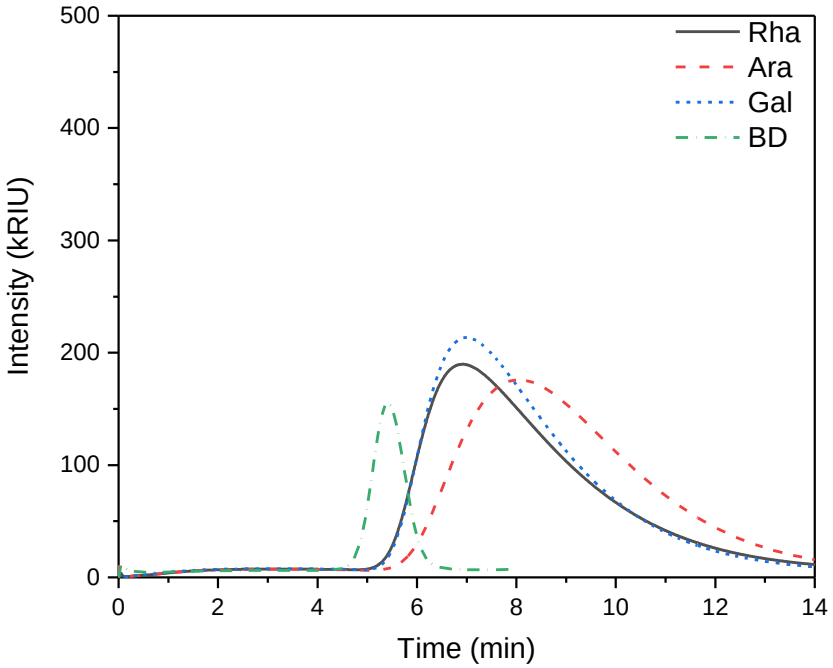

Figure 5-2: Batch separations of neutral monosaccharides a Monosphere 99 column in the Ca^{2+} form at 50°C. 100 µL injections of individual sugars (Ara, Rha and Gal (10 g L^{-1} each)) and blue dextran (1% w/v) were performed as described in Section 2.10 with the column prepared with 20 g of resin as described in Section 2.9. Rha, L-rhamnose; Ara, L-arabinose; Gal, D-galactose; BD, blue dextran.

While the selectivity is good, there are obvious problems with this resin under these conditions as both the peak shape and the resolution are poor. Figure 5-3 highlights this poor resolution. It shows a single injection of a mixture of all three sugars eluting as a single peak, with no evidence of its multicomponent composition. It is possible that these problems could both be rectified with the use of a longer column. Gotmar et al. [232] found that peak tailing could be reduced with the use of higher Stanton numbers (proportional to column length). This peak tailing could also be affecting the retention factors, as the values are taken from the maximum peak height, leading to inconsistencies at larger scales. It is possible that performance would thus improve on longer columns. Additionally, longer columns would improve the resolution by simply providing an increased number of theoretical plates. The use of longer columns, however, is somewhat limited by the pumps available for use on the SMB system, which have a maximum flow rate of 12 mL min^{-1}. A doubling of column length requires a doubling of all flow rates to maintain the same flow-rate ratios in SMB. As a result, alternative resins were sought with a smaller particle size to demonstrate SMB separation on this scale.

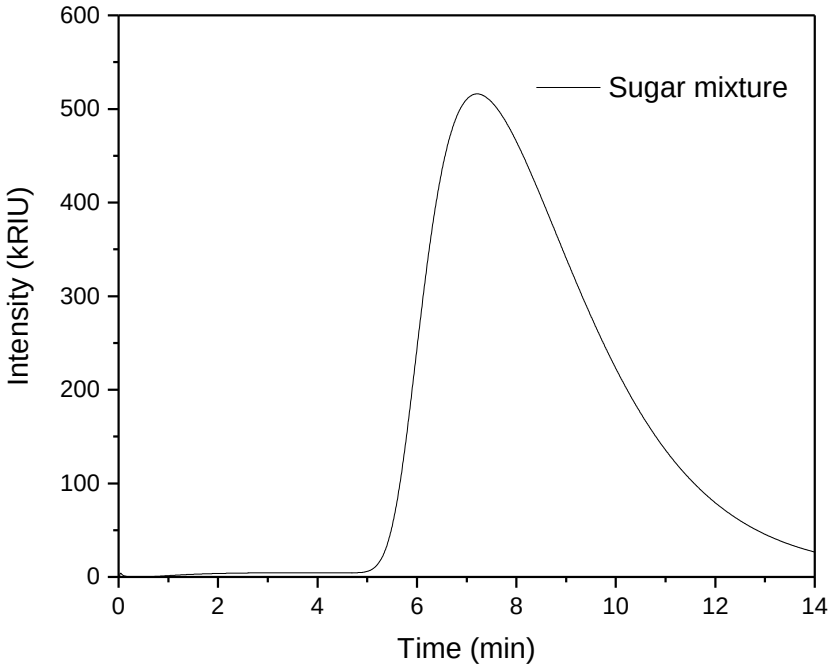

Figure 5-3: Chromatogram of a mixture of neutral sugars (Ara, Rha and Gal) injected onto a 20 g Monosphere 99 column in the Ca^{2+} form at 50°C. The injection volume was 100 µL containing 10 g L^{-1} of each sugar. This experiment was performed as described in Section 2.10 with the column prepared as described in Section 2.9.

5.2.2 Dowex 50W resins in the H^+ form

Three Dowex 50W cation exchange resins with different crosslinking percentages (2, 4 and 8%) were examined. Each had the smallest available mesh size (200-400 mesh ≈ 37-74 µm) and was first examined in the H^+ form. Larger mesh sizes for these resins are available and so can be used in much larger columns without introducing a significant pressure drop [233].

Figure 5-4 and Figure 5-5 show the overlaid chromatograms of individual Rha, Ara and Gal injections on a 20 g Dowex 50W X2 resin in H^+ form at room temperature and 50°C respectively. While the sugars appear to be quite well retained by the column (relative to blue dextran) and have much narrower peaks than the Monosphere 99 resin (Figure 5-1 and Figure 5-2), the selectivity of Rha and Gal to Ara is less than 1.1. Furthermore, there is little apparent difference in the retention factors or peak shape between room temperature and 50°C. Retention times, retention factors and selectivity to Ara are shown in Table 5-2.

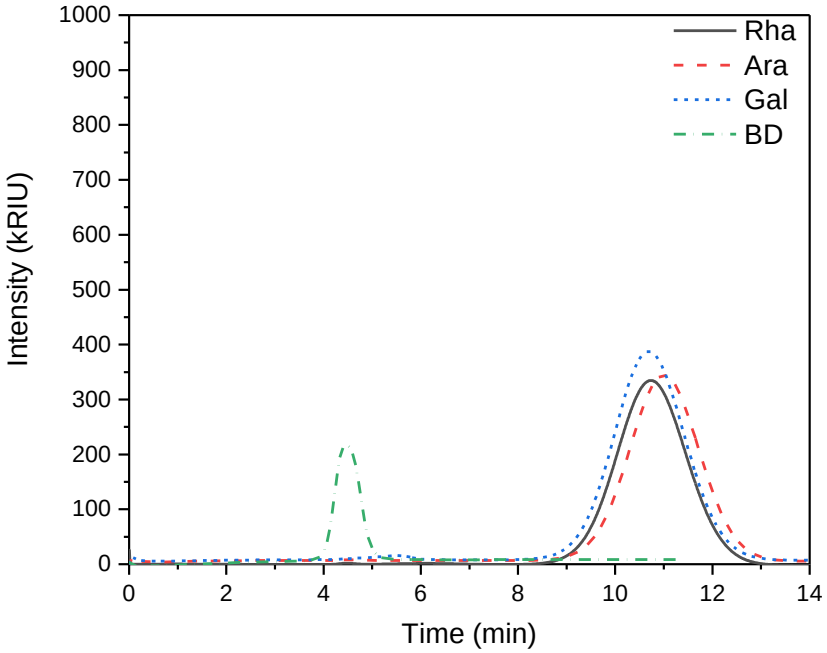

Figure 5-4: Batch separations of neutral monosaccharides a Dowex 50W X2 column in the H^+ form at room temperature. 100 µL injections of individual sugars (Ara, Rha and Gal (10 g L^{-1} each)) and blue dextran (1% w/v) were performed as described in Section 2.10 with the column prepared with 20 g of resin as described in Section 2.9. Rha, L-rhamnose; Ara, L-arabinose; Gal, D-galactose; BD, blue dextran.

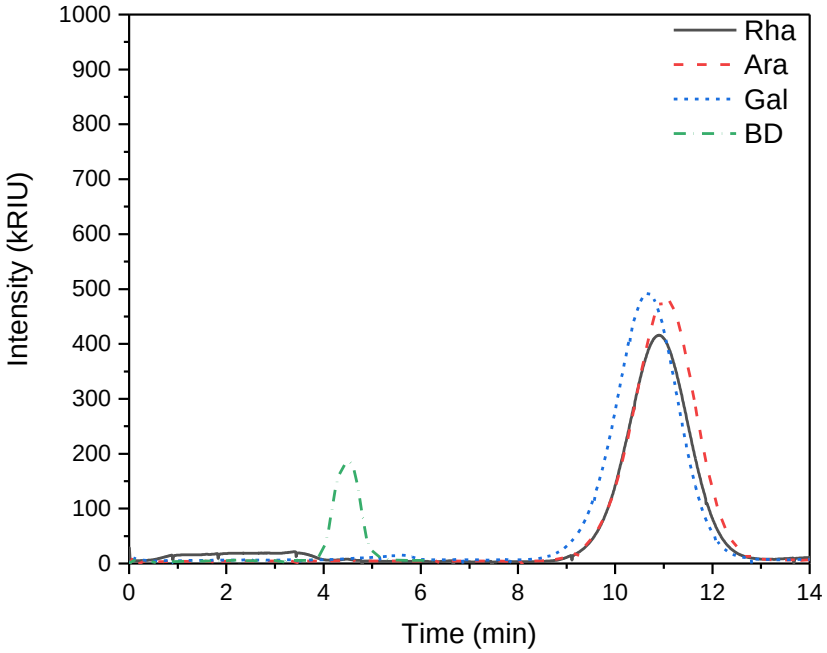

Figure 5-5: Batch separations of neutral monosaccharides a Dowex 50W X2 column in the H^+ form at 50°C. 100 µL injections of individual sugars (Ara, Rha and Gal (10 g L^{-1} each)) and blue dextran (1% w/v) were performed as described in Section 2.10 with the column prepared with 20 g of resin as described in Section 2.9. Rha, L-rhamnose; Ara, L-arabinose; Gal, D-galactose; BD, blue dextran.

Table 5-2: Retention times (t_i), retention factors (k_i^R) and selectivities (α^R) of individual sugars on a 20 g Dowex 50W X2 column in the H^+ form at room temperature (RT) and 50°C. The retention time of blue dextran is also given for reference. Experiments were performed as described in Section 2.10 with retention factors and selectivities also calculated as described in Section 2.10.

Sugar	t_i (RT)	k_i^R (RT)	α^R (RT)	t_i (50°C)	k_i^R (50°C)	α^R (50°C)
Rha	10.7	1.40	1.04	10.9	1.41	1.02
Ara	11.0	1.46	-	11.0	1.44	-
Gal	10.7	1.39	1.05	10.7	1.36	1.06
Blue Dextran	4.5	-	-	4.5	-	-

Separations on Dowex 50W X4, with 4% crosslinking in the H^+ form, is shown in Figure 5-6 and Figure 5-7, at room temperature and 50°C respectively, for sugars and blue dextran. Retention factors are lower than at 2% crosslinking, but all three sugars still elute at very similar times, with selectivity of Rha and Gal at 1.05 and 1.14 respectively at 50°C, slightly increased from the values at 2%. Similar to the 50W X2 resin, temperature appears to have little effect on retention factors and selectivity. Retention times, retention factors and selectivities are shown in Table 5-3.

Table 5-3: Retention times (t_i), retention factors (k_i^R) and selectivities (α^R) of individual sugars on a 20 g Dowex 50W X4 column in the H^+ form at room temperature (RT) and 50°C. The retention time of blue dextran is also given for reference. Experiments were performed as described in Section 2.10 with retention factors and selectivities also calculated as described in Section 2.10.

Sugar	t_i (RT)	k_i^R (RT)	α^R (RT)	t_i (50°C)	k_i^R (50°C)	α^R (50°C)
Rha	8.4	0.79	1.08	8.6	0.84	1.05
Ara	8.8	0.86	-	8.8	0.89	-
Gal	8.3	0.75	1.13	8.3	0.78	1.14
Blue Dextran	4.7	-	-	4.7	-	-

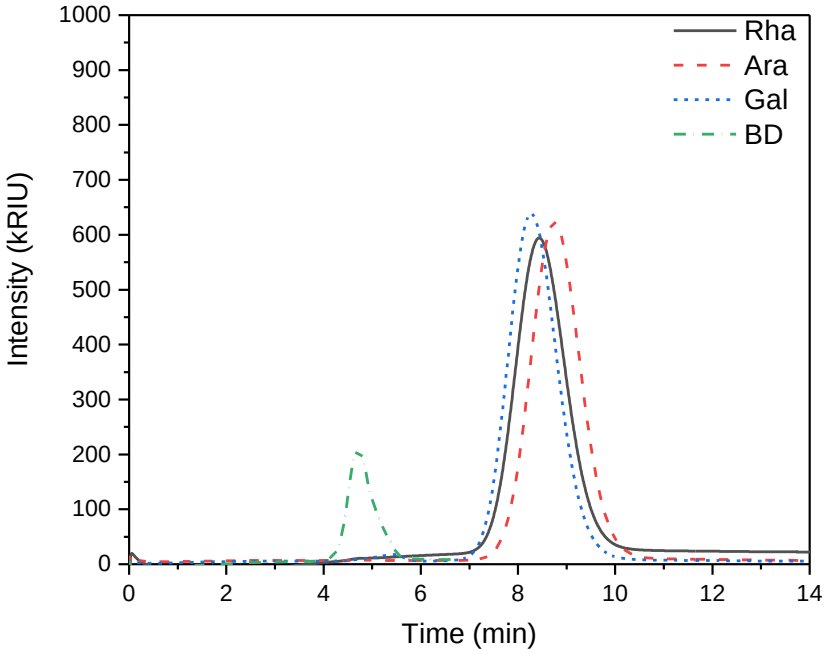

Figure 5-6: Batch separations of neutral monosaccharides a Dowex 50W X4 column in the H^+ form at room temperature. 100 µL injections of individual sugars (Ara, Rha and Gal (10 g L^{-1} each)) and blue dextran (1% w/v) were performed as described in Section 2.10 with the column prepared with 20 g of resin as described in Section 2.9. Rha, L-rhamnose; Ara, L-arabinose; Gal, D-galactose; BD, blue dextran.

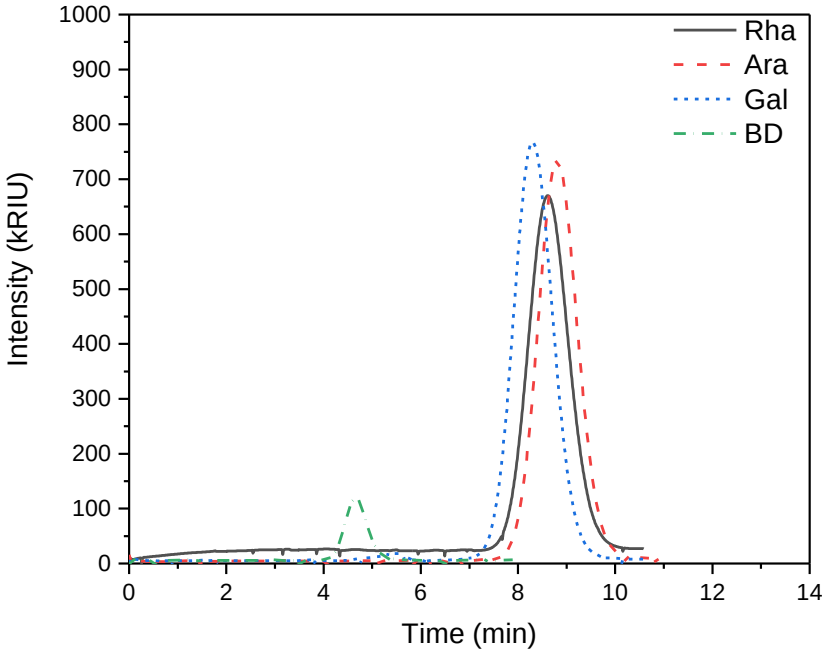

Figure 5-7: Batch separations of neutral monosaccharides a Dowex 50W X4 column in the H^+ form at 50°C. 100 µL injections of individual sugars (Ara, Rha and Gal (10 g L^{-1} each)) and blue dextran (1% w/v) were performed as described in Section 2.10 with the column prepared with 20 g of resin as described in Section 2.9. Rha, L-rhamnose; Ara, L-arabinose; Gal, D-galactose; BD, blue dextran.

At 8% crosslinking (Dowex 50W X8 resin), the retention factors drop further, but selectivity increases further. The selectivity of Gal to Ara is 1.27 at 50°C, although the selectivity of Rha to Ara is just 1.09. It appears that only the Rha is strongly influenced by the temperature on this resin. While all peaks narrow at higher temperature, the retention factors of Ara and Gal are effectively constant, while Rha moves closer to Ara. Chromatograms are shown in Figure 5-8 and Figure 5-9 at room temperature and 50°C respectively while retention times, retention factors and selectivities are shown in Table 5-4.

Table 5-4: Retention times (t_i), retention factors (k_i^R) and selectivities (α^R) of individual sugars on a 20 g Dowex 50W X8 column in the H^+ form at room temperature (RT) and 50°C. The retention time of blue dextran is also given for reference. Experiments were performed as described in Section 2.10 with retention factors and selectivities also calculated as described in Section 2.10.

Sugar	t_i (RT)	k_i^R (RT)	α^R (RT)	t_i (50°C)	k_i^R (50°C)	α^R (50°C)
Rha	5.4	0.32	1.18	5.6	0.35	1.09
Ara	5.7	0.38	-	5.7	0.38	-
Gal	5.3	0.30	1.26	5.4	0.30	1.27
Blue Dextran	4.1	-	-	4.1	-	-

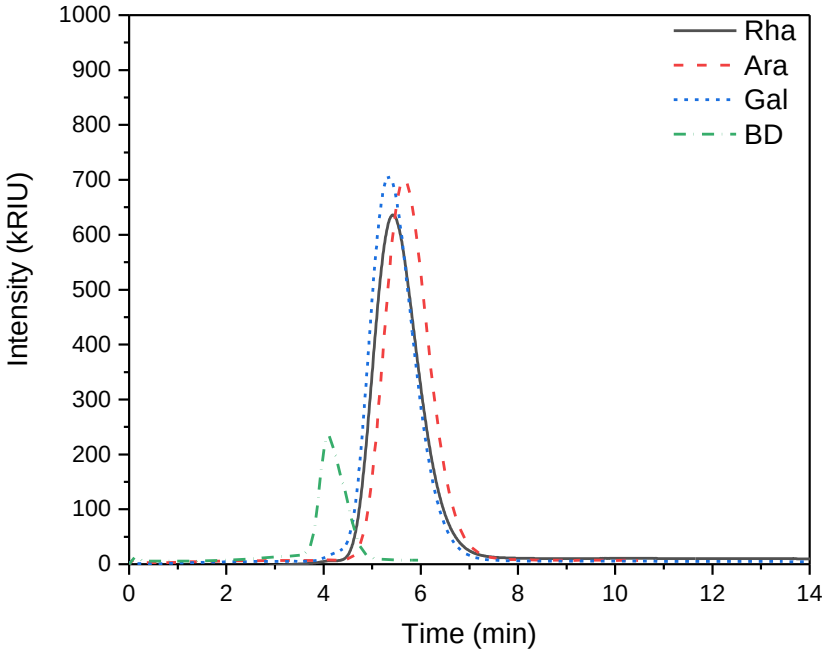

Figure 5-8: Batch separations of neutral monosaccharides a Dowex 50W X8 column in the H^+ form at room temperature. 100 µL injections of individual sugars (Ara, Rha and Gal (10 g L^{-1} each)) and blue dextran (1% w/v) were performed as described in Section 2.10 with the column prepared with 20 g of resin as described in Section 2.9. Rha, L-rhamnose; Ara, L-arabinose; Gal, D-galactose; BD, blue dextran.

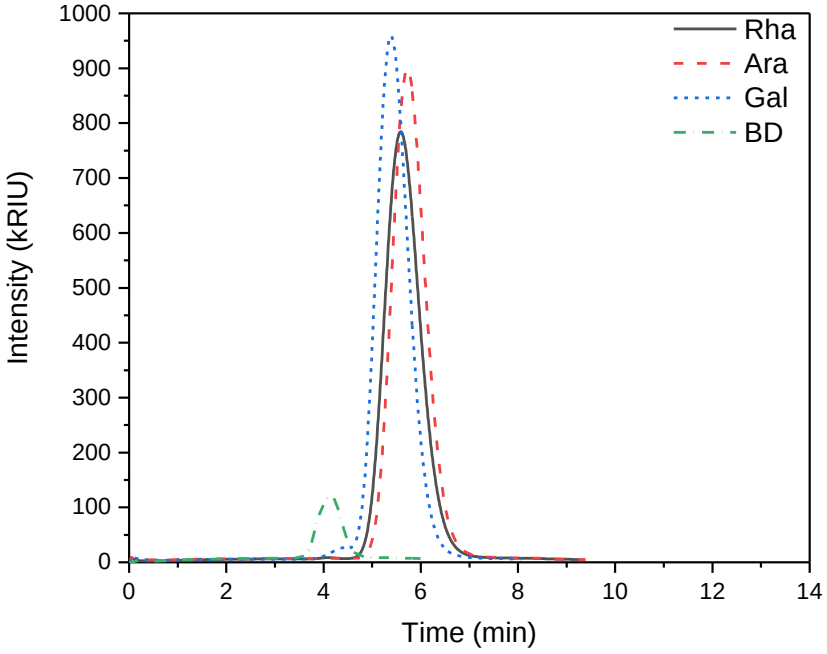

Figure 5-9: Batch separations of neutral monosaccharides a Dowex 50W X8 column in the H^+ form at 50°C. 100 µL injections of individual sugars (Ara, Rha and Gal (10 g L^{-1} each)) and blue dextran (1% w/v) were performed as described in Section 2.10 with the column prepared with 20 g of resin as described in Section 2.9. Rha, L-rhamnose; Ara, L-arabinose; Gal, D-galactose; BD, blue dextran.

The H^+ form of these three Dowex resins clearly have some interaction with the sugars based on the retention factors. Retention decreases with increasing crosslinking percentage of the resin, while the selectivity increases. However, each resin acts very similarly with all three of the sugars examined, with poor selectivity for all resins in all conditions. The best selectivity was found using the Dowex 50W X8 resin at room temperature that was able to achieve a selectivity of 1.18 and 1.26 for Rha and Gal respectively to Ara. While the selectivity of these resins is poor when compared to the Monosphere 99 resin, which achieved an optimum selectivity of 1.69 and 1.75 for Gal and Rha to Ara respectively, the peak shapes are much more symmetric than the Monosphere 99, even at 50°C. This could be a result of the much smaller particle size (37-74 µm for the Dowex 50W resins compared to 320 µm for the Monosphere 99). The use of longer columns could help to reduce the asymmetrical peak shapes present using the Monosphere 99 resin and so could be more appropriate for larger scale. The use of longer columns is, however, limited due to the Semba Octave 20 SMB system. While pressure is unlikely to be an issue when using longer columns, due to the large resin size, the pumps have a maximum flow rate of 12 mL min^{-1} and so could prove to be a bottle neck in an SMB application using this resin. The 50W resins, however, are not limited to smaller column sizes as they are also available at larger particle sizes (mesh sizes of 16-50 (1140-297 µm) and 50-100 (297-149 µm)). At larger scale the Monosphere 99 resin may be preferential due to its narrower particle size distribution assisting separation performance [234].

5.2.3 Dowex 50W resins in the Ca^{2+} form

The Dowex 50W resins were next examined in the Ca^{2+} form in an attempt to improve the selectivity of the separations. Figure 5-10 and Figure 5-11 show the overlaid chromatograms for the three individual sugars and blue dextran on a 20 g 50W X2 column in the Ca^{2+} form (room temperature and 50°C respectively). In comparison to all of the columns in the H^+ form (Figure 5-4 to Figure 5-9) it clearly has an improved selectivity; this is verified by the retention factor and selectivity values (1.17 and 1.14, for Rha and Gal respectively, at 50°C compared to 1.02 and 1.04 at 50°C in the H^+ form) shown in Table 5-5.

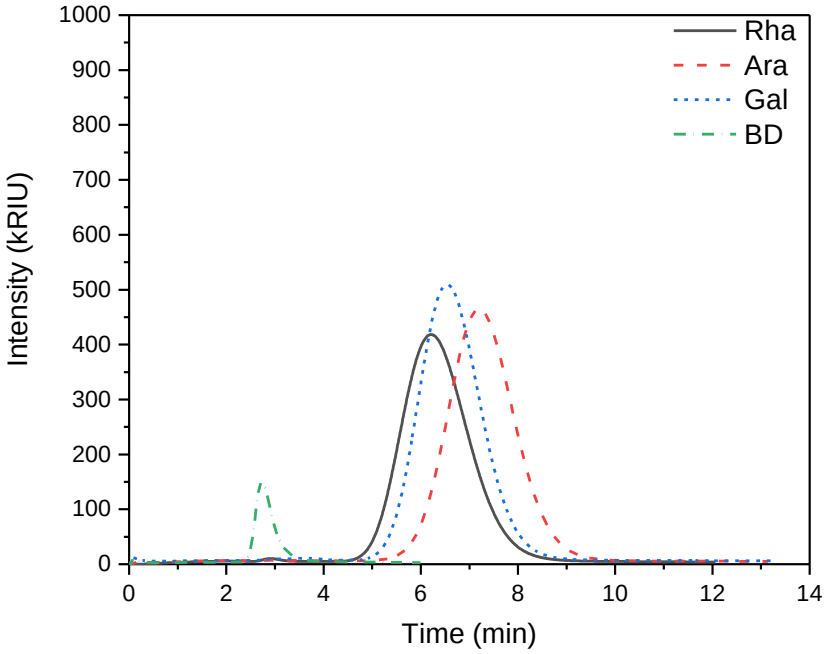

Figure 5-10: Batch separations of neutral monosaccharides a Dowex 50W X2 column in the Ca^{2+} form at room temperature. 100 µL injections of individual sugars (Ara, Rha and Gal (10 g L^{-1} each)) and blue dextran (1% w/v) were performed as described in Section 2.10 with the column prepared with 20 g of resin as described in Section 2.9. Rha, L-rhamnose; Ara, L-arabinose; Gal, D-galactose; BD, blue dextran.

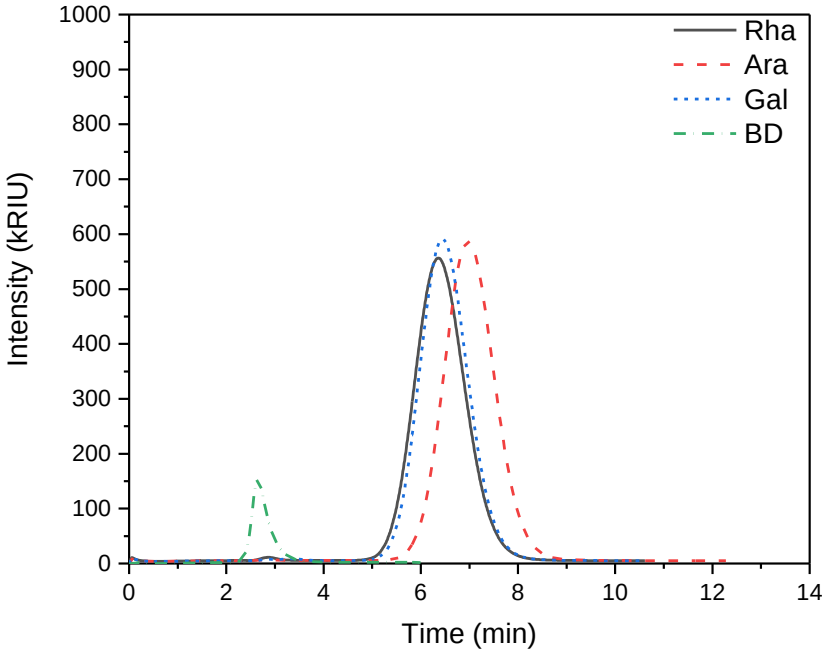

Figure 5-11: Batch separations of neutral monosaccharides a Dowex 50W X2 column in the Ca^{2+} form at 50°C. 100 µL injections of individual sugars (Ara, Rha and Gal (10 g L^{-1} each)) and blue dextran (1% w/v) were performed as described in Section 2.10 with the column prepared with 20 g of resin as described in Section 2.9. Rha, L-rhamnose; Ara, L-arabinose; Gal, D-galactose; BD, blue dextran.

Table 5-5: Retention times (t_i), retention factors (k_i^R) and selectivities (α^R) of individual sugars on a 20 g Dowex 50W X2 column in the Ca^{2+} form at room temperature (RT) and 50°C. The retention time of blue dextran is also given for reference. Experiments were performed as described in Section 2.10 with retention factors and selectivities calculated as described in Section 2.10.

Sugar	t_i (RT)	k_i^R (RT)	α^R (RT)	t_i (50°C)	k_i^R (50°C)	α^R (50°C)
Rha	6.2	1.27	1.28	6.4	1.40	1.17
Ara	7.2	1.63		7.0	1.63	-
Gal	6.5	1.39	1.18	6.5	1.43	1.14
Blue Dextran	2.7	-	-	2.7	-	-

Increasing the degree of crosslinking to 4% has a clear improvement on the selectivity, with the peaks at room temperature (Figure 5-12) and 50°C (Figure 5-13) appearing much more separated, although not base line resolved. Similar to 2% crosslinking, increasing the temperature narrows the peaks and appears to shift the Rha closer to the Gal, causing it to completely co-elute, and the Ara slightly closer to the Gal peak. While this has an impact on the selectivity to Ara of both Rha (1.46 to 1.27) and Gal (1.31 to 1.25) of both Rha and Gal to Ara, the effect could be outweighed by the narrower peaks. Comparing with 4% crosslinking in the H^+ form (Table 5-3), the lowest selectivity value at 50°C is improved from 1.05 (Rha) to 1.25 (Gal). The retention times, retention factors and selectivities are shown in Table 5-6.

Table 5-6: Retention times (t_i), retention factors (k_i^R) and selectivities (α^R) of individual sugars on a 20 g Dowex 50W X4 column in the Ca^{2+} form at room temperature (RT) and 50°C. The retention time of blue dextran is also given for reference. Experiments were performed as described in Section 2.10 with retention factors and selectivities calculated as described in Section 2.10.

Sugar	t_i (RT)	k_i^R (RT)	α^R (RT)	t_i (50°C)	k_i^R (50°C)	α^R (50°C)
Rha	6.9	0.70	1.46	7.1	0.79	1.27
Ara	8.2	1.02	-	8.0	1.00	-
Gal	7.2	0.77	1.31	7.2	0.80	1.25
Blue Dextran	4.1	-	-	4.0	-	-

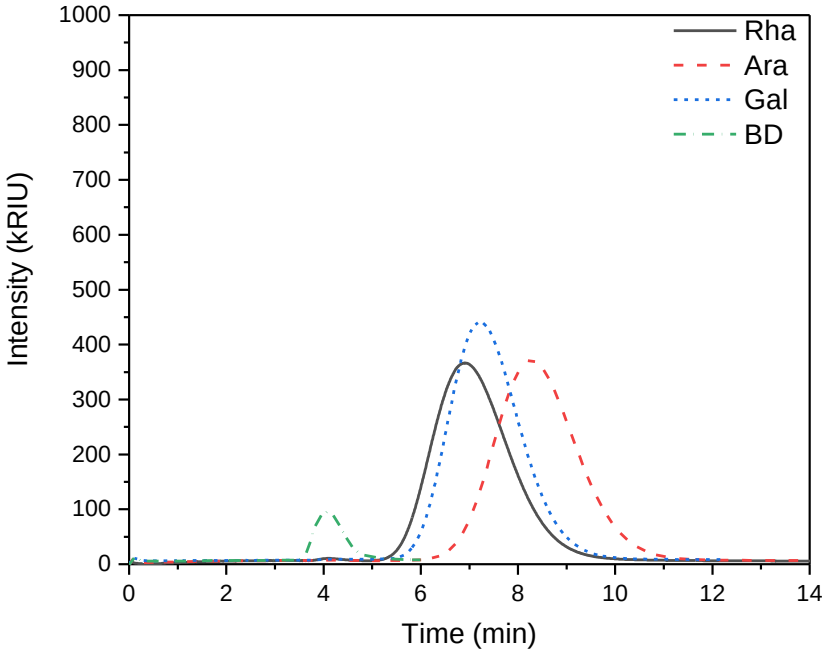

Figure 5-12: Batch separations of neutral monosaccharides a Dowex 50W X4 column in the Ca^{2+} form at room temperature. 100 µL injections of individual sugars (Ara, Rha and Gal (10 g L^{-1} each)) and blue dextran (1% w/v) were performed as described in Section 2.10 with the column prepared with 20 g of resin as described in Section 2.9. Rha, L-rhamnose; Ara, L-arabinose; Gal, D-galactose; BD, blue dextran.

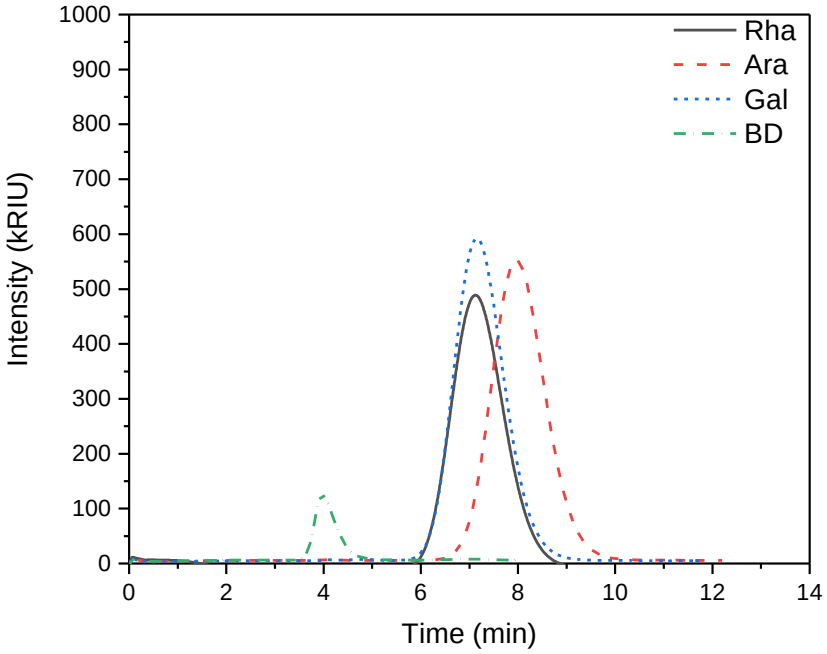

Figure 5-13: Batch separations of neutral monosaccharides a Dowex 50W X4 column in the Ca^{2+} form at 50°C. 100 µL injections of individual sugars (Ara, Rha and Gal (10 g L^{-1} each)) and blue dextran (1% w/v) were performed as described in Section 2.10 with the column prepared with 20 g of resin as described in Section 2.9. Rha, L-rhamnose; Ara, L-arabinose; Gal, D-galactose; BD, blue dextran.

A final increase in the percentage crosslinking to 8% lowers the retention factors but also appears to further improve the selectivity between Ara and the remaining sugars. At room temperature (Figure 5-14), the peak shapes show significant tailing, similar to the Monosphere 99 despite the much reduced particle size of the 50W X8 resin. At 50°C (Figure 5-15) this peak tailing is much reduced with more symmetric peaks as in the other resins. While the retention factors are reduced, the selectivity improves and this is a vitally important factor for separation in SMB, determining the size of the SMB separation region in the triangle theory (Section 1.6.2). Furthermore, the lower retention factors can actually improve the flexibility of the SMB separation, allowing a greater operating range for optimisation. The retention times, retention factors and selectivities at room temperature and 50°C are shown in Table 5-7.

Table 5-7: Retention times (t_i), retention factors (k_i^R) and selectivities (α^R) of individual sugars on a 20 g Dowex 50W X8 column in the Ca^{2+} form at room temperature (RT) and 50°C. The retention time of blue dextran is also given for reference. Experiments were performed as described in Section 2.10 with retention factors and selectivities calculated as described in Section 2.10

Sugar	t_i (RT)	k_i^R (RT)	α^R (RT)	t_i (50°C)	k_i^R (50°C)	α^R (50°C)
Rha	4.8	0.32	1.98	5.3	0.39	1.58
Ara	6.0	0.62	-	6.1	0.62	-
Gal	5.0	0.36	1.75	5.3	0.39	1.57
Blue Dextran	3.7	-	-	3.8	-	-

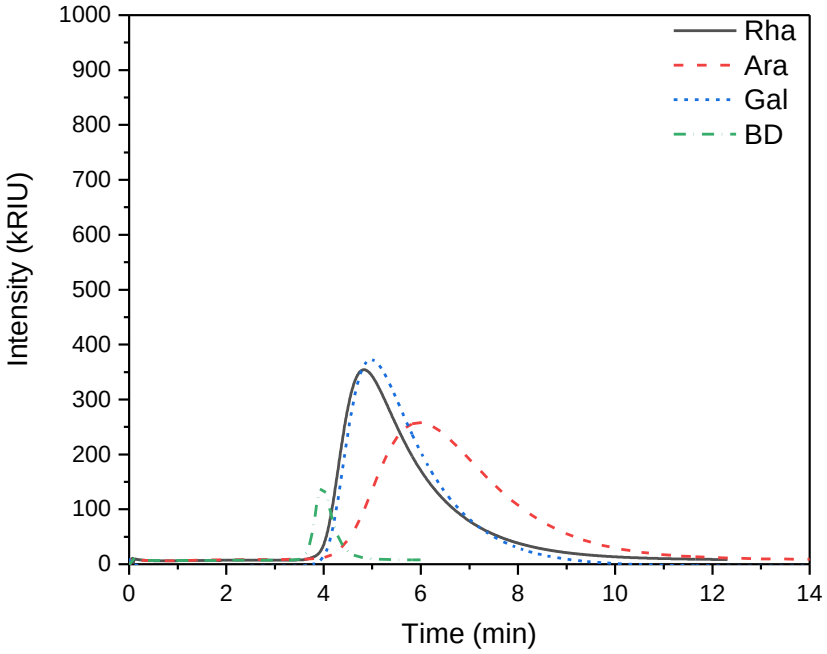

Figure 5-14: Batch separations of neutral monosaccharides a Dowex 50W X8 column in the Ca^{2+} form at room temperature. 100 µL injections of individual sugars (Ara, Rha and Gal (10 g L^{-1} each)) and blue dextran (1% w/v) were performed as described in Section 2.10 with the column prepared with 20 g of resin as described in Section 2.9. Rha, L-rhamnose; Ara, L-arabinose; Gal, D-galactose; BD, blue dextran.

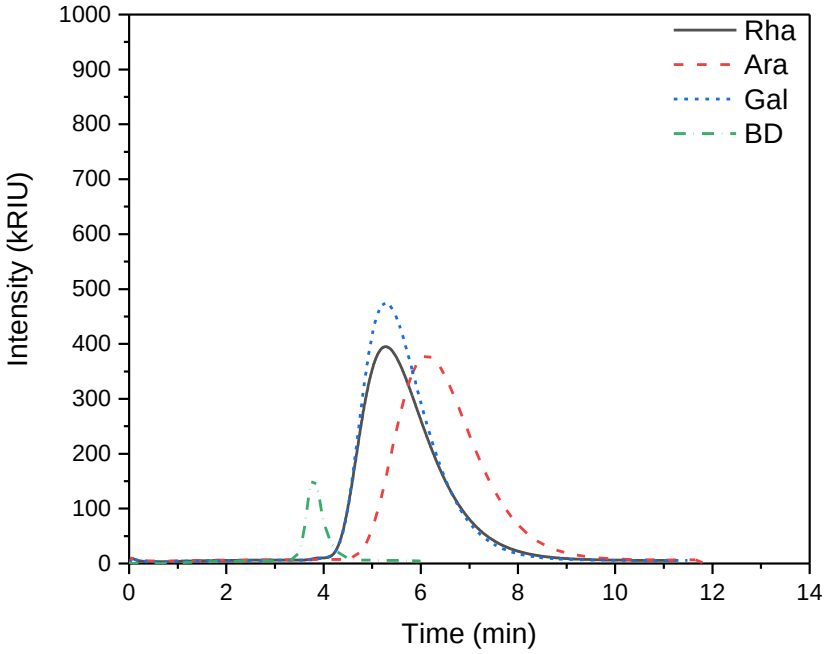

Figure 5-15: Batch separations of neutral monosaccharides a Dowex 50W X8 column in the Ca^{2+} form at 50°C. 100 µL injections of individual sugars (Ara, Rha and Gal (10 g L^{-1} each)) and blue dextran (1% w/v) were performed as described in Section 2.10 with the column prepared with 20 g of resin as described in Section 2.9. Rha, L-rhamnose; Ara, L-arabinose; Gal, D-galactose; BD, blue dextran.

While, at room temperature, the 50W X8 resin in calcium form has the highest selectivities (Ara to Gal: 1.75, Ara to Rha: 1.98), the tailing peak shape led to this option being discarded. At 50°C, the peak shape is markedly improved and the selectivity of Rha and Gal to Ara are effectively identical (1.58 for Rha and 1.57 for Gal).

As there is also some Glu in the crude SBP pectin hydrolysate (Section 1.1.4), albeit less than Ara, Rha or Gal, its retention time must also be considered to see if it will affect the separation. For various conditions and resins tested it was found that Glu always eluted prior to the Rha and Gal and so would have an even higher selectivity. As the SMB is a binary separation and the target is to purify Ara in the extract, the Glu will follow the same route as the Rha and Gal and elute in the raffinate. Due to its higher selectivity and lower concentration in the crude it was not included on the chromatograms in this section.

Based on the results in this section, the 50W X8 resin in the Ca^{2+} form, operated in the Ca^{2+} form at 50°C, was selected for SMB separations. This resin and condition had the second highest selectivity values (Table 5-7), surpassed only by Monosphere 99 resin (Table 5-1). However, the Monosphere 99 resin was deemed unsuitable due to its poor peak shape (Figure 5-2) relative to the Dowex 50W X8 resin (Figure 5-15).

5.3 Column packing comparison

With the resin, ionic form and operating temperature selected in Section 5.2, it is next necessary to pack 8 identical columns in order to perform SMB separations. The columns were packed with 28g of dry resin as described in Section 2.11. The increased column length was chosen to provide a greater difference in the retention factors of the columns, allowing for more flexibility for optimisation in the SMB separation. The retention factors and selectivities should be identical with an increasing column length and also any variation in the dead volume. For the column packing comparison experiments, a larger dead volume was used to incorporate the system into the SMB and simplify experimental setup.

Table 5-8 shows the retention times of blue dextran; and the retention times, retention factors and selectivities of pure Rha, Ara and Gal for each of the 8 columns. The relative standard deviations (RSD), calculated as described in Equation 2-7 in Section 2.11, are used to compare the columns: the retention times all have an RSD of <1%, the selectivities of Rha and Gal are both at an RSD of approximately 1%, and the retention factors all have an RSD below 2.5%. This shows a high level of similarity between the columns and so the columns were deemed to be sufficiently equally packed for SMB.

Table 5-8: Retention times of blue dextran (t_0) and retention times (t_i), retention factors (k_i^R) and selectivities (α^R) of individual sugars at room temperature on 8 identical columns, packed with 28 g of Dowex 50W X8 in the Ca^{2+} form. The mean values (± one standard deviations) and relative standard deviations (RSD) are also shown. Columns are packed as described in Section 2.9. Batch experiments are performed as described in Section 2.10, with retention factors and selectivities calculated as described in Section 2.10. The RSD is calculated as described in Section 2.11.

Column	t_0 (min)	Rha			Ara			Gal		
		t_{Rha} (min)	k_{Rha}^R	α^R	t_{Ara} (min)	k_{Ara}^R	α^R	t_{Gal} (min)	k_{Gal}^R	α^R
1	5.6	7.5	0.34	1.92	9.3	0.66	-	7.7	0.38	1.75
2	5.5	7.3	0.34	1.97	9.1	0.67	-	7.5	0.38	1.77
3	5.5	7.4	0.35	1.93	9.2	0.68	-	7.6	0.39	1.76
4	5.5	7.4	0.35	1.94	9.2	0.67	-	7.6	0.38	1.76
5	5.6	7.4	0.34	1.95	9.2	0.65	-	7.7	0.38	1.74
6	5.6	7.4	0.33	1.97	9.2	0.64	-	7.6	0.36	1.8
7	5.5	7.4	0.34	1.94	9.2	0.66	-	7.6	0.38	1.76
8	5.6	7.5	0.33	1.98	9.3	0.65	-	7.7	0.37	1.74
Mean	5.5±0.0	7.4±0.0	0.34±0.01	1.95±0.02	9.2±0.0	0.66±0.01	-	7.6±0.1	0.37±0.01	1.76±0.02
RSD	0.90%	0.59%	2.47%	1.06%	0.42%	1.73%	-	0.69%	2.11%	0.98%

5.4 SMB separations

5.4.1 General considerations

Comparison of the retention factors and selectivities at room temperature achieved with the 20 g columns in Table 5-7 (Section 5.2) and the 28 g columns in Table 5-8 (Section 5.3) shows some variation between the two column lengths (Table 5-9). There could be some difference in the dead volume either side of the column that is causing this small change in the retention factors, which should be dimensionless parameters independent of the amount of resin or the column dimensions. However, the magnitude of the difference is small and so the retention times, retention factors and selectivities at 50°C (also shown in Table 5-7 in Section 5.2) were used for SMB modelling without requiring additional batch experiments on the 28 g columns. Additionally, in all of the resin and condition screening experiments in Section 5.2, the retention time of blue dextran was effectively constant with a temperature shift from room temperature to 50°C and so this was assumed to be the case for the 28 g columns. The average value shown in Table 5-8 was thus the value used for the SMB model at 50°C.

Table 5-9: Comparison of retention factors (k_i^R) and selectivities (α^R) of individual sugars on two columns of different lengths. Experiments were performed on the Dowex 50W X8 resin in the Ca^{2+} form at room temperature and prepared with 20 g (from Table 5-7 in Section 5.2) or 28 g of resin (average values ± one standard deviation from Table 5-8 in Section 5.3).

Sugar	k_i^R (20 g)	k_i^R (28 g)	α^R (20 g)	α^R (28 g)
Rha	0.32	0.34±0.01	1.98	1.95±0.02
Ara	0.62	0.66±0.01	-	-
Gal	0.36	0.37±0.01	1.75	1.76±0.02

On the batch columns in Section 5.2, for the resin and conditions selected (Dowex 50W X8 at 50°C), a column length (C_L) of 9.5 cm was determined. Additionally, a dead volume (V_D) of 0.5 mL was calculated. On the longer SMB columns, a C_L of 13.9 cm was determined with a V_D of 1.7 mL. These values were used for the SMB model at the two scales, as described in Section 2.12.

Column lengths of 13.9 cm give a resin volume per column of approximately 28 mL (using a column diameter of 1.6 cm), and thus the SMB, with 8 columns, has a total resin volume of approximately 224 mL.

On the batch column, the Rha and Gal were found to have identical retention times of 5.3 min (Table 5-7) and so this value was used to calculate a Henry constant, with the retention time of Ara used for the other. Following the protocol in Section 2.12 requires the calculation of the adjusted retention time for blue dextran (t_0'); the adjusted retention times (t_i') and adjusted retention factors ($k_i^{R\prime}$) of the two components (1, Rha/Gal; 2, Ara); and the void fraction of the resin (ϵ). These values were then used to calculate the Henry constant of each component and are shown in Table 5-10. These Henry constants were used to set the limits for the SMB model (Equation 5-1 from Equation 2-20) and the column dimensions of the longer columns for SMB were then used to calculate the flow rate ratios (m_n) at different operating conditions as described in Section 2.12.

Table 5-10: Calculated values of adjusted retention times for blue dextran (t'_0), Rha/Gal (t'_1) and Ara (t'_2); adjusted retention factors for Rha/Gal ($k_1^{R'}$) and Ara ($k_2^{R'}$); void fraction (ε); Henry constants of for Rha/Gal (H_1) and Ara (H_2); and the adjusted selectivity between Rha/Gal and Ara ($\alpha^{R'}$). All values were calculated as described in 2.12 with retention times taken from Table 5-7 for the Dowex 50W X8 resin in the Ca^{2+} form at 50°C and a dead volume of 0.5 mL.

Measurement	Value
t_0'	3.55
t_1'	5.05
t_2'	5.85
$k_1^{R\prime}$	0.42
$k_2^{R\prime}$	0.65
ϵ	0.37
H_1	0.25
H_2	0.38
$\alpha^{R\prime}$	1.53

$$m_1 > 0.38 > m_3 > m_2 > 0.25 > m_4 \qquad \textbf{Equation 5-1}$$

5.4.2 4-zone, closed loop SMB setup

5.4.2.1 Selecting initial SMB operating conditions

A 4-zone, closed loop setup, described in Section 2.13.2, gives 5 input variables and, so, it could take considerable time to find a solution with a trial and error approach. Thus, a method was developed that allowed for a systematic selection of appropriate

SMB conditions which satisfy the requirements for the flow rate ratios m_1, m_2, m_3 and m_4, set by the Henry constants:

1. Select a switch time (T_S).
2. Find the recycle flow rate (Q_{Rec}) range which satisfies the requirements for m_4 ($H_1>m_4>0$) and select a value.
3. Find the minimum desorbent flow rate (Q_D) to satisfy the requirements for m_1 ($m_1>H_2$) and select a value.
4. Find the extract flow rate (Q_E) range which satisfies m_2 ($H_2>m_2>H_1$) and select a value.
5. Find a feed flow rate (Q_F) range which satisfies m_3 ($H_2>m_3>H_1$).
6. If no solution is possible, return to point 4 and select a new extract flow rate.
7. If no solution is possible, return to point 3 and select a new desorbent flow rate.
8. If no solution is possible, return to point 2 and select a new recycle flow rate.
9. If no solution is possible, return to point 1 and select a new switch time.

Table 5-11 shows a number of potential operating conditions that satisfy all of the flow rate ratio requirements with increasing switch times. The model results show that increasing the switch team leads to lower flow rates on all pumps and in all zones. In order to increase the overall throughput per resin volume, it would be advantageous to operate at higher feed flow rates and, consequently, lower switch times. One limitation of the pumps on the Semba SMB system is that they have a maximum flow rate of 12 mL min^{-1}. This effectively sets a minimum switch time of 61 s to allow for an m_4 above 0. Switch times below this would not be able to achieve a suitable m_4 value without a recycle flow rate above 12 mL min^{-1}.

While there are clearly a number of potential operating conditions that satisfy all of the required constraints, it was decided to pick a single condition and use this as a basis for optimisation. Model condition 2 in Table 5-11 was selected as it has a low switch time but is not right on the limit of operability as is the case in model condition 1.

Model condition 2 is shown as Experiment 1 in Table 5-12 along with the operating conditions of all of the 4-zone SMB experiments performed in this section.

Table 5-11: Example SMB variables (switch time and flow rates of the feed (Q_F), desorbent (Q_D), extract (Q_E) and recycle (Q_{Rec}) pumps) for the 4-zone SMB setup based on the Dowex 50W X8 resin in the Ca^{2+} form at 50°C. The input variables give flow rates (Q_n) and flow rate ratios (m_n) in each zone (n) which satisfy the equilibrium theory model described in Section 2.12.

Model Condition	1	2	3	4	5	6	7
Switch time (s)	65	90	120	150	200	250	300
Q_{feed}, (mL min^{-1})	1.3	1.0	0.8	0.8	0.6	0.5	0.4
$Q_{desorbent}$, (mL min^{-1})	7.0	6.0	4.0	3.0	2.0	2.0	1.5
$Q_{extract}$, (mL min^{-1})	3.0	4.0	2.5	1.4	1.0	1.0	0.7
$Q_{recycle}$, (mL min^{-1})	12.0	9.0	7.0	5.0	4.0	3.0	2.5
$Q_{raffinate}$, (mL min^{-1})	5.3	3.0	2.3	2.4	1.6	1.5	1.2
Q_1 (mL min^{-1})	19.0	15.0	11.0	8.0	6.0	5.0	4.0
Q_2 (mL min^{-1})	16.0	11.0	8.5	6.6	5.0	4.0	3.3
Q_3 (mL min^{-1})	17.3	12.0	9.3	7.4	5.6	4.5	3.7
Q_4 (mL min^{-1})	12.0	9.0	7.0	5.0	4.0	3.0	2.5
m_1	0.48	0.59	0.56	0.45	0.45	0.50	0.45
m_2	0.30	0.25	0.28	0.25	0.26	0.26	0.25
m_3	0.38	0.34	0.37	0.37	0.37	0.38	0.37
m_4	0.05	0.08	0.11	0.02	0.07	0.02	0.02

Table 5-12: Experimental conditions (switch time and flow rates of the feed (Q_F), desorbent (Q_D), extract (Q_E) and recycle (Q_{Rec}) pumps) used for SMB separation using the 4-zone SMB setup. Flow rates of the raffinate (Q_{Raf}) and through each zone (Q_n) are given in addition to the flow rate ratios in each zone (m_n) and were calculated as described in Section 2.12. SMB separations were performed as described in Section 2.13.1 with details specific to the 4-zone setup in Section 2.13.2.

Experiment	1	2	3	4	5	6
Switch time (s)	90	90	90	90	90	90
Q_F, (mL min^{-1})	1	2	3	2	3	2
Q_D, (mL min^{-1})	6	6	6	7	7	6
Q_E, (mL min^{-1})	4	4	4	4	4	3
Q_{Rec}, (mL min^{-1})	9	9	9	9	9	9
Q_{Raf}, (mL min^{-1})	3	4	5	5	6	5
Q_1 (mL min^{-1})	15	15	15	16	16	15
Q_2 (mL min^{-1})	11	11	11	12	12	12
Q_3 (mL min^{-1})	12	13	14	14	15	14
Q_4 (mL min^{-1})	9	9	9	9	9	9
m_1	0.59	0.59	0.59	0.68	0.68	0.59
m_2	0.25	0.25	0.25	0.34	0.34	0.34
m_3	0.34	0.42	0.51	0.51	0.59	0.51
m_4	0.08	0.08	0.08	0.08	0.08	0.08

Figure 5-16 shows the operating conditions in Experiment 1 on the m_2-m_3 plane, and the position within the operating triangle window.

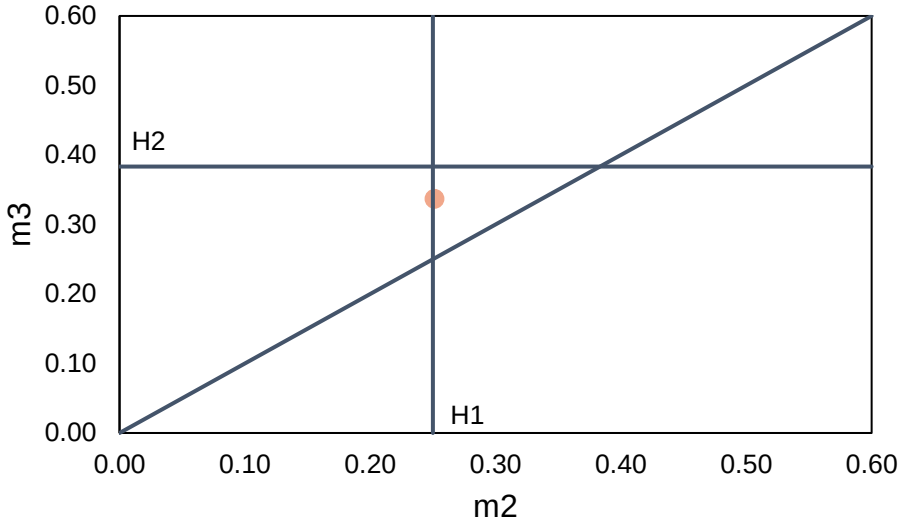

Figure 5-16: The m_2-m_3 plane showing SMB Experiment 1 and the boundaries set by the Henry constants. in Equation 5-1. The area within the triangle represents operating conditions where the SMB model, described in Section 2.12, predicts pure raffinate and extract streams. m_2 and m_3 refer to the flow rate ratios in zones 2 and 3 respectively and are shown in Table 5-12.

Looking at the results shown in Table 5-13, almost 100% of each sugar is eluted in the extract. A small amount of highly pure (96%) Ara is eluted in the raffinate. However, it would be expected the Rha and Gal to be more likely to elute in the raffinate, relative to the Ara, due to their faster elution times on the resin and condition screening experiments in Section 5.2. This effect could be a result of the increased feed concentration of Ara and so results in a broader peak that overlaps with the Rha and Gal peaks and, thus, a proportion elutes more quickly, in the raffinate.

Table 5-13: Concentration, purity and recovery of Rha, Ara and Gal in the Extract and Raffinate streams after 4-zone SMB separation using the variables defined in Experiment 1 in Table 5-12. SMB operation was performed as described in Section 2.13.1 using the 4-zone setup described in Section 2.13.2. A solution of Rha, Ara and Gal at concentrations of 1, 13 and 3 g L^{-1} respectively was used as the feed and water as the desorbent. Concentration, purity and recovery values were calculated using ICS analysis as described in Section 2.13.4.

Experiment 1	Rha	Ara	Gal
Extract conc. (g L^{-1})	0.22	2.49	0.64
Extract purity	7%	74%	19%
Extract recovery	100%	98%	100%
Raffinate conc. (g L^{-1})	0	0.2	0.01
Raffinate purity	0%	96%	4%
Raffinate recovery	0%	2%	0%

Additionally, the Ara in the raffinate represents just 2% by weight of the total Ara output, with the remaining 98% eluting in the extract. The results show that, while the experiment fits within the operating triangle in Figure 5-16, there is not complete separation of the sugars with Ara in the extract and Rha and Gal in the raffinate.

This could mean that there is some mistake in one or more of the measurements made, for example the dead volume calculation, and so the H_1 and H_2 values are, in effect, miscalculated and it may be necessary to operate beyond the operating triangle window to achieve separation. Furthermore, the triangle theory approximates the process to a TMB with infinite number of columns and so does not take the number of columns used in the SMB process into account [235]. It operates solely based on the Henry constants and so the large peak overlaps seen in the resin and condition screening experiments, in Section 5.2, could be affecting the SMB performance. However, one would expect at least some elution of the sugars in the raffinate if the model was working as intended. Further experiments were based on improving and optimising the separation on an experimental basis by manipulating the relative flow rates in each zone (m_1, m_2, m_3 and m_4).

5.4.2.2 Optimisation by increasing feed flow rate

With all of the sugars eluting in the extract, the feed flow rate was increased in Experiment 2, (from 1 mL min^{-1} to 2 mL min^{-1}, see Table 5-12), in order to increase the zone 3 flow rate, and allow the Rha and Gal to elute in the raffinate. This increases

the value of m_3 only (from 0.34 to 0.42), and does not affect the values of m_1, m_2 or m_4. The raffinate flow rate increases from 3 mL min^{-1} to 4 mL min^{-1} as a result of the increase in feed flow rate. The extract flow rate stays constant at 4 mL min^{-1} as this is defined by the extract pump (Section 2.13.2). The new value of m_3 pushes it above the H_2 value (0.38) and so outside of the requirements set by Equation 5-1 and the operating triangle in the m_2-m_3 plane (Figure 5-17).

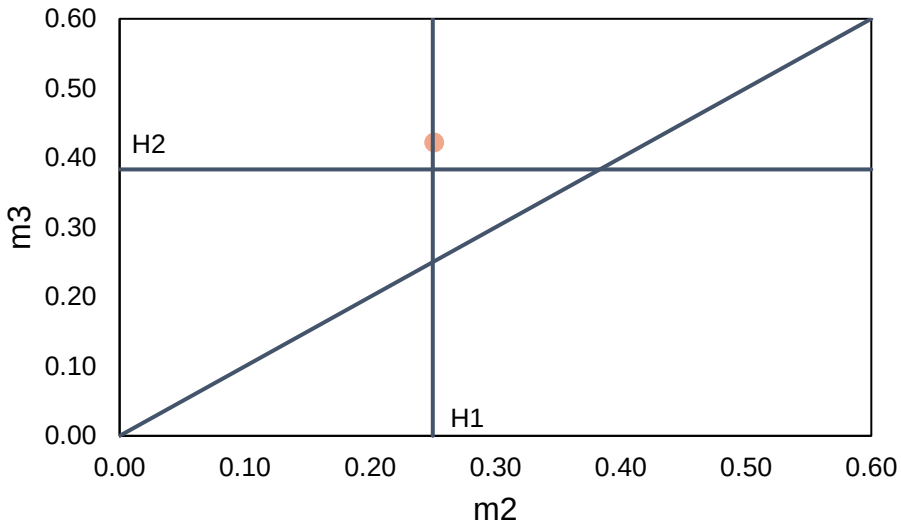

Figure 5-17: The m_2-m_3 plane showing SMB Experiment 2 and the boundaries set by the Henry constants in Equation 5-1. The area within the triangle represents operating conditions where the SMB model, described in Section 2.12, predicts pure raffinate and extract streams. m_2 and m_3 refer to the flow rate ratios in zones 2 and 3 respectively and are shown in Table 5-12.

The results, shown in Table 5-14, show some adjustments in the separation profile, however the results appear to get worse. Very little Rha and Gal are eluted in the raffinate (1-2%) but even more of the Ara is eluted there (up from 2% to 23%). The result is a very pure (98%) Ara stream in the raffinate, however, this is still unexpected behaviour with the slower eluting compound eluting in both the extract and raffinate. While it may be possible to use this method as an Ara purification technique by recycling the extract, and collecting the purer Ara in the raffinate, it would dramatically decrease the overall throughput per resin volume.

Table 5-14: Concentration, purity and recovery of Rha, Ara and Gal in the Extract and Raffinate streams after 4-zone SMB separation using the variables defined in Experiment 2 in Table 5-12. SMB operation was performed as described in Section 2.13.1 using the 4-zone setup described in Section 2.13.2. A solution of Rha, Ara and Gal at concentrations of 1, 13 and 3 g L^{-1} respectively was used as the feed and water as the desorbent. Concentration, purity and recovery values were calculated using ICS analysis as described in Section 2.13.4.

Experiment 2	Rha	Ara	Gal
Extract conc. (g L^{-1})	0.48	4.52	1.51
Extract purity	7%	69%	23%
Extract recovery	98%	77%	99%
Raffinate conc. (g L^{-1})	0.01	1.32	0.02
Raffinate purity	1%	98%	2%
Raffinate recovery	2%	23%	1%

The lack of Rha and Gal in the raffinate indicates that the zone 3 flow rate may still be too low and so the feed flow rate was increased further to 3 mL min^{-1} in Experiment 3 (detailed in Table 5-12). This further pushes up the m_3 value to 0.51 (shown in Figure 5-18) and the raffinate flow rate to 5 mL min^{-1} while not affecting the flow rates in any other zone.

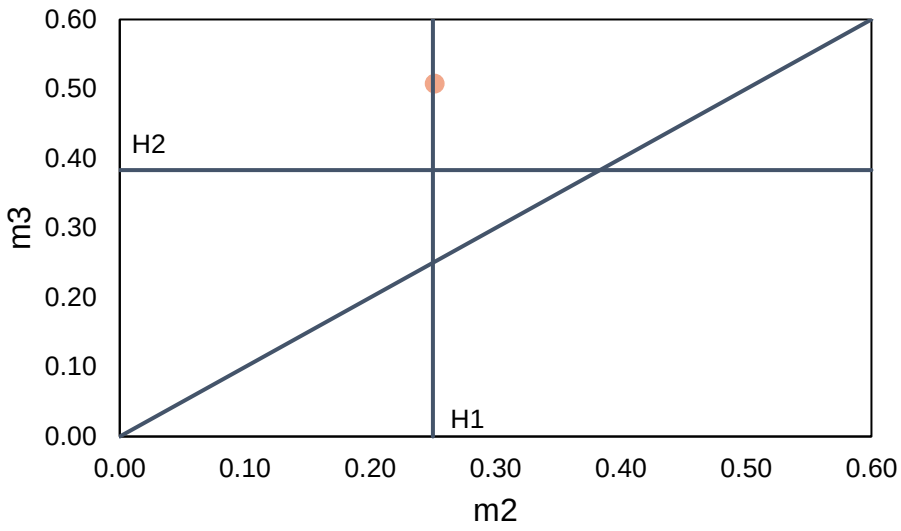

Figure 5-18: The m_2-m_3 plane showing SMB Experiment 3 and the boundaries set by the Henry constants in Equation 5-1. The area within the triangle represents operating conditions where the SMB model, described in Section 2.12, predicts pure raffinate and extract streams. m_2 and m_3 refer to the flow rate ratios in zones 2 and 3 respectively and are shown in Table 5-12.

The separation results, shown in Table 5-15, are markedly improved, demonstrating that the increase in zone 3 flow rate has helped to elute the Rha and Gal in the raffinate, without a large increase in the amount of Ara eluted in the raffinate. The raffinate recovery of Rha and Gal increases from just 1-2% in Experiment 2 (Table 5-14) to 86-88%. The Ara extract recovery is slightly reduced from 71 to 77%, but the purity in the extract is increased 69 to 95%. The separation is now behaving as expected with the faster compounds eluting in the raffinate and the more retarded compounds primarily eluting in the extract. It is interesting to note that, in isocratic SMB, increasing the feed flow rate can result in improved separation results as well as the obvious benefits of increased throughput.

Table 5-15: Concentration, purity and recovery of Rha, Ara and Gal in the Extract and Raffinate streams after 4-zone SMB separation using the variables defined in Experiment 3 in Table 5-12. SMB operation was performed as described in Section 2.13.1 using the 4-zone setup described in Section 2.13.2. A solution of Rha, Ara and Gal at concentrations of 1, 13 and 3 g L^{-1} respectively was used as the feed and water as the desorbent. Concentration, purity and recovery values were calculated using ICS analysis as described in Section 2.13.4.

Experiment 3	Rha	Ara	Gal
Extract conc. (g L^{-1})	0.09	5.77	0.23
Extract purity	2%	95%	4%
Extract recovery	14%	71%	12%
Raffinate conc. (g L^{-1})	0.45	1.86	1.32
Raffinate purity	12%	51%	36%
Raffinate recovery	86%	29%	88%

With the high purity of Ara and low recoveries of Rha and Gal in the extract, further optimisation was sought in other ways than increasing the flow rate. While increasing the flow rate could improve the purity further, it would inevitably lead to reduced recovery as more Ara elutes in the raffinate. It should be possible to recycle the raffinate back to the feed, however, this may reduce the overall throughput per column volume as the amount of fresh feed added to the SMB would be reduced.

The Ara concentration in the extract is 5.77 g L^{-1}. This value gives an overall dilution factor of the Ara of approximately 2.3 from its input concentration of 13 g L^{-1} while increasing the purity from 76 to 95%. This low dilution factor highlights the effectiveness of SMB due to the shorter solute migration distance [178].

5.4.2.3 Additional optimisation

Increasing the desorbent flow rate is an alternative method of increasing the m_3 flow rate and was explored in Experiment 4. Without adjusting the extract flow rate to compensate for the increased zone 1 and 2 flow rates, the increased desorbent flow rate is passed onto zone 3. Zone 4 is not affected as it is controlled by the recycle pump. Thus, increasing the desorbent flow rate therefore increases m_1, m_2 and m_3.

The results of Experiment 4 (in Table 5-16) show an Ara extract purity of 96% with an Ara extract recovery of 63%. While this is an improvement on Experiment 2 (Table 5-14), the results do not quite compare with the results of Experiment 3 (Table 5-15)

which achieved 95% Ara purity, an Ara extract recovery of 71%, an increased throughput due to a feed flow rate of 3 mL min^{-1} and a higher extract concentration (5.77 g L^{-1}).

Table 5-16: Concentration, purity and recovery of Rha, Ara and Gal in the Extract and Raffinate streams after 4-zone SMB separation using the variables defined in Experiment 4 in Table 5-12. SMB operation was performed as described in Section 2.13.1 using the 4-zone setup described in Section 2.13.2. A solution of Rha, Ara and Gal at concentrations of 1, 13 and 3 g L^{-1} respectively was used as the feed and water as the desorbent. Concentration, purity and recovery values were calculated using ICS analysis as described in Section 2.13.4.

Experiment 4	Rha	Ara	Gal
Extract conc. (g L^{-1})	0.03	2.86	0.08
Extract purity	1%	96%	3%
Extract recovery	7%	63%	6%
Raffinate conc. (g L^{-1})	0.39	1.32	1.13
Raffinate purity	14%	46%	40%
Raffinate recovery	93%	37%	94%

Increasing the feed flow rate to 3 mL min^{-1} (Experiment 5 in Table 5-12) increases the extract purity to 98% (shown in Table 5-17), however, the recovery of Ara in the extract drops to 27%, meaning that significantly more Ara is eluted in the raffinate stream rather than the purer extract. This is likely a result of the increased m_3 value, causing Ara to be eluted in the raffinate.

Table 5-17: Concentration, purity and recovery of Rha, Ara and Gal in the Extract and Raffinate streams after 4-zone SMB separation using the variables defined in Experiment 5 in Table 5-12. SMB operation was performed as described in Section 2.13.1 using the 4-zone setup described in Section 2.13.2. A solution of Rha, Ara and Gal at concentrations of 1, 13 and 3 g L^{-1} respectively was used as the feed and water as the desorbent. Concentration, purity and recovery values were calculated using ICS analysis as described in Section 2.13.4.

Experiment 5	Rha	Ara	Gal
Extract conc. (g L^{-1})	0.02	2.16	0.03
Extract purity	1%	98%	2%
Extract recovery	2%	27%	2%
Raffinate conc. (g L^{-1})	0.45	3.80	1.27
Raffinate purity	8%	69%	23%
Raffinate recovery	98%	73%	98%

Decreasing the extract flow rate increases the m_2 and m_3 values without adjusting m_1 or m_4 and could be used as another method of shifting the Rha and Gal from the extract to the raffinate. Experiment 2 was adjusted by dropping the extract flow rate from 4 to 3 mL min^{-1} (Experiment 6 in Table 5-12). Experiment 6a (using the same synthetic neutral mixture as Experiments 1-5, defined in Section 2.7.4) resulted in a high purity Ara (98%) extract stream with an extract recovery of 48%, shown in Table 5-18. The purity matches what was achieved in Experiment 5 (Table 5-17), but with a much higher Ara recovery. Comparing with Experiment 4 (Table 5-16), the only difference in the zone flow rates is a reduced zone 1 flow rate. Zone 1 desorbs the more strongly retained, slower eluting compounds, so slowing it down means that these compounds enter zone 2 later in the step and are less likely to be passed through to zone 3. While this allows for higher Ara extract purity than Experiment 4 (Table 5-16), the lower extract flow rate results in a lower recovery of Ara eluting in the extract.

Table 5-18: Concentration, purity and recovery of Rha, Ara and Gal in the Extract and Raffinate streams of Experiment 6a after 4-zone SMB separation. The variables used are defined in Experiment 6 in Table 5-12. SMB operation was performed as described in Section 2.13.1 using the 4-zone setup described in Section 2.13.2. A solution of Rha, Ara and Gal at concentrations of 1, 13 and 3 g L^{-1} respectively was used as the feed and water as the desorbent. Concentration, purity and recovery values were calculated using ICS analysis as described in Section 2.13.4.

Experiment 6a	Rha	Ara	Gal
Extract conc. (g L^{-1})	0.02	2.86	0.05
Extract purity	1%	98%	2%
Extract recovery	3%	48%	3%
Raffinate conc. (g L^{-1})	0.36	1.85	1.05
Raffinate purity	11%	57%	32%
Raffinate recovery	97%	52%	97%

5.4.2.4 Recycling of the raffinate stream to increase recovery

The raffinate from Experiment 6a contained 52% of the available Ara, therefore, the possibility of using this directly as a feed stream for another identical SMB operation was examined in order to increase the overall recovery. The concentrations and purities of the synthetic neutral feed, used to produce the raffinate, and the 'raffinate feed', used in Experiment 6b, are shown in Table 5-19. While the concentrations are lower, the purities of each sugar are broadly similar.

Table 5-19: Comparison of the concentrations and purity of the synthetic neutral feed used for Experiment 6a and the "Raffinate feed" used for Experiment 6b. This raffinate feed is the collected raffinate stream from Experiment 6a (Table 5-18). Concentration and purity values were calculated using ICS analysis as described in Section 2.13.4.

Feed	Rha	Ara	Gal
Original Feed concentration (g L^{-1})	1	13	3
Synthetic neutral feed purity	6%	76%	18%
Raffinate Feed concentration (g L^{-1})	0.45	3.8	1.27
Raffinate feed purity	8%	69%	23%

The results from Experiment 6b, using this raffinate feed, are shown in Table 5-20. The purity achieved is not quite as high as with fresh synthetic neutral feed (dropping to 93%, however, the recovery in the extract is slightly higher, at 62%. The overall Ara extract recovery of both systems is around 81%.

Table 5-20: Concentration, purity and recovery of Rha, Ara and Gal in the Extract and Raffinate streams of Experiment 6b after 4-zone SMB separation. The collected Raffinate from Experiment 6a (Table 5-18) is used as the feed and the variables defined in Experiment 6 in Table 5-12. SMB operation was performed as described in Section 2.13.1 using the 4-zone setup described in Section 2.13.2. Water was used as the desorbent. Concentration, purity and recovery values were calculated using ICS analysis as described in Section 2.13.4.

Experiment 6b	Rha	Ara	Gal
Extract conc. (g L^{-1})	0.01	0.68	0.03
Extract purity	2%	93%	5%
Extract recovery	6%	62%	5%
Raffinate conc. (g L^{-1})	0.13	0.26	0.41
Raffinate purity	17%	32%	51%
Raffinate recovery	94%	38%	95%

This method of using the raffinate as a feed in a tandem SMB to perform the same separation would likely not be practical in reality. On top of the additional capital costs of another SMB system, the initial separation produces raffinate at a rate of 5 mL min^{-1}, and so the second SMB may need larger columns in order to process this higher feed flow rate. While it may be possible to find a method that results in a raffinate flow rate equal to that of the feed process, this places an additional restriction on the operating conditions. Alternatively, it may be possible to simply recycle a portion of the raffinate back to feed. While this would reduce the flow rate of fresh feed to the system, it would negate the need for a tandem SMB format. Again though, the fact that the raffinate

flow rate is higher than the feed flow rate makes any attempt to increase the Ara extract recovery difficult.

5.4.2.5 4-zone, closed loop SMB summary

The results in this section show that it is possible to achieve high purity Ara in the extract (Table 5-18) although there is an apparent trade-off with the recovery that is achievable. What is important to note is that it is possible to improve the separation performance by increasing the feed flow rate (Section 5.4.2.2), which has dramatic effects on the total throughput. A brief comparison of the three best SMB results (Experiments 3, 4 and 6a) in terms of Ara purity, Ara extract recovery and feed flow rates are shown in Table 5-21.

Table 5-21: Summary of results from Experiments 3, 4 and 6a showing the Ara concentration, purity and recovery in the Extract; the feed and desorbent flow rates used; and the Table reference showing the full results from each Experiment. The feed flow rate is shown as an indicator of the total throughput while the desorbent flow rate shows the solvent usage. Concentration, purity and recovery values were calculated using ICS analysis as described in Section 2.13.4.

Experiment	3	4	6a
Ara extract concentration (g L^{-1})	5.77	2.86	2.86
Ara extract purity	95%	96%	98%
Ara extract recovery	71%	64%	48%
Feed flow rate (mL min^{-1})	3	2	2
Desorbent flow rate (mL min^{-1})	6	7	6
Source	Table 5-15	Table 5-16	Table 5-18

Potentially further optimisation is still achievable. This could come in terms of using different switch times; or a reduced desorbent flow rate, compensated for by increasing the extract flow rate. This would decrease the m_1 value without affecting the m_2, m_3 or m_4 values, while also reducing the dilution of the Ara in the extract. However, due to the problems experienced with the SMB model predicting separation (as shown by the poor separation in Experiment 1 in Section 5.4.2.1), this may require significant further experimental work.

5.4.3 3-zone, open loop SMB setup

In an effort to simplify the SMB separation, a 3-zone (open loop) SMB setup was also examined (Section 1.6.3). The 3-zone setup removes zone 4, allowing more of the

columns to be used in zones 2 and 3 for separation. It also removes a degree of freedom from the SMB model (Section 2.12.2.3) as there is now no recycle pump, but the flow rate of fresh desorbent usage will likely be higher. In this section, 2 columns are used in zone 1 (as in Section 5.4.2), while zones 2 and 3 contain an additional column (3 columns each), totalling 8 columns (Figure 2-7 in Section 2.13.3).

In Section 5.4.2, it was observed that the SMB model did not fit with the experimental data and that separation performance was improved with increasing the m_3 value. As a result, the method used here aimed for an m_3 value around 0.5-0.6, similar to what was used in Experiments 3 to 6 in Section 5.4.2. As the sum of the recycle and desorbent flow rates used in the 4-zone SMB are all above the pump limit of 12 mL min^{-1}, the methods cannot easily be transferred. As a result, a higher switch time (225 s) was required in order to reduce the 3-zone desorbent flow rates to below 12 mL min^{-1}. The experimental conditions, zone flow rates and m values are shown in Table 5-22.

Table 5-22: Experimental conditions (switch time and flow rates of the feed (Q_F), desorbent (Q_D) and extract (Q_E) pumps) used for SMB separation using the 3-zone SMB setup. Flow rates of the raffinate (Q_{Raf}) and through each zone (Q_n) are given in addition to the flow rate ratios in each zone (m_n) and were calculated as described in Section 2.12. SMB separations were performed as described in Section 2.13.1 with details specific to the 3-zone setup in Section 2.13.3.

Experiment	7	8
Switch time (s)	225	225
Q_F, (mL min^{-1})	1.00	1.00
Q_D, (mL min^{-1})	9.50	9.50
Q_E, (mL min^{-1})	4.50	5.00
Q_{Raf}, (mL min^{-1})	6.00	5.50
Q_1 (mL min^{-1})	9.50	9.50
Q_2 (mL min^{-1})	5.00	4.50
Q_3 (mL min^{-1})	6.00	5.50
m_1	1.40	1.40
m_2	0.39	0.28
m_3	0.62	0.51

The results of Experiment 7 are shown in Table 5-23 and show a very high purity of Ara in the extract (98%), although the Ara recovery is low, at 33%. This performance is between that of Experiments 5 and 6 in Section 5.4.2, however, the extract

concentration is 4-5 times lower than in the 4-zone system due to the reduced feed flow rate and the increased extract flow rate. The result shows that the separation is occurring as expected and can likely be improved with optimisation.

Table 5-23: Concentration, purity and recovery of Rha, Ara and Gal in the Extract and Raffinate streams after 3-zone SMB separation using the variables defined in Experiment 7 in Table 5-22. SMB operation was performed as described in Section 2.13.1 using the 3-zone setup described in Section 2.13.3. A solution of Rha, Ara and Gal at concentrations of 1, 13 and 3 g L^{-1} respectively was used as the feed and water as the desorbent. Concentration, purity and recovery values were calculated using ICS analysis as described in Section 2.13.4.

Experiment 7	Rha	Ara	Gal
Extract conc. (g L^{-1})	0.00	0.56	0.01
Extract purity	0%	98%	1%
Extract recovery	1%	33%	1%
Raffinate conc. (g L^{-1})	0.17	0.87	0.51
Raffinate purity	11%	56%	33%
Raffinate recovery	99%	67%	99%

In order to improve the recovery of Ara in the extract, the extract flow rate was increased from 4.5 to 5.0 mL min^{-1}, reducing both the zone 2 and zone 3 flow rates by 0.5 mL min^{-1}, as shown by Experiment 8 in Table 5-22. The results, Table 5-24, show a slight drop in Ara extract purity from 98% to 94%, however, importantly, this is achieved with a 99% recovery. This high recovery allows for the Ara extract concentrations (2.16 g L^{-1}) to be approximately three-quarters of their value in Experiments 4 and 6 (2.86 g L^{-1}) in Section 5.4.2, despite halving the feed flow rate, although it is well below the value of 5.77 g L^{-1} in Experiment 3 (see Table 5-21).

Table 5-24: Concentration, purity and recovery of Rha, Ara and Gal in the Extract and Raffinate streams after 3-zone SMB separation using the variables defined in Experiment 8 in Table 5-22. SMB operation was performed as described in Section 2.13.1 using the 3-zone setup described in Section 2.13.3. A solution of Rha, Ara and Gal at concentrations of 1, 13 and 3 g L^{-1} respectively was used as the feed and water as the desorbent. Concentration, purity and recovery values were calculated using ICS analysis as described in Section 2.13.4.

Experiment 8	Rha	Ara	Gal
Extract conc. (g L^{-1})	0.04	2.16	0.11
Extract purity	2%	94%	5%
Extract recovery	27%	99%	22%
Raffinate conc. (g L^{-1})	0.10	0.02	0.33
Raffinate purity	23%	4%	73%
Raffinate recovery	73%	1%	78%

It is possible that the dilution factor and the solvent usage could be reduced by lowering the desorbent flow rate and extract flow rates by equal amounts. This would reduce the m_1 value but keep the m_2 and m_3 values constant. For example, keeping the switch time at 225 s and the feed flow rate at 1 mL min^{-1} but dropping the desorbent flow rate to 6.5 mL min^{-1} and the extract flow rate to 1.5 mL min^{-1} results in an m_1 of 0.70 with the same m_2 and m_3 values as in Experiment 8 (Table 5-22). It is clear that there is considerable potential for further optimisation of this SMB separation.

While Experiment 7 is eclipsed in performance by Experiment 6, offering higher Ara extract concentration and recovery, and equal purity, Experiment 8 can be fairly compared with Experiments 3, 4 and 6. Table 5-25 shows a summary of the Ara extract results for Experiments 3, 4, 6 and 8, and the feed and desorbent flow rates. Experiment 8 has the highest purity and recovery combination with both above 90%, however, the feed flow rate is the lowest, indicating a low throughput per resin volume, and the desorbent flow rate is the highest due to the lack of recycling.

The feed flow rate is shown as an indicator of the total throughput while the desorbent flow rate shows the solvent usage. Feed flow rates of 1, 2 and 3 mL min^{-1} give throughputs of 4.6, 9.1 and 13.7 g L^{-1}_{resin} h^{-1} respectively, based on a total resin volume of 224 mL and a total sugars concentration of 17 g L^{-1}.

Table 5-25: Summary of results from Experiments 3, 4, 6a and 8 showing the zone setup used; the Ara concentration, purity and recovery in the Extract; the feed and desorbent flow rates; and the Table reference showing the full results from each Experiment. The SMB method inputs for the Experiments in the 4-zone and 3-zone SMB setups are detailed in Table 5-12 and Table 5-22 respectively. Concentration, purity and recovery values were calculated using ICS analysis as described in Section 2.13.4.

Experiment	3	4	6a	8
3 or 4 zone setup	4	4	4	3
Ara extract concentration (g L^{-1})	5.77	2.86	2.86	2.16
Ara extract purity	95%	96%	98%	94%
Ara extract recovery	71%	64%	48%	99%
Feed flow rate (mL min^{-1})	3	2	2	1
Desorbent flow rate (mL min^{-1})	6	7	6	9.5
Table shown	Table 5-15	Table 5-16	Table 5-18	Table 5-24

It is not clear whether the improvements are a result of the 3-zone SMB system, allowing an additional column to be present in each the separation zones (zones 2 and 3), or due to the use of a higher switch time, reducing the overall flow rates within the SMB system. Further experiments on the 4-zone SMB setup at higher switch times, and on the 3-zone SMB setup at lower switch times would be required distinguish between these possible explanations.

Figure 5-19 and Figure 5-20 shows the RI trace of the raffinate from Experiment 7 and the extract from Experiment 8 as representative examples of a functioning SMB. It is clear that the raffinate features a steady rise in refractive index units (RIU) as sugars begin to elute from the end of the final column in zone 3 and then a rapid drop with every port switch as elution switches to a fresh column. Conversely, the extract features a sharp jump and then a drop in RIU with every port switch, corresponding with the switch to a column loaded with sugar which is gradually desorbed

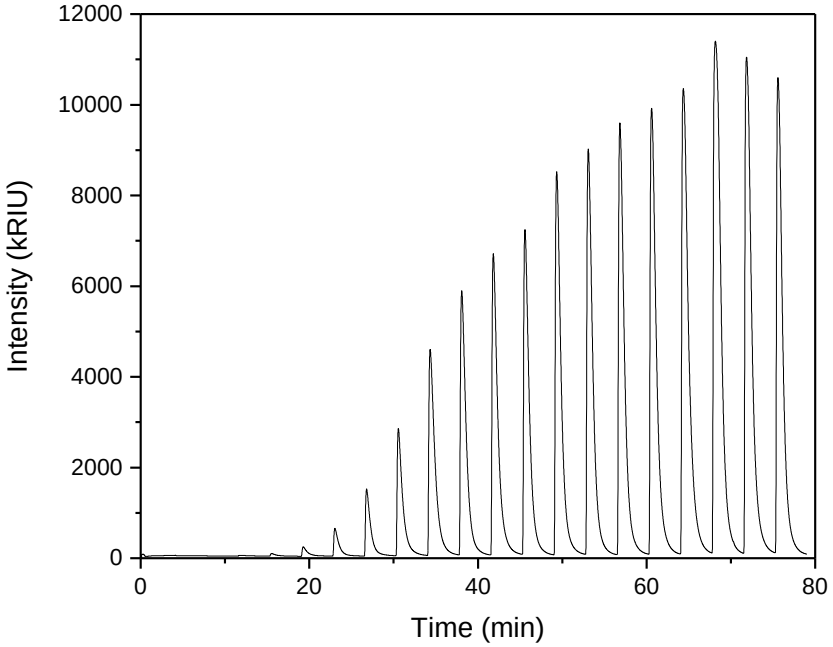

Figure 5-19: Refractive index trace of the Extract from SMB Experiment 7 for the separation of Ara from Rha and Gal. SMB separation was performed in the 3-zone setup as described in Section 2.13 with operating conditions for Experiment 7 given in Table 5-22.

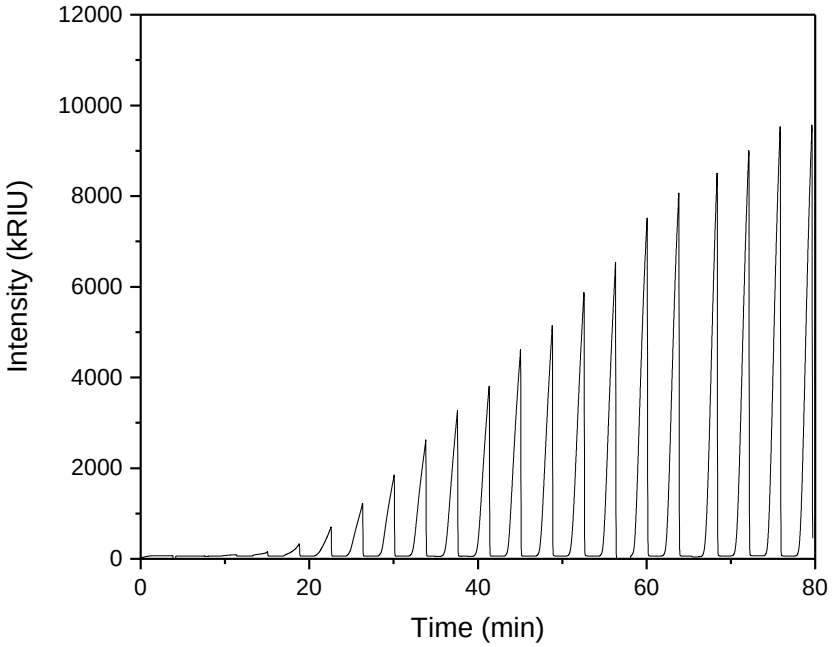

Figure 5-20: Refractive index trace of the Raffinate from SMB Experiment 8 for the separation of Ara from Rha and Gal. SMB separation was performed in the 3-zone setup as described in Section 2.13 with operating conditions for Experiment 8 given in Table 5-22.

5.5 Chapter summary

The work presented in this chapter demonstrates the application of simulated moving bed chromatography to the isolation of Ara from a synthetic neutral mixture of sugars comprising Ara, Gal and Rha. Simulated moving bed technology can be used at very large scales (Section 1.6.4) with high throughputs and the results in this chapter show the potential for it to be used for isolating sugars from a purified hydrolysate stream.

The aim of this chapter was to develop a method for isolating L-arabinose from a synthetic neutral mixture of the neutral sugars in hydrolysed SBP pectin using SMB. The main conclusions of this chapter are:

- Various resins and temperatures were screened based their retention times, selectivities and peak shapes of individual sugar injections. Dowex 50W X8 resin in the Ca^{2+} form at 50°C was selected as the optimal resin and condition for the isolation of Ara (Figure 5-15), providing selectivities to Ara of 1.57 and 1.58 for Rha and Gal respectively (Table 5-7).

- Glucose was found to elute prior to the Rha and Gal and so would have a higher selectivity to Ara. In SMB, the glucose would likely elute in the raffinate stream with the Rha and Gal.

- Column packing of the 8 columns for SMB showed relative standard deviations within 1% of the mean for retention times; within 2.5% of the mean for retention factors; and within 2% of the mean for selectivities (Table 5-8).

- The SMB equilibrium theory model was found to not provide sufficient separation, with almost all of the components eluting in the Extract (Table 5-13).

- SMB separation was improved in the 4-zone, closed loop setup by increasing the feed flow rate and thus increasing the flow rate ratio in zone 3 (Table 5-14 and Table 5-15).

- Using the 4-zone, closed loop, SMB it was possible to achieve an extract with 95-98% pure L-arabinose with a recovery of 71-48% (Table 5-21). Feed flow rates of 2-3 mL min^{-1} were used, giving throughputs of 9.1-13.7 g L^{-1}_{resin} h^{-1}.

- Using the 3-zone, open loop, SMB it was possible to achieve an extract with 94% pure L-arabinose with a recovery of 99% and a feed flow rate of 1 mL min^{-1}, giving a throughput of 4.6 g L^{-1}_{resin} h^{-1} (Table 5-25).

- For both the 4-zone and 3-zone SMB setups there remains a larger amount of possible further optimisation in terms of L-arabinose purity and recovery, feed throughput, and desorbent usage.

The next chapter will look at the isolation of D-galacturonic acid from a synthetic crude mixture and develop pretreatment methods, including decolourising resins and activated carbon, for the complete processing of the crude hydrolysate.

Chapter 6 Development of methods for crude pretreatment and the isolation of D-galacturonic acid towards SMB separation with crude hydrolysates

6.1 Introduction, aims and objectives

As described in Section 5.1, it would be necessary to isolate the GA and remove contaminants from the crude hydrolysate prior to isolation of the Ara using SMB. In this chapter, the isolation of GA will be considered from both a synthetic crude mixture of sugars (Section 2.5) and the crude hydrolysate. Furthermore, the removal of contaminants and coloured compounds will be examined that could impact on both the GA and SMB separations.

The ionic nature of GA (Figure 1-4) means that it could interfere with the cation exchange columns used in SMB (Section 5.2) and affect the isolation of Ara from Gal and Rha. As GA is ionic and the neutral sugars are not, a method was sought to isolate the GA from the neutral sugars so that it can then be used for further applications (Section 1.1.6) and the neutral sugars can be separated on the SMB using the method described in Chapter 5. An anion exchange chromatography method will be examined for isolating the GA from a synthetic crude mixture, binding the galacturonate ions while allowing the neutral sugars to pass through unimpeded. The neutral sugars could then be run on an SMB separation from Chapter 5 to assess the impact of the anion exchange step on SMB separation performance. In addition, pretreatment using resins and activated carbon (Section 1.3) will be examined for decolourisation and contaminant removal from the crude SBP hydrolysate. Finally, the effects of the pretreatment methods will be examined on the isolation of GA and SMB separation of Ara from the crude hydrolysate in order to move towards a complete bioprocessing strategy for use within an integrated SBP biorefinery (Section 1.1.1).

The aim of this chapter is to develop a method of isolating D-galacturonic acid from a synthetic crude mixture and develop pretreatment methods to move towards complete processing of the crude hydrolysate. The specific objectives of this chapter are to:

- Screen for an anion exchange resin that both allows D-galacturonic acid to bind and readily elute.
- Determine the dynamic binding capacities of the resins and perform preparative separations for the isolation of D-galacturonic acid from neutral sugars in a synthetic crude mixture of sugars.
- Perform simulated moving bed chromatography on the neutral sugars, after D-galacturonic acid removal, according to the 3-zone SMB method developed in Chapter 5.
- Develop methods of decolourising the crude hydrolysate using resins or activated carbon while minimising losses of sugar.
- Assess the effect of decolourisation on D-galacturonic acid isolation from decolourised crude hydrolysate.

6.2 D-galacturonic acid isolation from neutral sugars

6.2.1 Screening of resin ionic form

A method of isolating GA from a synthetic crude mixture of GA, Ara, Rha and Gal (defined in Section 2.7.5) was first explored using anion exchange resins in different ionic forms as detailed in Section 2.14.2. Using the resins in the hydroxide form, it was found that the galacturonate bound easily, however, it was not readily eluted with NaOH, but could be eluted with NaCl (data not shown). The neutral sugars did not bind to the column and eluted in the solvent front. While this method demonstrates the potential of anion exchange chromatography for the isolation of GA from the neutral sugars, it would require a large amount of desorbent in what would likely be a six step process:

1. Load: Synthetic crude mixture is loaded onto the column in the OH^- form. The GA binds and the neutral sugars flow through.
2. Wash: Water is passed through the column to remove any unbound sugars.
3. Elute: NaCl is passed through the column, exchanging with the GA which elutes from the column.
4. Wash: Water is passed through the column to remove any residual salts.
5. Regeneration: Large volumes of NaOH are passed through the column to exchange the binding sites back to the OH^- form for further GA loading.
6. Wash: Water is passed through the column to remove any residual salts.

A preferable process, in terms of desorbent usage, would be to combine the elution and regeneration steps and remove one of the wash steps. However, this can only occur if the elution salt is the same ionic form as the regeneration salt and depends on the selectivity of the salt [164]. Too high a selectivity and the GA will not bind to the column; too low a selectivity and the GA will not easily be removed from the column; at an intermediate selectivity, the GA can both bind to the column and easily be eluted.

A proposed four step process based on an ionic form (X^-) of intermediate selectivity is outlined below:

1. Load: Synthetic crude mixture is loaded onto the column in the X^- form. The GA binds and the neutral sugars flow through.
2. Wash: Water is passed through the column to remove any unbound sugars.
3. Elution/regeneration: A salt containing X is passed through the column, exchanging for GA, which elutes from the column and converts the column back into the X^- form.
4. Wash: Water is passed through the column to remove any residual salts.

Knowing that NaCl was capable of eluting the GA from the resin, it was explored if the GA could bind to the resin in the Cl^- form. However, it was found that GA eluted immediately from the column with the neutral sugars. Thus, the Cl^- form was deemed to have too high a selectivity for GA binding and, so, an anionic form with a selectivity that is intermediate of OH^- and Cl^- was sought.

Based on work in the literature on separating uronic acids (galacturonic acid from glucuronic acid) on acetate ion exchangers [162]; and analytical ion chromatography methods where GA does not elute in the OH^- form with a NaOH eluent, but elutes in the acetate form with a NaOAc eluent [163]; the acetate form was next considered. According to DOW [164], the acetate form has a type 1 anion exchange selectivity of 3.2, higher than OH^- (1.0) and lower than Cl^- (22), and so could fall into this intermediate selectivity range, allowing GA to bind to the column, and elute with an acetate salt.

Separation in the acetate form, as detailed in Section 2.14.2, showed that it was capable of binding the GA, allowing the neutral sugars to flow through. Furthermore, elution with NaOAc showed that GA was readily eluted from the column, and the column was thus easily regenerated back into the acetate form ready for further loading.

6.2.2 Screening for resins

Multiple resins (Table 2-4) in the acetate form were compared for their capacity based on the breakthrough curve and relative dynamic binding capacities, as detailed in

Section 2.14.3, by continuously adding GA until it overloads the column. Figure 6-1 shows the breakthrough curves using an RI detector in order to view all of the salts eluting from the column.

The results for each resin show that there are four clear stages and each can be mapped based on the presence of GA in samples collected at various time points. The four stages of the RI-time profile are given with times based on the Dowex 1x8 resin profile:

1. 0-5 min: GA binds to column, exchanging acetate ions off the column which begin to elute, forcing up the RI intensity – no GA detected
2. 5-16 min: RI intensity levels off as acetate ions exchange at the same rate as GA is fed into the column – no GA detected
3. 17-28 min: RI intensity increases as breakthrough is reached and GA begins to elute from the column – (small amounts of GA detected)
4. 29-40 min: RI intensity levels off as the column reaches maximum capacity and no more GA binds to the column. GA concentration of the outlet is equal to the GA concentration of the feed.

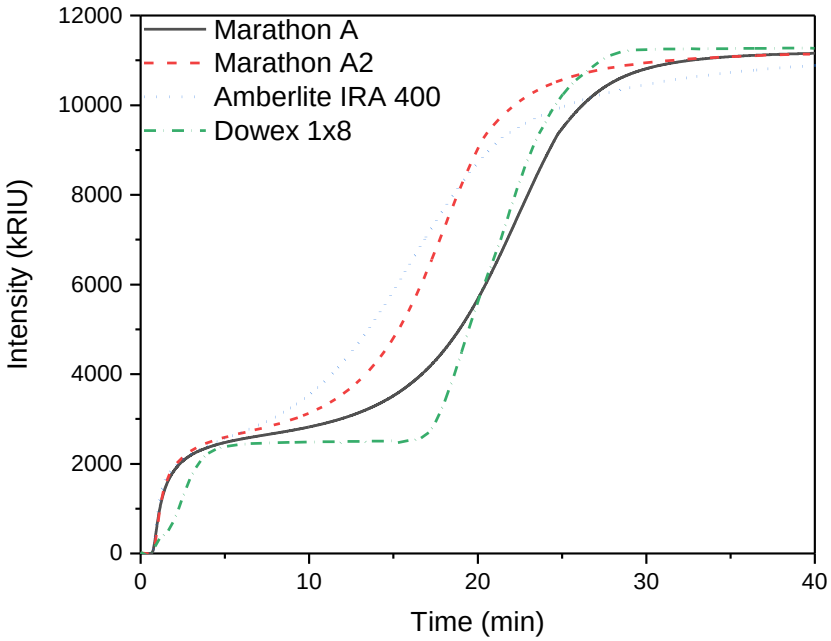

Figure 6-1: Refractive index profile of the breakthrough curves of D-galacturonic acid (GA) on different resins. GA was loaded at a flow rate of 5 mL min^{-1} and a concentration of 10 g L^{-1} onto anion exchange columns packed with 3 g of different resins prepared in the acetate form. Columns were prepared and packed as described in Section 2.14.1. Experiments were performed as described in Section 2.14.3.

It is evident that the Dowex 1x8 resin has significantly later breakthrough than the other resins. It has a fully developed binding step, with initial breakthrough of GA after approximately 17 min and a steeper breakthrough curve. Conversely, the other resins begin to elute GA after approximately 5 min, and feature gentler breakthrough curves. Based on these breakthrough times, the 1x8 column has approximately 3 times the dynamic binding capacity of the other resins and was used for further studies. It is possible that the advantage of this resin lies predominantly in the smaller particle size (Table 2-4 in Section 2.14.3), an effect that would not have been detected using a batch static binding capacity experiment.

The columns here were packed with just 3 g of resin and it is possible that longer columns may cause an increased pressure drop using the 1x8 resin due to its smaller particle size. However, due to the high selectivity of the separation, the column length is not envisaged to be an important factor for separation. Furthermore, by utilising continuous processing in a simultaneous multicolumn chromatography (SMCC) method, it will be possible to use shorter column lengths and achieve increased throughputs by utilising the column capacity above the DBC. The effect of column length is examined in Section 6.2.4 and an SMCC process method is proposed in Section 6.2.5.

While it is difficult to make detailed comparisons of the other resins, some observations can be made. Marathon A, Marathon A2 and Amberlite IRA-400 each reach a breakthrough point at around 5 min. The Marathon A and A2 resins are broadly similar resins but contain different anion exchanger types (A, type 1 anion exchanger; A2, type 2 anion exchanger). The Marathon A2 resin shows a steeper curve than Marathon A, reaching full capacity the soonest of all of the resins examined. This could be a result of the anion exchanger type, with type 2 anion exchangers exhibiting lower affinity for galacturonate. This is supported by work from the DOW Chemical Company that type 1 anion exchange resins have a greater affinity for weak acids than type 2 anion exchange resins [236].

Dowex 1x8 was selected for further development based on its apparent higher DBC, likely a result of its smaller particle size. Quantitative values of the DBC are measured in Section 6.2.3.

6.2.3 Quantification of dynamic binding capacities

Having selected the Dowex 1x8 resin, a quantitative DBC was determined for the same column by overloading a 3 g column with the synthetic crude mixture (defined in Section 2.7.5) as described in Section 2.14.4. Fractions were then analysed by ICS to determine the GA concentration and the area of the combined neutral sugars peak as described in Section 2.14.4. DBC values were calculated using Equation 2-30 and Equation 2-31 in Section 2.14.4.

Figure 6-2 shows the neutral sugars (given as the area of the combined neutral sugars peak) rapidly eluting in the initial fractions showing no effective retention on the column. No GA is detected until 38 min (190 mL), and the GA concentration reaches above 0.5 mg mL^{-1} (10% of the loading concentration) after 42 min (210 mL). This gives a $DBC_{0\%}$ of 1.49 mmol g^{-1}_{resin} and a $DBC_{10\%}$ of 1.65 mmol g^{-1}_{resin}. The resin reaches 100% breakthrough at 60 min (300 mL).

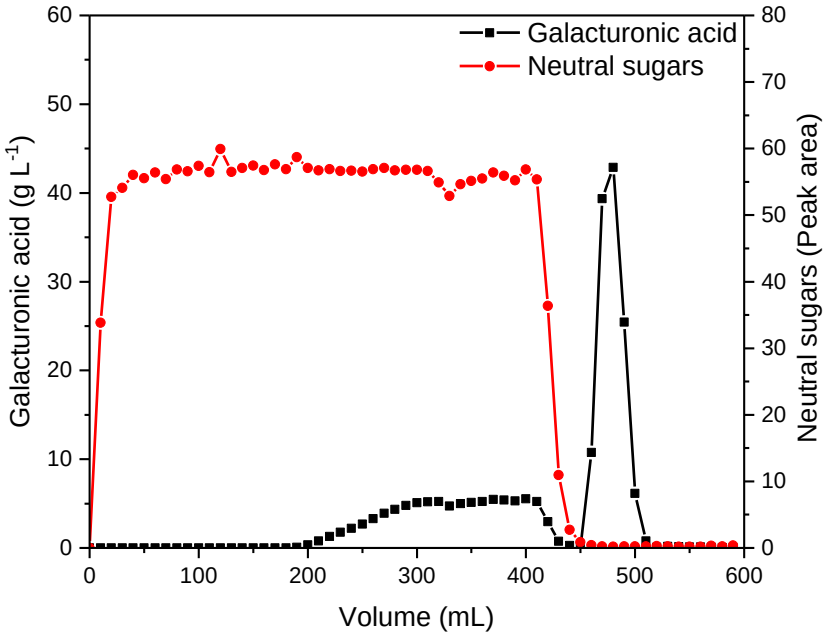

Figure 6-2: Breakthrough curve and elution profile of a synthetic crude mixture of D-galacturonic acid and neutral sugars on a Dowex 1x8 column in the acetate form. A column containing 3 g of Dowex 1x8 resin in the acetate form was used, packed as described in Section 2.14.1. The separation consisted of 4 steps: load (400 mL of synthetic crude mixture), wash (50 mL of deionised water), elute (100 mL of 200 mM NaOAc), and wash (50 mL of deionised water) detailed in Section 2.14.4. Fractions were collected every 10 mL and analysed for GA concentration and the combined neutral sugar peak area as described in Section 2.14.4.

The loading step was stopped after 80 min (400 mL) and flushed with deionised water for 10 min (50 mL). It is clear that all of the residual neutral sugars and unbound GA were washed out within this time before the start of the elution step from 90 min (450 mL). During the elution step, no neutral sugars were eluted, indicating that none was bound to the column. The GA was rapidly eluted, peaking at a concentration above 42 g L^{-1}. An important point to note here is that this method to isolate GA will only marginally dilute the neutral sugars (during the start of the load step and the wash step), but will allow for concentration of the GA.

A batch process is thus proposed for the separation of neutral sugars and GA using this column and was found to give neutral sugars with no detectable GA in the collected load fraction, and GA with no detectable neutral sugars in the collected elution fraction:

1. 38 min (190 mL) load step leading up to initial breakthrough of GA.
2. 10 min (50 mL) wash step to flush all residual sugars from the load step.
3. 25 min (125 mL) elution step with NaOAc to elute the GA.
4. 10 min (50 mL) wash step to flush out all residual salts from the elution step.

6.2.4 Effect of column length

The column explored in Section 6.2.3 uses just 3 g of resin creating a very short bed length (1.8 cm, ~3.6 mL in the acetate form) in the XK16 column. A longer column using 14 g of resin was used to give a more representative operating condition as well as increase the capacity of the column for preparative separations. This gave a bed length of 8.5 cm and a column volume of 17 mL in the acetate form. The quantitative DBC experiment performed in Section 6.2.3 was repeated on the longer 14 g column with the same synthetic crude mixture (detailed in Section 2.14.2). The method is detailed in Section 2.14.4 and outlined as follows:

1. Load for 325 min (1600 mL)
2. Wash with water for 20 min (100 mL)
3. Elution with 200 mM NaOAc for 50 min (250 mL)
4. Wash with water for 20 min (100 mL).

To reduce the amount of ICS analysis required in order to assess the separation, the conductivity was used as a metric for comparison between the 3 g and the 14 g columns. Figure 6-3 shows the GA concentration on the 3 g column (from Figure 6-2) overlaid with the conductivity profile. The profile begins with an increase in conductivity to (0.24 mS cm^{-1}) as GA exchanges with the acetate bound to the column which is consequently eluted. The trace then follows a similar rise as GA breakthrough begins and levels off (at 0.98 mS cm^{-1}) once the column reaches saturation. The conductivity then drops with the GA concentration during the water wash step at 400 mL. It is during the elution step where the conductivity profile begins to differ slightly from the GA concentration due to the use of NaOAc as an eluent. The conductivity rapidly increases as GA is eluted from the column and then doesn't drop with GA concentration but, after a small step, begins to rise again and quickly levels off (at 13.5 mS cm^{-1}) as the NaOAc elutes from the column. The conductivity rapidly drops at the end of the profile as the final water wash step begins. It is clear from this comparison that the conductivity profile can be used to demonstrate the breakthrough curve and elution profile of GA.

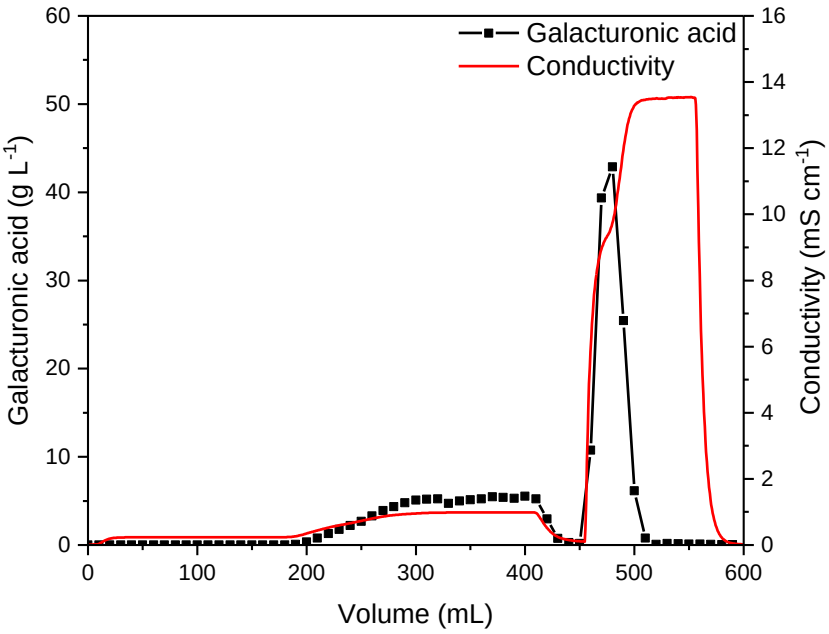

Figure 6-3: Comparison of D-galacturonic acid concentration and conductivity from a synthetic crude mixture applied to a Dowex 1x8 column in the acetate form. The column was packed with 3 g of resin as described in Section 2.14.1. The separation consisted of 4 steps: load (400 mL of synthetic crude mixture), wash (50 mL of deionised water), elute (100 mL of 200 mM NaOAc), and wash (50 mL of deionised water) detailed in Section 2.14.4. Fractions were collected every 10 mL and analysed for GA concentration, and the conductivity was measured online as described in Section 2.14.4.

The conductivity profile on a 14 g column is shown in Figure 6-4, with noise filtered out as described in Section 2.14.4. The profile is broadly similar to the conductivity profile on the 3 g column, with a clear breakthrough curve and more developed two-step profile in the elution step.

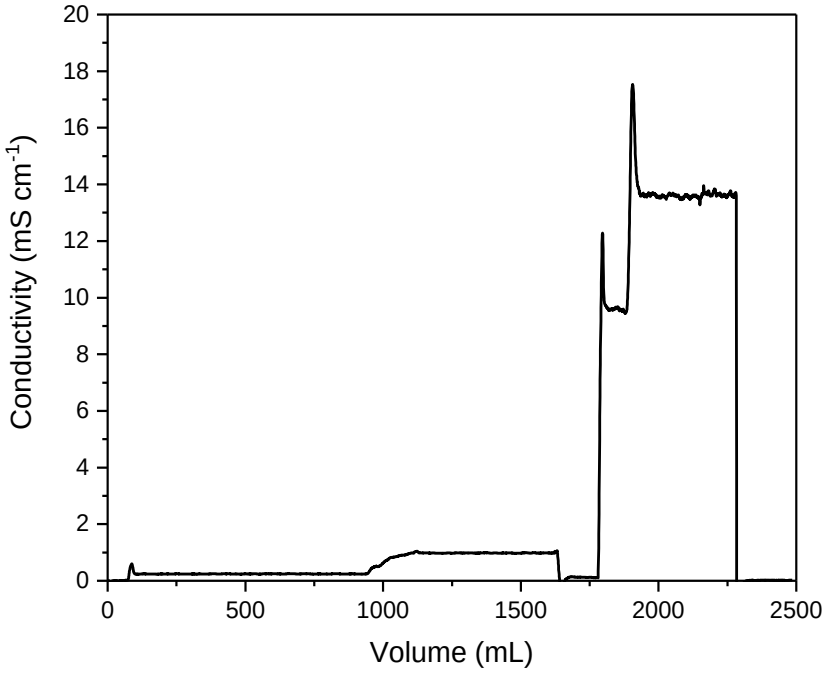

Figure 6-4: Conductivity profile showing the breakthrough and elution of D-galacturonic acid from a synthetic crude mixture applied to a Dowex 1x8 column in the acetate form. Noise reduction was performed with a 21 point symmetric moving average as described in Section 2.14.4. The column was packed with 14 g of the resin as described in Section 2.14.1. The separation consisted of 4 steps: load (1600 mL of synthetic crude mixture), wash (100 mL of deionised water), elute (250 mL of 200 mM NaOAc), and wash (100 mL of deionised water) detailed in Section 2.14.4.

The breakthrough curve begins at approximately 944 mL, giving a $DBC_{0\%}$ of 1.59 mmol g^{-1}_{resin} (1.31 mmol mL^{-1}_{resin}). The 10% breakthrough volume can also be estimated, assuming a linear response between the conductivity and the GA elution. Prior to breakthrough is a conductivity of 0.24 $mS.cm^{-1}$ and at 100% breakthrough is 0.98 mS cm^{-1}, therefore, 10% breakthrough correlates to a conductivity of 0.31, with a volume of 949 mL giving a $DBC_{10\%}$ of 1.60 mmol g^{-1}_{resin} (1.32 mmol mL^{-1}_{resin}).

For direct comparison, the conductivity method for determining the DBC should also be performed on the shorter 3 g column. This gives an initial breakthrough of 186 mL (37.2 min), giving a $DBC_{0\%}$ of 1.46 mmol g^{-1}_{resin}; and a 10% breakthrough volume of

197 mL (39.4 min), giving a $DBC_{10\%}$ of 1.55 mmol g^{-1}_{resin}. The results of these conductivity determined DBC values are given in Table 6-1.

Table 6-1: Comparison of dynamic binding capacities and breakthrough curves for the binding of D-galacturonic acid on two columns of Dowex 1x8 in the acetate form at different lengths. Columns were packed as described in Section 2.14.1. Experiments were performed as described in Section 2.14.4 and values were determined using the conductivity profiles.

Mass of resin (g_{resin})	$DBC_{0\%}$ (mmol g^{-1}_{resin})	$DBC_{10\%}$ (mmol g^{-1}_{resin})	Breakthrough volume per mass of resin (mL g^{-1}_{resin})	Breakthrough curve length (mL)
3	1.46	1.55	62	127
14	1.59	1.60	67	158

The longer column appears to have a slightly higher DBC, considering an almost 5 times longer column. Looking at the initial breakthrough volume per mass of resin, Table 6-1, shows a similar result with only a small increase in the breakthrough volume per mass of resin. Additionally, the length of the breakthrough curve is longer on the 14 g column. The variations in both the breakthrough volume per mass of resin and the breakthrough curve length are small, considering an almost 5 times increase in resin mass, indicating that the effect could be associated purely with experimental error, such as a small change in feed concentration. A constant breakthrough curve length and a breakthrough volume proportional to the column length are important observations when selecting a column length for a large-scale batch system or for the design of a continuous process such as SMCC.

Examining the elution step on the conductivity profile shows a much more defined stepwise profile than on the 3 g column. This is simply a result of the longer column length allowing the GA elution profile to fully develop before the elution begins to complete and acetate is eluted from the column. The required length of the elution step can be calculated on both columns from the start of the conductivity rise to the balancing out of conductivity during acetate elution. The 3 g column gives an elution volume of ~50 mL while the 14 g column gives an elution volume of 150 mL. It appears that the elution volume required per mass of resin decreases with increased resin mass (from ~17 mL g^{-1}_{resin} on the 3 g column to ~11 mL g^{-1}_{resin} on the 14 g column). However, due to the shortage in data points it is not possible to comment on the trend beyond 14 g, for example, if it tends towards a certain value with increasing

column length. It may be useful to add additional volume to the elution step, or an independent regeneration step, in order to ensure total regeneration of the column to the acetate form.

Looking at the GA concentration of the fractions collected on the 3 g column gives an elution time of approximately 70 mL from the first to the last observed GA in the collected fractions, however, this may overstate the elution volume due to the relatively large fraction volume of 10 mL.

It is thus possible to generate an idealised batch separation method for the 14 g column. The load step is more than 3 times as long as the remaining steps combined. There is therefore an obvious opportunity for the process to benefit from SMCC, further discussed in Section 6.2.5.

1. Load step: 940 mL of feed
2. Wash: 50 mL water
3. Elution: 150 mL 200 mM NaOAc
4. Regeneration: 50 mL 200 mM NaOAc
5. Wash: 50 mL water

6.2.5 Proposed SMCC process

A possible SMCC operation is proposed in Table 6-2 with the 14 g column split into 4 smaller (3.5g) columns, with 1 undergoing the first wash, elution, regeneration and second wash steps; and the other 3 in the load step.

Table 6-2: A proposed simulated multicolumn chromatography setup with a four step cycle consisting of 4 columns.

Cycle	Step	Column1	Column2	Column3	Column4	Step volume (mL)
Cycle1	Step1	Load1	Load2	Load3	Wash	50
Cycle1	Step2	Load1	Load2	Load3	Elute	59.5
Cycle1	Step3	Load1	Load2	Load3	Regenerate	50
Cycle1	Step4	Load1	Load2	Load3	Wash	75.5
Cycle2	Step1	Wash	Load1	Load2	Load3	50
Cycle2	Step2	Elute	Load1	Load2	Load3	59.5
Cycle2	Step3	Regenerate	Load1	Load2	Load3	50
Cycle2	Step4	Wash	Load1	Load2	Load3	75.5
Cycle3	Step1	Load3	Wash	Load1	Load2	50
Cycle3	Step2	Load3	Elute	Load1	Load2	59.5
Cycle3	Step3	Load3	Regenerate	Load1	Load2	50
Cycle3	Step4	Load3	Wash	Load1	Load2	75.5
Cycle4	Step1	Load2	Load3	Wash	Load1	50
Cycle4	Step2	Load2	Load3	Elute	Load1	59.5
Cycle4	Step3	Load2	Load3	Regenerate	Load1	50
Cycle4	Step4	Load2	Load3	Wash	Load1	75.5

As only 3 of the columns are in the load step, the step is reduced by a quarter from 940 to 705 mL, which gives a cycle volume of 235 mL between column switches. Keeping the wash and regeneration steps as 50 mL and reducing the elution step from 11 mL g^{-1}_{resin} to 17 mL g^{-1}_{resin} (as in the 3 g column) gives an elution volume of 59.5 mL and a total cycle volume of 209.5 mL. The second wash step was therefore increased from 50 mL to 75.5 mL to maintain the volumetric flow rate across all steps, giving a cycle volume of 235 mL, equal to the column switch time volume.

The SMCC process effectively allows for a higher proportion of the resin to be active in the separation of the neutral sugars from GA. In the batch process, the throughput is 940 mL of feed for every 248 min (3.8 mL min^{-1}). In the proposed SMCC process, the throughput is 940 mL of feed for every 188 min (5 mL min^{-1}) as the feed is always being loaded onto some of the columns.

The SMCC process can theoretically be improved further by using the length of the mass transfer zone (the breakthrough curve volume) to determine the column length. This allows for the use of 3 columns, reducing the required resin volume, with one

becoming saturated, one containing the breakthrough curve and one undergoing the wash, elution and regeneration steps.

6.3 Crude pretreatment

6.3.1 Crude D-galacturonic acid isolation

The isolation of GA from the crude hydrolysate was examined using the 14 g Dowex 1x8 column in the acetate form described in Section 6.2.4. No pretreatment was performed prior to the separation with the crude hydrolysate loaded directly onto the column using the method outlined in Section 2.14.5. By loading 350 mL of crude onto the column there was no apparent binding of the GA which eluted in the load step. Furthermore, a portion of the coloured compounds bound to the column. It is possible that the coloured compounds have a higher selectivity for the resin than the GA and so preferentially exchange. Washing the column sequentially with 2 M NaCl and 1 M NaOH reduced the colouration on the resin, exchanging to Cl^- and OH^- respectively, however, some colour remained on the resin, indicating permanent adsorption. Smaller load steps of 10 mL also resulted in no GA binding onto the column. It is clear that some form of pretreatment is required in order for the D-galacturonic acid isolation method developed in Section 6.2 to be successful when separating the crude hydrolysate. The next sections examine pretreatment methods for the decolourisation of the crude in order to allow for further processing to recover the GA and neutral sugars via anion exchange and simulated moving bed chromatography respectively.

6.3.2 Resin decolourisation

Resins are routinely used for decolourisation of crude feedstocks, generally as alternatives to activated carbon as they can be more easily regenerated. They tend also tend to be ion exchange resins, operating based on reversible exchange onto the resin. Various ion exchange resins (both anion and cation) were explored in batch experiments (described in Section 2.15.1) to determine their decolourisation performance. The Cl^- form was used as it has been shown in Section 2.14 to not allow exchange of GA.

Figure 6-5 shows the UV profiles of the crude before and after pretreatment with a range of different resins. There are clear differences in the effectiveness of the different resins at removing the UV absorbing compounds. However, they tend to show a similar profile, absorbing similar proportions across the range 230-400 nm (as shown in Figure 6-6). The mean average value across the range 230-400 nm appears to be representative of the UV absorption and so was used for numerical observations. The UV range is shown as it was difficult to get quantifiable data in the visible range, however, the reductions in the UV absorbance correlated with a visible reduction in colouration. The level of decolourisation was calculated as described in Section 2.15.1.

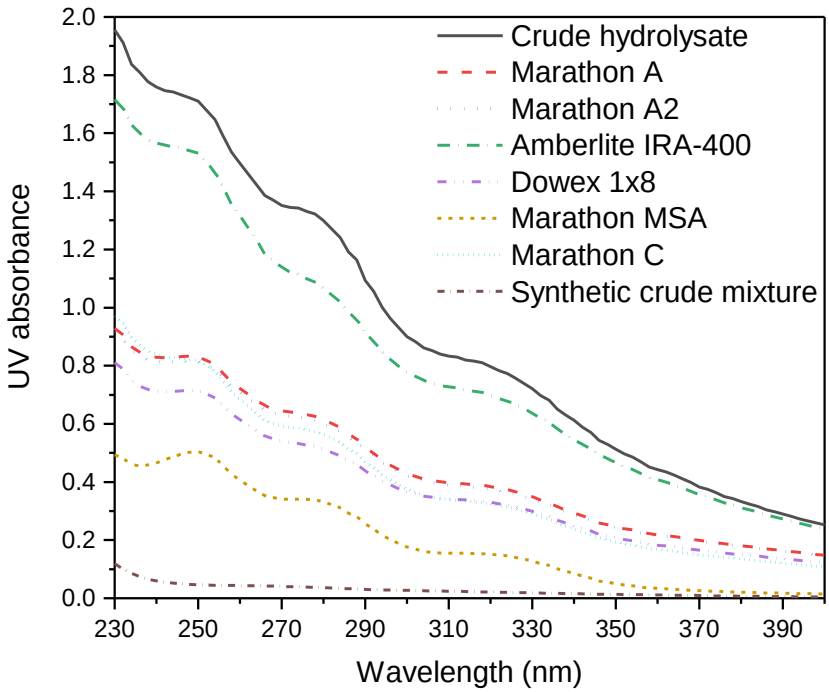

Figure 6-5: Decolourisation of crude hydrolysate using different resins. Decolourisation was performed with a resin loading of 200 mg mL^{-1} of resin and a contact time of 16 hours as described in Section 2.15.1. UV analysis was performed as described in Section 2.15.1.

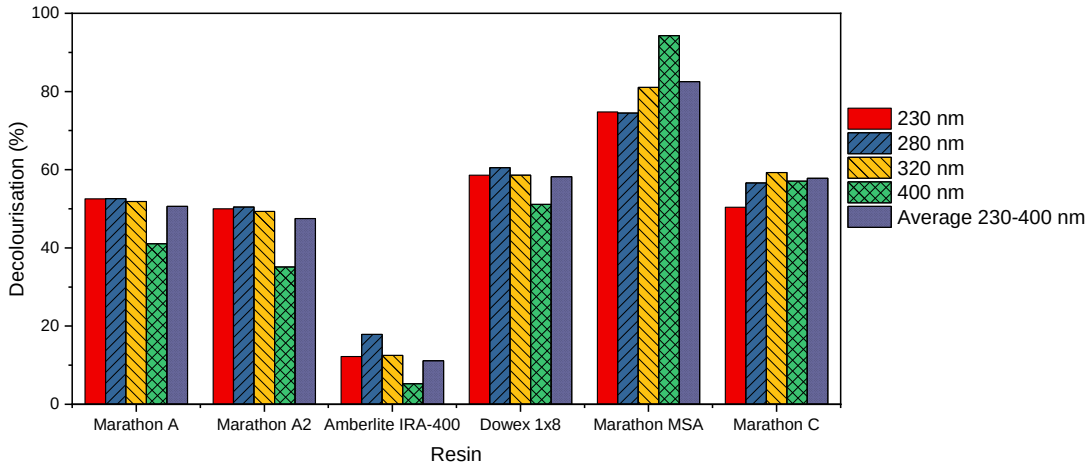

Figure 6-6: Decolourisation of crude hydrolysate at different wavelengths using different resins. Decolourisation was performed with a resin loading of 200 mg mL^{-1} of resin and a contact time of 16 hours as described in Section 2.15.1. UV analysis was performed as described in Section 2.15.1.

Figure 6-5 also shows the UV profile of the synthetic crude mixture. The profile is much lower than the crude indicating that the UV profile is caused by other compounds in the crude and not by the sugars, which have very little UV absorbance.

While it is clear that Marathon MSA facilitates the highest decolourisation, it is necessary to look at whether there is any loss of sugars during the pretreatment step. Figure 6-7 shows the decrease in concentration of each sugar and the level of decolourisation across the 230-400 nm range. It can be seen that the concentration of all the sugars decreases, generally less than 15%. This effect is unlikely to be an ion exchange one, particularly as the only ionic sugar (GA) has similar decreases to the neutral sugars, and appears to be equally affected by the cation exchange resin (Marathon C). It could be a simple hydrophilic interaction with the resin or some effect caused by the resin hydration, as the resins were not hydrated prior to use. Furthermore, it was seen in Section 6.2.1 that neutral sugars and GA eluted immediately from the Dowex 1x8 resin in the Cl^- form in a column setup. As such it was assumed that the concentration decrease for the sugars was insignificant and the Marathon MSA resin was selected based on its superior decolourisation.

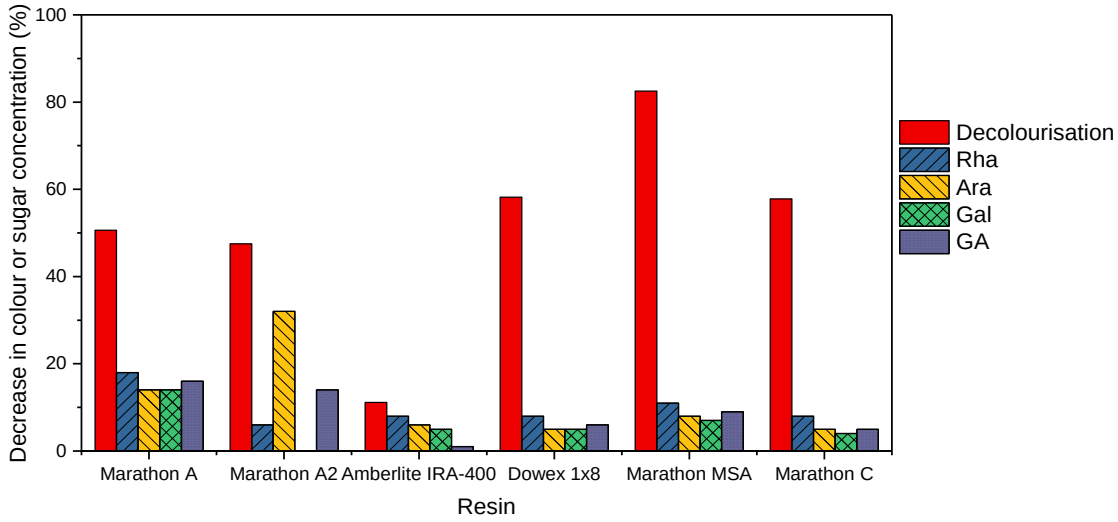

Figure 6-7: Decrease in colour and sugar concentrations of crude hydrolysate after decolourisation with different resins. Decolourisation was performed with a resin loading of 200 mg mL^{-1} of resin and a contact time of 16 hours as described in Section 2.15.1. UV analysis was performed as described in Section 2.15.1. Sugar concentrations were calculated using ICS for both GA and neutral sugars as described in Section 2.8.3.

Next, the kinetics of the decolourisation step were examined and the UV profiles are shown in Figure 6-8. The rate of change slows dramatically from 40-90 min, however, it does not reach zero and the decolourisation continues such that at 960 min (overnight), it is significantly further reduced (see Figure 6-9). The reasons for this are unclear, however, it shows that, a long contact time may be necessary to maximise the decolourisation and the kinetics will be an important factor in any process design. In addition, the concentration of sugars was found not to be affected by the contact time, further demonstrating that the variation in concentration may not be a binding effect.

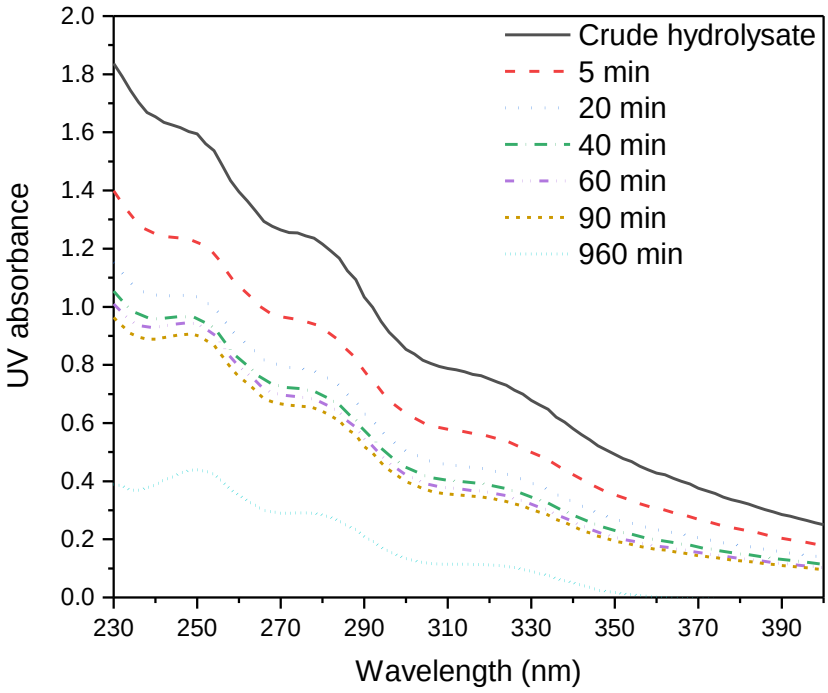

Figure 6-8: Decolourisation of crude hydrolysate using Marathon MSA resin at different contact times. Decolourisation was performed with a resin loading of 200 mg mL^{-1} and varying the contact time as described in Section 2.15.1. UV analysis was performed as described in Section 2.15.1.

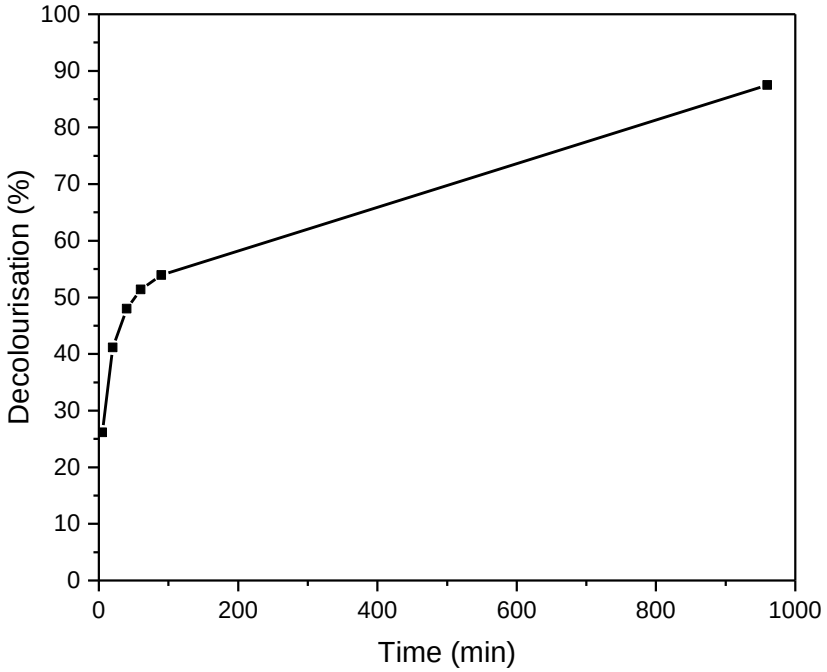

Figure 6-9: Effect of contact time on the average level of crude hydrolysate decolourisation performed with a Marathon MSA resin. Decolourisation was performed on the Marathon MSA resin with a loading of 200 mg mL^{-1} and varying the contact time as described in Section 2.15.1. UV analysis was performed as described in Section 2.15.1.

Subsequently, the impact of resin loading was examined to ascertain the maximum decolourisation achievable. Figure 6-10 shows the UV traces of increasing resin loading relative to the original crude, while Figure 6-11 shows the tailing off of the level of decolourisation at approximately 90%.

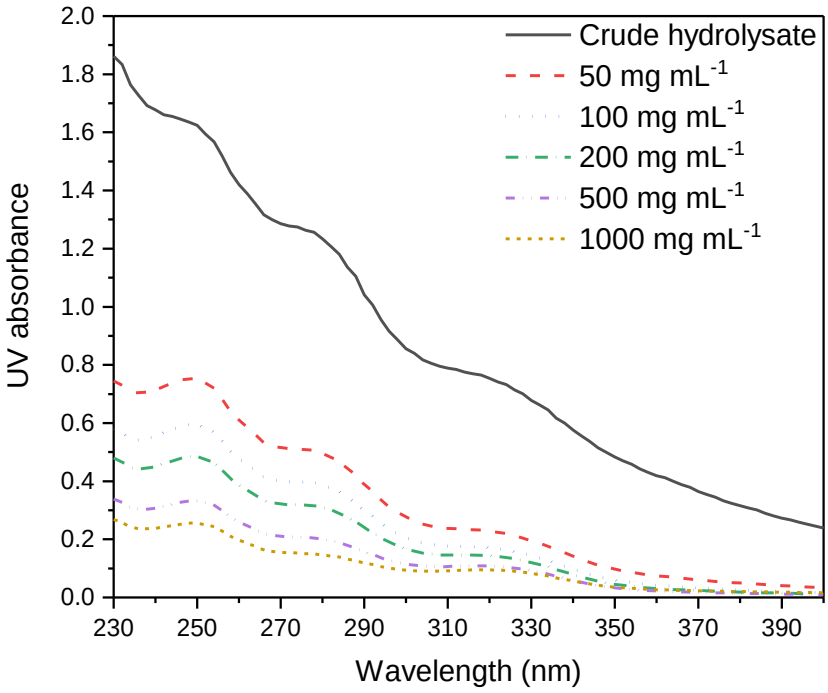

Figure 6-10: Decolourisation of crude hydrolysate using Marathon MSA resin at different resin loadings. Decolourisation was performed on the Marathon MSA resin with a varying resin loading and a contact time of 16 hours as described in Section 2.15.1. UV analysis was performed as described in Section 2.15.1.

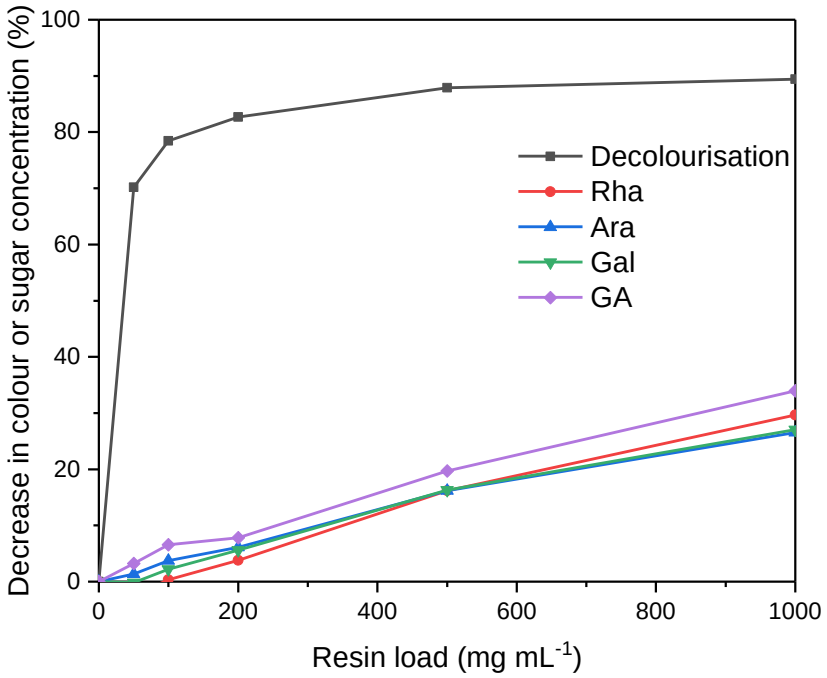

Figure 6-11: Effect of resin loading on the decolourisation and decrease in sugar concentrations. Decolourisation was performed on the crude hydrolysate using the Marathon MSA resin with a varying resin loading and a contact time of 16 hours as described in Section 2.15.1. UV analysis was performed as described in Section 2.15.1.

The percentage decrease in sugar concentration for each sugar in the supernatant are also shown in Figure 6-11. The trends show a steady linear increase in losses for all sugars, with higher loadings resulting in a reduced sugar concentration. The constant rate between all sugars helps to further justify that the effect may be non-binding, and could be a dilution or hydration effect caused by the resin and indicates that the effect would unlikely be of importance in a column format.

The results show that the Marathon MSA resin could be an effective method for decolourising the crude up to 90%, however this may require long contact times and large amounts of resin. Further work needs to focus on column experiments for decolourisation to demonstrate the decolourisation effect; impact of the sugar 'binding' in column runs; and effectiveness of column regeneration. In the next section, the possibility of using activated carbon was examined for decolourisation of the crude.

6.3.3 Activated carbon decolourisation

Activated carbon is an effective decolourising agent and capable of the adsorption of a wide range of compounds (Section 1.3.2). They are widely used in water purification for industrial wastewaters and drinking water [139] and have been used for the decolourisation of sugar liquors [143], indicating that they are capable of removing contaminating compounds without significant adsorption of the sugars Batch activated carbon decolourisation of the crude hydrolysate was explored based on the colour removal and the changes in sugar concentration and compared with the resins examined in Section 6.3.2

Figure 6-12 shows the effect of activated carbon on the overnight decolourisation compared with the original crude hydrolysate, the synthetic crude mixture and the Marathon MSA resin from Section 6.3.2. Activated carbon decolourisation was performed as described in Section 2.15.1. The effect of activated carbon loading was also examined. At a loading of 20 mg mL^{-1}, the activated carbon performance is similar to that of the Marathon MSA resin at a loading of 200 mg mL^{-1}). At equal loading (200 mg mL^{-1}), the activated carbon shows superior decolourisation with the UV profile similar to that of the synthetic crude mixture.

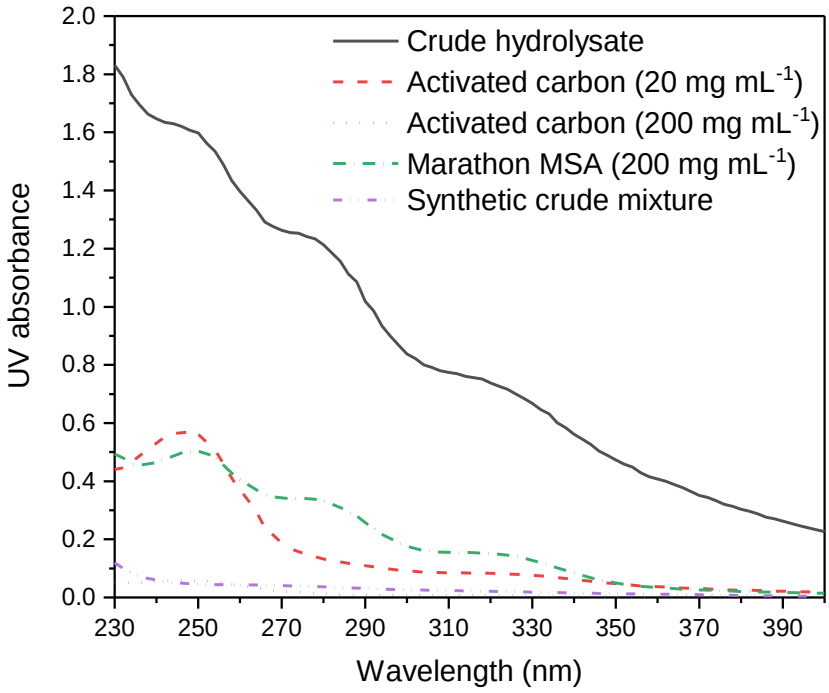

Figure 6-12: Decolourisation of crude hydrolysate with different decolourising agents and loadings. Decolourisation was performed with activated carbon at loadings of 20 and 200 mg mL^{-1}, and Marathon MSA at 200 mg mL^{-1}, as described in Section 2.15.1 with a contact time of 16 hours. The UV profile of a synthetic crude mixture is shown for comparison. Decolourisation experiments were performed with a contact time of 16 hours as described in Section 2.15.1. UV analysis was performed as described in Section 2.15.1.

Figure 6-13 shows the decreases in sugar concentrations and levels of decolourisation of activated carbon decolourisation at the two loadings, alongside the values for Marathon MSA decolourisation, from Figure 6-7. At the higher loading there is a clear adsorption of the neutral sugars, although interestingly not of GA. At the lower loading, only Ara is adsorbed, with a 28% decrease in concentration. This is higher than the values observed in Marathon MSA. At this low loading, the other sugars appear to show a small increase in sugar concentration. It is possible that there is some exclusion of the sugars while the water hydrates the activated carbon, and it has a specific adsorption for L-arabinose. These activated carbon experiments were equilibrated overnight although visual observations show the decolourisation occurring within minutes.

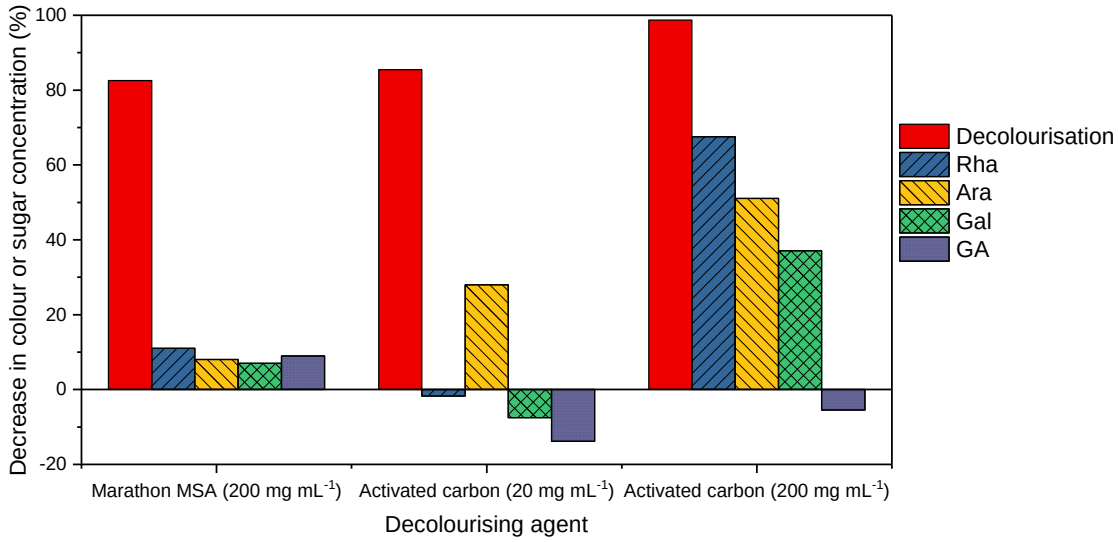

Figure 6-13: Effect of different decolourising agents and loadings on the decolourisation and decrease in sugar concentrations. Decolourisation was performed on the crude hydrolysate with activated carbon at loadings of 20 and 200 mg mL^{-1}, and Marathon MSA resin at 200 mg mL^{-1}, as described in Section 2.15.1, with a contact time of 16 hours. UV analysis was performed as described in Section 2.15.1. Sugar concentrations were calculated using ICS for both GA and neutral sugars as described in Section 2.8.3. Negative values indicate an apparent increase in sugar concentration.

Using an intermediate activated carbon loading of 100 mg mL^{-1} and a reduced contact time of 10 min gives an average decolourisation (230-400 nm) of 97%, identical to the 200 mg mL^{-1} loading. Additionally, the Ara concentration is only reduced by ~15%, lower than either loading on the overnight experiments, while the other sugars have very little change in concentration. This indicates that the kinetics of decolourisation is fast, occurring completely in 10 min to a maximum of 97%, and the adsorption of sugars is much slower.

It is clear that optimisation is possible and it is likely possible to perform the decolourisation with less reduction of L-arabinose concentration. Additionally to the loading and contact time, it may be useful to look at the effects of temperature and pH on the level of decolourisation and sugar concentrations. The 10% activated carbon loading with a contact time of 10 min was used for scale-up experiments in Section 6.3.4.

6.3.4 Scaling up activated carbon decolourisation

Scaling up the 10% activated carbon loading and 10 min contact time from 100 mg of activated carbon with 1 mL of crude to 5g of activated carbon with 50 mL of crude

was performed as described in Section 2.15.2. The scale-up yielded similar results, with 96% decolourisation, a decrease in Ara concentration of 14%, and negligible changes in the concentrations of the other sugars. Figure 6-14 shows the visual effect of decolourisation from the crude on the left to the decolourised sample on the right. This decolourised crude hydrolysate was used for GA isolation experiments with decolourised crude hydrolysate in Section 6.3.5.

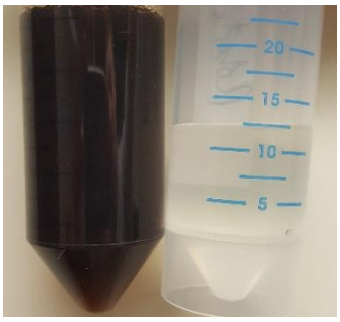

Figure 6-14: Visual comparison of the crude hydrolysate (left) and the decolourised crude hydrolysate (right). Decolourisation was performed as described in Section 2.15.2.

6.3.5 D-galacturonic acid isolation using decolourised crude hydrolysate

The decolourised crude hydrolysate prepared in Section 6.3.4 was then used for GA isolation experiments on a 14 g Dowex 1x8 column in the acetate form as described in Section 2.15.3. Initially, 350 mL of the decolourised crude hydrolysate was loaded onto the column, but resulted in no binding of the GA to the column, with both neutral sugars and GA eluting in the loading step, including in the first 50 mL fraction.

Next, a much smaller, 10 mL injection was attempted. This resulted in approximately 55% of the GA being bound to the column and eluted in the elution step, with the remaining 45% eluting in the loading step with the neutral sugars. Reducing the injection volume further to 5 mL resulted in 79% of the GA bound to the column and eluted in the elution step, while for a 1 mL injection, the value rose to 88%. In both instances 100% of the neutral sugars eluted in the load step. In order to verify the lack of GA binding was caused by the decolourised crude hydrolysate and not some damage to the column, a 10 mL synthetic crude mixture sample (described in Section 2.7.5) was injected and resulted in complete binding of the GA, and elution in the elution step.

After the loading of multiple decolourised crude hydrolysate samples onto the column, a small section at the top of the column began to darken. This could be a result of the incomplete decolourisation, with the remaining coloured compounds binding to the column. It is noted that some additional column cleaning may be necessary for processing large volumes of decolourised crude hydrolysate.

The problem with the GA not binding, particularly for larger sample volumes could be to do with the presence of other salts in the crude. The acid hydrolysis with H_2SO_4 and subsequent neutralisation with NaOH will result in the presence of Na^+ and SO_4^{2-} ions. These salts are unlikely to be removed by the activated carbon pretreatment and the sulphate ions could be binding to the anion exchange column more selectively than the GA. The sulphate anion is reported to have a selectivity coefficient of 85 on type 1 anion exchangers, demonstrating that it is much more selective than the chloride anion (22) and the acetate anion (3.2) [164]. Given that GA was found to not bind to anion exchangers in the chloride form but could bind in the acetate form and be eluted with NaOAc indicates a selectivity coefficient somewhere around 3.2. It is therefore likely that the sulphate ions present in the decolourised crude hydrolysate, with a selectivity coefficient of 85, preferentially bind to the column and readily exchange with any GA that does bind.

Comparing the conductivities of the synthetic crude mixture, crude hydrolysate and decolourised crude hydrolysate (Table 6-3) can help to indicate the quantity of salts in the samples. It was found that the crude hydrolysate had a significantly higher conductivity than the synthetic crude mixture and that the decolourisation process with activated carbon did not affect the conductivity. This indicates that the coloured compounds removed in the decolourisation process are non-ionic, or have low relative conductivities.

Table 6-3: Conductivities of different samples. The decolourised crude hydrolysate was prepared as described in Section 2.15.2. The synthetic crude mixture was a solution of GA, Ara, Rha and Gal (5, 13, 1, 3 g L^{-1} respectively). Conductivity was determined as described in Section 2.8.4.

Sample	Conductivity (mS cm^{-1})
Synthetic crude mixture	1.0
Crude hydrolysate	45.3
Decolourised crude hydrolysate	45.3

It is likely that the presence of these additional salts is prohibiting the binding of GA to the anion exchange column in the acetate form. As a result, it may be necessary to find an alternative method to isolate the GA and neutral sugars. For example, it may be possible to completely demineralise the decolourised crude hydrolysate through a two-step series of cation and anion exchange resins in the H^+ and OH^- forms respectively, and collecting the mixture of neutral sugars for SMB operation. It may then be possible to isolate the GA from the anion exchange column in a gradient or sequential stepwise elution method.

The pretreatment methods discussed in this chapter could also be of benefit to the crude CPC separations in Chapter 4. For example, decolourisation using activated carbon could allow for an increased sample load without affecting separation performance. Furthermore, if an effective demineralisation method could be found, it could allow for more flexibility in the CPC sample preparation, allowing for increases in sample concentration, separation performance and throughput.

6.3.6 SMB separations with synthetic GA removed

Although it was not possible to isolate the GA using the decolourised crude hydrolysate with this method, the impact of successful GA isolation on the performance of SMB separation of the neutral sugars (described in Chapter 5) was studied. Experiment 8 in Chapter 5 (Section 5.4.3) was repeated with a synthetic crude mixture that had been passed through the 14 g anion exchange column (from Section 6.2.4) to remove the GA from the remaining neutral sugars. 5 mM Ca^{2+} ions, in the form of calcium ($CaCl_2$) was added to the desorbent in order to compensate for the presence of any H^+ or Na^+ ions present in the feed as a result of the anion exchange, GA removal step. All other conditions were kept identical. This method resulted in a

93% Ara purity in the extract with a recovery of 99%, comparable with the synthetic neutral mixture performed in Section 5.4.3 (Table 5-25).

These results show that the GA removal is a viable option prior to the SMB neutral sugars separations proposed in Chapter 5. It may also not be necessary to add $CaCl_2$ to the desorbent if the neutral sugars solution is demineralised by passing through a cation exchange column in the H^+ form and an anion exchange column in the OH^- form. Furthermore, if the correct pretreatment methods can be found, this sequential anion exchange chromatography and SMB method could be an effective, high throughput and scalable separation path for the isolation of monosaccharides from an SBP hydrolysate.

6.4 Chapter summary

This chapter demonstrates the effectiveness of anion exchange resins for the isolation of D-galacturonic acid from a synthetic crude mixture. The isolation of L-arabinose from the remaining neutral sugars using simulated moving bed chromatography was also shown to be successful. Decolourisation methods were explored in order to move from processing synthetic crude mixtures to real crude hydrolysed sugar beet pulp.

The aim of this chapter was to develop a method of isolating D-galacturonic acid from a synthetic crude mixture and develop pretreatment methods to move towards complete processing of the crude hydrolysate.

The main conclusions of this chapter are:

- Anion exchange resins in the acetate form are highly effective at binding D-galacturonic acid with no retention of the neutral sugars in synthetic crude mixtures. The bound D-galacturonic acid can be readily eluted with sodium acetate.
- A Dowex 1x8 resin was selected and resulted in a dynamic binding capacity for D-galacturonic acid of 1.59 mmol g^{-1}_{resin} (Figure 6-2). This allows 944 mL of a synthetic crude mixture to be loaded onto a 14 g column with complete separation of the D-galacturonic acid from the neutral sugars (Figure 6-4).

- The method developed for synthetic crude mixtures did not translate to the isolation of D-galacturonic acid from the crude hydrolysate, thus some pretreatment method was sought.
- Activated carbon was found to be much more effective at decolourisation than resins but may result in larger irretrievable sugar losses than resins (Figure 6-13). An activated carbon treatment of 100 mg of activated carbon per mL of crude and a contact time of 10 min was capable of 97% decolourisation with a 15% loss of Ara and was scalable up to 50 mL of crude in a single batch.
- While decolourisation reduced the amount of irreversible binding to the column, it failed to allow for isolation of the D-galacturonic acid. This could be related to the high levels of other salts present in the crude and decolourised crude hydrolysate.
- L-arabinose can successfully be isolated from the remaining neutral sugars after removal of the D-galacturonic acid from a synthetic crude mixture using the simulated moving bed method developed in Chapter 5.

In the final chapter the SMB approach proposed in Chapter 5 and Chapter 6 will be compared to CPC separation from Chapter 3 and Chapter 4. Overall conclusions of this thesis will be presented along with proposals for future work.

Chapter 7 Conclusions and future work

7.1 Overall conclusions

The overall aim of this thesis was to establish novel scalable separation pathways for the isolation of the component monosaccharides from crude hydrolysed sugar beet pulp pectin (Section 1.7). Two possible process routes have been developed, both of which show the potential for the isolation of monosaccharides from SBP pectin hydrolysates within an integrated, whole crop biorefinery. The first, utilising CPC to separate the sugars from the crude hydrolysate in a single step process was described in Chapter 4, with phase system development in Chapter 3. The second involved utilising SMB to isolate L-arabinose from neutral sugars (Chapter 5), with ion exchange chromatography to isolate the D-galacturonic acid (Section 6.2) but required pretreatment of the crude hydrolysate steps prior to the separations (Section 6.3). An overview of the two process paths is shown in Figure 7-1.

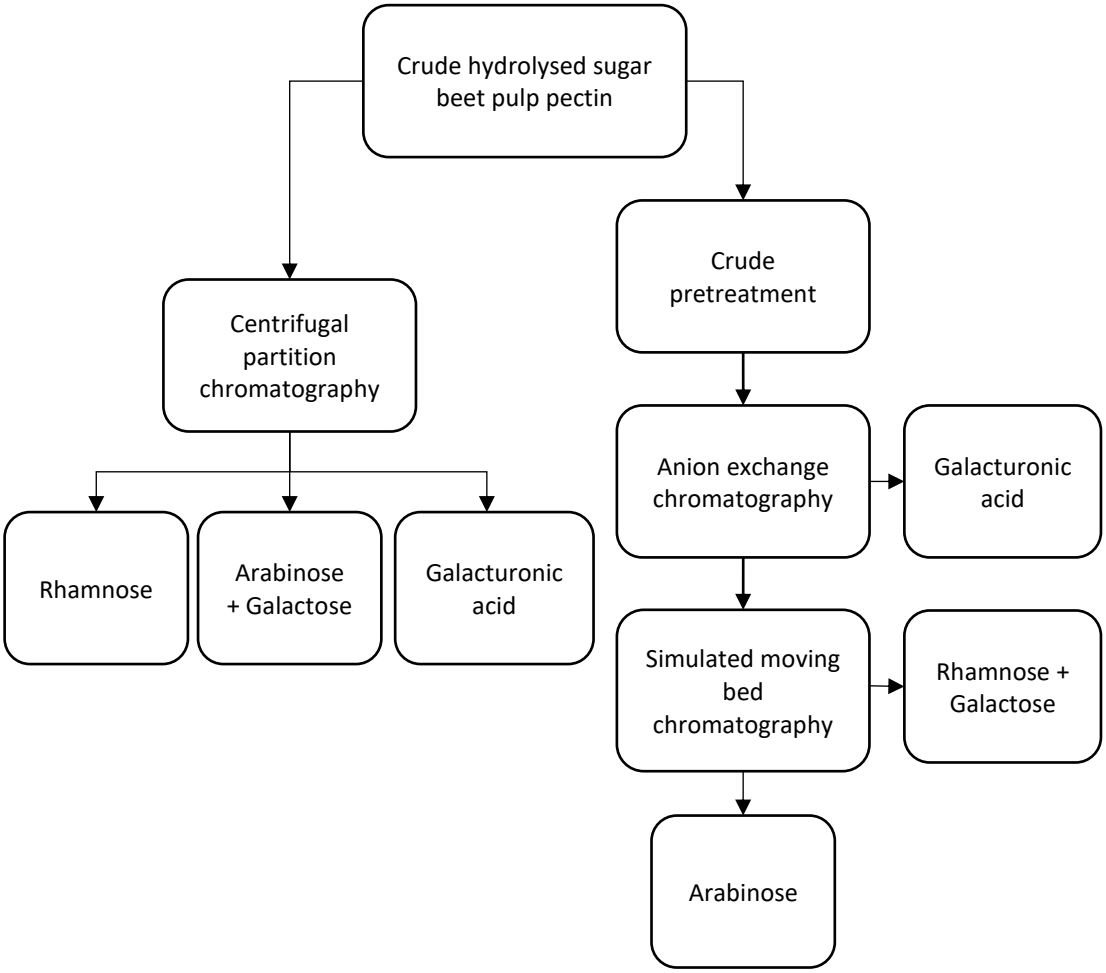

Figure 7-1: Overview of the two process paths established in this thesis. This figure also illustrates the isolated sugar beet pectin fractions obtained from each path.

Chapter 3 examined possible two-phase systems for the separation of a model synthetic mixture of sugars using a novel CPC approach. Pure solvent based phase systems and ion exchange phase systems were ruled out due to poor partition coefficients and extreme settling times respectively. Alcohol-salt phase systems provided promising partition coefficients and were studied in detail, primarily focussed on ethanol : aqueous ammonium sulphate two-phase systems with various modifiers. The highly polar phase system ethanol : DMSO : aqueous ammonium sulphate (300 g L^{-1}) (0.8:0.1:1.8 v:v:v) was selected for CPC separations (phase system XV in Table 3-3) and gave a stationary phase retention of 57% with a rotational speed of 1000 rpm and 8 mL min^{-1} in the ascending mode (Figure 3-5). Using these conditions, a model synthetic mixture of Rha, Ara, Gal and GA was separated into three fractions with high purity: Rha (>90%); Ara (76%) and Gal; and GA (>90%) (Figure 3-8).

Chapter 4 modified the CPC method developed in Chapter 3 to the processing of a crude SBP hydrolysate and scale-up of the separation. DMSO was removed from the phase system as it was shown to have only a minor impact on separation performance (Table 4-2) and complicates further processing. The crude sample was prepared in the stationary phase (LP) to allow for full solubilisation of the sample and showed improved separation performance to the model synthetic mixture (Figure 4-5) while simultaneously removing the coloured contaminants in an early elution fraction. Throughput maximisation was achieved by increasing the sample volume from 4 to 16% of the column volume (Figure 4-10) and applying the elution-extrusion mode (Section 4.6) to extrude the final GA fraction and regenerate the column (Figure 4-11). Linear scale-up of the sample injection volume and flow rate based on the column volume allowed for comparable separation performance and a final throughput of 1.9 g L^{-1}_{column} h^{-1} of monosaccharides and 9.4 g L^{-1}_{column} h^{-1} of total dissolved solids. Ara was purified to 94% purity with a recovery of 98% while GA was purified to 96% purity with a recovery of 95% from the crude SBP hydrolysate (Section 4.7).

Having established the feasibility of CPC as a novel technology for the isolation of monosaccharides from crude hydrolysates, Chapter 5 demonstrated SMB chromatography, an existing technology used in industrial sugar separations, as a potential method for purifying Ara from a synthetic neutral mixture of sugars (Ara, Gal and Rha). A number of different resins, ionic forms and operating conditions were examined in a batch column format. After these initial results a Dowex 50W X8 resin in the Ca^{2+} form at 50°C was selected for SMB experiments based on the selectivities and the peak shapes. Selectivities to Ara of 1.57 and 1.58 were found for Rha and Gal respectively. An equilibrium theory SMB model was used to determine initial SMB operating conditions with 8 columns (Section 5.4.1). A 4-zone, closed-loop SMB (Section 5.4.2) purified Ara to 95-98% purity with 71-48% recovery in the extract and feed flow rates of 2-3 mL min^{-1} (Table 5-21) giving throughputs of 9.1-13.7 g L^{-1}_{resin} h^{-1}. A 3-zone, open-loop SMB (Section 5.4.3) purified Ara to 94% purity with 99% recovery and a feed flow rate of 1 mL min^{-1}, giving a total throughput of 4.6 g L^{-1}_{resin} h^{-1} (Table 5-25).

Finally, Chapter 6 examined methods for isolating GA from neutral sugars in a synthetic crude mixture. Anion exchangers in the acetate form were found to allow

binding of GA and simple elution with sodium acetate while not interacting with the neutral sugars (Section 6.2.1). Anion exchange resins were then screened for the qualitative binding capacity of GA and Dowex 1x8 was selected. The quantitative dynamic binding capacity was determined to be 1.59 mmol g^{-1}_{resin} (Figure 6-2) allowing 944 mL of the synthetic crude mixture to pass through a 14 g column and fully separate the neutral sugars and GA (Figure 6-4).

Chapter 6 also examined crude pretreatment methods in order to allow for crude hydrolysate processing of the GA anion exchange isolation and SMB purification of neutral sugars steps. Various resins and activated carbon were examined for their decolourising ability and the impact they had on sugar concentrations. Marathon MSA was found to be capable of 83% decolourisation with minimal sugar losses; however, long contact times were required. Activated carbon was found to be capable of more effective and rapid decolourisation (97% in 10 min), however, 15% of the Ara was irretrievably lost. While a large amount of the coloured contaminants were removed in this decolourised crude hydrolysate, it did not allow for subsequent GA isolation and additional pretreatment may be required. After the removal of GA from a synthetic crude mixture using anion exchange, the remaining neutral sugars were run on an SMB with comparable performance to the synthetic neutral mixture used in Chapter 5, indicating that the SMB separation performance is not affected by the anion exchange step.

The most direct comparisons of these processes would be to a batch chromatography system for SMB, and a liquid-liquid extractor such as a Podbielniak contactor for the CPC. Batch chromatography does not look practical for these monosaccharide separations due to the poor separation efficiency and resolutions achieved in Section 5.2. To compete with the throughput of SMB (4.6 g L^{-1} h^{-1}), a single 20 mL column (as in Section 5.2)) would be required to process 92 mg h^{-1}. Assuming a run time of 10 minutes, the mass loading required becomes 15.3 mg per injection (or ~0.9 mL at the feed concentration used for SMB). The chromatograms in Section 5.2 show the separation performance based on sample injections of 0.1 mL is poor, indicating that purities and recoveries would be far from those achieved in SMB even with a much reduced sample volume. While adjusting the column geometry may provide improved

separation performance, it is unlikely that it would be able to overcome the shortcomings in purity, recovery and throughput when operated in batch mode.

Countercurrent extractors such as the Podbielniak contactor may be a useful addition to the process but are unlikely to be able to compete with CPC as they act as a traditional liquid-liquid extraction process. The difficulties associated with the highly hydrophilic nature of the target monosaccharides make an extraction of targets into different phases difficult except as a potential prepurification step to remove less hydrophilic impurities from the crude.

With over 8 million tonnes of sugar beet grown in the UK each year, giving approximately 448,000 tonnes of dried sugar beet pulp [237], supply of SBP would likely outstrip the demand for value added products . Processing 1 % of the dried SBP would give a total of 4,480 tonnes per year, or 13.6 tonnes per day based on a 330 day operating year. Ignoring the impact of any pre-processing, estimates were made for the operating scales required to process 13.6 tonnes of dried sugar beet pulp per day.

Based on a total monosaccharides throughput of 4.6 g L^{-1}_{resin} h^{-1} for a 3-zone SMB from Chapter 5, 1 tonne per day would require a total volume of ~9 m^3 (~1.1 m^3 per column). To reach an operating throughput of 13.6 tonnes per day would thus require a total volume of ~123 m^3 (15.4 m^3 per column). While SMB is almost unhindered by scale considerations, the current generation of CPC machines have a maximum working volume of 50 L [238]. Working with a total dissolved solids throughput of 9.4 g L^{-1} h^{-1} (Chapter 4) would give a total throughput of ~11.3 kg per day. To process 13.6 tonnes per day would thus require ~1206 machines. While this ignores any potential benefits that may be achieved by scaling up further to these machines (Appendix B), it is clear that with the current generation of CPC machines, a fleet of machines would be required in order to process this quantity of material reducing the practicality relative to SMB.

However, if a smaller amount of material was required, CPC may become more desirable. To match the throughput of a single 50 L CPC a much smaller SMB would be required (~12.7 L per column), however, the operational complexities of operating

an SMB would remain and may make the process less favourable at a smaller scale. Therefore, CPC may prove to be a simpler and more robust option at smaller scales.

Process purities are also an important factor to consider. Current generation CPC may struggle to dramatically increase the purity of Ara from 84% to >95% without compromising on process throughput. SMB on the other hand could conceivably purify Ara to >99% purity with additional optimisation and without applying significant constraints to throughput. As a result, the purity requirements of further processes would play a major role in process selection and SMB may be able to provide higher purities.

In summary, both CPC and SMB have been established as potential scalable separation methods for the isolation of monosaccharides from crude hydrolysates in a biorefinery context. CPC has been developed as a novel separation technology for preparative biorefinery separations and has been shown to allow separation of the crude hydrolysate in a single step, isolating multiple fractions to high purity. However, additional aspects still need to be considered such as additional scale-up to industrial scales, as well as potential limits to scalability, and phase system recycling. On the other hand, SMB is a more established technology for large scale separations with potential for high throughput, high purity separations and has fewer scalability problems. However, SMB is operationally complex and requires a multistep process, with pretreatment and isolation of the D-galacturonic acid prior to SMB separation, and further work is needed on these aspects to establish a complete crude processing option.

7.2 Future work

7.2.1 CPC separations

The CPC method developed in Chapter 3 and Chapter 4 allows for direct separation of the crude hydrolysate with no prior pretreatment or additional processing. However, while the final sugar fractions are isolated from the coloured contaminants, they contain ethanol and ammonium sulphate from the phase system. The extrusion step, used to rapidly elute the GA fraction, uses a higher concentration of ammonium sulphate, but a lower concentration of ethanol. Future work will need to examine

methods for demineralisation of the collected fractions to remove the ammonium sulphate and drying to remove the ethanol. Demineralisation could be performed by passing the fractions through a sequence of anion and cation exchange columns (in the OH^- and H^+ forms respectively) [142][239]. GA would likely bind to any demineralisation column (as seen by the anion exchange behaviour in Chapter 6) and so may require selective elution to obtain a pure GA sample. These demineralisation problems would also be an issue for both fractions of the GA isolation: the neutral sugars fraction, containing acetate exchanged off the column; and the GA, containing acetate from the elution step.

During the demineralisation steps, particularly for the CPC fractions, it may be possible to recover a large proportion of the ammonium sulphate during regeneration of the demineralisation columns, however, the presence of any other salts in the crude may complicate this. Recovery of the ethanol may also be possible during the drying steps, particularly due to the presence of existing bioethanol facilities at sugar beet refineries such Wissington.

7.2.2 CPC Scale-up

CPC scale-up has been demonstrated successfully in Chapter 4 without detriment to separation performance. However, the scale-up was performed on similar size equipment with a similar rotor geometry. In order to scale-up significantly from here, larger equipment can adopt new rotor geometries, allowing for retention of the stationary phase without significant increases in hydrostatic pressure. Appendix B contains a preliminary experimental study on the scale up of a model synthetic mixture to a 2 L RotaChrom CPC which is capable of operating 50 L columns. Additional development of the method will be required in transferring to this new type of equipment. In a more general sense, further scale-up of CPC is dependent on innovations by equipment manufacturers for industrial scale machines, which are beginning to enter the market.

7.2.3 SMB optimisation

In Chapter 5, the equilibrium theory model did not accurately predict the SMB separation results (Table 5-13), with all of the compounds eluting in the extract, and

optimisation was performed purely experimentally. Future work should focus on understanding why the equilibrium theory model failed, such that it could be used for additional optimisation and developing scale up models. Further experimental optimisation could also be performed, aimed at further improving Ara purity or recovery, or feed flow rates in both the 4-zone, closed loop SMB and the 3-zone open loop SMB.

Furthermore, longer columns could be explored for the SMB using the Monosphere 99 Ca/320 resin. Longer columns provide higher Stanton numbers which reduce peak tailing, which could allow the superior retention factors of this resin to be effective. However, this may be hardware limited, as longer columns would require increased flow rates, and the SMB pumps are limited to a maximum of 12 mL min^{-1}.

In addition, when scaling up, it may be necessary to use a column with a larger mesh size (such as the Dowex 50W X8 resin at 16-50 mesh, or the Monosphere 99 Ca/320 resin) in order to prevent excessive backpressure in an SMB system. The long term effects on the resin lifetime and separation performance should also be examined.

7.2.4 Sequential multicolumn chromatography

In Chapter 7 a sequential multicolumn chromatography process is proposed for the continuous isolation of GA from neutral sugars and should be tested experimentally. It could also be further improved by reducing the number of columns from 4 to 3 by utilising the length of the mass transfer zone in the column length, reducing the amount of resin required.

7.2.5 Decolourisation

In Chapter 7 it was shown that activated carbon was highly effective at rapidly decolourising the crude hydrolysate, but did remove 15% of the Ara. Future work could look at alternative activated carbons, and the effects of temperature and pH as well as additional studies into the carbon loading and contact time in order to reduce the losses of Ara. While decolourisation was not examined at volumes higher than 50 mL of crude per batch, suitable scale-up methods may also need to be examined to increase the scale further.

Resins may be beneficial due to their simple regeneration and it may be useful to use multiple resins in series to improve the decolourisation, however, the required contact time was the primary issue and would need to be dramatically improved for resin decolourisation to be feasible. Additionally, resin lifetime and reductions in capacity would need to be examined.

7.2.6 Additional pretreatment and crude processing

It was also seen in Chapter 7 that the GA isolation method using anion exchange chromatography was not successfully transferred from the synthetic crude mixture to the decolourised crude hydrolysate. Future work should focus on additional pretreatment methods, looking at reducing the salt concentrations without affecting the sugars.

It could also be useful to examine whether the pretreatment processes developed for reducing the coloured contaminants and the salts could be used to improve the throughput of the CPC methods. Synthetic separations in Chapter 3 were successful with sugar concentrations as high as 100 g L^{-1} and, removing contaminants could allow for concentration of the crude from ~20 g L^{-1} to closer to 100 g L^{-1}.

7.2.7 Process route selection

After the process optimisation and further scale-up options described in this future work section, it will be important to compare the two main process options: CPC or SMB. This could be performed based on mathematical process modelling of the two routes, incorporating capital expenditure, operating costs, throughput requirements and the potential value of the isolated monosaccharides. The analysis would allow for a costed decision on which technology would be most suited for biorefinery applications of sugar beet pulp pectin.

Appendix A HPLC and ICS chromatograms

Calibration curves for analytical HPLC and ICS methods were performed daily in order to ensure accurate concentration calculations due to some variations in retention times over multiple sample injections. All chromatograms in this section were performed as described in Section. Example calibrations and example separations are shown in this Appendix, with a list shown in Table A-1.

Table A-1: List of chromatograms and calibration curves shown in this Appendix for HPLC-RI and ICS analyses.

System	Separation/calibration	Figure
HPLC-RI	Retention times of all sugars	Figure A-1
HPLC-RI	Calibration of all sugars	Figure A-2
HPLC-RI	Lower phase and upper phase composition	Figure A-3
HPLC-RI	Calibration of Ethanol and DMSO	Figure A-4
ICS	Neutral sugars calibration on CarboPac PA1	Figure A-5
ICS	GA calibration on CarboPac PA1	Figure A-6
ICS	GA separation on CarboPac PA1	Figure A-7
ICS	Neutral sugars calibration on AminoPac PA10	Figure A-8
ICS	Neutral sugars separation on AminoPac PA10	Figure A-9
ICS	GA separation on AminoPac PA10	Figure A-10
ICS	Neutral sugars calibration on AminoPac PA10	Figure A-11
ICS	GA calibration on AminoPac PA10	Figure A-12

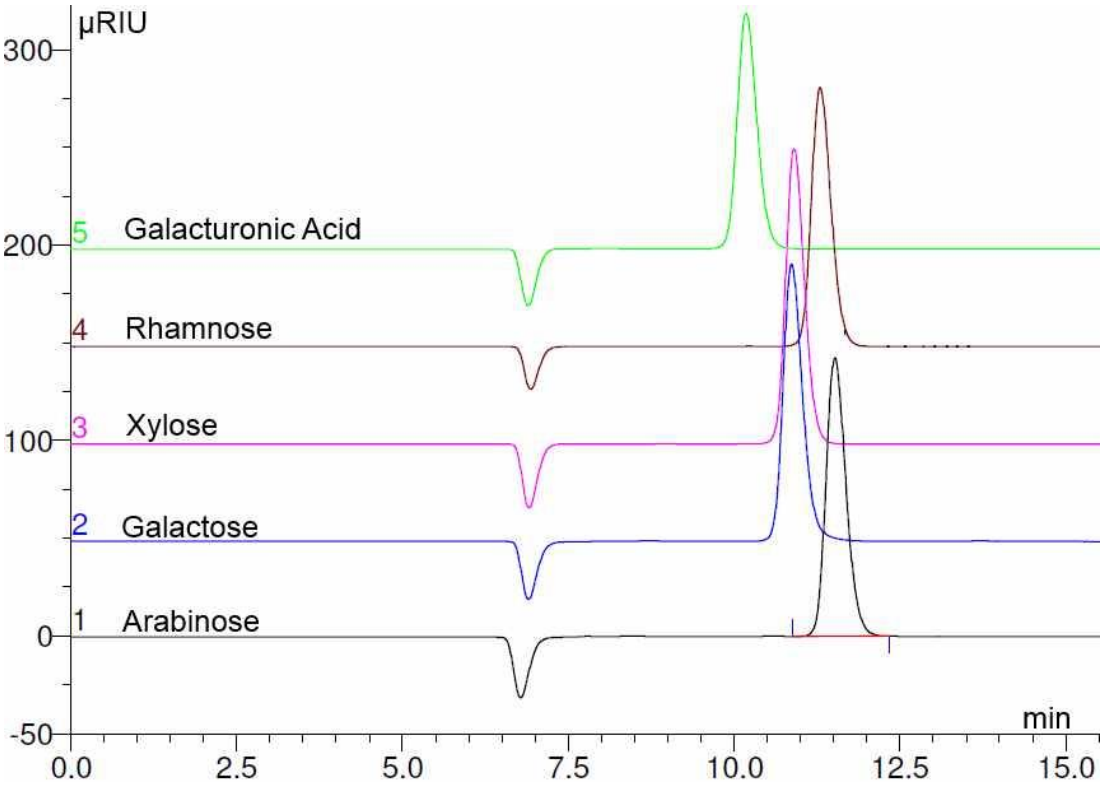

Figure A-1: Example HPLC-RI analysis of the sugars D-galacturonic acid, L-rhamnose, D-galactose and L-arabinose. The analytical methods used are detailed in Section 2.8.1.

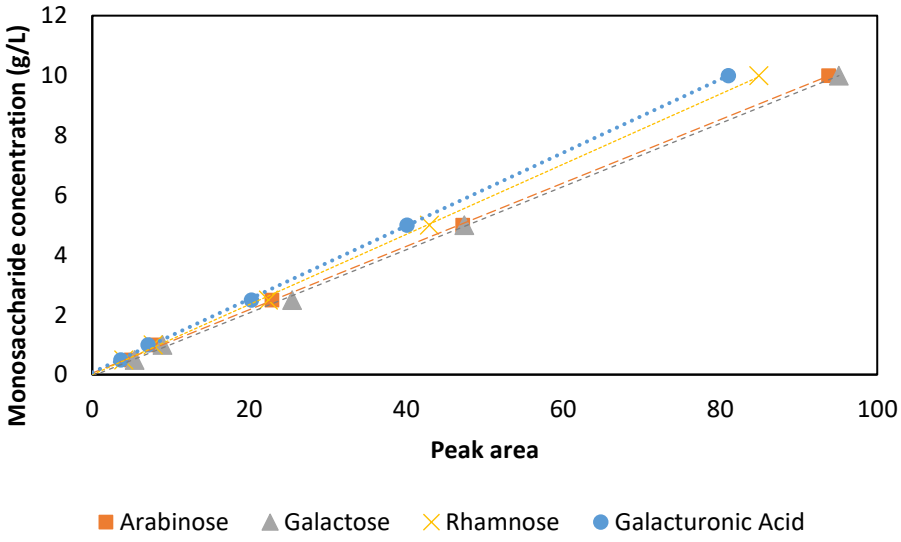

Figure A-2: Example HPLC-RI calibration curves of the sugars Ara, Gal, Rha and GA. The analytical methods used are detailed in Section 2.8.1.

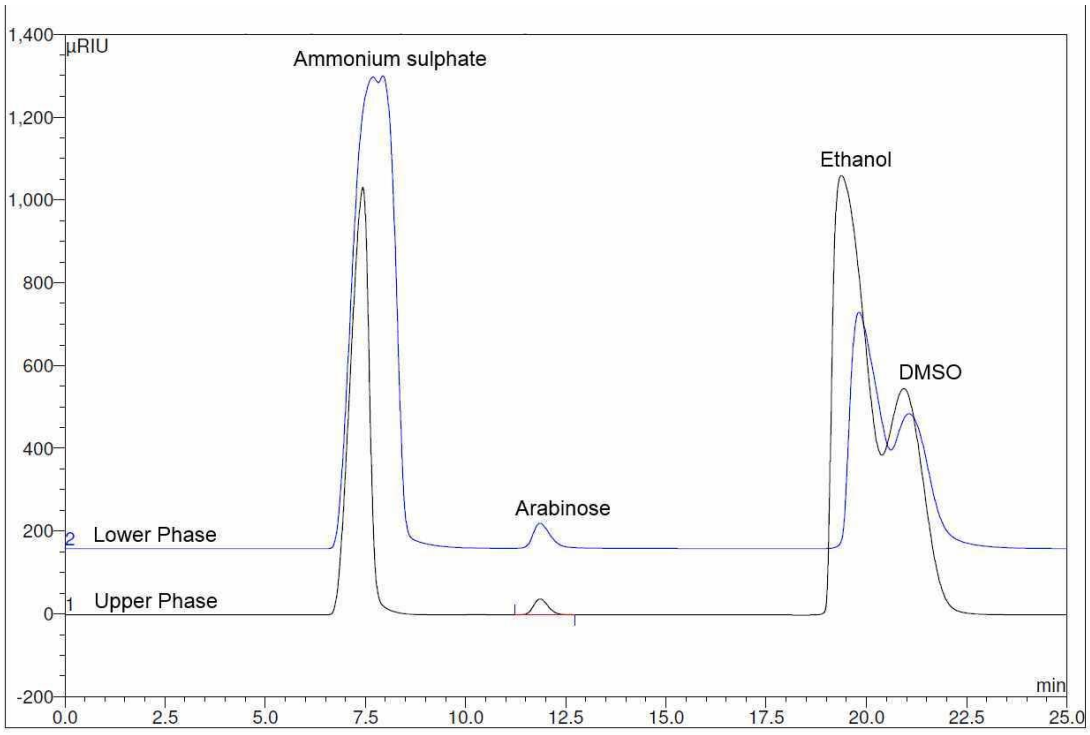

Figure A-3: HPLC-RI analysis of the upper phase and lower phase of the phase system ethanol : DMSO : ammonium sulphate (300 g L^{-1}) (0.8:0.1:1.8) showing peaks for ammonium sulphate, Ara, ethanol and DMSO. The analytical methods used are detailed in Section 2.8.1.

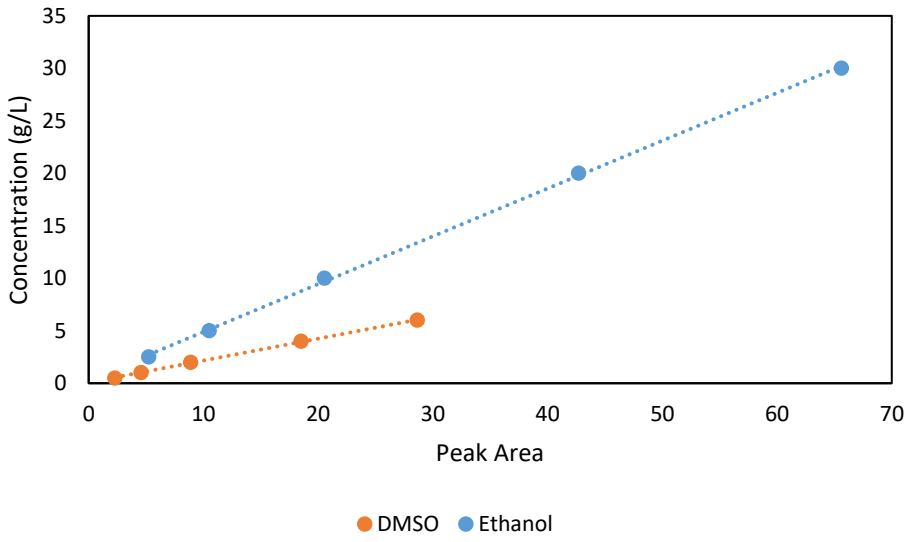

Figure A-4: Example HPLC-RI calibration curves of the ethanol and DMSO. The analytical methods used are detailed in Section 2.8.1.

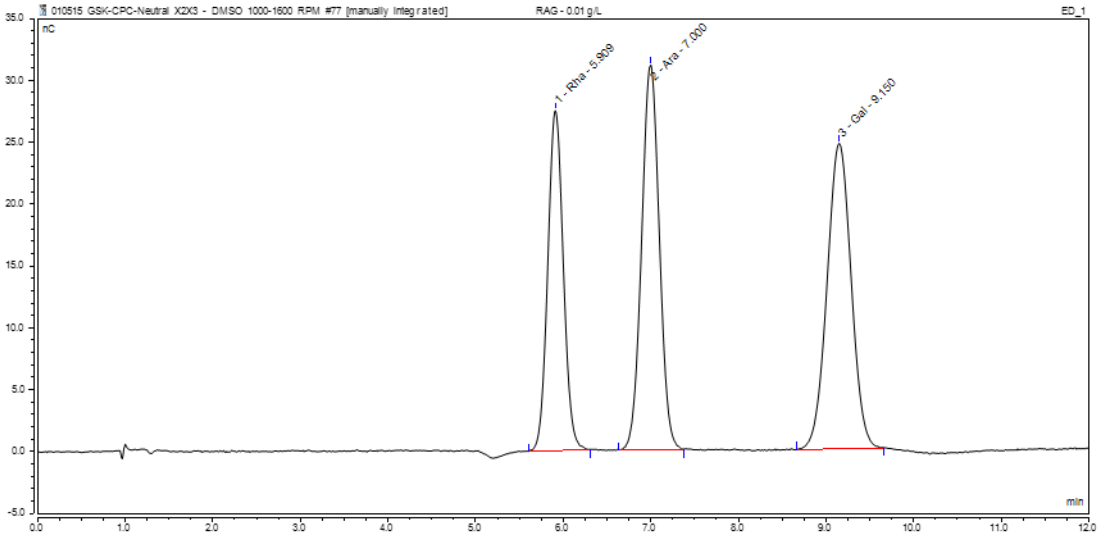

Figure A-5: ICS calibration of neutral sugar standards (Rha, Ara and Gal) on the CarboPac PA1 column using 15 mM NaOH. The analytical methods used are detailed in Section 2.8.3.

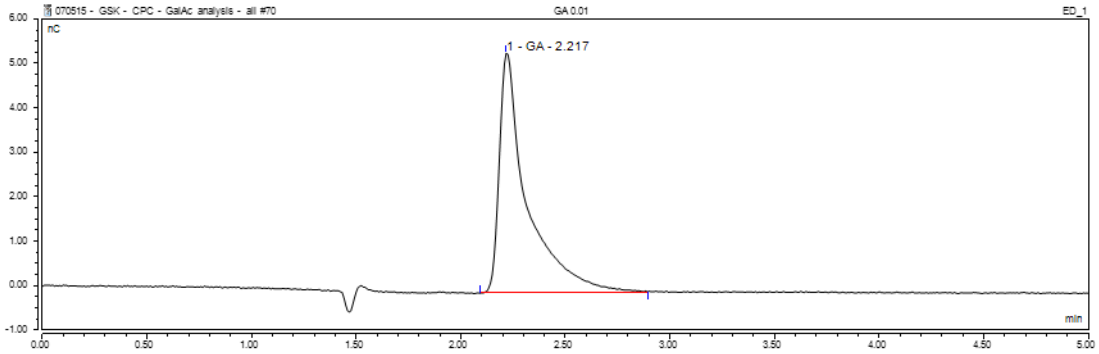

Figure A-6: ICS calibration of GA on the CarboPac PA1 column, using 250 mM NaOAc. The analytical methods used are detailed in Section 2.8.3.

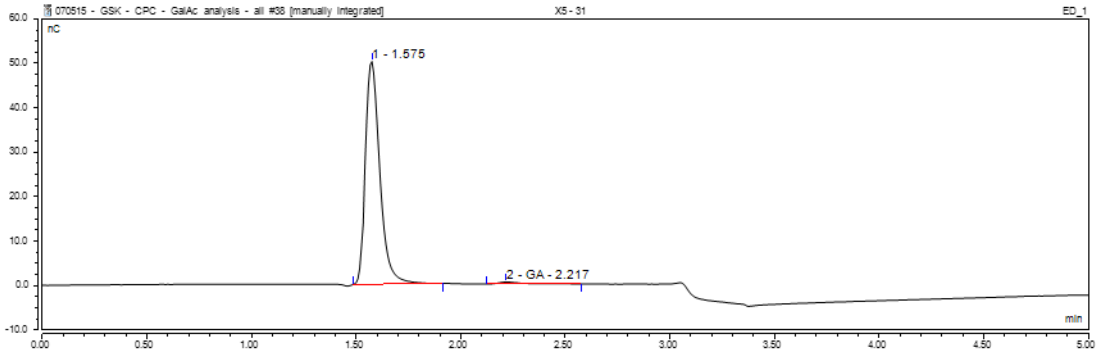

Figure A-7: Example ICS chromatogram showing the combined neutral sugars peak (1) and GA (2) on the CarboPac PA1 column, using 250 mM NaOAc. The analytical methods used are detailed in Section 2.8.3.

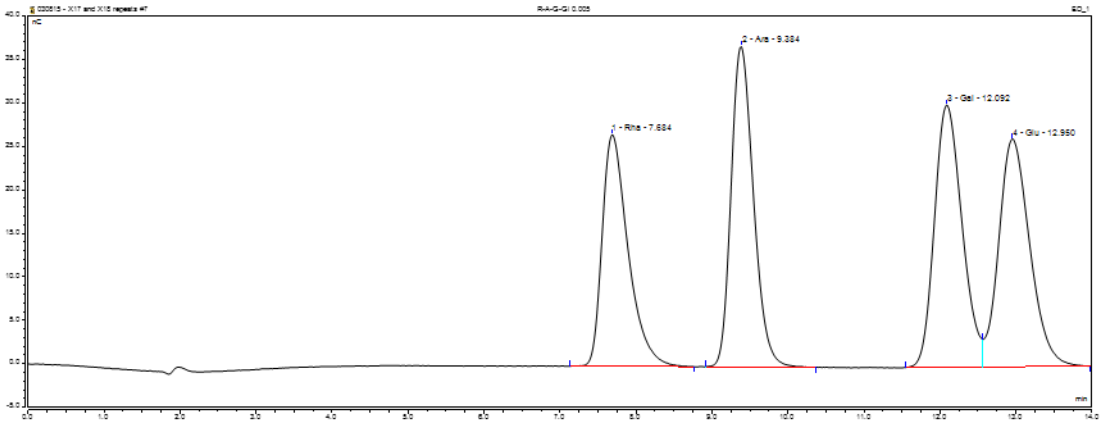

Figure A-8: ICS calibration of neutral sugars (Rha, Ara, Gal and Glu) using the AminoPac PA10 column with 7.5 mM NaOH. The analytical methods used are detailed in Section 2.8.3.

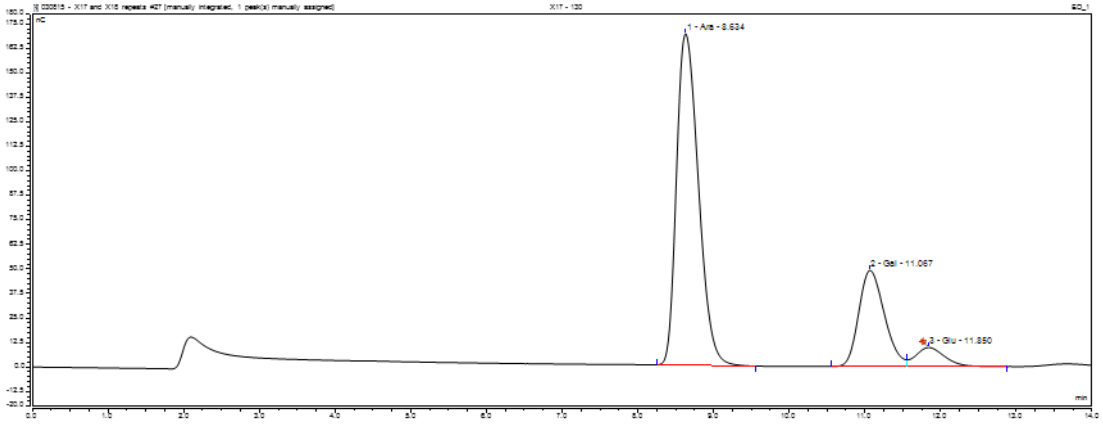

Figure A-9: Example ICS chromatogram showing neutral sugars (Ara, Gal, Glu) using the AminoPac PA10 column with 7.5 mM NaOH. The analytical methods used are detailed in Section 2.8.3.

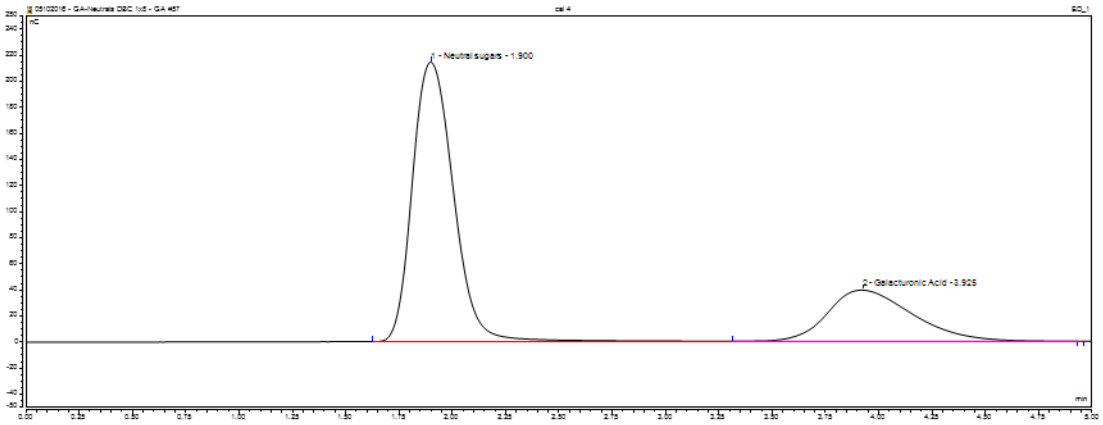

Figure A-10: Example ICS chromatogram showing the combined neutral sugars peak (1) and GA (2) on the AminoPac PA10 column, using 50 mM NaOAc. The analytical methods used are detailed in Section 2.8.3.

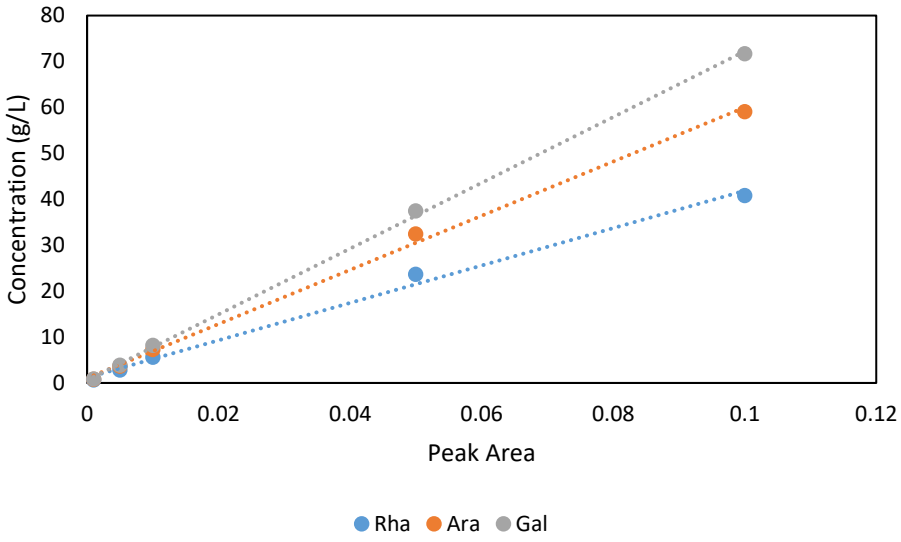

Figure A-11: Example ICS calibration curves of the sugars Rha, Ara and Gal performed on the AminoPac PA10 using the neutral sugars method. The analytical methods used are detailed in Section 2.8.3.

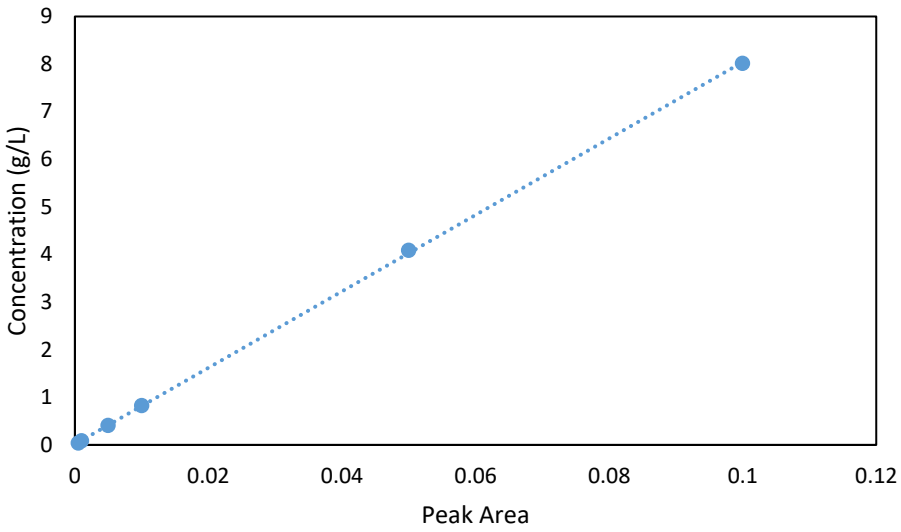

Figure A-12: Example ICS calibration curves of GA performed on the AminoPac PA10 using the GA method. The analytical methods used are detailed in Section 2.8.3.

Appendix B Industrial scale CPC

B.1 Introduction

Industrial scale CPC is generally limited by operating pressures which increase with increasing scale due to the hydrostatic nature of the devices. Laboratory preparative devices generally have a maximum column volume of 1 L and a new piece of equipment is required for larger scale systems. Kromaton offer two industrial scale CPC devices based on a similar operating principle to their laboratory scale CPC, utilising a scaled up version of the disks shown in Figure 1-6. These devices are available at 5 L and 18 L scales. An alternative to these devices has been developed by RotaChrom (Dabas, Hungary) utilising a novel cell design (Figure B-1) attached to a modular cell stack on the rotor (Figure B-2). This cell stack design allows for a variable number of cells to be used for the separation, allowing for adjustment of the column volume from 2 L to 50 L.

In this Appendix, the potential for larger scale CPC separations is examined on a 2 L RotaChrom rCPC, based on scale-up of the CPC separations performed in Chapter 3and Chapter 4.

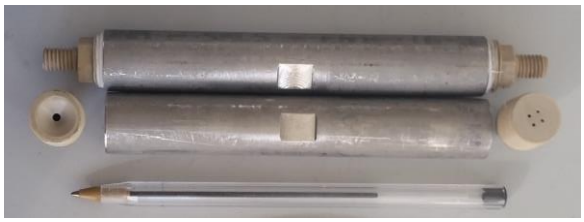

Figure B-1: Individual cells (~18.75 mL) for the RotaChrom CPC.

Figure B-2: RotaChrom rCPC with two cell stacks containing 32 cells each.

B.2 Materials and Methods

CPC separation was performed on a RotaChrom rCPC with a total volume of 2 L, 96 cells with a total cell volume of 1.8 L. The cells were set up in the ascending mode and a rotational speed of 450 rpm (RCF of 120 *g*) was used. An ethanol : aqueous ammonium sulphate (300 g L^{-1}) (0.8:1.8 v:v) phase system was used in the ascending mode, as in Chapter 3. A model synthetic mixture was prepared by dissolving the sugars in the LP (stationary phase) and consisted of: Rha, 1.3 g L^{-1}; Ara, 13.4 g L^{-1}; Gal 2.2 g L^{-1}; GA, 3.2 g L^{-1}; total dissolved sugars, 20.1 g L^{-1}. A 100 mL sample was injected directly onto the column with no prior equilibration at a flow rate of 200 mL min^{-1} (0.5 min).

The elution-extrusion mode (Section 1.2.7) was used with a flow rate of 150 mL min^{-1} throughout. The mobile phase (UP) flow began immediately after sample injection and extrusion was performed 36 min later. In the elution step, fractions were collected every 150 mL (1 min) with the first fraction collected 12 min after sample injection had finished. In the extrusion step, fractions were collected every 90 seconds (225 mL

fractions). Fractions were analysed on ICS using the AminoPac PA10 column as described in Section 2.8.

B.3 Results

The CPC separation was scaled up beyond the values given by a linear scale up. 950 mL to 2 L gives a scale-up factor of ~2.1. Thus, a flow rate 63.8 mL min^{-1} should have been used based on linear scale-up criteria. Instead, the flow rate was increased almost by a factor of 5 from 30.4 mL min^{-1} to 150 mL min^{-1}. Initial breakthrough occurred after 580 mL of elution, giving a stationary phase retention of 61% using Equation 2-3, with a V_C of 2000 mL, and a V_D of 200 mL. This is increased from a stationary phase retention of 50% on the preparative 1 L column in Chapter 4 (Table 4-8), indicating that the RotaChrom rCPC may have superior stationary phase retention in spite of the increased mobile phase flow rate.

The results, in Figure B-3, show good separation between the various solutes. The Rha peak eluted earlier than expected and so was not fully collected, however, it appears that the separation between Rha and Ara is comparable to that observed in the Kromaton CPC device on the preparative (950 mL) column (Figure 4-14). Additionally, the GA and Gal peaks are better separated from the Ara peak. This superior separation performance indicates that it may be possible to achieve an additional fraction with further optimisation, separating the sugars into four fractions from a single separation: Rha, Ara, Gal and GA. The increased stationary phase retention could be a key factor in the apparent improvement in separation performance, however, it is difficult to specifically link this due to the differences in cell design and geometry. Another caveat is that this separation was performed using a model synthetic mixture with a total sugars concentration of 20 g L^{-1}. Model synthetic mixture separations were performed previously in Chapter 3 and Chapter 4 using a sugars concentration of 100 g L^{-1} to match the total dissolved solids concentrations in the crude.

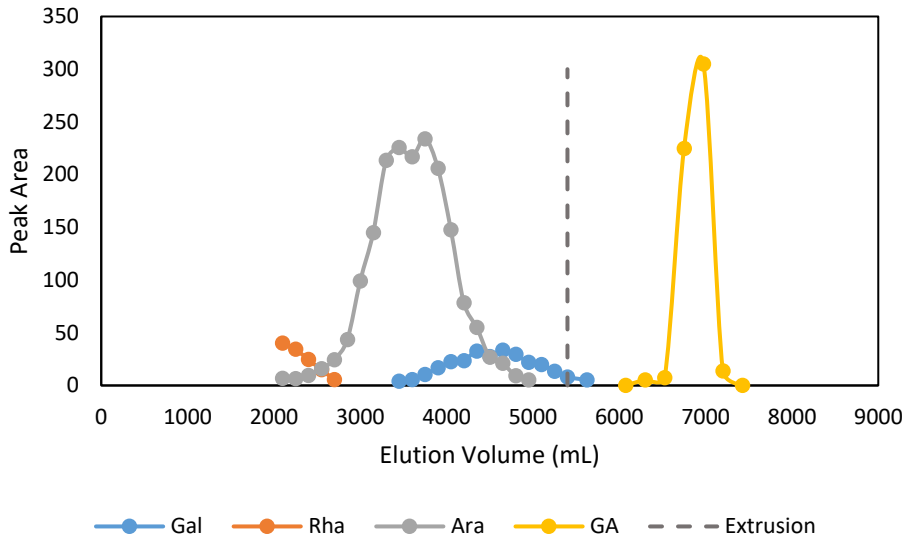

Figure B-3: CPC separation of a 100 mL model synthetic mixture sample performed on a 2 L RotaChrom rCPC column. A mobile phase flow rate of 150 mL min^{-1} was used. Extrusion was performed 36 min (5400 mL) after sample injection. Full experimental methods are described in Section B.2 in Appendix B.

Overall the separation performance appears to be superior at this larger scale, however, full quantification has not been performed and additional work needs to be performed to transfer the method to the crude hydrolysate and increase the sample loading to the levels seen in Chapter 4. Furthermore, the 2 L column is the minimum column volume that is achievable on the RotaChrom rCPC and the unique cell design allows for additional cells to be added to increase the total column volume while providing the potential for increased separation performance. Larger cells are also available on the industrial scale RotaChrom iCPC which has a potential column volume of 50 L. The work in this Appendix demonstrates the potential of these larger, industrially scalable machines

References

[1] H.J. Huang, S. Ramaswamy, Overview of biomass conversion processes and separation and purification technologies in biorefineries, in: Sep. Purif. Technol. Biorefineries, 2013: pp. 1–36. doi:10.1002/9781118493441.ch1.

[2] R. Kumar, S. Singh, O. V. Singh, Bioconversion of lignocellulosic biomass: biochemical and molecular perspectives, *J. Ind. Microbiol. Biotechnol.* 35

(2008) 377–391. doi:10.1007/s10295-008-0327-8.

[3] C.O. Tuck, E. Perez, I.T. Horvath, R.A. Sheldon, M. Poliakoff, Valorization of biomass: deriving more value from waste, *Science (80-.).* 337 (2012) 695–699. doi:10.1126/science.1218930.

[4] L. Wang, J. Littlewood, R.J. Murphy, Environmental sustainability of bioethanol production from wheat straw in the UK, *Renew. Sustain. Energy Rev.* 28 (2013) 715–725. doi:10.1016/j.rser.2013.08.031.

[5] B. Kamm, M. Kamm, Principles of biorefineries, *Appl. Microbiol. Biotechnol.* 64 (2004) 137–145. doi:10.1007/s00253-003-1537-7.

[6] Y. Zheng, C. Yu, Y.-S. Cheng, C. Lee, C.W. Simmons, T.M. Dooley, R. Zhang, B.M. Jenkins, J.S. VanderGheynst, Integrating sugar beet pulp storage, hydrolysis and fermentation for fuel ethanol production, *Appl. Energy*. 93 (2012) 168–175. doi:10.1016/j.apenergy.2011.12.084.

[7] V. Micard, C.M.G.C. Renard, J.F. Thibault, Enzymatic saccharification of sugar-beet pulp, *Enzyme Microb. Technol.* 19 (1996) 162–170. doi:10.1016/0141-0229(95)00224-3.

[8] P.T. Pienkos, M. Zhang, Role of pretreatment and conditioning processes on toxicity of lignocellulosic biomass hydrolysates, *Cellulose*. 16 (2009) 743–762. doi:10.1007/s10570-009-9309-x.

[9] Y. Zheng, Z. Pan, R. Zhang, Overview of biomass pretreatment for cellulosic ethanol production, *Int. J. Agric. Biol. Eng.* 2 (2009) 51–68. doi:10.3965/j.issn.1934-6344.2009.03.051-068.

[10] V.B. Agbor, N. Cicek, R. Sparling, A. Berlin, D.B. Levin, Biomass pretreatment: Fundamentals toward application, *Biotechnol. Adv.* 29 (2011) 675–685. doi:10.1016/j.biotechadv.2011.05.005.

[11] A.G.M. Leijdekkers, J.P.M. Bink, S. Geutjes, H.A. Schols, H. Gruppen,

Enzymatic saccharification of sugar beet pulp for the production of galacturonic acid and arabinose; a study on the impact of the formation of recalcitrant oligosaccharides, *Bioresour. Technol.* 128 (2013) 518–25. doi:10.1016/j.biortech.2012.10.126.

[12] M. Spagnuolo, Fractionation of sugar beet pulp into pectin, cellulose, and arabinose by arabinases combined with ultrafiltration, *Biotechnol. Bioeng.* 64 (1999) 685–691. doi:10.1002/(SICI)1097-0290(19990920)64:6<685::AID-BIT7>3.0.CO;2-E.

[13] H. Günan Yücel, Z. Aksu, Ethanol fermentation characteristics of *Pichia stipitis* yeast from sugar beet pulp hydrolysate: Use of new detoxification methods, *Fuel*. 158 (2015) 793–799. doi:10.1016/j.fuel.2015.06.016.

[14] S. Kühnel, H. a Schols, H. Gruppen, Aiming for the complete utilization of sugar-beet pulp: Examination of the effects of mild acid and hydrothermal pretreatment followed by enzymatic digestion, *Biotechnol. Biofuels*. 4 (2011) 14. doi:10.1186/1754-6834-4-14.

[15] Y. Zheng, C. Lee, C.W. Yu, Y.-S. Cheng, R.H. Zhang, B.M. Jenkins, J.S. VanderGheynst, Dilute acid pretreatment and fermentation of sugar beet pulp to ethanol, *Appl. Energy*. 105 (2013) 1–7. doi:10.1016/j.apenergy.2012.11.070.

[16] B. Foster, B. Dale, J. Doran-Peterson, Enzymatic hydrolysis of ammonia-treated sugar beet pulp, *Appl. Biochem. Biotechnol.* 91 (2001) 269–282.

[17] C. Hamley-Bennett, G.J. Lye, D.J. Leak, Selective fractionation of sugar beet pulp for release of fermentation and chemical feedstocks; optimisation of thermo-chemical pre-treatment, *Bioresour. Technol.* 209 (2016) 259–264. doi:10.1016/j.biortech.2016.02.131.

[18] P.E. Shaw, J.H. Tatum, R.E. Berry, Acid-catalyzed degradation of d-fructose, *Carbohydr. Res.* 5 (1967) 266–273. doi:10.1016/S0008-6215(00)80500-5.

[19] T. Popoff, O. Theander, Formation of aromatic compounds from carbohydrates.

Part 1. Reaction of D-glucuronic Acid, D-glacturonic Acid, D-xylose, and L-arabinose in slightly acidic, aqueous solution, *Carbohydr. Res.* 22 (1972) 135–149. doi:10.1016/S0008-6215(00)85733-X.

[20] T. Hofmann, Characterization of the most intense coloured compounds from Maillard reactions of pentoses by application of colour dilution analysis, *Carbohydr. Res.* 313 (1998) 203–213. doi:10.1016/S0008-6215(98)00279-1.

[21] M.A. Bornik, L.W. Kroh, D-galacturonic acid as a highly reactive compound in nonenzymatic browning. 1. Formation of browning active degradation products, *J. Agric. Food Chem.* 61 (2013) 3494–3500. doi:10.1021/jf303855s.

[22] S. Wegener, M.-A. Bornik, L.W. Kroh, D-Galacturonic acid: a highly reactive compound in nonenzymatic browning. 2. formation of amino-specific degradation products, *J. Agric. Food Chem.* 63 (2015) 6457–6465. doi:10.1021/acs.jafc.5b01121.

[23] S. Venkatesan, Adsorption, in: S. Ramaswamy, H.-J. Huang, B.V. Ramarao (Eds.), Sep. Purif. Technol. Biorefineries, Wiley, 2013: pp. 101–148. doi:10.1002/9781118493441.ch5.

[24] P. Richard, R. Verho, M. Putkonen, J. Londesborough, M. Penttilä, Production of ethanol from L-arabinose by *Saccharomyces cerevisiae* containing a fungal L-arabinose pathway, *FEMS Yeast Res.* 3 (2003) 185–189. doi:10.1016/S1567-1356(02)00184-8.

[25] M. Bettiga, O. Bengtsson, B. Hahn-Hägerdal, M.F. Gorwa-Grauslund, Arabinose and xylose fermentation by recombinant *Saccharomyces cerevisiae* expressing a fungal pentose utilization pathway., *Microb. Cell Fact.* 8 (2009) 40. doi:10.1186/1475-2859-8-40.

[26] F.M. Gírio, C. Fonseca, F. Carvalheiro, L.C. Duarte, S. Marques, R. Bogel-Łukasik, Hemicelluloses for fuel ethanol: A review, *Bioresour. Technol.* 101 (2010) 4775–4800. doi:10.1016/j.biortech.2010.01.088.

[27] J.B. Doran, J. Cripe, M. Sutton, B. Foster, Fermentations of pectin-rich biomass with recombinant bacteria to produce fuel ethanol, *Appl. Biochem. Biotechnol.* 84–86 (2000) 141–152. doi:10.1385/ABAB:84-86:1-9:141.

[28] T. Werpy, G. Petersen, Top value added chemicals from biomass: volume I - results of screening for potential candidates from sugars and synthesis gas, Office of Scientific and Technical Information (OSTI), (2004). doi:10.2172/15008859.

[29] H. Zhang, X. Li, X. Su, E.L. Ang, Y. Zhang, H. Zhao, Production of Adipic Acid from Sugar Beet Residue by Combined Biological and Chemical Catalysis, *ChemCatChem*. 8 (2016) 1500–1506. doi:10.1002/cctc.201600069.

[30] M.R. Borges, R.D.C. Balaban, L-Arabinose (pyranose and furanose rings)-branched poly(vinyl alcohol): enzymatic synthesis of the sugar esters followed by free radical polymerization, *J. Biotechnol.* 192 (2014) 42–49. doi:10.1016/j.jbiotec.2014.10.005.

[31] F. Subrizi, M. Cárdenas-Fernández, G.J. Lye, J.M. Ward, P.A. Dalby, T.D. Sheppard, H.C. Hailes, Transketolase catalysed upgrading of L-arabinose: the one-step stereoselective synthesis of L-gluco-heptulose, *Green Chem.* 18 (2016) 3158–3165. doi:10.1039/C5GC02660A.

[32] C. DeAmicis, N. a Edwards, M.B. Giles, G.H. Harris, P. Hewitson, L. Janaway, S. Ignatova, Comparison of preparative reversed phase liquid chromatography and countercurrent chromatography for the kilogram scale purification of crude spinetoram insecticide, *J. Chromatogr. A.* 1218 (2011) 6122–7. doi:10.1016/j.chroma.2011.06.073.

[33] W.D. Conway, Counter-current chromatography, *J. Chromatogr. A.* 538 (1991) 27–35. doi:10.1016/S0021-9673(01)91618-8.

[34] I.A. Sutherland, D. Hawes, S. Ignatova, L. Janaway, P. Wood, Review of progress toward the industrial scale-up of CCC, *J. Liq. Chromatogr. Relat. Technol.* 28 (2005) 1877–1891. doi:10.1081/JLC-200063521.

[35] G.F. Pauli, S.M. Pro, J.B. Friesen, Countercurrent separation of natural products, *J. Nat. Prod.* 71 (2008) 1489–1508.

[36] Y. Pan, Y. Lu, Recent progress in countercurrent chromatography, *J. Liq. Chromatogr. Relat. Technol.* 30 (2007) 649–679. doi:10.1080/10826070701190948.

[37] Y. Ito, Golden rules and pitfalls in selecting optimum conditions for high-speed counter-current chromatography, *J. Chromatogr. A.* 1065 (2005) 145–168. doi:10.1016/j.chroma.2004.12.044.

[38] Y. Ito, R. Bhatnagar, Preparative counter-current chromatography with a rotating coil assembly, *J. Chromatogr. A.* 207 (1981) 171–180. doi:10.1016/S0021-9673(00)89929-X.

[39] Y.H. Guan, R. van den Heuvel, Y.-P. Zhuang, Visualisation of J-type counter-current chromatography: a route to understand hydrodynamic phase distribution and retention, *J. Chromatogr. A.* 1239 (2012) 10–21. doi:10.1016/j.chroma.2012.03.039.

[40] P. Wood, Critical beta-values of all coil planet centrifuges, *J. Chromatogr. A.* 1217 (2010) 1283–92. doi:10.1016/j.chroma.2009.12.038.

[41] Y.H. Guan, R. van den Heuvel, The three-dimensional model for helical columns on type-J synchronous counter-current chromatography, *J. Chromatogr. A.* 1218 (2011) 5108–14. doi:10.1016/j.chroma.2011.05.078.

[42] C. Schwienheer, J. Merz, G. Schembecker, Investigation, comparison and design of chambers used in centrifugal partition chromatography on the basis of flow pattern and separation experiments, *J. Chromatogr. A.* 1390 (2015) 39–49. doi:10.1016/j.chroma.2015.01.085.

[43] I.A. Sutherland, Recent progress on the industrial scale-up of counter-current chromatography, *J. Chromatogr. A.* 1151 (2007) 6–13. doi:10.1016/j.chroma.2007.01.143.

[44] A. Berthod, T. Maryutina, B. Spivakov, O. Shpigun, I.A. Sutherland, Countercurrent chromatography in analytical chemistry (IUPAC Technical Report), *Pure Appl. Chem.* 81 (2009) 355–387. doi:10.1351/PAC-REP-08-06-05.

[45] K. Faure, E. Bouju, P. Suchet, A. Berthod, Use of limonene in countercurrent chromatography: a green alkane substitute, *Anal. Chem.* 85 (2013) 4644–50. doi:10.1021/ac4002854.

[46] J.B. Friesen, J.B. McAlpine, S.N. Chen, G.F. Pauli, Countercurrent separation of natural products: an update, *J. Nat. Prod.* 78 (2015) 1765–1796. doi:10.1021/np501065h.

[47] I. Garrard, Simple approach to the development of a CCC solvent selection protocol suitable for automation, *J. Liq. Chromatogr. Relat. Technol.* 28 (2005) 1923–1935. doi:10.1081/JLC-200063571.

[48] A.P. Foucault, L. Chevolot, Counter-current chromatography: instrumentation, solvent selection and some recent applications to natural product purification, *J. Chromatogr. A.* 808 (1998) 3–22. doi:10.1016/S0021-9673(98)00121-6.

[49] Q.-B. Han, L. Wong, N.-Y. Yang, J.-Z. Song, C.-F. Qiao, H. Yiu, Y. Ito, H.-X. Xu, A simple method to optimize the HSCCC two-phase solvent system by predicting the partition coefficient for target compound, *J. Sep. Sci.* 31 (2008) 1189–94. doi:10.1002/jssc.200700582.

[50] J.B. Friesen, G.F. Pauli, G.U.E.S.S. — A generally useful estimate of solvent systems for CCC, *J. Liq. Chromatogr. Relat. Technol.* 28 (2005) 2777–2806. doi:10.1080/10826070500225234.

[51] A. Berthod, S. Carda-Broch, Determination of liquid–liquid partition coefficients by separation methods, *J. Chromatogr. A.* 1037 (2004) 3–14. doi:10.1016/j.chroma.2004.01.001.

[52] S. Adelmann, G. Schembecker, Influence of physical properties and operating

parameters on hydrodynamics in centrifugal partition chromatography, *J. Chromatogr. A.* 1218 (2011) 5401–5413. doi:10.1016/j.chroma.2011.01.064.

[53] S. Adelmann, T. Baldhoff, B. Koepcke, G. Schembecker, Selection of operating parameters on the basis of hydrodynamics in centrifugal partition chromatography for the purification of nybomycin derivatives, *J. Chromatogr. A.* 1274 (2013) 54–64. doi:10.1016/j.chroma.2012.11.031.

[54] A. Berthod, Countercurrent chromatography and the journal of liquid chromatography: A love story, *J. Liq. Chromatogr. Relat. Technol.* 30 (2007) 1447–1463. doi:10.1080/10826070701277067.

[55] P. Wood, D. Hawes, L. Janaway, I.A. Sutherland, Stationary phase retention in CCC: modelling the J-type centrifuge as a constant pressure drop pump, *J. Liq. Chromatogr. Relat. Technol.* 26 (2003) 1373–1396. doi:10.1081/JLC-120021256.

[56] N. Fumat, A. Berthod, K. Faure, Effect of operating parameters on a centrifugal partition chromatography separation, *J. Chromatogr. A.* 1474 (2016) 47–58. doi:10.1016/j.chroma.2016.10.014.

[57] L.-J. Chen, D.E. Games, J. Jones, Isolation and identification of four flavonoid constituents from the seeds of Oroxylum indicum by high-speed counter-current chromatography, *J. Chromatogr. A.* 988 (2003) 95–105. doi:10.1016/S0021-9673(02)01954-4.

[58] J. Shi, G. Li, H. Wang, J. Zheng, Y. Suo, J. You, Y. Liu, One-step separation of three flavonoids from *Poacynum hendersonii* by high-speed counter-current chromatography., *Phytochem. Anal.* 22 (2011) 450–4. doi:10.1002/pca.1301.

[59] J.B. Friesen, G.F. Pauli, Rational development of solvent system families in counter-current chromatography, *J. Chromatogr. A.* 1151 (2007) 51–9. doi:10.1016/j.chroma.2007.01.126.

[60] F.D.N. Costa, G.G. Leitão, Strategies of solvent system selection for the

isolation of flavonoids by countercurrent chromatography, *J. Sep. Sci.* 33 (2010) 336–47. doi:10.1002/jssc.200900632.

[61] E. Hopmann, W. Arlt, M. Minceva, Solvent system selection in counter-current chromatography using conductor-like screening model for real solvents., *J. Chromatogr. A.* 1218 (2011) 242–50. doi:10.1016/j.chroma.2010.11.018.

[62] E. Hopmann, A. Frey, M. Minceva, A priori selection of the mobile and stationary phase in centrifugal partition chromatography and counter-current chromatography, *J. Chromatogr. A.* 1238 (2012) 68–76. doi:10.1016/j.chroma.2012.03.035.

[63] J.B. Friesen, S. Ahmed, G.F. Pauli, Qualitative and quantitative evaluation of solvent systems for countercurrent separation, *J. Chromatogr. A.* 1377 (2015) 55–63. doi:10.1016/j.chroma.2014.11.085.

[64] M. Iqbal, Y. Tao, S. Xie, Y. Zhu, D. Chen, X. Wang, L. Huang, D. Peng, A. Sattar, M.A.B. Shabbir, H.I. Hussain, S. Ahmed, Z. Yuan, Aqueous two-phase system (ATPS): an overview and advances in its applications, *Biol. Proced. Online*. 18 (2016) 18. doi:10.1186/s12575-016-0048-8.

[65] S. Raja, V.R. Murty, V. Thivaharan, V. Rajasekar, V. Ramesh, Aqueous two phase systems for the recovery of biomolecules – a review, *Sci. Technol.* 1 (2012) 7–16. doi:10.5923/j.scit.20110101.02.

[66] C.-W. Shen, T. Yu, Protein separation and enrichment by counter-current chromatography using reverse micelle solvent systems., *J. Chromatogr. A.* 1151 (2007) 164–168. doi:10.1016/j.chroma.2007.01.079.

[67] Y.H. Guan, E.C. Bourton, P. Hewitson, I.A. Sutherland, D. Fisher, The importance of column design for protein separation using aqueous two-phase systems on J-type countercurrent chromatography, *Sep. Purif. Technol.* 65 (2009) 79–85. doi:10.1016/j.seppur.2008.07.016.

[68] C. Schwienheer, J. Merz, G. Schembecker, Selection and use of poly ethylene

glycol and phosphate based aqueous two-phase systems for the separation of proteins by centrifugal partition chromatography, *J. Liq. Chromatogr. Relat. Technol.* 38 (2015) 929–941. doi:10.1080/10826076.2014.951765.

[69] Y. Shibusawa, Y. Ito, Protein separation with aqueous-aqueous polymer systems by two types of counter-current chromatographs, *J. Chromatogr. A.* 550 (1991) 695–704. doi:10.1016/S0021-9673(01)88575-7.

[70] I.A. Sutherland, G. Audo, E. Bourton, F. Couillard, D. Fisher, I. Garrard, P. Hewitson, O. Intes, Rapid linear scale-up of a protein separation by centrifugal partition chromatography, *J. Chromatogr. A.* 1190 (2008) 57–62. doi:10.1016/j.chroma.2008.02.092.

[71] M.J. Ruiz-Angel, V. Pino, S. Carda-Broch, A. Berthod, Solvent systems for countercurrent chromatography: an aqueous two phase liquid system based on a room temperature ionic liquid, *J. Chromatogr. A.* 1151 (2007) 65–73. doi:10.1016/j.chroma.2006.11.072.

[72] Y. Wang, Y. Liu, J. Han, S. Hu, Application of water-miscible alcohol-based aqueous two-phase systems for extraction of dyes, *Sep. Sci. Technol.* 46 (2011) 1283–1288. doi:10.1080/01496395.2010.551168.

[73] Z. Li, H. Teng, Z. Xiu, Aqueous two-phase extraction of 2,3-butanediol from fermentation broths using an ethanol/ammonium sulfate system, *Process Biochem.* 45 (2010) 731–737. doi:10.1016/j.procbio.2010.01.011.

[74] K. Shinomiya, Y. Ito, Countercurrent chromatographic separation of biotic compounds with extremely hydrophilic organic-aqueous two-phase solvent systems and organic-aqueous three-phase solvent systems, *J. Liq. Chromatogr. Relat. Technol.* 29 (2006) 733–750. doi:10.1080/10826070500509298.

[75] J. Fahey, K. Wade, Separation and purification of glucosinolates from crude plant homogenates by high-speed counter-current chromatography, *J. Chromatogr. A.* 996 (2003) 85–93. doi:10.1016/S0021-9673(03)00607-1.

[76] B. Pinel, G. Audo, S. Mallet, M. Lavault, F.D.L. Poype, D. Séraphin, P. Richomme, Multi-grams scale purification of xanthanolides from *Xanthium macrocarpum*. Centrifugal partition chromatography versus silica gel chromatography, *J. Chromatogr. A.* 1151 (2007) 14–19. doi:10.1016/j.chroma.2007.02.115.

[77] M. Hamzaoui, J. Hubert, J. Hadj-Salem, B. Richard, D. Harakat, L. Marchal, A. Foucault, C. Lavaud, J.-H. Renault, Intensified extraction of ionized natural products by ion pair centrifugal partition extraction, *J. Chromatogr. A.* 1218 (2011) 5254–62. doi:10.1016/j.chroma.2011.06.018.

[78] A. Spórna-Kucab, S. Ignatova, I. Garrard, S. Wybraniec, Versatile solvent systems for the separation of betalains from processed *Beta vulgaris L.* juice using counter-current chromatography, *J. Chromatogr. B.* 941 (2013) 54–61. doi:10.1016/j.jchromb.2013.10.001.

[79] J. Hubert, N. Borie, S. Chollet, J. Perret, C. Barbet-Massin, M. Berger, J. Daydé, J.-H. Renault, Intensified separation of steviol glycosides from a crude aqueous extract of *Stevia rebaudiana* leaves using centrifugal partition chromatography, *Planta Med.* 81 (2015) 1614–1620. doi:10.1055/s-0035-1545840.

[80] K.D. Yoon, Y.-W. Chin, J. Kim, Centrifugal partition chromatography: application to natural products in 1994-2009, *J. Liq. Chromatogr. Relat. Technol.* 33 (2010) 1208–1254. doi:10.1080/10826076.2010.484374.

[81] Y. Ito, E. Kitazume, M. Bhatnagar, F. Trimble, Cross-axis synchronous flow-through coil planet centrifuge (type XLL): I. Design of the apparatus and studies on retention of stationary phase, *J. Chromatogr. A.* 538 (1991) 59–66. doi:10.1016/S0021-9673(01)91621-8.

[82] Y. Shibusawa, S. Iino, H. Shindo, Y. Ito, Separation of Chicken Egg White Proteins By High-Speed Countercurrent Chromatography, *J. Liq. Chromatogr. Relat. Technol.* 24 (2001) 2007–2016. doi:10.1081/JLC-100104442.

[83] I.A. Sutherland, Centrifugal liquid-liquid chromatography using aqueous two-

phase solvent (ATPS) systems: Its scale-up and prospects for the future production of high-value biologics, *Curr. Opin. Drug Discov. Devel.* 10 (2007) 540–549.

[84] I.A. Sutherland, P. Hewitson, R. Siebers, R. van den Heuvel, L. Arbenz, J. Kinkel, D. Fisher, Scale-up of protein purifications using aqueous two-phase systems: comparing multilayer toroidal coil chromatography with centrifugal partition chromatography, *J. Chromatogr. A.* 1218 (2011) 5527–30. doi:10.1016/j.chroma.2011.04.013.

[85] S. Deng, Z. Deng, Y. Fan, Y. Peng, J. Li, D. Xiong, R. Liu, Isolation and purification of three flavonoid glycosides from the leaves of *Nelumbo nucifera* (Lotus) by high-speed counter-current chromatography, *J. Chromatogr. B.* 877 (2009) 2487–92. doi:10.1016/j.jchromb.2009.06.026.

[86] C.Y. Kim, J. Kim, Preparative isolation and purification of geniposide from Gardenia fruits by centrifugal partition chromatography, *Phytochem. Anal.* 18 (2007) 115–117. doi:10.1002/pca.958.

[87] D. Fisher, I. Garrard, R. van den Heuvel, I. a. Sutherland, F.E. Chou, J.W. Fahey, Technology transfer and scale up of a potential cancer-preventive plant dynamic extraction of glucoraphanin, *J. Liq. Chromatogr. Relat. Technol.* 28 (2005) 1913–1922. doi:10.1081/JLC-200063563.

[88] A. Toribio, J.M. Nuzillard, J.-H. Renault, Strong ion-exchange centrifugal partition chromatography as an efficient method for the large-scale purification of glucosinolates, *J. Chromatogr. A.* 1170 (2007) 44–51. doi:10.1016/j.chroma.2007.09.004.

[89] C.S. Lau, K.A. Bunnell, E.C. Clausen, G.J. Thoma, J.O. Lay, J. Gidden, D.J. Carrier, Separation and purification of xylose oligomers using centrifugal partition chromatography, *J. Ind. Microbiol. Biotechnol.* 38 (2011) 363–370. doi:10.1007/s10295-010-0799-1.

[90] C.S. Lau, E.C. Clausen, J.O. Lay, J. Gidden, D.J. Carrier, Separation of xylose

oligomers using centrifugal partition chromatography with a butanol-methanol-water system, *J. Ind. Microbiol. Biotechnol.* 40 (2013) 51–62. doi:10.1007/s10295-012-1209-7.

[91] K. Bunnell, C.-S. Lau, J.O. Lay, J. Gidden, D.J. Carrier, Production and fractionation of xylose oligomers from switchgrass hemicelluloses using centrifugal partition chromatography, *J. Liq. Chromatogr. Relat. Technol.* 38 (2015) 801–809. doi:10.1080/10826076.2014.973505.

[92] M.H. Chen, K. Rajan, D.J. Carrier, V. Singh, Separation of xylose oligomers from autohydrolyzed *Miscanthus* × <i>giganteus<i> using centrifugal partition chromatography, *Food Bioprod. Process.* 95 (2015) 125–132. doi:10.1016/j.fbp.2015.04.006.

[93] H. Zhang, E.C. Brace, A.S. Engelberth, Selection of a non-aqueous two-phase solvent system for fractionation of xylooligosaccharides prebiotics using the conductor-like screening model for real solvents, *J. Liq. Chromatogr. Relat. Technol.* 39 (2016) 666–673. doi:10.1080/10826076.2016.1230552.

[94] L. Chevolot, A. Foucault, S. Colliec-Jouault, J. Ratiskol, C. Sinquin, Improvement purification of sulfated oligofucan by ion-exchange displacement centrifugal partition chromatography, *J. Chromatogr. A.* 869 (2000) 353–361. doi:10.1016/S0021-9673(99)01187-5.

[95] W. Murayama, T. Kobayashi, Y. Kosuge, H. Yano, Y. Nunogaki, K. Nunogaki, A new centrifugal counter-current chromatograph and its application, *J. Chromatogr. A.* 239 (1982) 643–649. doi:10.1016/S0021-9673(00)82022-1.

[96] K. Shinomiya, Y. Kabasawa, Y. Ito, Countercurrent chromatography separation of sugars and their p-nitrophenyl derivatives by cross-axis coil planet centrifuge, *J. Liq. Chromatogr. Relat. Technol.* 22 (1999) 579–592. doi:10.1081/JLC-100101683.

[97] I.A. Sutherland, L. Brown, S. Forbes, G. Games, D. Hawes, K. Hostettmann, E.H. McKerrell, A. Marston, D. Wheatley, P. Wood, Countercurrent

chromatography (CCC) and its versatile application as an industrial purification & production process, *J. Liq. Chromatogr. Relat. Technol.* 21 (1998) 279–298. doi:10.1080/10826079808000491.

[98] I.A. Sutherland, L. Brown, A.S. Graham, G.G. Guillon, D. Hawes, L. Janaway, R. Whiteside, P. Wood, Industrial scale-up of countercurrent chromatography: predictive scale-up., *J. Chromatogr. Sci.* 39 (2001) 21–28. doi:10.1093/chromsci/39.1.21.

[99] S. Chollet, L. Marchal, Jérémy Meucci, J. Renault, J. Legrand, A. Foucault, Methodology for optimally sized centrifugal partition chromatography columns, *J. Chromatogr. A.* 1388 (2015) 174–183. doi:10.1016/j.chroma.2015.02.043.

[100] G.F. Pauli, S.M. Pro, L.R. Chadwick, T. Burdick, L. Pro, W. Friedl, N. Novak, J. Maltby, F. Qiu, J.B. Friesen, Real-time volumetric phase monitoring: advancing chemical analysis by countercurrent separation, *Anal. Chem.* 87 (2015) 7418–7425. doi:10.1021/acs.analchem.5b01613.

[101] E. Bouju, A. Berthod, K. Faure, Scale-up in centrifugal partition chromatography: The “free-space between peaks” method, *J. Chromatogr. A.* 1409 (2015) 70–78. doi:10.1016/j.chroma.2015.07.020.

[102] A. Kotland, S. Chollet, C. Diard, J.-M. Autret, J. Meucci, J.-H. Renault, L. Marchal, Industrial case study on alkaloids purification by pH-zone refining centrifugal partition chromatography, *J. Chromatogr. A.* 1474 (2016) 59–70. doi:10.1016/j.chroma.2016.10.039.

[103] J.-H. Renault, P. Thépenier, M. Zèches-Hanrot, L. Le Men-Olivier, A. Durand, A. Foucault, R. Margraff, Preparative separation of anthocyanins by gradient elution centrifugal partition chromatograghy, *J. Chromatogr. A.* 763 (1997) 345–352. doi:10.1016/S0021-9673(96)00880-1.

[104] A. Toribio, J.M. Nuzillard, B. Pinel, L. Boudesocque, M. Lafosse, F. De La Poype, J.-H. Renault, Pilot-scale ion-exchange centrifugal partition

chromatography: Purification of sinalbin from white mustard seeds, *J. Sep. Sci.* 32 (2009) 1801–1807. doi:10.1002/jssc.200800651.

[105] E. Bouju, A. Berthod, K. Faure, Carnosol purification. Scaling-up centrifugal partition chromatography separations, *J. Chromatogr. A.* 1466 (2016) 59–66. doi:10.1016/j.chroma.2016.08.015.

[106] A. Berthod, M.J. Ruiz-Angel, S. Carda-Broch, Elution-extrusion countercurrent chromatography. Use of the liquid nature of the stationary phase to extend the hydrophobicity window, *Anal. Chem.* 75 (2003) 5886–5894. doi:10.1021/ac030208d.

[107] A. Berthod, M. Hassoun, G. Harris, Using the liquid nature of the stationary phase: the elution-extrusion method, *J. Liq. Chromatogr. Relat. Technol.* 28 (2005) 1851–1866. doi:10.1081/JLC-200063489.

[108] A. Berthod, J.B. Friesen, T. Inui, G.F. Pauli, Elution-extrusion countercurrent chromatography: Theory and concepts in metabolic analysis, *Anal. Chem.* 79 (2007) 3371–3382. doi:10.1021/ac062397g.

[109] E. Delannay, A. Toribio, L. Boudesocque, J.M. Nuzillard, M. Zèches-Hanrot, E. Dardennes, G. Le Dour, J. Sapi, J.-H. Renault, Multiple dual-mode centrifugal partition chromatography, a semi-continuous development mode for routine laboratory-scale purifications, *J. Chromatogr. A.* 1127 (2006) 45–51. doi:10.1016/j.chroma.2006.05.069.

[110] N. Rubio, S. Ignatova, C. Minguillón, I.A. Sutherland, Multiple dual-mode countercurrent chromatography applied to chiral separations using a (S)-naproxen derivative as chiral selector, *J. Chromatogr. A.* 1216 (2009) 8505–11. doi:10.1016/j.chroma.2009.10.006.

[111] N. Mekaoui, A. Berthod, Using the liquid nature of the stationary phase. VI. Theoretical study of multi-dual mode countercurrent chromatography, *J. Chromatogr. A.* 1218 (2011) 6061–71. doi:10.1016/j.chroma.2010.12.104.

[112] N. Rubio, C. Minguillón, Preparative enantioseparation of (±)-N-(3,4-cis-3-decyl-1,2,3,4-tetrahydrophenanthren-4-yl)-3,5-dinitrobenzamide by centrifugal partition chromatography, *J. Chromatogr. A.* 1217 (2010) 1183–1190. doi:10.1016/j.chroma.2009.12.023.

[113] A. Toribio, L. Boudesocque, B. Richard, J.-M. Nuzillard, J.-H. Renault, Preparative isolation of glucosinolates from various edible plants by strong ion-exchange centrifugal partition chromatography, *Sep. Purif. Technol.* 83 (2011) 15–22. doi:10.1016/j.seppur.2011.07.001.

[114] M. Hamzaoui, J. Hubert, R. Reynaud, L. Marchal, A. Foucault, J.-H. Renault, Strong ion exchange in centrifugal partition extraction (SIX-CPE): Effect of partition cell design and dimensions on purification process efficiency, *J. Chromatogr. A.* 1247 (2012) 18–25. doi:10.1016/j.chroma.2012.05.046.

[115] J.H. Renault, J.M. Nuzillard, G. Le Crouérour, P. Thépenier, M. Zèches-Hanrot, L. Le Men-Olivier, Isolation of indole alkaloids from *Catharanthus roseus* by centrifugal partition chromatography in the pH-zone refining mode, *J. Chromatogr. A.* 849 (1999) 421–431. doi:10.1016/S0021-9673(99)00495-1.

[116] Y. Ito, pH-zone-refining counter-current chromatography: origin, mechanism, procedure and applications, *J. Chromatogr. A.* 1271 (2013) 71–85. doi:10.1016/j.chroma.2012.11.024.

[117] F. Gula, D. Paillat, Decolorization of refinery liquors: A technical and economic comparison between the different systems using activated carbon or resins, *Int. Sugar J.* 107 (2005) 235–240.

[118] J.A. García Agudo, M.T. García Cubero, G.G. Benito, M.P. Miranda, Removal of coloured compounds from sugar solutions by adsorption onto anionic resins: equilibrium and kinetic study, *Sep. Purif. Technol.* 29 (2002) 199–205. doi:10.1016/S1383-5866(02)00083-7.

[119] V. Kochergin, W. Jacob, M. Kearney, W. Bornak, Ion Exchange Decolorization - Possibility of Resin Rejuvenation, in: Am. Soc. Sugar Beet Technol. - Proc.

from 34th Bienn. Meet., 2007.

[120] M. Coca, M.T. García, S. Mato, Á. Cartón, G. González, Evolution of colorants in sugarbeet juices during decolorization using styrenic resins, *J. Food Eng.* 89 (2008) 429–434. doi:10.1016/j.jfoodeng.2008.05.025.

[121] M. Asadi, Sugarbeet processing, in: Beet-Sugar Handb., Wiley, New Jersey, 2007.

[122] L.S.M. Bento, Application of Ion-Exchange Resins for Sugar Liquors Decolourisation, in: Int. Soc. Sugar Cane Technol., 1999.

[123] I.M. De Mancilha, M.N. Karim, Evaluation of ion exchange resins for removal of inhibitory compounds from corn stover hydrolyzate for xylitol fermentation, *Biotechnol. Prog.* 19 (2003) 1837–1841. doi:10.1021/bp034069x.

[124] M.L. Soto, A. Moure, H. Domínguez, J.C. Parajó, Recovery, concentration and purification of phenolic compounds by adsorption: A review, *J. Food Eng.* 105 (2011) 1–27. doi:10.1016/j.jfoodeng.2011.02.010.

[125] C.S. Gong, C.S. Chen, L.F. Chen, Pretreatment of sugar cane bagasse hernicellulose hydrolyzate for ethanol production by yeast, *Appl. Biochem. Biotechnol.* 39 (1993) 83–88. doi:10.1007/BF02918979.

[126] A.K. Chandel, R.K. Kapoor, A. Singh, R.C. Kuhad, Detoxification of sugarcane bagasse hydrolysate improves ethanol production by Candida shehatae NCIM 3501, *Bioresour. Technol.* 98 (2007) 1947–1950. doi:10.1016/j.biortech.2006.07.047.

[127] M. Okuno, H. Tamaki, A novel technique for the decolorization of sugarcane juice, *J. Food Sci.* 67 (2002) 236–238. doi:10.1111/j.1365-2621.2002.tb11390.x.

[128] Y. Ku, K.-C. Lee, Removal of phenols from aqueous solution by XAD-4 resin, *J. Hazard. Mater.* 80 (2000) 59–68. doi:10.1016/S0304-3894(00)00275-2.

[129] R.S. Juang, J.Y. Shiau, Adsorption isotherms of phenols from water onto macroreticular resins, *J. Hazard. Mater.* 70 (1999) 171–183. doi:10.1016/S0304-3894(99)00152-1.

[130] K. Abburi, Adsorption of phenol and p-chlorophenol from their single and bisolute aqueous solutions on Amberlite XAD-16 resin, *J. Hazard. Mater.* 105 (2003) 143–156. doi:10.1016/j.jhazmat.2003.08.004.

[131] N. Van Duc Long, T.H. Le, J. Il Kim, J.W. Lee, Y.M. Koo, Separation of D-psicose and D-fructose using simulated moving bed chromatography, *J. Sep. Sci.* 32 (2009) 1987–1995. doi:10.1002/jssc.200800753.

[132] B. Ataç, V. Gökmen, Adsorption of dark colored compounds in apple juice - Effects of initial soluble solid concentration on adsorption kinetics and mechanism, *J. Food Process Eng.* 34 (2011) 108–124. doi:10.1111/j.1745-4530.2008.00339.x.

[133] O. Ioannidou, A. Zabaniotou, Agricultural residues as precursors for activated carbon production-A review, *Renew. Sustain. Energy Rev.* 11 (2007) 1966–2005. doi:10.1016/j.rser.2006.03.013.

[134] G. Mezohegyi, F.P. van der Zee, J. Font, A. Fortuny, A. Fabregat, Towards advanced aqueous dye removal processes: A short review on the versatile role of activated carbon, *J. Environ. Manage.* 102 (2012) 148–164. doi:10.1016/j.jenvman.2012.02.021.

[135] M. Ahmedna, W.. Marshall, R.. Rao, Surface properties of granular activated carbons from agricultural by-products and their effects on raw sugar decolorization, *Bioresour. Technol.* 71 (2000) 103–112. doi:10.1016/S0960-8524(99)90069-X.

[136] E.C. Bernardo, R. Egashira, J. Kawasaki, Decolorization of molasses' wastewater using activated carbon prepared from cane bagasse, *Carbon N. Y.* 35 (1997) 1217–1221. doi:10.1016/S0008-6223(97)00105-X.

[137] A.H. Konsowa, M.E. Ossman, Y. Chen, J.C. Crittenden, Decolorization of industrial wastewater by ozonation followed by adsorption on activated carbon, *J. Hazard. Mater.* 176 (2010) 181–185. doi:10.1016/j.jhazmat.2009.11.010.

[138] J.M. Dias, M.C.M. Alvim-Ferraz, M.F. Almeida, J. Rivera-Utrilla, M. Sánchez-Polo, Waste materials for activated carbon preparation and its use in aqueous-phase treatment: A review, *J. Environ. Manage.* 85 (2007) 833–846. doi:10.1016/j.jenvman.2007.07.031.

[139] I.N. Najm, V.L. Snoeyink, B.W. Lykins, J.Q. Adams, Using powdered activated carbon: a critical review, *J. Am. Water Works Assoc.* 83 (1991) 65–76.

[140] C. Stoquart, P. Servais, P.R. Bérubé, B. Barbeau, Hybrid Membrane Processes using activated carbon treatment for drinking water: A review, *J. Memb. Sci.* 411–412 (2012) 1–12. doi:10.1016/j.memsci.2012.04.012.

[141] E.S. Hertzog, S.J. Broderick, Activated Carbon for Sugar Decolorization, *Ind. Eng. Chem.* 33 (1941) 1192–1198. doi:10.1021/ie50381a024.

[142] H.K. Atiyeh, Z. Duvnjak, Purification of Fructose Syrups Produced from Cane Molasses Media Using Ultrafiltration Membranes and Activated Carbon, *Sep. Sci. Technol.* 39 (2005) 341–362. doi:10.1081/SS-120027562.

[143] H.L. Mudoga, H. Yucel, N.S. Kincal, Decolorization of sugar syrups using commercial and sugar beet pulp based activated carbons, *Bioresour. Technol.* 99 (2008) 3528–3533. doi:10.1016/j.biortech.2007.07.058.

[144] K. Qureshi, I. Bhatti, R. Kazi, A.K. Ansari, Physical and chemical analysis of activated carbon prepared from sugarcane bagasse and use for sugar decolorisation, *Int. J. Chem. Biol. Eng.* 1 (2008) 144–148.

[145] B. Pendyal, M.M. Johns, W.E. Marshall, M. Ahmedna, R.M. Rao, Removal of sugar colorants by granular activated carbons made from binders and agricultural by-products, *Bioresour. Technol.* 69 (1999) 45–51. doi:10.1016/S0960-8524(98)00172-2.

[146] M. Ahmedna, W. Marshall, R. Rao, Production of granular activated carbons from select agricultural by-products and evaluation of their physical, chemical and adsorption properties, *Bioresour. Technol.* 71 (2000) 113–123. doi:10.1016/S0960-8524(99)00070-X.

[147] S.I. Mussatto, I.C. Roberto, Hydrolysate detoxification with activated charcoal for xylitol production by *Candida guilliermondii*, *Biotechnol. Lett.* 23 (2001) 1681–1684. doi:10.1023/A:1012492028646.

[148] J.C. Parajó, H. Dominguez, J.M. Dominguez, Charcoal adsorption of wood hydrolysates for improving their fermentability: Influence of the operational conditions, *Bioresour. Technol.* 57 (1996) 179–185. doi:10.1016/0960-8524(96)00066-1.

[149] P.V. Gurgel, I.M. Mancilha, R.P. Peçanha, J.F.M. Siqueira, Xylitol recovery from fermented sugarcane bagasse hydrolyzate, *Bioresour. Technol.* 52 (1995) 219–223. doi:10.1016/0960-8524(95)00025-A.

[150] L. Canilha, J.B. de Almeida e Silva, A.I.N. Solenzal, Eucalyptus hydrolysate detoxification with activated charcoal adsorption or ion-exchange resins for xylitol production, *Process Biochem.* 39 (2004) 1909–1912. doi:10.1016/j.procbio.2003.09.009.

[151] J. Buhner, F. a Agblevor, Effect of detoxification of dilute-acid corn fiber hydrolysate on xylitol production, *Appl. Biochem. Biotechnol.* 119 (2004) 13–30. doi:10.1385/ABAB:119:1:13.

[152] A. Converti, P. Perego, J.M. Domínguez, Xylitol production from hardwood hemicellulose hydrolysates by *Pachysolen tannophilus*, *Debaryomyces hansenii*, and *Candida guilliermondii*, *Appl. Biochem. Biotechnol.* 82 (1999) 141–152. doi:10.1385/ABAB:82:2:141.

[153] R.E. Berson, J.S.J. Young, S.N. Kamer, T.R. Hanley, Detoxification of actual pretreated corn stover hydrolysate using activated carbon powder, *Appl. Biochem. Biotechnol.* 121 (2005) 923–34. doi:10.1385/ABAB:124:1-3:0923.

[154] J.C. Parajó, H. Domínguez, J.M. Domínguez, Study of charcoal adsorption for improving the production of xylitol from wood hydrolysates, *Bioprocess Eng.* 16 (1996) 39. doi:10.1007/s004490050285.

[155] M. Ahmedna, M.M. Johns, S.J. Clarke, W.E. Marshall, R.M. Rao, Potential of agricultural by-product-based activated carbons for use in raw sugar decolourisation, *J. Sci. Food Agric.* 75 (1997) 117–124. doi:10.1002/(SICI)1097-0010(199709)75:1<117::AID-JSFA850>3.0.CO;2-M.

[156] E. Sabio, E. González, J.F. González, C.M. González-García, A. Ramiro, J. Gañan, Thermal regeneration of activated carbon saturated with p-nitrophenol, *Carbon N. Y.* 42 (2004) 2285–2293. doi:10.1016/j.carbon.2004.05.007.

[157] G. San Miguel, S.D. Lambert, N.J.D. Graham, The regeneration of field-spent granular-activated carbons, *Water Res.* 35 (2001) 2740–2748. doi:10.1016/S0043-1354(00)00549-2.

[158] B. Chai, H. Meng, Z. Zhao, Q. Huang, X. Fu, Removal of color compounds from sugarcane juice by modified sugarcane bagasse: equilibrium and kinetic study, *Sugar Tech*. 18 (2016) 317–324. doi:10.1007/s12355-015-0415-9.

[159] H. Arslanoglu, F. Tumen, A study on cations and color removal from thin sugar juice by modified sugar beet pulp, *J. Food Sci. Technol.* 49 (2012) 319–327. doi:10.1007/s13197-011-0288-1.

[160] M. Hamachi, B.. Gupta, R. Ben Aim, Ultrafiltration: a means for decolorization of cane sugar solution, *Sep. Purif. Technol.* 30 (2003) 229–239. doi:10.1016/S1383-5866(02)00145-4.

[161] T. Suzuki, K. Tomita-Yokotani, S. Yoshida, Y. Takase, I. Kusakabe, K. Hasegawa, Preparation and isolation of oligogalacturonic acids and their biological effects in cockscomb (*Celosia argentea L.*) seedlings, *J. Plant Growth Regul.* 21 (2002) 209–215. doi:10.1007/s003440010060.

[162] J.X. Khym, D.G. Doherty, The analysis and separation of glucuronic and

galacturonic acids by ion exchange, *J. Am. Chem. Soc.* 74 (1952) 3199–3200. doi:10.1021/ja01132a536.

[163] X. Wang, Y. Xu, L. Fan, Q. Yong, S. Yu, Simultaneous separation and quantitative determination of monosaccharides, uronic acids, and aldonic acids by high performance anion-exchange chromatography coupled with pulsed amperometric detection in corn stover prehydrolysates, *BioResources*. 7 (2012) 4614–4625. doi:10.15376/biores.7.4.4614-4625.

[164] DOW liquid separations, DOWEX ion exchange resins - using ion exchange resin selectivity coefficients - 177-01755-0207, 2007.

[165] J. Kumanotani, R. Oshima, Y. Yamauchi, N. Takai, Y. Kurosu, Preparative high-performance gel chromatography for acidic and neutral saccharides, *J. Chromatogr. A.* 176 (1979) 462–464. doi:10.1016/S0021-9673(00)89472-8.

[166] K.B. Hicks, S.M. Sondey, L.W. Doner, Preparative liquid chromatography of carbohydrates mono- and di-saccharides, uronic acids, and related derivatives, *Carbohydr. Res.* 168 (1987) 33–45. doi:10.1016/0008-6215(87)80004-6.

[167] R. Pecina, G. Bonn, E. Burtscher, O. Bobleter, High-performance liquid chromatographic elution behaviour of alcohols, aldehydes, ketones, organic acids and carbohydrates on a strong cation-exchange stationary phase, *J. Chromatogr. A.* 287 (1984) 245–258. doi:10.1016/S0021-9673(01)87701-3.

[168] D.C.S. Azevedo, A. Rodrigues, Fructose–glucose separation in a SMB pilot unit: modeling, simulation, design, and operation, *AIChE J.* 47 (2001) 2042–2051.

[169] H. Caruel, L. Rigal, a. Gaset, Carbohydrate separation by ligand-exchange liquid chromatography. Correlation between the formation of sugar-cation complexes and the elution order, *J. Chromatogr.* 558 (1991) 89–104. doi:10.1016/0021-9673(91)80114-V.

[170] M. Stefansson, D. Westerlund, Ligand-exchange chromatography of

carbohydrates and glycoconjugates, *J. Chromatogr. A.* 720 (1996) 127–136. doi:10.1016/0021-9673(95)00276-6.

[171] Z. El Rassi, Recent progress in reversed-phase and hydrophobic interaction chromatography of carbohydrate species, *J. Chromatogr. A.* 720 (1996) 93–118. doi:10.1016/0021-9673(94)01298-9.

[172] G. Karlsson, S. Winge, H. Sandberg, Separation of monosaccharides by hydrophilic interaction chromatography with evaporative light scattering detection, *J. Chromatogr. A.* 1092 (2005) 246–9. doi:10.1016/j.chroma.2005.08.025.

[173] T. Ikegami, K. Horie, N. Saad, K. Hosoya, O. Fiehn, N. Tanaka, Highly efficient analysis of underivatized carbohydrates using monolithic-silica-based capillary hydrophilic interaction (HILIC) HPLC., *Anal. Bioanal. Chem.* 391 (2008) 2533–42. doi:10.1007/s00216-008-2060-6.

[174] C. Corradini, A. Cavazza, C. Bignardi, High-Performance Anion-Exchange Chromatography Coupled with Pulsed Electrochemical Detection as a Powerful Tool to Evaluate Carbohydrates of Food Interest: Principles and Applications, *Int. J. Carbohydr. Chem.* 2012 (2012) 1–13. doi:10.1155/2012/487564.

[175] A. Rajendran, G. Paredes, M. Mazzotti, Simulated moving bed chromatography for the separation of enantiomers, *J. Chromatogr. A.* 1216 (2009) 709–738. doi:10.1016/j.chroma.2008.10.075.

[176] M. Juza, M. Mazzotti, M. Morbidelli, Simulated moving-bed chromatography and its application to chirotechnology, *Trends Biotechnol.* 18 (2000) 108–118. doi:10.1016/S0167-7799(99)01419-5.

[177] S. Imamoglu, Simulated moving bed chromatography (SMB) for application in bioseparation, *Mod. Adv. Chromatogr.* 76 (2002) 211–231. doi:10.1007/3-540-45345-8_6.

[178] Y. Xie, Y. Koo, N.-H.L. Wang, Preparative chromatographic separation:

Simulated moving bed and modified chromatography methods, *Biotechnol. Bioprocess Eng.* 6 (2001) 363–375. doi:10.1007/BF02932317.

[179] P. Sá Gomes, A.E. Rodrigues, Simulated moving bed chromatography: from concept to proof-of-concept, *Chem. Eng. Technol.* 35 (2012) 17–34. doi:10.1002/ceat.201100281.

[180] S. Abel, G. Erdem, M. Mazzotti, M. Morari, M. Morbidelli, Optimizing control of simulated moving beds - Linear isotherm, *J. Chromatogr. A.* 1033 (2004) 229–239. doi:10.1016/j.chroma.2004.01.049.

[181] S.-M. Song, M.-B. Park, I.H. Kim, Three-zone simulated moving-bed (SMB) for separation of cytosine and guanine, *Korean J. Chem. Eng.* 29 (2012) 952–958. doi:10.1007/s11814-011-0247-6.

[182] A. Rajendran, Equilibrium theory-based design of simulated moving bed processes under reduced purity requirements. Linear isotherms, *J. Chromatogr. A.* 1185 (2008) 216–222. doi:10.1016/j.chroma.2008.01.054.

[183] C. Nobre, M.J. Santos, A. Dominguez, D. Torres, O. Rocha, a M. Peres, I. Rocha, E.C. Ferreira, J. a Teixeira, L.R. Rodrigues, Comparison of adsorption equilibrium of fructose, glucose and sucrose on potassium gel-type and macroporous sodium ion-exchange resins, *Anal. Chim. Acta*. 654 (2009) 71–6. doi:10.1016/j.aca.2009.06.043.

[184] J. a. Vente, H. Bosch, A.B. De Haan, P.J.T. Bussmann, Evaluation of sugar sorption isotherm measurement by frontal analysis under industrial processing conditions, *J. Chromatogr. A.* 1066 (2005) 71–79. doi:10.1016/j.chroma.2004.12.071.

[185] Y. Xie, S. Mun, J. Kim, N.-H.L. Wang, Standing wave design and experimental validation of a tandem simulated moving bed process for insulin purification, *Biotechnol. Prog.* 18 (2002) 1332–1344. doi:10.1021/bp025547r.

[186] S. Mun, Improving performance of a tandem simulated moving bed process for

sugar separation by making a difference in the adsorbents and the column lengths of the two subordinate simulated moving bed units, *J. Chromatogr. A.* 1277 (2013) 48–57. doi:10.1016/j.chroma.2012.12.056.

[187] Y. Xie, C.Y. Chin, D.S.C. Phelps, C.-H. Lee, K.B. Lee, S. Mun, N.-H.L. Wang, A five-zone simulated moving bed for the isolation of six sugars from biomass hydrolyzate, *Ind. Eng. Chem. Res.* 44 (2005) 9904–9920. doi:10.1021/ie050403d.

[188] R. Wooley, A Nine-Zone Simulating Moving Bed for the Recovery of Glucose and Xylose from Biomass Hydrolyzate, 5885 (1998) 3699–3709.

[189] D. Antos, A. Seidel-Morgenstern, Application of gradients in the simulated moving bed process, *Chem. Eng. Sci.* 56 (2001) 6667–6682. doi:10.1016/S0009-2509(01)00342-6.

[190] D. Antos, A. Seidel-Morgenstern, Two-step solvent gradients in simulated moving bed chromatography: Numerical study for linear equilibria, *J. Chromatogr. A.* 944 (2002) 77–91. doi:10.1016/S0021-9673(01)01365-6.

[191] A.L. Zydney, Continuous downstream processing for high value biological products: A Review, *Biotechnol. Bioeng.* (2015). doi:10.1002/bit.25695.

[192] L. Aumann, M. Morbidelli, A continuous multicolumn countercurrent solvent gradient purification (MCSGP) process, *Biotechnol. Bioeng.* 98 (2007) 1043–1055. doi:10.1002/bit.21527.

[193] L.C. Keßler, L. Gueorguieva, U. Rinas, A. Seidel-Morgenstern, Step gradients in 3-zone simulated moving bed chromatography. Application to the purification of antibodies and bone morphogenetic protein-2, *J. Chromatogr. A.* 1176 (2007) 69–78. doi:10.1016/j.chroma.2007.10.087.

[194] C.Y. Chin, N.H.L. Wang, Simulated moving-bed technology for biorefinery applications, in: Sep. Purif. Technol. Biorefineries, 2013: pp. 167–202. doi:10.1002/9781118493441.ch7.

[195] H.J. Subramani, K. Hidajat, A.K. Ray, Optimization of simulated moving bed and Varicol processes for glucose–fructose separation, *Chem. Eng. Res. Des.* 81 (2003) 549–567. doi:10.1205/026387603765444500.

[196] S. Katsuo, M. Mazzotti, Intermittent simulated moving bed chromatography: 1. Design criteria and cyclic steady-state, *J. Chromatogr. A.* 1217 (2010) 1354–1361. doi:10.1016/j.chroma.2009.12.065.

[197] Z. Zhang, M. Mazzotti, M. Morbidelli, PowerFeed operation of simulated moving bed units: Changing flow-rates during the switching interval, *J. Chromatogr. A.* 1006 (2003) 87–99. doi:10.1016/S0021-9673(03)00781-7.

[198] H. Schramm, A. Kienle, M. Kaspereit, A. Seidel-Morgenstern, Improved operation of simulated moving bed processes through cyclic modulation of feed flow and feed concentration, *Chem. Eng. Sci.* 58 (2003) 5217–5227. doi:10.1016/j.ces.2003.08.015.

[199] L.C. Keßler, A. Seidel-Morgenstern, Improving performance of simulated moving bed chromatography by fractionation and feed-back of outlet streams, *J. Chromatogr. A.* 1207 (2008) 55–71. doi:10.1016/j.chroma.2008.08.022.

[200] M. Holzer, H. Osuna-Sanchez, L. David, Multicolumn Chromatography, *Bioprocess Int.* September (2008) 74.

[201] N. Gottschlich, V. Kasche, Purification of monoclonal antibodies by simulated moving-bed chromatography, *J. Chromatogr. A.* 765 (1997) 201–206. doi:10.1016/S0021-9673(96)00932-6.

[202] D.B. Broughton, C.G. Gerhold, Continuous Sorption process employing fixed bed of sorbent and moving inlets and outlets, (1961).

[203] C. Ching, D. Ruthven, K. Hidajat, Experimental study of a simulated counter-current adsorption system—III. Sorbex operation, *Chem. Eng. Sci.* 40 (1985) 1411–1417.

[204] C. Ching, D. Ruthven, An experimental study of a simulated counter-current adsorption system—I. Isothermal steady state operation, *Chem. Eng. Sci.* 40 (1985). doi:10.1016/0009-2509(85)85001-6.

[205] K. Lee, Continuous separation of glucose and fructose at high concentration using two-section simulated moving bed process, *Korean J. Chem. Eng.* 20 (2003) 532–537. doi:10.1007/BF02705561.

[206] A.S. Kurup, K. Hidajat, A.K. Ray, Optimal operation of an industrial-scale parex process for the recovery of p-xylene from a mixture of C8 aromatics, *Ind. Eng. Chem. Res.* 44 (2005) 5703–5714. doi:10.1021/ie0488694.

[207] V.F.D. Martins, A.M. Ribeiro, M.G. Plaza, J.C. Santos, J.M. Loureiro, A.F.P. Ferreira, A.E. Rodrigues, Gas-phase simulated moving bed: Propane/propylene separation on 13X zeolite, *J. Chromatogr. A.* 1423 (2015) 136–148. doi:10.1016/j.chroma.2015.10.038.

[208] Z. Bubnik, V. Pour, A. Gruberova, H. Starhova, A. Hinkova, P. Kadlec, Application of continuous chromatographic separation in sugar processing, *J. Food Eng.* 61 (2004) 509–513. doi:10.1016/S0260-8774(03)00221-8.

[209] H. Heikkilä, G. Hyöky, K. Jarmo, Method for the fractionation of molasses, US Patent 6,649,066, 2003.

[210] M.S. Coelho, D.C.S. Azevedo, J. a Teixeira, A. Rodrigues, Dextran and fructose separation on an SMB continuous chromatographic unit, *Biochem. Eng. J.* 12 (2002) 215–221. doi:10.1016/S1369-703X(02)00071-2.

[211] D.C.S. Azevedo, A.E. Rodrigues, Separation of fructose and glucose from cashew apple juice by SMB chromatography, *Sep. Sci. Technol.* 40 (2005) 1761–1780. doi:10.1081/SS-200064559.

[212] J. Tiihonen, T. Sainio, A. Kärki, E. Paatero, Co-eluent effect in partition chromatography. Rhamnose–xylose separation with strong and weak cation-exchangers in aqueous ethanol, *J. Chromatogr. A.* 982 (2002) 69–84.

doi:10.1016/S0021-9673(02)01522-4.

[213] H.J. Lee, Y. Xie, Y.M. Koo, N.H.L. Wang, Separation of lactic acid from acetic acid using a four-zone SMB, *Biotechnol. Prog.* 20 (2004) 179–192. doi:10.1021/bp025663u.

[214] C.S. López-Garzón, A.J.J. Straathof, Recovery of carboxylic acids produced by fermentation, 2014. doi:10.1016/j.biotechadv.2014.04.002.

[215] N.L. Mai, N.T. Nguyen, J.-I. Kim, H.-M. Park, S.-K. Lee, Y.-M. Koo, Recovery of ionic liquid and sugars from hydrolyzed biomass using ion exclusion simulated moving bed chromatography, *J. Chromatogr. A.* 1227 (2012) 67–72. doi:10.1016/j.chroma.2011.12.030.

[216] B.R. Caes, T.R. Van Oosbree, F. Lu, J. Ralph, C.T. Maravelias, R.T. Raines, Simulated moving bed chromatography: separation and recovery of sugars and ionic liquid from biomass hydrolysates, *ChemSusChem*. 6 (2013) 2083–2089. doi:10.1002/cssc.201300267.

[217] M. Minceva, P.S. Gomes, V. Meshko, A.E. Rodrigues, Simulated moving bed reactor for isomerization and separation of p-xylene, *Chem. Eng. J.* 140 (2008) 305–323. doi:10.1016/j.cej.2007.09.033.

[218] M. Kawase, A. Pilgrim, T. Araki, K. Hashimoto, Lactosucrose production using a simulated moving bed reactor, *Chem. Eng. Sci.* 56 (2001) 453–458. doi:10.1016/S0009-2509(00)00248-7.

[219] D.C.S. Azevedo, A.E. Rodrigues, Design methodology and operation of a simulated moving bed reactor for the inversion of sucrose and glucose–fructose separation, *Chem. Eng. J.* 82 (2001) 95–107. doi:10.1016/S1385-8947(00)00359-4.

[220] A. Kurup, H. Subramani, K. Hidajat, A. Ray, Optimal design and operation of SMB bioreactor for sucrose inversion, *Chem. Eng. J.* 108 (2005) 19–33. doi:10.1016/j.cej.2004.12.034.

[221] Y. Zhang, K. Hidajat, A. Ray, Optimal design and operation of SMB bioreactor: production of high fructose syrup by isomerization of glucose, *Biochem. Eng. J.* 21 (2004) 111–121. doi:10.1016/j.bej.2004.05.007.

[222] G. Storti, M. Mazzotti, M. Morbidelli, S. Carrà, Robust design of binary countercurrent adsorption separation processes, *AIChE J.* 39 (1993) 471–492. doi:10.1002/aic.690390310.

[223] Y. Wang, Y. Mao, J. Han, Y. Liu, Y. Yan, Liquid-liquid equilibrium of potassium phosphate / potassium citrate / sodium citrate + ethanol aqueous two-phase systems at (298.15 and 313.15) K and correlation, *J. Chem. Eng. Data*. 55 (2010) 5621–5626.

[224] R. Kohn, P. Kovác, Dissociation constants of D-galacturonic and D-glucuronic acid and their O-methyl derivatives, *Chem. Zvesti*. 32 (1978) 478–485.

[225] J.W. Fahey, K. Wade, Separation and purification of glucosinolates from crude plant homogenates by high-speed counter-current chromatography, *J. Chromatogr. A*. 996 (2003) 85–93. doi:10.1016/S0021-9673(03)00607-1.

[226] K.V. Balakin, Y.A. Ivanenkov, A.V. Skorenko, Y. V. Nikolsky, N.P. Savchuk, A.A. Ivashchenko, In silico estimation of DMSO solubility of organic compounds for bioscreening, *J. Biomol. Screen.* 9 (2004) 22–31. doi:10.1177/1087057103260006.

[227] D.S. Jackson, Solubility behaviour of granular corn starches in methyl sulfoxide (DMSO) as measured by high performance size exclusion chromatography, *Starch - Stärke*. 43 (1991) 422–427. doi:10.1002/star.19910431103.

[228] A. Berthod, Countercurrent chromatography: the support-free liquid stationary phase (Comprehensive analytical chemistry, Vol. 38), Elsevier, Amsterdam, 2002.

[229] Z. Zhang, D. Huang, M. Lv, P. Jia, D. Sun, W. Li, Entrainer selection for separating tetrahydrofuran/water azeotropic mixture by extractive distillation,

Sep. Purif. Technol. 122 (2014) 73–77. doi:10.1016/j.seppur.2013.10.051.

[230] L. Marchal, O. Intes, A. Foucault, J. Legrand, J.M. Nuzillard, J.H. Renault, Rational improvement of centrifugal partition chromatographic settings for the production of 5-n-alkylresorcinols from wheat bran lipid extract: I. flooding conditions - optimizing the injection step, *J. Chromatogr. A.* 1005 (2003) 51–62. doi:10.1016/S0021-9673(03)00879-3.

[231] DOW liquid separations, DOWEX MONOSPHERE ion exchange resins - chromatographic separation of fructose and glucose with DOWEX MONOSPHERE ion exchange resins 177-01566-0209, 2006.

[232] G. Gotmar, T. Fornstedt, G. Guiochon, Peak tailing and mass transfer kinetics in linear chromatography Dependence on the column length and the linear velocity of the mobile phase, 831 (1999) 17–35. doi:10.1016/S0021-9673(98)00648-7.

[233] Dow liquid separations, DOWEX fine mesh spherical ion exchange resins for fine chemical and pharmaceutical column separations - 177-01509-904, n.d.

[234] DOW liquid separations, DOWEX ion exchange resins - the advantages of uniform particle sized ion exchange resins - 177-01842-0306, 2006.

[235] A. Jupke, A. Epping, H. Schmidt-Traub, Optimal design of batch and simulated moving bed chromatographic separation processes, *J. Chromatogr. A.* 944 (2002) 93–117. doi:10.1016/S0021-9673(01)01311-5.

[236] DOW liquid separations, DOWEX ion exchange resins - fundamentals of ion exchange - 177-01837-600QRP, 2000.

[237] W.. van Zeist, M. Marinussen, R. Broekema, E. Groen, A. Kool, M. Dolman, H. Blonk, LCI data for the calculation tool Feedprint for greenhouse gas emissions of feed production and utilization: Sugar Industry, *Blonk Consult.* (2012) 1–15.

[238] L. Lorántfy, L. Németh, Development of Industrial Scale Centrifugal Partition Chromatography, *Poster Present. 63rd Int. Congr. Annu. Meet. Soc. Med. Plant Nat. Prod. Res. (GA2015), Budapest*. (2015).

[239] M. Berrios, J.A. Siles, M.A. Martín, A. Martín, Ion Exchange, in: S. Ramaswamy, H.-J. Huang, B.V. Ramarao (Eds.), Sep. Purif. Technol. Biorefineries, Wiley, 2013: pp. 149–165. doi:10.1002/9781118493441.ch6.